THE
PHYSICAL REVIEW

A journal of experimental and theoretical physics established by E. L. Nichols in 1893

SECOND SERIES, VOL. 63, NOS. 7 AND 8 APRIL 1 AND 15, 1943

Radioactive Isotopes of Mercury

GERHART FRIEDLANDER* AND CHIEN-SHIUNG WU**
Radiation Laboratory, Department of Physics, and Department of Chemistry, University of California, Berkeley, California
(Received December 18, 1942)

The radioactive mercury isotopes produced by the bombardment of mercury with neutrons and by the bombardment of gold with deuterons have been studied. Two activities with half-lives of 23 hours and 64 hours, respectively, both decaying by *K*-electron capture, have been assigned to Hg^{197}, on the basis of critical absorption measurements made on the x-rays emitted. The same method was used to show that the 43-minute activity produced by fast neutrons in mercury belongs to an excited state of a mercury isotope and decays by an isomeric transition to the ground state. A 51.5-day beta-emitter was studied; it is probably to be assigned to Hg^{203}.

IN the present paper, we are reporting in detail the results of studies on radioactive mercury isotopes which we have already published in preliminary form.[1] Most of the bombardments were made with the 14-Mev deuterons of the 60-inch cyclotron and with neutrons produced by the bombardment of beryllium with these 14-Mev deuterons.

PREVIOUS WORK

The first artificially radioactive isotope of mercury was discovered by Anderson[2] in 1936. He reported a half-life period of 40 ± 5 hours induced in mercury by slow neutrons, and he tentatively assigned it to Hg^{205}. Shortly afterward, Pool, Cork, and Thornton[3] reported a 45-minute period produced by fast neutron bombardment of mercury. The authors did not identify the chemical nature of this isotope. Heyn[4] also found a 43-minute period from fast neutron bombardment of mercury and showed that it was due to a mercury isotope. McMillan, Kamen, and Ruben[5] investigated the radiations from this 43-minute activity, and found negative beta-rays with an upper energy limit of 0.42 Mev and gamma-radiation of 70- to 250-kev energy. They assigned this period to Hg^{203}. The same authors also reported a 25-hour activity, weakly induced in mercury by fast neutrons, and chemically identified as mercury.

This was all the work that had been published on artificially radioactive mercury isotopes when the present research was begun in 1940. Shortly afterward, however, Krishnan and Nahum[6] published a paper on deuteron bombardments of some heavy metals, in which they discussed

* Now at the Department of Chemistry, University of Idaho, Moscow, Idaho.
** Now at the Department of Physics, Smith College, Northampton, Massachusetts.
[1] C. S. Wu and G. Friedlander, Phys. Rev. **60**, 747 (1941).
[2] E. B. Anderson, Nature **137**, 457 (1936).
[3] M. L. Pool, J. M. Cork, and R. L. Thornton, Phys. Rev. **52**, 239 (1937).
[4] F. A. Heyn, Nature **139**, 842 (1937).
[5] F. M. McMillan, M. Kamen, and S. Ruben, Phys. Rev. **52**, 375 (1937).
[6] R. S. Krishnan and E. A. Nahum, Proc. Camb. Phil. Soc. **36**, 490 (1940).

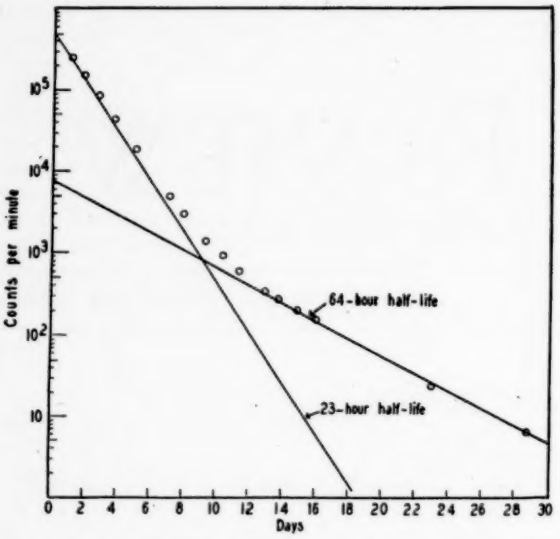

FIG. 1. Decay of Hg^{197} produced by the bombardment of gold with 14-Mev deuterons. The first part of the curve, above 10^4 counts per minute, was measured on an electroscope with thin window (2.5 mg/cm²) which was calibrated against the counter used.

several mercury isotopes: a 48-minute period induced in mercury by fast neutrons as well as by deuterons and assigned to Hg^{197} for reasons which will be discussed later; a 36-hour period produced by fast neutron or deuteron bombardments of mercury and by deuteron bombardment of gold, and assigned to an excited state of Hg^{198} (whose ground state is stable); finally a 5.5-minute period produced in the deuteron bombardment of mercury and assigned to Hg^{205}. Later, Krishnan[7] revised the half-life of the activity assigned by him to Hg^{198*} to 32 hours.

The conflicting assignments of the 43 to 48-minute period[5,6] and particularly the fact that various authors[2,5–7] had reported periods of from 25 to 40-hours' half-life with otherwise very similar properties, led the present authors to make a systematic study of the radioactive mercury isotopes.

Sherr, Bainbridge, and Anderson[8] have recently published results on the transmutation of mercury by fast neutrons, which include a discussion of a 43-minute and a 25-hour activity in mercury. These results are in agreement with ours and will be discussed later in this paper.

[7] R. S. Krishnan, Proc. Camb. Phil. Soc. **37**, 186 (1941).
[8] R. Sherr, K. T. Bainbridge, and H. H. Anderson, Phys. Rev. **60**, 473 (1941).

CHEMICAL SEPARATIONS

Chemical separations were made after all bombardments. In most of the neutron bombardments of mercury, metallic mercury was used, which was then distilled after the addition of gold and platinum carriers. In a few cases, mercury salts were bombarded; in those cases the mercury fractions were isolated by the precipitation of HgO in the presence of gold carrier.

The deuteron-bombarded gold samples were cut up into small strips; a small amount of mercury was amalgamated with the gold, and the mercury then distilled away from the gold in vacuum. The distillate was mixed with some inactive gold and redistilled. In some cases an alternative procedure was used: The gold was dissolved in aqua regia, a few milligrams each of mercuric chloride and platinic chloride were added, and the solution was evaporated to about 0.5 cc. The residue was taken up in water, and gold and mercury were then extracted with ethyl acetate by the procedure of Noyes and Bray.[9] The separation of gold and mercury was then carried out according to Noyes and Bray. The mercury was finally precipitated in the form of the compound $HgO \cdot HgINH_2$.

Hg^{197}: ISOMERS WITH HALF-LIVES OF 23 HOURS AND 64 HOURS

When mercury was first bombarded with fast neutrons from the Be+D reaction, the decay curve of the mercury fraction was a composite of three half-lives, the shortest one being about 45 minutes, the longest one about 50 days. The intermediate half-life, however, varied between 25 and 45 hours, depending upon the thickness of the sample and that of the window of the measuring instrument. Absorption measurements with aluminum absorbers showed the presence of very soft electrons belonging to this activity; but since the 50-day activity was present in rather high intensity, the properties of the intermediate period could not be studied very well. But a similar mercury activity had been found[6] as a product of the deuteron bombardment of gold; and since gold has only one

[9] A. A. Noyes and W. C. Bray, *A System of Qualitative Analysis for the Rare Elements* (Macmillan Company, New York, 1927), pp. 113–116.

stable isotope, it was decided to bombard gold with 14-Mev deuterons and to study the mercury activities produced, and then to investigate whether they were identical with any of those found in neutron bombardments of mercury.

The half-life of the mercury fraction separated from the gold was again found to vary between about 30 and 45 hours, when different samples and different instruments were used. After the chemical identity had been definitely proved by repeated distillations, a thin sample was prepared by amalgamating a silver surface with the active mercury, and its decay was carefully followed on a Lauritsen electroscope. It was then found that the decay curve (when plotted on semilog paper) was not a straight line, but showed a slight curvature, the apparent half-life varying from 26 hours, a few hours after bombardment, to about 48 hours, after two weeks. This suggested immediately that there were two activities of rather similar half-lives. After following the decay of one sample for over a month on a Geiger-Mueller counter with a thin mica window, the decay curve could be resolved into two straight lines, corresponding to half-lives of 23 and 64 hours, respectively (Fig. 1). Aluminum absorption curves taken at various intervals

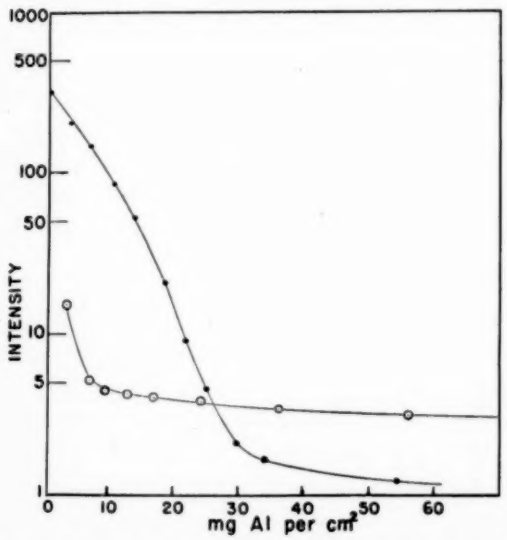

FIG. 2. Absorption in aluminum of the radiation from Hg^{197} produced by the bombardment of gold with 14-Mev deuterons. Dots indicate points taken two days after bombardment (mixture of 23-hour and 64-hour activities). Circles indicate points taken 15 days after bombardment (practically pure 64-hour activity). Two different aliquots were used for the two absorption curves.

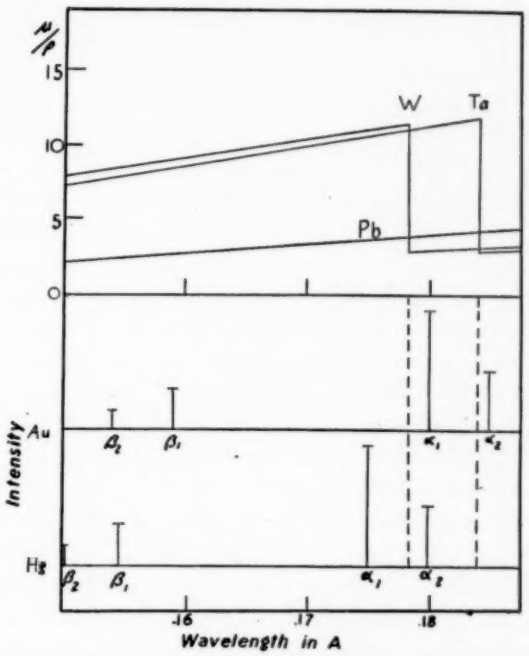

FIG. 3. The bottom part of the figure shows the K-emission lines of mercury and gold, with their relative intensities. The top part shows the mass absorption coefficients μ/ρ of tungsten, tantalum, and lead in the same wave-length region.

also showed clearly the presence of two different activities. Figure 2 shows absorption curves taken 2 days and 15 days, respectively, after bombardment. At the time the second curve was taken, the decay curve showed that the 23-hour period had practically completely disappeared. The end points of the absorption curves indicate maximum energies of about 200 and 90 kev respectively for the 23-hour and 64-hour activities. Dr. A. C. Helmholz[10] investigated the internal conversion electrons from some of our samples in his magnetic spectrograph and found K, L, and M lines from two gamma-rays decaying with a 25-hour half-life and L and M lines from a gamma-ray decaying with a 64-hour half-life. Valley[11] has also reported electron lines from mercury formed by deuteron bombardment of gold.

The only two mercury isotopes that can be formed in the deuteron bombardment of Au^{197} (if we assume the ordinary nuclear reactions) are Hg^{197} and Hg^{198}, the former by a d-$2n$, the latter by a d-n reaction. The fact that, in the

[10] A. C. Helmholz, Phys. Rev. **61**, 204 (1942).
[11] G. E. Valley, Phys. Rev. **60**, 167 (1941).

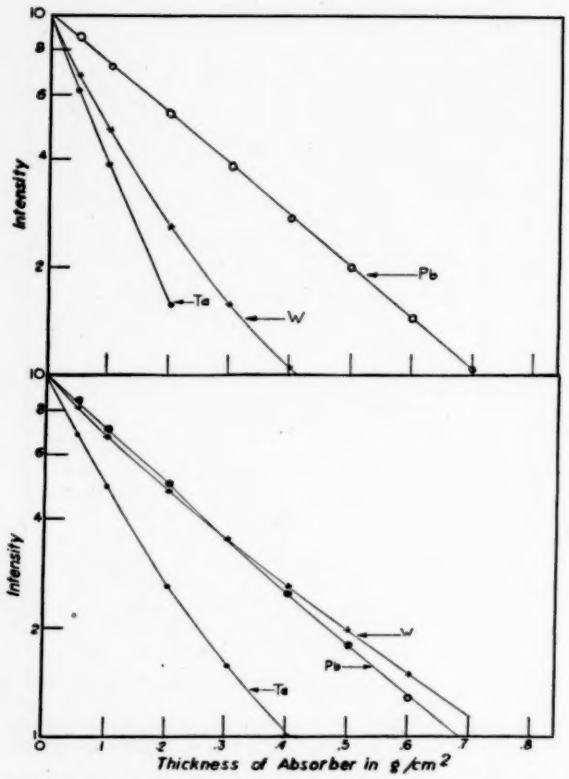

FIG. 4. Calculated curves for the absorption of the K radiations of mercury (upper curve) and gold (lower curve) in tungsten, tantalum, and lead.

bombardment of gold with 8-Mev deuterons from the 37-inch Berkeley cyclotron, we obtained an exceedingly small yield of mercury activity suggested that both periods were due to Hg^{197}, because at that bombardment energy the probability of a d-$2n$ reaction would be expected to be much lower than that of a d-n reaction. The possibility that one of the two activities was due to an excited state of Au^{197} or to Au^{198} growing out of active Hg^{197} or Hg^{198*} was eliminated: Chemical separations of gold and mercury were carried out by distillation at various intervals after bombardment, and in all cases the total activity stayed in the mercury fraction.

The final assignment of the two activities was made by means of critical absorption measurements of the x-rays emitted. The method was based on the following reasoning: Hg^{197} would be expected to decay by K-electron capture[12] to Au^{197}. The product of the disintegration would, therefore, be a gold atom with a vacancy in the K shell. Hence, outer electrons would be expected to cascade down to the K shell, with the emission of gold x-rays. An isomeric transition in mercury, on the other hand (e.g., from Hg^{198*} to Hg^{198}, or possibly from an upper to a lower level in Hg^{197}), would leave a mercury atom with a missing K electron as the reaction product; hence it would be followed by the emission of mercury x-rays. Thus, it could be hoped that an investigation of the x-rays emitted by the two mercury isotopes would throw some light on their modes of disintegration.

The four prominent K lines in the x-ray emission spectra of elements in the region of gold are (in the order of decreasing intensity): α_1, α_2, β_1, β_2. The wave-lengths and relative intensities of these lines are shown for mercury and gold in Fig. 3. On the same figure are shown the x-ray absorption spectra of tungsten, tantalum, and lead (the mass absorption coefficient

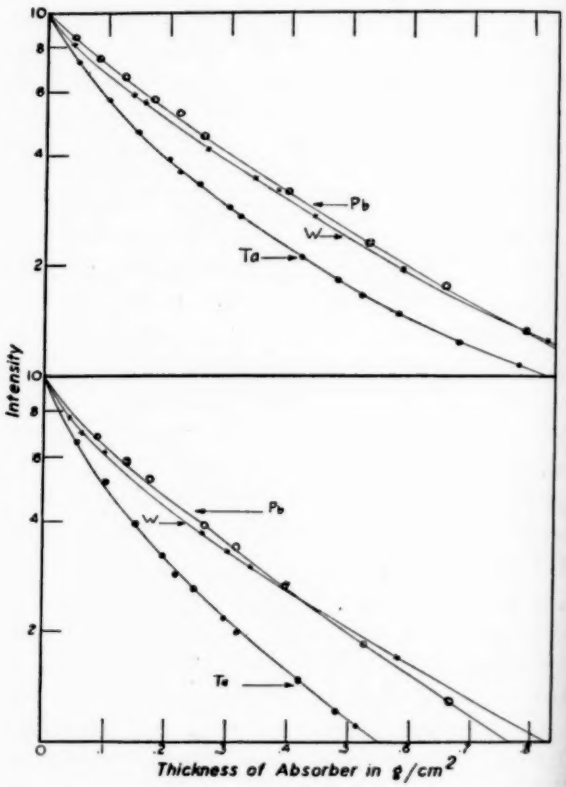

FIG. 5. Absorption in tungsten, tantalum, and lead of the x-rays emitted by Hg^{197}. The upper set of curves was taken 2 to 4 hours after the bombardment of gold with deuterons, the lower set of curves two weeks later.

[12] The alternative process of positron emission is very rare in the region of the heaviest elements. Furthermore, we were unable to detect experimentally any positrons in the mercury activities considered.

μ/ρ is plotted against wave-length). It is seen that the absorption edges of tungsten and tantalum fall in the region of the K-emission lines of gold and mercury. The data represented in Fig. 3 are taken from the book by Compton and Allison.[13] Absorption curves for the K x-rays of gold and mercury in tantalum, tungsten, and lead were calculated from these data and are shown in Fig. 4. If the original intensity of radiation is I_0, the intensity I which is transmitted through a thickness x of an absorber of density ρ is given by the formula $I = I_0 e^{-\mu x} = I_0 \cdot e^{-(\mu/\rho)\cdot(x\rho)}$. μ is the fractional reduction of intensity per cm of path length, and μ/ρ is called the mass absorption coefficient. Thus, if μ/ρ is known for a given wave-length (say, that of the $K\alpha_1$ radiation of gold) and a given absorber (say, tantalum), the intensity transmitted can be calculated as a function of the product of thickness and density ($x\rho$, expressed in g/cm^2). In this way the absorption curves in Fig. 4 were calculated. (They show the integrated effect of the 4 principal K-emission lines.)

Actual absorption curves of the x-rays emitted by the mercury fraction of the gold+deuteron bombardment were taken with tungsten, tantalum, and lead absorbers, at frequent intervals from the time of the chemical isolation of the mercury until two weeks later. The measurements were made with a freon-filled ionization chamber connected to a vacuum-tube electrometer with a sensitive galvanometer. In all the measurements an aluminum absorber of sufficient thickness to cut out all the electrons emitted was interposed between the sample and the window of the ionization chamber. This absorber also cut out the L radiations of gold and mercury, which are very much softer than the K radiations. Lead and tantalum foils were available in thicknesses from 0.001 inch up. But thin tungsten absorbers had to be made from tungstic oxide (WO_3). Suspensions of weighed amounts of WO_3 in an acetone solution of "Duco cement" were filtered quantitatively through sintered-glass funnels covered with filter paper. The dried precipitates were quite uniform and adhered well to the paper. The absorption of x-rays by the paper and by the oxygen in the WO_3 is negligible.

Two of the sets of experimental absorption curves are reproduced in Fig. 5. One was taken two hours after bombardment, the other one two weeks later. The two sets of curves are very similar (as are all the sets taken at various times) and both agree rather well with the calculated absorption curves for gold x-rays while they are very different from the calculated curves for mercury x-rays (Fig. 4). The deviations from the theoretically expected curves are due to the fact that both the 23-hour and the 64-hour periods have groups of soft gamma-rays associated with them. Although an attempt has been made to correct for the absorption of the gamma-rays, this could not be done quite satisfactorily, because of the complexity of the gamma-ray spectra and, in the later measurements, because of the weak activity of the samples.

The results of the x-ray absorption measurements leave no doubt that both the 23-hour and the 64-hour activities emit the K radiations of gold, and, therefore, that they decay by K-electron capture to form gold isotopes. The rather improbable case that one of them is an excited state of Hg^{198} and decays by K-electron capture to Au^{198} (which itself decays with a 2.7-day half-life to stable Hg^{198}) is completely ruled out by the fact that no growth of gold activity was observed. Thus, both periods can be assigned to Hg^{197}. Apparently the two isomeric states decay independently to Au^{197}, both by K-electron capture.

It should be pointed out here that Krishnan[6,7] has also used the critical absorption of x-rays to assign what he calls the 32-hour mercury activity, produced by deuteron bombardment of gold (probably a mixture of the 23-hour and 64-hour periods). His data agree with those of the present authors; but he merely compared the absorption curves of the x-rays from the "32-hour" mercury activity in tungsten, tantalum, and lead with those obtained with the x-rays emitted by the 43-minute mercury activity (cf. below). Finding the two sets of curves very different and having assigned the 43-minute period to Hg^{197} because it is produced by fast and not by slow neutrons in mercury, he concluded that the 43-minute activity emitted gold x-rays;

[13] A. H. Compton and S. K. Allison, *X-Rays in Theory and Experiment* (D. Van Nostrand Company, New York, 1935).

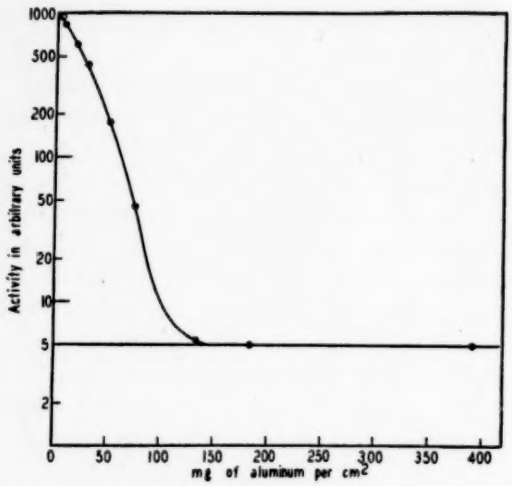

FIG. 6. Absorption in aluminum of the radiation from the 43-minute mercury activity.

the 32-hour activity mercury x-rays. He therefore assigned the latter to Hg^{198*}.

X-ray absorption curves were also taken on neutron-bombarded mercury samples, and the curves obtained after the 43-minute period had decayed completely agree very well with those taken on the mercury samples extracted from deuteron-bombarded gold. Thus it is probable that the complex activities at intermediate half-lives produced by neutron bombardment of mercury as mentioned at the beginning of this section are identical with the 23-hour and 64-hour periods produced from gold with deuterons. Apparently both slow and fast neutrons produce these periods in mercury, slow neutrons, however, in low intensity.

THE 43-MINUTE ACTIVITY

In fast neutron bombardments of mercury, a 43-minute mercury period is strongly induced. Slow neutron bombardments yield very little, if any, of this activity. The radiations associated with this period consist of conversion electrons, soft gamma-rays and x-rays.

Absorption measurements with aluminum absorbers (Fig. 6) suggest the presence of a line of electrons, rather than a beta-ray spectrum. The range of the electrons is about 140 mg/cm² of aluminum, corresponding to an energy of about 460 kev, according to the data of Varder and Eddy.[14]

[14] E. Rutherford, J. Chadwick, and C. D. Ellis, *Radiations from Radioactive Substances* (Cambridge University Press, 1930), p. 422.

The x-rays emitted by the 43-minute activity were investigated by the critical absorption method described in the preceding section. After the proper corrections were made for the rather intense gamma-rays of the 43-minute activity and for the presence of the 23-hour and 64-hour periods, the absorption curves in lead, tungsten, and tantalum agreed reasonably well with those calculated for the K radiation of mercury, as is seen from the set of experimental absorption curves reproduced in Fig. 7. Hence, the 43-minute period is associated with an isomeric transition in mercury.

To decide on the assignment of this activity, several additional experiments were performed. A careful search for the 43-minute period was made in the mercury fraction obtained from the bombardment of gold with 14-Mev deuterons. But no trace of this period was found. Hence it cannot be due to Hg^{197} or Hg^{198}. Very likely, it is an isomer of one of the stable isotopes of mercury (their mass numbers are: 196, 198, 199, 200, 201, 202, 204). The large yield of 43-minute activity from fast neutron bombardment of mercury makes the assignment to Hg^{196*} quite unreasonable, because Hg^{196} has an abundance of only 0.15 percent. If, on the other hand, the 43-minute period is associated with an isomeric state in one of the isotopes 199, 200, 201, or 202, the very low yield from slow neutron bombardment of mercury is difficult to explain, since any one of the isotopes named would be expected to be formed by an n-γ reaction from the next lower stable isotope. The best assignment, then, would seem to be Hg^{204*}, formed from stable Hg^{204} by excitation either with fast neutrons or with

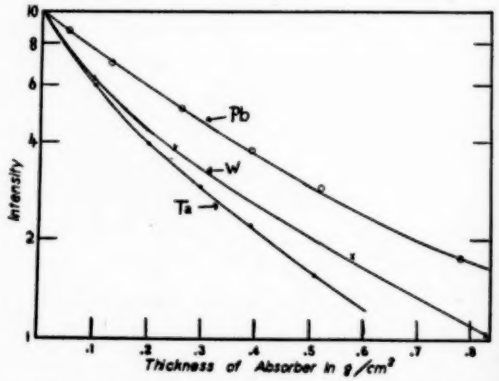

FIG. 7. Absorption in tungsten, tantalum, and lead of the x-rays emitted by the 43-minute mercury activity.

deuterons.[6] To test this assignment, it was thought advisable to bombard lead with fast neutrons, in the hope of forming Hg^{204*} from Pb^{207} by an n-α reaction. Spectroscopically pure lead was bombarded for several hours with the neutrons formed in the bombardment of beryllium with 14-Mev deuterons. The lead was amalgamated after bombardment and the mercury distilled off in vacuum. In each of two bombardments the mercury activity obtained was too small to be measured with any accuracy (0 ± 10 counts per minute on a Geiger-Mueller counter). It is to be remembered, however, that the neutrons used have an energy of about 18 Mev and that this may be below or near the threshold of the n-α reaction for an element as heavy as lead. The evidence against the assignment of the 43-minute period to Hg^{204*} may therefore not be conclusive.

Sherr, Bainbridge, and Anderson[8] have discussed the assignment of the 43-minute mercury activity. These authors produced that activity by fast neutron bombardment of mercury, and their results are in agreement with the ones discussed above. However, they have also obtained a 43-minute activity (chemically not identified) from the bombardment of platinum with alpha-particles. The properties of this activity are very similar to those of the 43-minute mercury. If the two are identical, then the assignment is limited to Hg^{199*} or Hg^{201*}, and the abnormally low yield with slow neutrons on mercury remains unexplained.

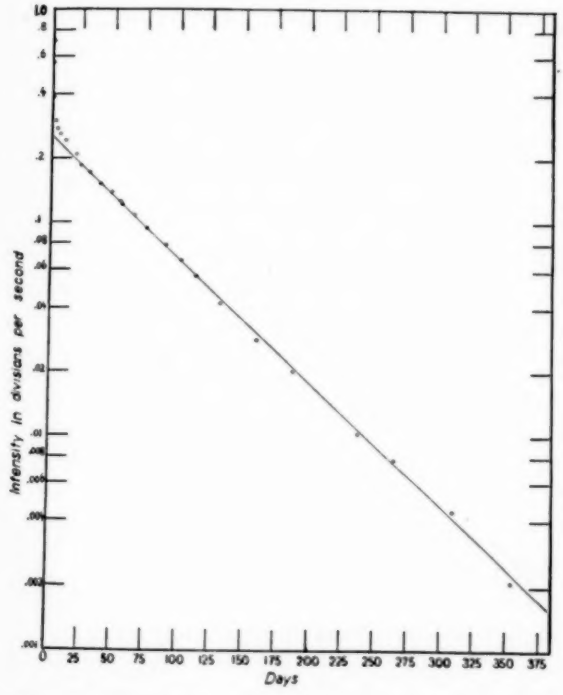

FIG. 8. Decay of the long-lived mercury activity produced by slow neutron bombardment of mercury. Half-life is 51.5 ± 1.5 days.

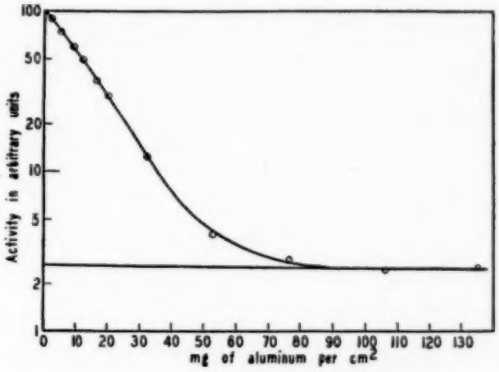

FIG. 9. Absorption in aluminum of the radiation from the 51.5-day mercury activity.

THE 51.5-DAY ACTIVITY

Krishnan and Nahum[6,7] mention that they have obtained a period of 60 days in their deuteron bombardments of mercury, but have not investigated this activity. Sherr, Bainbridge, and Anderson[8] observed a 50-day period in neutron bombardments of mercury, but did not study this activity. We have observed a period of similar half-life in the bombardment of mercury with slow or fast neutrons. Chemical separations proved this period to be associated with a mercury isotope. One sample was followed for one year (about seven half-lives) and found to decay with a half-life of 51.5 ± 1.5 days (Fig. 8).

This activity emits beta- and gamma-rays. The sign of the beta-rays was investigated by means of a magnetic field, in conjunction with a Geiger-Mueller counter. No positrons could be detected. A search for annihilation radiation also failed. The range of the beta-rays in aluminum (Fig. 9) is about 90 mg/cm², corresponding to a maximum energy of about 460 kev. The gamma-rays have a half-thickness of 1.25 g/cm² in lead corresponding[15] to an energy of 300 kev. No x-rays are emitted by this activity.

[15] W. Gentner, Physik. Zeits. **38**, 836 (1937).

The assignment of the 51.5-day activity is probably limited to Hg^{203} and Hg^{205}, since it decays by the emission of negative beta-particles to thallium. Tl^{203} and Tl^{205} are the only stable thallium isotopes, and no active thallium has been found to grow from the 51.5-day mercury. Since both slow and fast neutrons produce the activity, the best assignment is Hg^{203} which can be produced by n-γ reaction from Hg^{202}, and by n-$2n$ reaction from Hg^{204}.

THE 5-MINUTE ACTIVITY

In short slow neutron bombardments of mercury, an activity with a half-life of about 5 minutes was produced. No chemical identification of this activity was attempted. Its yield at saturation was about one-tenth of that of the 43-minute activity, which has itself an abnormally low yield in slow neutron bombardments. It cannot, therefore, be decided whether or not this period is due to an impurity. It may, however, be identical with the 5.5-minute mercury, reported by Krishnan and Nahum,[6] and assigned by them to Hg^{205}. We have not studied the radiations emitted by the 5-minute activity.

It is a pleasure to express our gratitude to Professor E. O. Lawrence for his interest and to the staff of the Radiation Laboratory for their cooperation. We are indebted to Professor G. T. Seaborg, Dr. J. W. Kennedy, and Dr. E. G. Segrè for numerous stimulating discussions and suggestions. The financial support of the Research Corporation and the Rockefeller Foundation is gratefully acknowledged.

PHYSICAL REVIEW VOLUME 63, NUMBERS 7 AND 8 APRIL 1 AND 15, 1943

Further Tests of the Atom-Annihilation Hypothesis as to the Origin of the Cosmic Rays

R. A. MILLIKAN, H. VICTOR NEHER, AND WILLIAM H. PICKERING
California Institute of Technology, Pasadena, California

(Received January 28, 1943)

1. Tests in Mexico. The authors had predicted that since the hypothetical silicon-annihilation rays should have enough energy (13.2 Bev) to get vertically through the earth's magnetic field at the equator in Peru, though not in India, there should be found, both at sea level and at all altitudes in the Americas, when vertically incoming rays alone are under test, a very long plateau of uniform cosmic-ray intensities extending north from Mollendo, Peru to about the latitude of Victoria, Mexico (mag. lat. 32.8°). There the strong band due to oxygen annihilation rays (7.5 Bev) should first appear, to be followed in going still further north when the latitude of 40° N magnetic had been reached, by the full entrance of the nitrogen annihilation band (6.5 Bev). The experimental findings were in accord with these predictions. 2. Tests in the United States. In going from Pasadena (mag. lat. 40.7° to St. George, Utah, but 4.1° (280 miles) nearer to the N magnetic pole than Pasadena, the carbon-annihilation band (5.6 Bev) was expected to appear, to be followed by a flat plateau clear up to latitude 54° N magnetic, when helium annihilation rays (1.88 Bev) were expected to appear. A balloon flight at St. George (mag. lat. 44.8°) and another at Pocatello, Idaho (mag. lat. 51°) yielded preliminary results in harmony with these predictions. 3. Evidence that the act of atom-annihilation actually transforms the rest mass energy of an atom into an electron pair. The flat plateau between St. George and Pocatello (mag. lat. 51°) corresponding to the absence of abundant atoms of atomic weight between that of carbon and that of helium, and the definite appearance of a new band between Omaha (mag. lat. 51.3°) and Bismarck (mag. lat. 56°) constitute new and strong evidence for the transformability of the complete rest mass energy of an atom into an electron pair.

I. THE FUNDAMENTALS OF THE HYPOTHESIS

IN a former paper[1] we have presented what may be called the atom-annihilation hypothesis of the origin of cosmic rays and the preliminary evidence found for its utility. This hypothesis assumes that an atom out in interstellar space has the capacity not possessed by an atom in the stars or in any other region in which it is continuously subjected to bombardment from neighboring atoms, of occasionally transforming the whole of its rest mass energy into a charged-particle pair which for the present

[1] Millikan, Neher, and Pickering, Phys. Rev. **61**, 397–413 (1942).

may be called an "electron pair." The kinetic energy of such an electron pair can then easily be computed from the known rest mass of the atom m with the aid of the equation $E=mc^2$, c denoting the velocity of light and E energy in ergs.

Bowen and Wise have recently made the discovery[2] that in ring nebulae (and, therefore, in interstellar space) there are but five abundant atoms (save hydrogen, which could yield for the present purposes no observable effects anyway), namely, He, C, N, O, Si, the last four of which are, according to Bowen, about equally abundant and the first about ten times their abundance, no other atom having as much as a tenth of the abundance of any of these five.

In view of this discovery the foregoing hypothesis requires that the only "*field-sensitive*" cosmic rays that can get into the earth's atmosphere so as to be observable in balloon flights would have to be the annihilation rays of one or another of these five atoms.

To understand fully the reasons for this conclusion it is also necessary to be familiar with the Lemaitre-Vallarta analysis of the effects of the earth's magnetic field on incoming electrons, an analysis which, when combined with Millikan and Neher's observations on the longitude effect in cosmic rays, shows that it requires vertically incoming electrons of an energy of 17 Bev to get through the earth's magnetic field at the magnetic equator in southern India, while it requires not more than 13 Bev to get through at the magnetic equator in the neighborhood of Peru. This difference is due to the fact that the earth's magnetic field is weaker on the Peru side of the earth than on the India side.

II. WHY EVIDENCE FOR THE LATITUDE OF ENTRANCE OF SILICON-ANNIHILATION RAYS HAD TO BE SOUGHT IN INDIA

From the mass of the atom of silicon, the silicon-annihilation rays are easily computed to have an energy of 13.2 Bev. Also from the Lemaitre-Vallarta curves one can compute that the magnetic latitude in India at which vertically incoming silicon-annihilation rays could first break through the earth's magnetic field as one moves northward from say Madura, which is on the magnetic equator, is about 20° N magnetic. This is less than 200 miles north of Agra, where is located the most important meteorological observing station of the British Indian Meteorological Service. Agra therefore possessed special advantages as a flight point.

However, vertically incoming silicon-annihilation rays, though they could not get in at Agra should be found in full strength, for example, at Peshawar (mag. lat. 25°), the northernmost meteorological observing station available in India, for we had computed that the energy necessary to get through there should be but 12.4 Bev.

But since there are no abundant atoms of rest mass energy between 17 Bev and 13.2 Bev, according to the present hypothesis there could be no new cosmic rays entering the earth vertically between Madura and Agra, where we computed that the energy necessary to get through was 15.4 Bev.

Further, since there are no abundant elements of rest mass energy between 13.2 Bev and 7.5 Bev —the latter being the rest mass energy of the oxygen atom—there should be found no new vertically incoming cosmic rays other than those of silicon anywhere in any latitude south of about 32° or 33° N magnetic, where the oxygen annihilation rays ought first to begin to break through the blocking effect of the earth's magnetic field.

To test experimentally the requirements of this hypothesis as to the silicon annihilation rays it was clearly necessary, then, to go to India and measure *the total vertical incoming cosmic-ray energy at or near the magnetic equator* and then to make similar measurements both at a latitude just a little south of the computed latitude of first entrance of the silicon annihilation rays and, second, at a latitude definitely north of that of first entrance of silicon rays. These considerations, supplemented by the local conveniences for observing, dictated the choice of Bangalore (mag. lat. 3° N), Agra (mag. lat. 17.3° N), and Peshawar (mag. lat. 25° N) as the three best locations in India for measuring by high balloon flights the total incoming cosmic-ray energy.

The predicted flat plateau of vertically incoming cosmic-ray energies between the magnetic

[2] I. S. Bowen and A. B. Wise, Bull. Lick Observatory 19, 1 (1939).

equator and Agra and the definitely predicted entrance between Agra and Peshawar of a new band corresponding to silicon annihilation rays could, of course, be tested only when vertically arranged coincidence counters were used as the measuring instrument in high flights, since it was the energies of vertically incoming rays that were the subjects of the foregoing computations.

When the measuring instruments used are either single counters or electroscopes—instruments which respond to rays coming in from all directions, the Lemaitre-Vallarta curves[3] show clearly that the flat plateau for vertically incoming rays between the equator and Agra should be replaced by an incoming cosmic-ray energy which should increase continuously with increasing latitude. The measurements made in India by all three of these methods, double coincidence counters, electroscopes and single counters, showed in every case the behavior predicted by the hypothesis. So far, then, as the observations in India went (there were made between November 30, 1939 and February 10, 1940 over forty successful flights) the predictions of the hypothesis were fully satisfied.

III. PREDICTION OF A VERY LONG PLATEAU OF CONSTANT VERTICALLY INCOMING COSMIC-RAY INTENSITY FROM SOUTHERN PERU UP TO MIDDLE MEXICO

There was also presented in the former reports upon this work such evidence as a careful study of earlier observations made by some of the authors offered in support of the atom-annihilation hypothesis. All of these data, however, had been taken with electroscopes rather than with vertical coincidence counters, and this made the interpretation somewhat uncertain.

For example, since, on the Peru side of the earth vertically incoming silicon rays can get through the earth's magnetic field at the equator, and since there should be no other rays of lower energy than those of silicon (13.2 Bev) to get to earth until one reaches the latitude of about 33° N, where the vertically incoming oxygen annihilation rays (7.5 Bev) should be able to get to earth, *the hypothesis clearly predicted a long flat plateau of unchanging vertically incoming cosmic-ray energy extending from the magnetic equator near Mollendo, Peru, clear up to about the latitude of Victoria, Mexico* (mag. lat. 32.8° N).

There had been found some evidences for the existence of this plateau in flights made in 1932 in both Panama and Peru in which *electroscopes* had been taken up to altitudes of 22,000 feet without showing any differences in their readings whether the flights were made in Peru on the magnetic equator or in Panama (mag. lat. 20° N). This was entirely different from the results obtained with electroscopes in India between the same latitudes. Also, in sea-level readings made in '32, '33, and '34 in voyages from Mollendo to Los Angeles there had been found in electroscope readings no change until a magnetic latitude of about 21° N was reached, at which point the readings began to rise and continued to do so until Los Angeles was reached. It was accordingly predicted that if one had taken, or could take, these readings with vertical coincidence counters instead of with electroscopes, there would be no increase at all in going from the magnetic equator in Peru clear up to the magnetic latitude of about 33° N (Victoria in Mexico).

The foregoing prediction made it possible to obtain a very crucial test for the hypothesis, especially since its critics were willing to concede that if a flat plateau was found on the Peru-Mexico side of the earth between magnetic 0° and 33° N, it would be convincing evidence in its favor. They were not so sure that the flat plateau which had already been found in India between magnetic latitudes 3° and 17.3° was entirely convincing evidence, since in any case the *rate* of change in incoming energy would be expected to be small near the equator, even for such *continuous* laws of distribution of incoming energy with latitude as had been suggested by others.

IV. NEW EQUIPMENT FOR MAKING CRUCIAL TESTS IN MEXICO

In view, then, of the crucial character of observational work in Mexico, in spite of the absorption of all the authors in war duties it was decided to be essential to take a month off in December, 1941, and to try to make in Mexico observations similar to those made in India

[3] See curve 1, Fig. 2 in Phys. Rev. **61**, 401 (1942); or Fig. 10, Phys. Rev. **50**, 503 (1936).

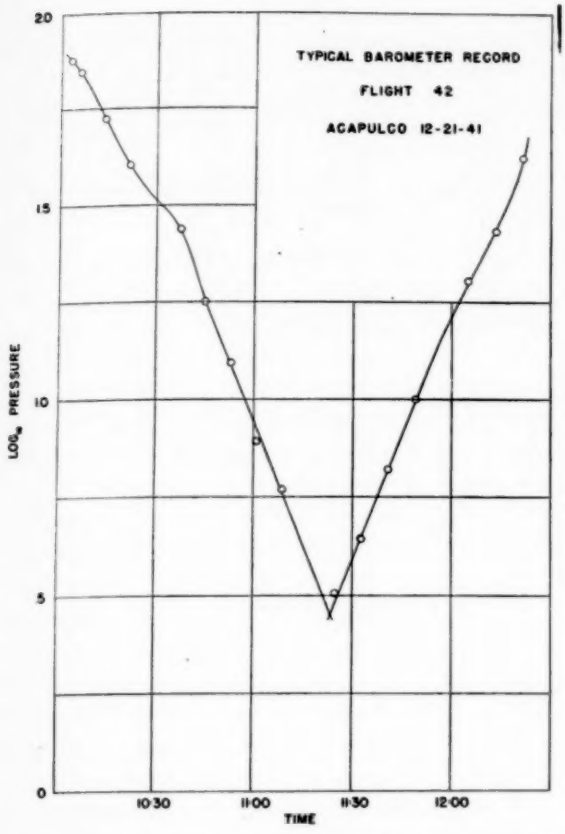

FIG. 1. Shows method of determining the pressure in mm of mercury at any instant during the flight, also the time and altitude at which one of the two supporting balloons burst.

between November, 1939 and February, 1940, save that the Mexico experiments were to be made only on vertically incoming cosmic-ray energies and hence not with electroscopes or single counters.

In order, however, to render the Mexico tests independent of such flight facilities as are usually available only in well-equipped meteorological stations, and in order to be in position to change the desired latitudes for the flights independently of the locations of such stations, in November, 1941 there was fitted out a covered truck as a travelling cosmic-ray laboratory. This left Pasadena on December 2nd and was driven via Laredo, Texas, from Pasadena to the most southerly accessible point in Mexico, *viz.*, Acapulco, and then back to Pasadena. Enroute careful measurements were made on vertically incoming cosmic-ray energies by balloon flights at or near Acapulco, Mexico (mag. lat. 25.8° N), Valles, Mexico (mag. lat. 31.15° N), Victoria, Mexico (mag. lat. 32.8° N), and Pasadena, U. S. A. (mag. lat. 40.7° N).

Also, careful measurements were made with vertical coincidence counters in from four- to ten-hour runs on the "ground rate of cosmic-ray counts" at all these places, and also at San Antonio, Laredo, and Monterrey (Mexico). This series of ground measurements was taken first because they were needed as reference rates at all the places at which balloon flights were to be made, but also because the ground rates, though representing but a trifling part of the vertically incoming energy ought clearly to present a correct reflection of *the variation with latitude* of the whole vertically incoming cosmic-ray energy such as was to be measured in the balloon flights.

The technique of measuring the vertically incoming energy was the same as that used in India, save that one of the authors, Pickering, introduced the improvement of inserting the "scaling mechanism" at the receiving end instead of at the transmitting end, which had of course to be taken up with the balloon.

This scaling mechanism provides that only every second, or every fourth, or eighth, or sixteenth, or thirty-second cosmic-ray shot is registered on the recording tape. It will be described in *The Review of Scientific Instruments.*

This arrangement, though operating on 1.7 meter waves is sensitive to the waves emitted by automobile spark plugs—a condition which made it necessary to choose observing locations some miles distant from paved highways or other lines of automobile travel. This is not as difficult a condition to fulfill in Mexico as in the United States.

V. THE OBSERVING TECHNIQUES

The standard procedure followed in all flights at a particular location is as follows: On the day or night preceding the flight the coincidence counter-pair to be used in the flight is carefully compared with a standard counter-pair by setting the two up side by side in the truck laboratory, each being provided with a mechanical counter which registers the number of shots traversing each counter-set throughout say a six-hour run. This establishes the standardized

TABLE I. Summary of ground level counts with standard set.

	Counts	Time in minutes	Rate per minute	Paulin bar. reading	Corrected rate	Mean rate	
Acapulco (mag. lat. 25.8°)	5004	208	24.0	29.91	24.9	90	90.5
Valles (mag. lat. 31.15°)	6005	246	24.4	29.92	25.3	91	
Victoria (mag. lat. 32.8°) Dec. 10	13585	504	27.0	29.03	25.9	94	94
Victoria (mag. lat. 32.8°) Dec. 28	8086	304	26.6	29.30	26.1	94	
Monterrey (mag. lat. 34.6°)	5797	197	29.5	28.42	26.5	96	95.3
Laredo (mag. lat. 36.65°)	16408	633	25.9	29.70	26.4	95	
San Antonio (mag. lat. 38.5°)	6747	239	28.2	29.25	27.6	100	98
Junction, Texas (mag. lat. 38.5°)	11171	370	30.2	28.17	26.6	96	
Pasadena (mag. lat. 40.7°)	29736	1073	27.7	29.50	27.7	100	100

Corrected rates to Paulin reading of 29.50.
Correction 0.9% per 0.1".

ground-level-rate of cosmic-ray bombardment at the given locality.

During the same period another observer has calibrated the aneroid to be carried up in the flight. This is done by having in the truck-laboratory an air pump and a closed chamber with glass top and sides in which the aneroid can be placed and the pressure reduced by any desired number of steps as read off on a mercury barometer column, also connected into the variable pressure chamber. In this way the movements of the aneroid arm as recorded in the immediately succeeding flight on the tape of the so-called "Galcit" meteorograph (of the Olland type) give at once the pressure in millimeters of mercury at any instant of the flight. Indeed, the barometer readings recorded on the moving tape of the meteorograph in this artificial flight made in the truck-laboratory, just before the actual flight, with the aid of the mercury-column-barometer and the variable pressure chamber constitute exactly the same series of readings that the aneroid will record immediately thereafter when it is sent aloft. For, although the barometers used have, in fact, a very nearly negligible temperature coefficient, it has been found that in practice, by suitably covering with black paper the basket in which the instruments are sent up, the temperature inside the baskets, as read also on the tape of the Galcit meteorograph, is actually held very nearly constant throughout a flight, so that barometer errors due to stratosphere temperatures are quite fully eliminated. As in all high altitude flights, however, in spite of great care used in the calibration of the barometers, when the pressures fall to the values between ten and forty millimeters of mercury, the barometer readings introduce one of the chief sources of inaccuracy in the duplication of flight-curves.

VI. METHOD OF COMPUTING AND PLOTTING THE CURVES

In all high altitude flights the most satisfactory method of handling the barometer record as recorded on the tape is much the same as that used by Millikan and Bowen in 1922 in the first cosmic-ray flights made to altitudes requiring the use of automatic recording electroscopes in place of human observers. The procedure is as follows. After the pressures have been read off in mm of Hg from the tape-record and the barometer calibration curve obtained as above, the logs of the pressures in mm of Hg are plotted as ordinates against the times measured from the instant of release of the balloons as abscissae.

Since in a quiet atmosphere of uniform temperature the rate of ascent is practically constant, in such an ideal atmosphere the logs of the pressure plotted against time of ascent should be a straight line. In practice the curve shows some departures from linearity, especially below the stratosphere, less so in it. A very typical curve is shown in Fig. 1. In general it is found that the most consistent curves are obtained by very carefully joining the series of observed log-pressure points by straight lines, as shown in the figure. The point of intersection of the lines corresponding to ascent and descent then gives with much reliability the time of bursting of one of the balloons and the altitude at which this event occurred. Errors in drawing this time log-pressure curve are, however, responsible for no small part of the observed straggling of the

points, and such lack of duplicability, amounting to possibly five or six percent, as sometimes appears between different flights taken but a few hours apart and apparently under the same conditions.

VII. TESTING IN MEXICO OF THE PREDICTIONS OF THE HYPOTHESIS

1. The first and simplest prediction, actually made and published in April, 1941, was that if sea-level or ground observations reduced to the same level were taken with vertical coincidence counters instead of with electroscopes, the heretofore observed increase in cosmic-ray rate which sets in with electroscopes at mag. lat. 21° or 22° [see Fig. 3, Phys. Rev. **61**, 402 (1942)] would not appear until about the latitude at which oxygen annihilation rays would be expected to get vertically through the earth's magnetic field, say at mag. 33° N. Here a rapid rise should set in and be completed when the observers had moved northward, say 6° or 7°, or enough to enable both oxygen annihilation rays (7.5 Bev) and nitrogen annihilation rays (6.6 Bev) to break vertically through the earth's magnetic field. This latitude of full appearance at sea level of nitrogen rays was expected, from previous experiments in taking electroscopes south on shipboard from Los Angeles harbor, to be within a degree or so of that harbor, which is itself half a degree south of Pasadena.

No further sea-level rise was expected in going north of the latitude of entrance of the nitrogen-annihilation rays since carbon annihilation rays (of energy 5.6 Bev) were not thought able to extend their influence down as far as to sea level. Indeed, electroscopes taken on sea-level, summer, voyages had never shown any rise in going north of Pasadena.

The observed ground-level counts on this trip taken with the same standard set and corrected as indicated to reduce them to a common elevation were as shown in Table I, the accurate value at Pasadena, representing 29,736 counts (18 hours), being taken as 100. Since the readings at Acapulco, Valles, Monterrey, San Antonio, and Junction contain but from 5000 to 10,000 counts each, it is estimated that they should be assigned an uncertainty of about two percent, or twice the statistical "probable

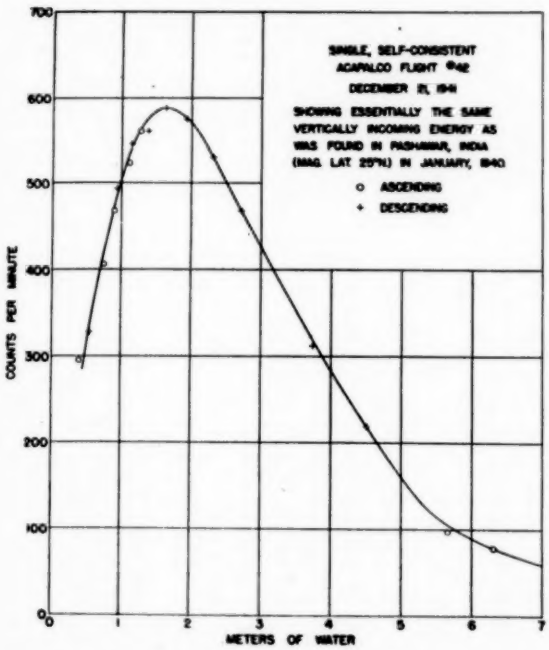

FIG. 2. Best single flight curve taken at Acapulco. Area about 5.8 percent less than the corresponding curve taken at Peshawar (see page 411 of reference 1).

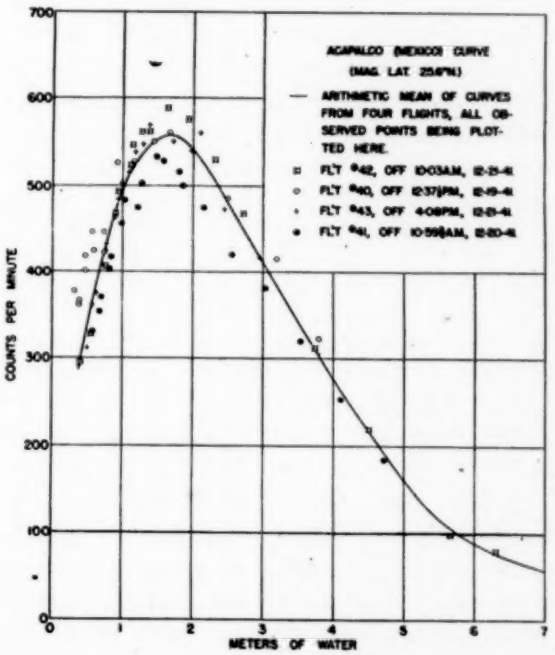

FIG. 3. Every individual observation taken in all four of the Acapulco flights is recorded in Fig. 3. The best obtainable smooth curve is drawn for each of the four flights. The final full curve shown is the arithmetic mean of these four curves.

In general, in all these curves each recorded point is the actual counting rate in a four-minute interval in that flight at the recorded mean pressure in that interval.

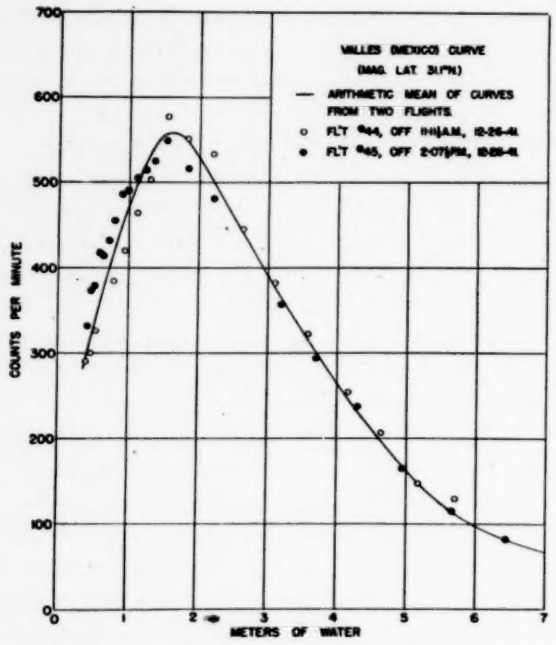

FIG. 4. The full curve is the arithmetic mean of the curves from the flights, two only, made at Valles, all observed points being recorded as in Fig. 3.

error" which for 6000 counts is about one percent. Within these limits the readings all show a satisfactory consistency though those at San Antonio and Junction show the maximum permissible divergence. Their mean is doubtless a better reflection of the condition at that latitude than is either one of the two readings. The significance of the last mean column of Table I in terms of the hypothesis is: (a) that the oxygen annihilation rays are fully in at Monterrey, about three degrees above the latitude at which their effect first began to appear, *viz.*, just a little south of Victoria (the effective angles covered by the counter-pair were 25° crosswise, 45° lengthwise); (b) that at Laredo, two degrees above Monterrey, the effects of vertically entering nitrogen rays have not begun to appear; *in other words, that there is here some evidence for the existence of a very short but possibly observable plateau between the latitudes of first entrance of vertically incoming oxygen and nitrogen annihilation rays;* (c) that nitrogen annihilation rays have *begun* to appear in the two degree interval between Laredo and San Antonio, i.e., at about mag. lat. 37°; (d) that, as in the case of oxygen, three degrees farther north, i.e., by lat. 40°, they are fully in, as the Pasadena reading at lat. 40.7° shows; (e) that, as Bowen's spectroscopic observations indicated, the incoming oxygen and nitrogen rays are very closely equal in energy, the additional percentage of counts brought in by oxygen being $95.3-90.5=4.8$ and that by nitrogen $100-95.3=4.7$.

So far, then, as vertically incoming ground-level readings are concerned, the predictions of the hypothesis are verified with unexpected completeness.

2. The second test of a prediction from the hypothesis is found in a comparison of the *total* energy coming in vertically at Peshawar, India (mag. lat. 25°) and Acapulco (mag. lat. 25.8°).

The hypothesis requires that the vertically incoming rays measurable at both places be simply silicon-annihilation rays. They should, therefore, be of the same total energy unless the intensity of these rays had changed in the two-year interval between the times of measurement at these two widely different localities.

On the other hand, any kind of a continuous distribution in the energy of the vertically

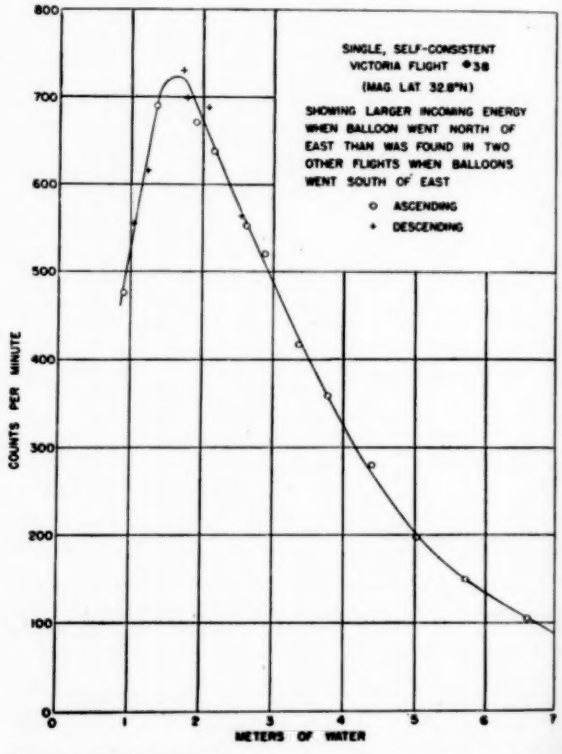
SINGLE, SELF-CONSISTENT
VICTORIA FLIGHT #38
(MAG. LAT. 32.8°N)
SHOWING LARGER INCOMING ENERGY WHEN BALLOON WENT NORTH OF EAST THAN WAS FOUND IN TWO OTHER FLIGHTS WHEN BALLOONS WENT SOUTH OF EAST
○ ASCENDING
+ DESCENDING
COUNTS PER MINUTE
METERS OF WATER

FIG. 5. Flight showing largest energy-area of any of the three flights made at Victoria. In this flight the balloon went north of east.

incoming rays requires that the energy coming in at Acapulco be larger than that at Peshawar, and that for two reasons: First, Acapulco is 0.8° farther north than is Peshawar, and hence should let through more rays for this reason alone. But, second, the earth's retarding magnetic field is in fact notably weaker at Acapulco than at Peshawar, so that, with any *continuous* distribution of incoming energies, more rays should have the energy to get through at the same latitude in the Americas than in Asia. The hypothesis in question denies the possibility of either of these effects.

Five different flights were made in Acapulco to test this point, four of them being reasonably successful. The fifth was not usable. The best of these flights (Fig. 2) gave within 6 percent the same vertical cosmic-ray energy as that found in the observations taken in Peshawar two years earlier. The mean in Acapulco, however (see Fig. 3), was 8.3 percent lower, not higher, than that in Peshawar. This result, then, is definitely

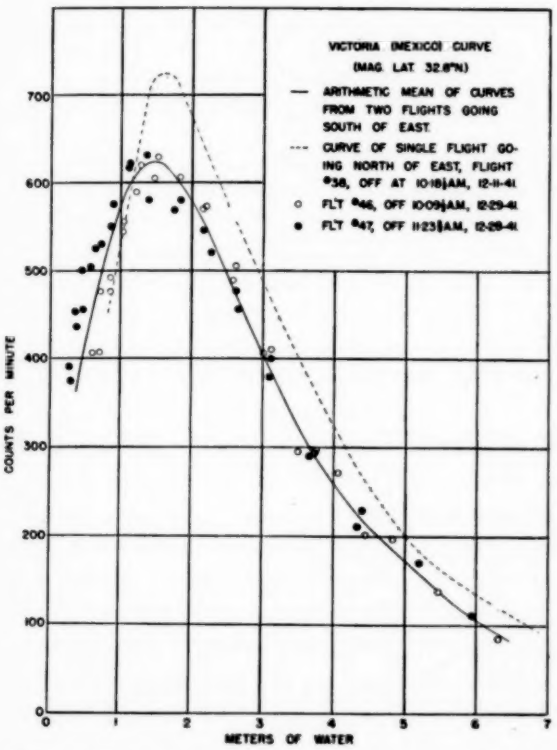
VICTORIA (MEXICO) CURVE
(MAG. LAT. 32.8°N)
— ARITHMETIC MEAN OF CURVES FROM TWO FLIGHTS GOING SOUTH OF EAST.
--- CURVE OF SINGLE FLIGHT GOING NORTH OF EAST, FLIGHT #38, OFF AT 10·18½AM, 12-11-41
○ FLT #46, OFF 10·09½AM, 12-29-41
● FLT #47, OFF 11·23½AM, 12-29-41
COUNTS PER MINUTE
METERS OF WATER

FIG. 6. The full curve is the mean of two flights at Victoria when the balloons went south of East, the broken curve the single flight in which the balloons went north of east. Therefore lat. of Victoria, mag. 32.8° N is thought to be very close to the latitude of first entrance of oxygen annihilation rays.

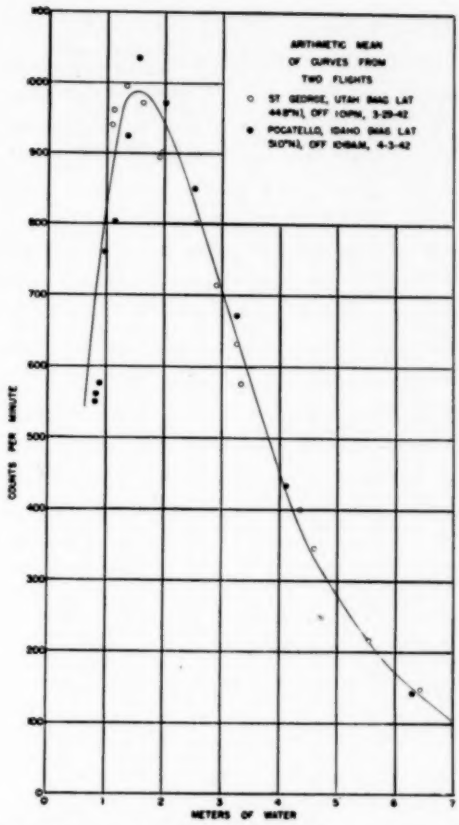
ARITHMETIC MEAN OF CURVES FROM TWO FLIGHTS
○ ST. GEORGE, UTAH (MAG. LAT. 44.8°N), OFF 1·04PM, 3-29-42
● POCATELLO, IDAHO (MAG. LAT. 51.0°N), OFF 10·18AM, 4-3-42
COUNTS PER MINUTE
METERS OF WATER

FIG. 7. Shows that there is practically no new energy entering vertically in the long latitude stretch between St. George and Pocatello, although there is clear evidence of the entrance of carbon annihilation rays between Pasadena and St. George (Utah).

inconsistent with the continuous energy distribution hypothesis unless a very considerable reduction in incoming cosmic-ray energy be assumed to have taken place since January, 1940, when the measurements at Peshawar were made. On the other hand, a much smaller change, or possibly no change at all, would be necessary to bring the readings into harmony with the atom-annihilation hypothesis since the observed differences could be more than covered by a 5 percent uncertainty such as we had estimated might exist both at Peshawar and at Acapulco. However, two sets of observations taken five years apart (1935–1940) in both Madras, India, and San Antonio, Texas, have shown no evidence of a time-change in this particular five-year interval, so that it is perhaps better to explain the 4.2 percent divergence of both the Peshawar and the Acapulco curves from their mean as falling within the limits of observational uncertainties,

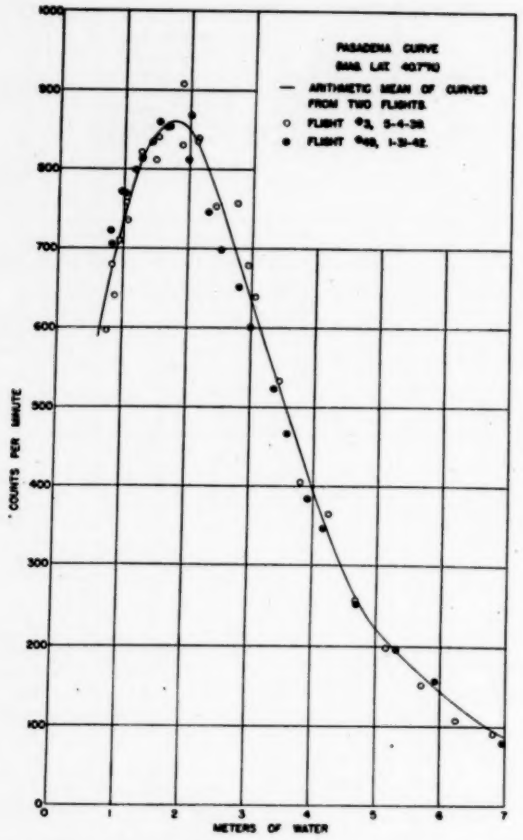

FIG. 8. At the latitude of Pasadena the annihilation rays of both oxygen and nitrogen appear to be able to get fully in vertically.

especially since different modes of recording were used in taking them.

3. A third and a most striking and unambiguous verification of prediction is seen by comparing the mean curve at Acapulco (Fig. 3) with the mean curve at Valles 5.3° farther north. (See Fig. 4.) These curves show no differences at all. This result, taken in conjunction with the result of the airplane flights at Panama and Arequipa in 1932[4] furnish excellent proof of the existence of the long plateau of constant cosmic-ray intensity extending from the equatorial latitude in Peru clear up to about mag. lat. 33° in Mexico. Furthermore, these results are in full agreement with the "ground-level" findings stated in VII (1) above.

4. Although there were found, in going north from Acapulco to Valles (370 miles) no additions at all to the vertical rays coming in at Acapulco, yet in going only 112 miles still farther north, *viz.*, from Valles to Victoria, both the ground level counts and the total vertically incoming energy obtained from the Victoria flight curves show an unambiguous increase. (See Figs. 5 and 6.)

5. There is evidence in the flight curves taken at Victoria that it is within a very few miles of Victoria that the oxygen annihilation rays begin to get in vertically. The ground-level reading was taken in the hotel grounds in the middle of the city. To avoid interference during the flight the truck was driven out into the "bush" not over four miles southeast of the town and the flight there in which the wind carried the balloons a little north of east revealed notably more incoming energy (see dotted curve Fig. 6) than did either of the two flights in which the wind carried the balloons a little south of east, so that *it seems to be right at the latitude of Victoria that the oxygen annihilation rays first get in vertically.*

VIII. A FIRST ATTEMPT TO TEST IN THE UNITED STATES THE PREDICTIONS OF THE HYPOTHESIS OF THE EXISTENCE OF THE CARBON AND HELIUM ANNIHILATION RAYS

The authors took off one week at the end of March, 1942 to try to test the prediction of the hypothesis, first, as to entrance not far north of Pasadena of a band of carbon annihilation rays (5.6 Bev); second, of the existence north of this latitude of a flat plateau of constant cosmic-ray intensity extending up to the latitude of entrance of the predicted band of helium annihilation rays (1.88 Bev). Because of unfavorable weather and several mishaps they got but two good flights, one at St. George, Utah (mag. lat. 44.8° N), which is but 4 degrees, or 266 miles nearer the north magnetic pole than Pasadena (mag. lat. 40.7° N), and one at Pocatello (mag. lat. 51° N), which is 6.2 degrees or 428 miles nearer the north magnetic pole than St. George. These two flights are plotted in Fig. 7 and the mean of two good flights at Pasadena in Fig. 8. It is to be regretted that the limited time and other conditions did not permit more flights at each of the two foregoing most northerly latitudes so as to add the weight of multiple observations to the evidence, and it is proposed to repeat and extend these observations as soon as

[4] See Fig. 4, Phys. Rev. **61**, 403 (1942).

peacetime conditions prevail. However, these two flights as recorded on the moving tape showed excellent consistency, so that the results obtained in them should have a very considerable degree of reliability. They seem to show with great certainty, first, the entrance of the carbon-annihilation rays between Pasadena and St. George, and, second, the altogether flat plateau extending from St. George to Pocatello. The latitude of entrance of the helium rays, as computed from the Lemaitre-Vallarta curves, is at mag. 54° N, only three degrees above Pocatello. Further, it is certain from preceding flights with electroscopes that between Omaha (mag. lat. 51.3°) and Bismarck (mag. lat. 56°) a group of new rays of energy about two billion electron volts does appear. *So far, then, as experiments have now gone no results have been obtained from the studies in India, in South America, in Mexico, or in the United States which are out of harmony with the predicions of the atom-annihilation hypothesis of the origin of cosmic rays.*

IX. COMPARISON OF OBSERVATION WITH THE COMPUTATIONS OF LEMAITRE AND VALLARTA ON THE ENERGIES OF VERTICALLY INCOMING ELECTRONS AT DIFFERENT LATITUDES

The curve labeled 1 on the original Lemaitre-Vallarta diagram[5] gives the computation of these authors of the energy required for an electron to reach the earth vertically as a function of latitude. This curve, however, is computed on the assumption of a magnetic field symmetrical about a north pole situated at lat. 78° 30″, long. 69° 0″ W, and having a field strength at the magnetic equator which requires an electron to have an energy of 15 Bev to reach the earth vertically there. From Millikan and Neher's measurements on the longitude effect at sea level at the equator these authors have estimated the energy necessary to get in at the equator in India as 17 Bev and in Peru as 13 Bev. In order, then, to find the energy necessary for an electron to reach the earth vertically at Victoria, mag. lat. 32.8°, the value found at that latitude from the Lemaitre-Vallarta curve has been multiplied by 13/15. This procedure yields 7.5 Bev, so that the Lamaitre-Vallarta curve modified in this way predicts exactly the latitude at which oxygen annihilation rays of energy 7.5 Bev do actually appear first to reach the earth vertically.

In order to make a similar computation for the electronic energy required to reach the earth vertically at Pasadena, it was for this case thought more legitimate to use as the base in the computations the equatorial value 15 Bev instead of 13 Bev, the reasons being, first, that the nearer one approaches to the pole the less should be the influence of the dissymmetry that produces the equatorial longitude effect; and, second, the farther west one moves in America the more should the stronger equatorial field in the Orient influence this base. Using, then, for Pasadena the Lemaitre-Vallarta base of 15 Bev

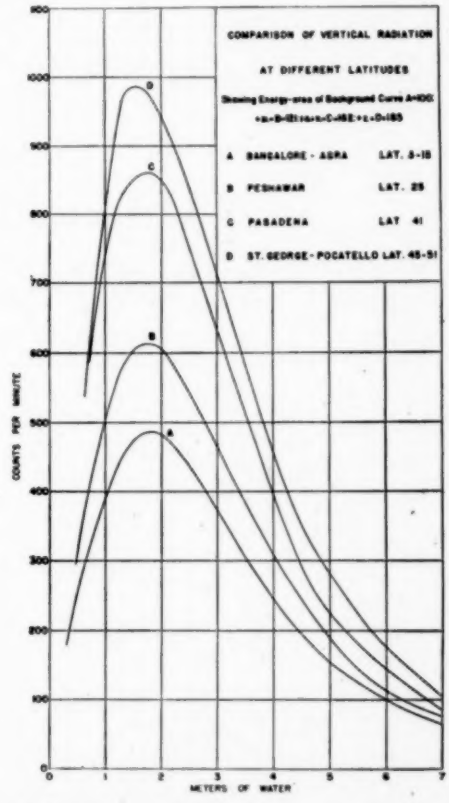
COMPARISON OF VERTICAL RADIATION
AT DIFFERENT LATITUDES
A BANGALORE - AGRA LAT. 8-18
B PESHAWAR LAT. 25
C PASADENA LAT 41
D ST. GEORGE - POCATELLO LAT. 45-51
COUNTS PER MINUTE
METERS OF WATER

FIG. 9. Shows that the cosmic-ray energy brought to earth vertically by silicon annihilation rays (curves *B–A*) is 21 percent of the energy of the earth's cosmic-ray nonfield sensitive or background energy (curve *A*); that oxygen and nitrogen annihilation rays bring in a joint energy (curves *C–B*) of 162 − 121 = 41 percent of curve *A*, the equivalent of 20½ percent each: that carbon annihilation rays (curves *D–C*) bring in an energy 185 − 162, or 23 percent of curve *A*; so that Si, O, N, C atoms are all thought to contribute nearly equal amounts of atom-annihilation cosmic-ray energy.

[5] See Fig. 10, Phys. Rev. **50**, 503 (1936); also reproduced in Fig. 2, Phys. Rev. **61**, 401 (1942).

instead of 13 Bev one finds the energy necessary for an electron to get in vertically to be 5.84×10^9, somewhat too large to enable the carbon annihilation rays of energy 5.6 Bev to reach the earth vertically at Pasadena, as in fact the experiments of the last section show that they actually fail to do.

In the same way and again using the base 15×10^9 the vertical energy necessary to get in at St. George comes out 4.41 Bev, so that the carbon rays of energy 5.6 Bev should be fully in at St. George as they were in fact seen to be from Fig. 8.

By the same procedure the latitude at which helium annihilation rays of energy 1.88×10^9 should first enter vertically comes out mag. 54° N. This is only 3 degrees above that of Pocatello where the total area beneath the curve comes out quite the same as that corresponding to St. George. So that the evidence for the existence of the flat plateau in the stretch of latitudes requiring an energy of vertical entry between 5.6×10^9 and 1.88×10^9 appears to be quite good.

X. COMPARISON OF THE VERTICALLY INCOMING, FIELD SENSITIVE, COSMIC-RAY ENERGIES BROUGHT TO EARTH BY THE ANNIHILATION RAYS OF SI, O, N, AND C.

It has been shown in preceding articles[1] that the background of non-field-sensitive cosmic-ray energy is not more than forty percent of the total cosmic-ray energy with which the earth is being continuously bombarded.

In terms of the total of this non-field sensitive cosmic-ray energy taken as a base one can estimate with considerable certainty the relative field-sensitive cosmic-ray energies brought to earth by the annihilation rays of the four atoms Si, O, N, and C, as follows: To get a numerical value for the base one measures with a planimeter the total area underneath the mean Bangalore curve *A*, Fig. 9. The best measure now obtainable for the energy brought in by vertical silicon rays will then be the difference between the area of the mean Peshawar curve *B* and the mean Bangalore curves, *A* (Fig. 9). Similarly, the difference between the area underneath the mean Pasadena curve *C* and the Peshawar curve *B* is a measure of the joint energy brought in vertically by the field sensitive annihilation rays of the oxygen and nitrogen atoms. Some evidence has already been brought forward in §7 for the conclusion that these two annihilation rays have an approximately equal energy content. Similarly, the difference between the mean St. George-Pocatello curve *D* and the mean Pasadena curve *C* gives the energy brought in vertically by carbon annihilation rays. The actually measured areas underneath these four curves are given in the second column of Table II, while the third column gives the relative values in terms of Bangalore-Madras as a base.

TABLE II. Areas under curves, numerical and relative values.

Bangalore-Madras	65.7	100
Peshawar	79.0	121
Pasadena	106.2	162
St. George-Pocatello	122.1	185

The energy content of these four annihilation rays is thus seen to be very nearly the same. This is not quite the conclusion drawn from Bowen's spectroscopic measurements on ring nebulae, for according to them the relative *abundance*, rather than the relative energy, of these four atoms in interstellar space is the same for the four. If all these four atoms have the same chance of undergoing the transformation of their rest mass energy into an electron pair, then these cosmic-ray measurements are in agreement with Bowen's spectroscopic measurements to the extent that the same relative abundance is assigned by both methods to carbon, nitrogen, and oxygen atoms. Since, however, the rest mass energy of silicon is about double that of each of the other three atoms, the foregoing evidence from cosmic-ray data would indicate an *abundance* of silicon atoms in interstellar space of about half that of each of the carbon, nitrogen, and oxygen atoms. This much of a discrepancy would probably not be outside the limits of Bowen's own estimate of his uncertainty.

To account for the fact that about 60 percent of the total incoming cosmic-ray energy is field sensitive and only 40 percent non-field sensitive (this non-field sensitive part corresponding to the area underneath the Bangalore curve) it would be necessary to assign to helium annihila-

tion rays an incoming cosmic-ray energy in terms of Bangalore as a base of $(100/.40)-185.=65$, or about three times the energy brought in by say carbon annihilation rays. But since helium's rest-mass is but one-third that of carbon its *abundance* would from these figures have to be about nine times that of carbon. It will be recalled that Bowen's spectroscopic measurements assigned helium about ten times the abundance of the atoms of carbon. *So far, then, as the abundance of the elements in interstellar space is concerned the present atom-annihilation hypothesis as to the origin of cosmic rays assigns to the different atoms involved an abundance in interstellar space that is in quite reasonable agreement with Bowen's spectroscopic findings.*

XI. THE NATURE OF THE INCOMING PARTICLES

If the foregoing evidence as to the latitudes of first entrance of the annihilation rays of Si, O, N, C, and He is considered convincing, then the incoming particles must be *electrons* and not essentially heavier particles like protons or even mesotrons, though in view of the short lifetime of the mesotron that particle seems to be barred out for other reasons than its available mass. If, then, the transformation of rest mass energy in the case of the helium atom gave rise to a pair of protons rather than a pair of electrons, then the total available energy for getting these protons through the earth's magnetic field would be not 1.88 Bev, but 0.94 Bev, in which case the latitude of first entrance of these helium annihilation rays would be considerably north of Saskatoon (mag. lat. 60°). But in fact as one goes north, the latitude of entrance of the last significant group of new rays, designated herein as helium-annihilation rays, does appear between the latitude of Omaha (mag. 51.3° N) and that of Bismarck (mag. 56° N). This is certainly very close to the lat. mag. 54° N computed from the Lemaitre-Vallarta curves as the first latitude of entrance of helium annihilation rays on the assumption that the whole rest mass of the helium is transformed into an electron pair.

Thus far no new rays coming in north of Bismarck have been found by anyone. It is true that as yet the energies of *vertically* incoming rays have not been determined north of Pocatello (mag. 51° N) as the authors plan to do as soon as world conditions permit. Since, however, the Lemaitre-Vallarta curves show that in these northern latitudes the differences between the curves of incoming energies obtained from electroscope readings should show but small differences from those obtained from vertical counter readings the following conclusion from already existing measurements seems to be fully justified, *namely, that from the standpoint of the atom annihilation hypothesis as to the origin of cosmic rays the incoming cosmic-ray charged particles must be electrons rather than protons or any other particles essentially more massive than electrons.*

The foregoing investigations and a long series of preceding ones upon which these depend have been supported for years by grants from the Carnegie Corporation of New York administered by the Carnegie Institution of Washington. For this aid the authors wish to express their keen appreciation. They wish also to make acknowledgments to the Indian Meteorological Service for cordial and well-nigh unlimited assistance to their work in India and also to express their thanks for similar cooperation in Mexico by the Mexican Meteorological Service.

The Spectrum of Neutral Tungsten, W I

O. LAPORTE, *University of Michigan, Ann Arbor, Michigan*
AND
J. E. MACK, *University of Wisconsin, Madison, Wisconsin*

(Received June 29, 1942)

An analysis of the W I spectrum has yielded 300 levels, of which 201 have been given tentative magnetic g values. Configurations, as well as L and S values, have been assigned to the 65 levels $5d^46s^2\,{}^5D\,{}^3HGFDP$, $5d^56s\,{}^{7,5}S\,{}^5G$, $5d^46s(^6D)7s\,{}^{7,5}D$, $5d^46s(^6D)6p\,{}^{7,5}FDP$ with 18 definite ambiguities due to a mixing of eigenfunctions. All the low levels are believed to be known. The ionization potential is (7.94 ± 0.1) volts. A rectangular array of the transitions is given.

1. INTRODUCTION, AND SUMMARY OF RESULTS

THE science of the classification of atomic spectra has progressed so far in the last fifteen years that it seems desirable to view what has been accomplished and where knowledge is still lacking.

Naturally classification began with the simplest spectra. A spectrum may be called simple if it shows one or both of the following traits:

(1) It has but few lines.

(2) It shows pronounced coupling character.

Passing over the trivial case of the alkali-like spectra, we see that to the first category there belong the spectra of the occupants of those columns of the periodic table characterized by partly filled p shells. The spectra of the alkaline earths and of Ni, Pd, Pt, with almost closed d shells, also belong in this category. In most of these elements, notably among the heavier ones of them, regularities consisting of constant differences, i.e., levels, have been known for a long time (Runge, Paschen, Paulson).

The most typical representatives of the second category are the famous spectra of Cr and Mn, in which multiplets were first discovered. Other, though not such typical, representatives are the spectra of the other elements of the iron group. For all these the classification has been carried through to a high degree of completion. Some of the spectra of the second long period and a few rare earths are also to be counted in this category although the latter exhibit their characteristic features to a still slighter degree.

Spectra that cannot be regarded as belonging to either of the above categories are the most numerous, and most of them are as yet incompletely or not at all investigated. They exhibit multitudes of lines of approximately equal intensity. From a theoretical point of view only little that is helpful may be said about them. Interactions are so general and so complex that no quantum numbers other than J and the parity value can be ascribed. No grouping of the levels is apparent, and the assignment of further quantum numbers, whether vector sums of electronic quantum numbers or electronic quantum numbers (configurations) themselves, would in general therefore be unjustified. Fortunately there often occur among spectra of this uninviting class, groups of levels that exhibit traces of coupling simply because the chances for perturbing interactions are relatively small among the lowest levels. In a few of these somewhat tractable spectra rather complete classifications have been published, notably those of certain rare earths by Albertson, Harrison, Meggers, Russell, and their co-workers.

The spectrum of neutral tungsten, W I, on which we are reporting here, is of the kind described in the previous paragraph. Its investigation was begun at the Bureau of Standards seventeen years ago, in the heyday of multiplet spectroscopy, in an attempt to find multiplets in a spectrum of an element of the third long period. W I was expected to be the easiest spectrum in this period, since both Cr I and Mo I showed from the then prevailing point of view a relatively simple structure. As we know now, this simplicity arises from the occurrence of configurations involving five equivalent d-electrons, for which spin-orbit interaction vanishes.[1] On the other hand it has become clear that in W I the simplifying influence of d^5 is considerably obscured

[1] W. Albertson, Astrophys. J. **84**, 26 (1936), points out the corresponding fact for seven f-electrons and its bearing upon the relative simplicity of portions of certain spectra in the middle of the rare earth group.

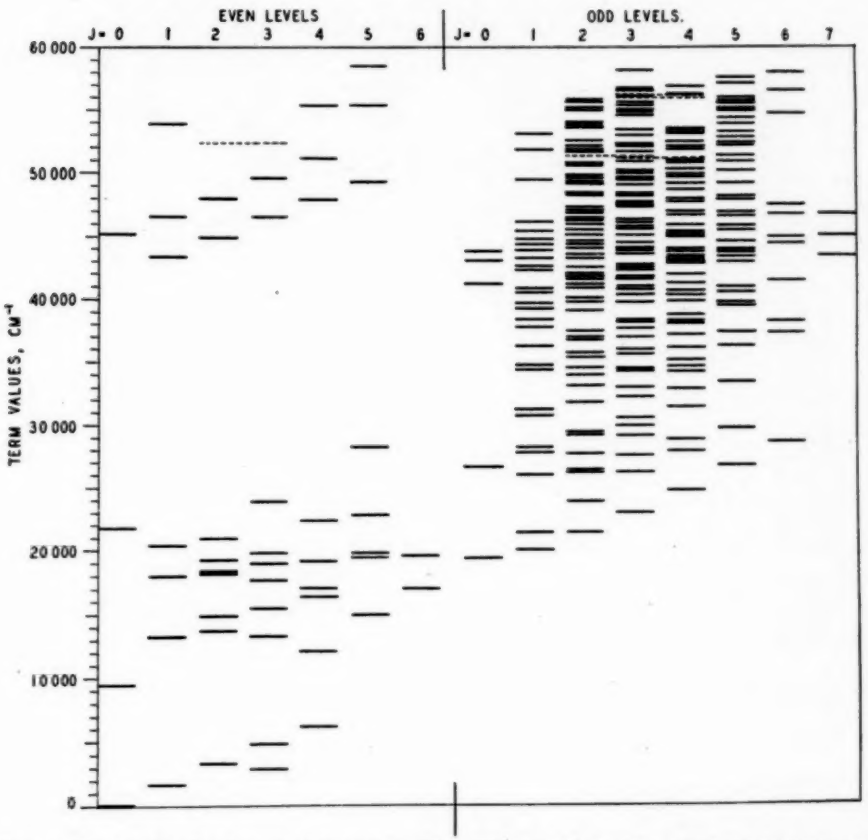

FIG. 1. Energy levels of neutral tungsten, W I. The first ionization level, W II $5d^46s\ ^6S$, lies at 64.4×10^3 cm^{-1}.

by its relative instability and by mixture with other configurations, and that, as compared with its neighbors in the Pt group, the spectrum of W shows no such singularly simple structure as was exhibited by those of Cr and Mo in the Fe and Pd groups, respectively.

Most of the new material in this paper is incorporated in Table I, which is a rectangular array in which an attempt has been made to gather all the important information available concerning the properties of the neutral tungsten atom. Closely related to Table I is Table II, the list of classified lines. Because Tables I and II are designed for reference rather than continuous reading, and on account of the length of the explanatory matter that accompanies them, the presentation of this matter is postponed to Section 4, which is devoted to it.

Briefly stated, the present status of W I is that 2378 lines have been given assignment as 2567 transitions (including 169 double and 10 triple assignments) among 50 even and 250 odd levels (of which 16 are established only tentatively and listed with question marks), and tentative g values have been assigned to 201 of the levels. Figure 1 is the general level diagram. As for the assignment of quantum numbers, of course parity and J values are given for all the levels (except for ambiguities in J, in 4 cases). Further than that, surprisingly enough for an atom in this part of the periodic table, it has been found practical to assign approximate configuration and LS-coupling quantum numbers, with only 18 cases of evident mixing of eigenfunctions, to 65 levels: $5d^46s^2\ ^5D\ ^3HGFDP$, $5d^56s\ ^{7,5}S\ ^5G$, $5d^46s(^6D)7s\ ^{7,5}D$, $5d^46s(^6D)6p\ ^{7,5}FDP$. Clues as to possible structural properties are given for about 10 other levels. The rest of the odd levels cannot at present be interpreted. In the study of the low levels, formulas have been used for the configuration d^4 (LS interaction is neglected) after Ostrofsky,[2] and for the configuration d^5 (where the LS in-

[2] M. Ostrofsky, Phys. Rev. **46**, 604 (1934); see also for corrected formulae: O. Laporte, Phys. Rev. **61**, 302 (1942).

TABLE I. Level and transition array for W I.

Structure	Name		$5d^46s(^6D)6p$ (cm^{-1})	g	$^7F_0$ $19_{30}°$ 19389.38 0/0	$^7F_1$ $20_{01}°$ 20064.26 1.54A	$^7F_2$ $21_{42}°$ 21448.66 1.48A	$^7D_1$ $21_{41}°$ 21453.80 2.51A	$^7F_3$ $23_{02}°$ 23047.19 1.53B	$^7D_2$ $23_{92}°$ 23964.58 1.93B	$^7F_4$ $24_{74}°$ 24763.30 1.50B
$5d^46s^2$	$^5D_0$	D_0	0.00	0/0		$5KZ$ −04		$6Z$ −03			
	$^5D_1$	D_1	1670.27	1.51A	2 −18	$3z$ −03	$5K?z$ +01	$8KZ$ +02		$6KZd$ 00C	
$5d^56s$	$^7S_3$	S_3	2951.27	1.98A			—		—	$4Kz$ −01C	—
$5d^46s^2$	$^5D_2$	D_2	3325.50	1.48A		2 +13	—	$7K?\zeta$ −21	$6K?z$ +01	$6Kz$ +01	
	$^5D_3$	D_3	4829.99	1.50A			0u −1		$2z$ +04	$6KZ$ +03	$6K?z$ 00
	$^5D_4$	D_4	6219.30	1.49A					1u −07C		1 −01
	$^3P_0$	09_0	9528.01	0/0		—		2 +01			
	$^3H_4$	12_4	12161.96	0.99B					—		—
	$^3P_1$	13_1	13307.09	1.32B						—	
	$^3G_3$	13_3	13348.53	0.92A					—	—	—
	$^3F_2$	13_2	13777.71	1.09B						1.0 +13	
	$^3P_2$	14_2	14976.17	1.06B							
	$^3H_5$	15_5	15069.94	1.05B							—
	$^3F_3$	15_3	15460.00	1.17B							
	$^3G_4$	16_4	16431.30	1.02B							
	$^3H_6$	17_6	17008.48	1.4 C							
	$^3F_4$	17_4	17107.01	1.19B							
—	—	17_3	17701.16	1.02C							
$5d^46s^2$	^3D	18_1	18082.84	0.7 C							
	$^5G_2$	18_2	18116.83	1.08C							
	$^5S_2$	$18_2'$	18280.48	1.43C							
	$^5G_3$	18_3	18974.48	1.06A							
$5d^46s^2$	$^3D_2$	19_2	19253.59	1.18A							
$5d^56s$	$^5G_4$	19_4	19256.22	1.20B							
	$^5G_5$	19_5	19535.00	1.21B							
	$^5G_6$	19_6	19648.48	1.32B							
$5d^46s^2$	$^3G_5$	$19_5'$	19826.02	1.20A							
	$^3D_3$	19_3	19827.67	1.28A							
$5d^56s$	$^5P_1?$	20_1	20427.82	2.1 C							
—	—	20_2	20983.07								
$5d^56s$	$^5D_0?$	21_0	21856.3	0/0							
	$^5D_4?$	22_4	22476.65	1.48C							
	$^5F_5?$	22_5	22852.82	1.2 C							
—	—	23_3	23930.07	1.4 C							
—	—	28_5	28233.41								
$5d^46s(^6D)7s$	$^7D_1$	43_1	43451.89	2.83B	2Z 00	$3fZ$ +06	3ζ −03	1 −03		2 −01	
	$^7D_2$	44_2	44919.74	1.9 C		3ζ +02C	$5=$ +03	$3z$ +01c	$4K?Z$ −01	0 +02	
	$^5D_0$	45_0	45225.18	0/0		0 −02		1u 00			
	$^5D_1$	46_1	46458.20		—	—	$0z$ −04	$2=$ +03		0 +08	
	$^7D_3$	46_3	46496.50	1.74B			$2z$ +02		5 +02	$3z$ −03C	$4Z$ 00
	$^7D_4$	47_4	47975.45	1.68A					$2z$ −01		1= −02
	$^5D_2$	48_2	48078.33	1.55B		—	0u 00	0 +03	$1z$ −09	—	0 −05C
	$^7D_5$	49_5	49354.58	1.7 C							
	$^5D_3$	49_3	49655.95	1.66B			—		3 +03C	0 −02	—
	$^5D_4$	51_4	51123.08	1.4 C					—		—
—	—	52_{23}	52284.71			—	$3Kz$ 00	—	1 00	—	—
—	—	53_1	53847.81		—	—	0 +01	—		—	
—	—	55_4	55333.03	1.45B					0 −18		2 +02
—	—	55_5	55380.87								2 +13C
—	—	$?58_5$	58630.9								0 +28
					$19_{30}°$	$20_{01}°$	$21_{42}°$	$21_{41}°$	$23_{02}°$	$23_{92}°$	$24_{74}°$

teraction energy vanishes), as published by Laporte.[3]

At this point it is appropriate to consider the degree of completeness of the classification. The relative term "complete," applied to the classification of an atomic spectrum, carries quite different meanings from the two points of view of the experimental spectroscopist and the theoretician. The experimentalist considers a classification complete if it accounts for all the lines on a reasonably exposed plate, or at least for all that show by their behavior under various conditions that they belong to levels especially populous or stable, or otherwise interesting. The theoretician wants, of the infinite number of levels, the identification of certain limited sets, such as the approximately defined configurations. In any atom so complicated as tungsten, the two kinds of completeness are incompatible, for almost every configuration possesses some improbable levels, the discovery of which would require heavily exposed plates, that would present many new lines to be classified, that would yield new part-configurations, etc.

[3] O. Laporte, Phys. Rev. 61, 302 (1942).

TABLE I—*Continued.*

$^6F_1$ 2594° 25983.57 0.54*B*	$^7D_2$ 2611° 26189.11 1.80*B*	$^7P_2$ 2622° 26229.68 1.84*B*	$^7F_2$ 2632° 26367.22 0.87*B*	$^5D_0$ 2660° 26629.51 0/0	$^7F_0$ 2665° 26676.41 1.46*B*	$^7P_2$ 2748° 27488.05 1.72*A*	— 2762° 27662.44 1.21*A*	$^5D_1$ 2771° 27778.46 1.25*B*	
3/*K*?*Z* −10		4ζ −03	2 −02	3*Z* −03				3*Z* +04	D_0
4*Z* +01	6*GKZ* −01	6*rGKz* 00	5*fKZ* −01			6*e*′*K* −03	5*fZ* 00	3= +01	D_1
4*f*= −01*C*	3*z* −01	4*z* −01	—			5*fz* 00*c*	5*K*?*Z* −01 0 00	4*z* −02	S_2
	6*K*?*Z* −01	2 −01	1 +07*C*			4*f*= 00*C*	3ζ −03		D_2
	6*K*?*z* 00				6*K*?*z* −03	3*z* 00*c*			D_3
—								5*Z* 00	D_4
	1 00				—	—		3= +01	09_0
2 +01	—	1 +16	2 +02	2 +03			3 −01	3 −03	12_4
		2 +01				—	4 +02		13_1
—	1 +04	—	3 +03			1*u* −14	2 +03	3 −01	13_2
.5 +19	.7 +16	.4 −04	1 −05			—	2 +06	2 00	13_7
	.3 +12	.4 +13	.2 +28*C*		—	1 +03	—		14_2
	—					.0 +29			15_5
									15_3
					—	—			16_4
						—	—		17_6
						—	—		17_4
									17_3
							—	—	18_1
								.3 +12	18_2
									$18_2'$
									18_3
									19_2
									19_4
									19_5
									19_6
									$19_5'$
									19_3
									20_1
									20_2
									21_6
									22_4
									22_3
									23_3
									28_5
2*u* −37		4 00	2 −03	0*u* +3			—	0*u* −1	43_1
—	1*u* +03	2 +02	0 +05			4*z* −07	2 +09	1 −18	44_2
1*u* 00								—	45_0
—		—	—	0*u* −09			2 −03	1 +02	46_1
	0*u* +10	0*u* +14	—			2*z* +01	—		46_3
	4*z* −07				5*K*?*z* −05	—			47_4
—	—	—	—		—	—	0 −01	—	48_2
	—	—	1 −13*C*		3= +05	—	—		49_5
	—				2*z* −03	—			49_3
									51_4
—	0*u* +02	2 −13	1 +11			0 +01	—	—	52_{22}
—	0 00	1 −32	1	0 +05			—	—	53_1
	1 −01				—	—			55_4
					0 −01				55_2
					—				?58_3
259_1°	261_3°	262_2°	263_2°	266_0°	266_5°	274_3°	276_2°	277_1°	

From the theoretical point of view, of course, the present classification of W I is far from complete. Even in $5d^46s^2$, which is the lowest configuration, hardly more than one-half of the 34 levels are known. Experimentally, however, the situation can perhaps be compared favorably with that in almost any other spectrum of comparable complexity; see remarks made under 3(c).

2. CRITICAL RÉSUMÉ OF PREVIOUS DATA AND INTERPRETATIONS

Heretofore a large amount of experimental data but a relatively small amount of classification and interpretation on the arc spectrum of tungsten have been available. Although an exhaustive review is unnecessary, certain aspects of the problem and some of the most important previous work are discussed in the following historical and critical account.

(a) Line Measurements

The older line measurements are collected in Kayser's *Handbuch*.[4] The most extensive of all the lists is that of Exner and Haschek,[5] whose

[4] H. Kayser, *Handbuch der Spectroscopie* (1912), Vol. 6, p. 787.

[5] F. Exner and E. Haschek, *Die Spektren der Elemente bei normalem Druck* (Leipzig, 1911, 1912).

TABLE I—*Continued.*

	$^7P_4$ 278_4° 27889.56 1.71*A*	$^5P_1$ 281_1° 28187.84 2.34*A*	$^7F_6$?285_6° 28599.81	$^7D_4$ 287_4° 28797.21 1.61*A*	$^5F_3$ 291_3° 29139.10 1.06*B*	$^5D_2$ 291_2° 29195.84 1.28*A*	$^5P_2$ 293_2° 29393.38 1.83*A*	$^7D_3$ 297_3° 29773.27 1.55*A*	$^5D_3$ 299_3° 29912.80 1.31*A*
D_0		6*KZ* +02							
D_1		5*KZ* +05				5*z* −03	3*z* 00		
S_3	8*GKZ* +01			5*fK*?*Z* +01	6*Z* 00	5*Z* −02	5*zKz* +05		6*K*?*Z* +05
D_2		4*Z* 00			4*z* −01*C*	3= +03	5*fZ* −02		4*fz* −03
D_3	0 +12			5*z* +03	1*u* +25*C*	—	—		—
D_4	4= +01*c*			—	3*z* −02			4*K*?*z* +03*c*	5*z* +01
09_0		1*Z* 00*C*							
12_4	—			1 −02	—			2 −03*C*	2*K*? +11
13_1		2 −05				4 00	—		
13_3	—			—	—	1 +02	—		1*u* −27
13_2		—			2 +07	2 −02*c*	2 −04		1 −06
14_2		—			1 −05	—	4 −08		5*u* 00*c*
15_5	—		1 +05	—				2 −08	
15_3	1 −05			—	—	2 +03*C*	—		1 −07
16_4	—			—	2 +02			—	—
17_6			—					—	
17_4	—			—	—			—	—
17_3	—			—	2 −01	—	—		—
18_1		—				.4 −05*C*	—		
18_2		1.8 +16			.5 +09	.1 −24	1.5 +12		3 −01
$18_2'$		.1 +03			.2 +09	2.0*u* +04*C*	.4 +05*C*		3 −01
18_0				—	1.0 +16	.7 +04	.4 +07		.4 −03
19_2					—	—	.4 +14		.3 +12
19_4				.0 +21	.3 +20			(*C* +44)	2.5 +01
19_5								.8 +13	
19_6								1.2 +18	
$19_5'$								.4*n* −04	
19_3							.1*ud* +14		.3 +11
20_1									
20_2									
21_0									
22_4									
22_5									
23_3									
28_5									
43_1		2 +03				—	1 −06*c*		
44_2		2 −06			0*u* −1	—	—		—
45_0		1*u* +15							
46_1		0 +11				1*u* −03			
46_3	0 −01			4*z* −11*C*	2*u* −06	—	2 −04		2 +08
47_4	0 +08			2*f* −02	—			6*K*?*z* −02	—
48_2		0*u* −24*C*			0 +12	—	2 −08		(*C* −40)
49_5	3 −03		2 +04	0*u* −24*C*				2 +01	
49_3	—			0 −03	(*C* −53)	—	0*u* +28		0*u* −04*C*
51_4	—			0*f* +14	—			0 +01	0*u* −20
52_{23}	—			—	—	—	—		—
53_1						—	—		
55_4	0 +11			1*z* +04	—			0*u* 00	—
55_3	—			2 00				1*z* +02	
?58_5	—			—				—	
	278_4°	281_1°	?285_6°	287_4°	291_3°	291_2°	293_2°	297_3°	299_3°

comparison of arc and spark intensities was useful in isolating the transitions belonging to the neutral atom. The high accuracy of their measurements was exceeded only by that of Miss Belke's[6] important work, which justified the retention of seven digits, and by that of Kiess and Meggers[7] in the longer wave-lengths. In the farthest photographic infra-red we have made use of Cohen's[8] unpublished list, but have not classified any lines that occur exclusively on it. In the extreme ultraviolet the hitherto published material has been supplemented by a new list,[9]

[6] M. Belke, Zeits. f. Wiss. Photographie **17**, 132 and 145 (1918). In this paper 3179.964 should read 3179.064 and 5020.369 should read 5040.369.

[7] C. C. Kiess and W. F. Meggers, Sci. Pap. Bur. Stand. **16**, 51 (1920); C. C. Kiess, unpublished list of lines in the region ν11333 to ν9541, kindly placed at our disposal.

[8] I. Cohen, A. B. thesis, Wisconsin, 1937 (deposited at the Library of the University of Wisconsin). Belke's (reference 6) lines in the third order were used as standards.

[9] Obtained by Mack on Schumann plates with a Hilger E-1 quartz spectrograph at Palmer Physical Laboratory, with the valuable advice and aid of Professor Shenstone. Belke's lines, and beyond their limit, Shenstone's silver arc lines, were used as standards. Although the standards are believed to be good to about 0.2 cm^{-1}, it is evident from the disagreement of our tungsten lines with the combination principle that the lines listed are uncertain by several times that amount.

TABLE I—*Continued.*

$^5F_5$ $30\mathrm{5}_5°$ 30586.61 1.64*A*	— $30\mathrm{6}_7°$ 30683.45 1.39*A*	— $31\mathrm{3}_1°$ 31323.41 0.86*A*	$^5F_4$ $31\mathrm{4}_4°$ 31432.87 1.32*B*	— $31\mathrm{8}_5°$ 31817.61 1.52*B*	— $32\mathrm{2}_3°$ 32238.00 1.3*C*	$^5D_4$ $32\mathrm{8}_4°$ 32828.11 1.7*C*	— $32\mathrm{9}_3°$ 32957.56 1.43*B*	— $33\mathrm{1}_2°$ 33141.40 1.51*B*	
	2 +12	1*KZ* +04		3*z* 00				4*dKz* −02	D_0
	2*z* 00	2= +02*C*						4*KZ* +03*c*	D_1
8*rKZ* +05			5*z* −02	3*A*? +02	3= +02	0 +13	5*K*= +02	1 −04*c*	S_3
3*z* +05*C*	3*z* +03	6ζ +14*C*		3*f*/*z* −01	3*z* 00		3*Kz* +02		D_2
5*f*/*K*?*z* 00			3*f*/*z* −01	—	3*Az* +02	6ζ −07*C*	3*z* 00	?0 +44	D_3
5*p*′/*k*?*z* −04			2 −01		2*f* −02	3 −02*C*	2 +01*C*		D_4
	0 −06	3*Z* −06							09_0
—			—		—	0 −17*C*	2 +01		12_4
	1*u* −17	0*u* +3		?0 −43				2 00	13_1
1 −06			0*u* +29	0*u* −29	—	—	—	—	13_2
4 +08	1 00	2 −11		—	0 −20		0*u* +02	0*u* +5	13_3
4 −05	1 −14	2 00		—	—		0 −05	2*f* −10*c*	14_3
			—			0 +02			15_3
2*u* −03			2*u* −12	2 +01	0*u* −2	2*u* −22	—	0 −08	15_2
—			1*u* −07		0*u* 0	—	—		16_4
									17_6
—			—		2 −09	1*u* −05	—		17_4
1 −03			—		—	—	2 −04	1*u* +03	17_2
	—	2 +01		—				—	18_1
4 +05	1. −05	3 +05		—	—		—	—	18_2
3 +03	2 +04	?3 +03		3 −04	2 −03		2 +18*C*	—	$18_2'$
—			—	3 +02	3 −02	2 +03*C*	—	—	18_3
.1 +30	2 +03	—		2 00	1 00		1 −01	1 −08	19_2
.2 +17			?2 −01		2 +04	—	3 −04		19_4
			2 +03			—			19_5
									19_6
			3 +03			3 +05			$19_7'$
3*u* +10	.4 +10	.1 +05	2 −03	2 +02	2 −02	1 −04	3 +09	3 +01	19_8
2 +17	.0 +01	.2 +24		1 −09				2 −01	20_1
				2 +08	—		1 +04	1*u* +05	20_2
									21_0
					.4 +05	—	2.5 +10		22_4
						?.2*us* +52			22_5
									23_3
									28_3
	—	—		1 +01	1 +02		—	—	43_1
	—	—						—	44_2
	2 −12	1 +04		2 +04					45_0
	—	—		—				—	46_1
—			1*u* +17*C*	—	—	—	1 +06	—	46_2
2 +02			3 +02		0*u* +09	2*u* −14*C*	—		47_4
1*u* +34	2*u* −10	—		1*u* −34	—		3*u* −07	5*u* −30*C*	48_2
—			0*u* 00			—			49_5
			1 +02	1*z* +11	1*z* +07	1*u* −02*C*	0*ud* −09		49_3
0 +19			—		—	0*u* −1	(*C* −09)		51_4
—	—	—	—	—	2*z* +08*C*	—	—	—	52_{21}
	—	(*C* +46)		—				0 −03	53_1
2*z* −10*C*			0 +13		—		—		55_4
			—			—			55_{44}
			—						$?58_{16}$
$30\mathrm{5}_2°$	$30\mathrm{6}_1°$	$31\mathrm{3}_1°$	$31\mathrm{4}_4°$	$31\mathrm{8}_2°$	$32\mathrm{2}_2°$	$32\mathrm{8}_4°$	$32\mathrm{9}_3°$	$33\mathrm{1}_2°$	

whose lines are much more intense than Exner and Haschek's and extend to considerably higher frequencies, but are less accurately measured.

Since the completion of what we thought was to be our final list, the M.I.T. tables[10] have appeared, covering almost the whole range of all the previous lists. The accuracy of the tungsten lines in this list, as judged by self-consistency under the combination principle, compares favorably with that in any of the other lists except the middle portions of those of Belke, Kiess, and Meggers. The list is rich in lines although it needs to be supplemented by others throughout its range. If our work were starting now we should undoubtedly use the M.I.T. list as the principal basis for our work throughout the spectrum, instead of limiting our principal changes to the region $\nu > 40{,}000$ cm^{-1} as we have done for the sake of economy.

(b) Special Excitation Conditions

Certain lines evidently belonging to the lowest levels are distinguished by their reversal in the arc or their presence among de Gramont's[11] or

[10] G. R. Harrison, *Massachusetts Institute of Technology Wavelength Tables* (John Wiley and Sons, 1939).

[11] A. de Gramont, Comptes rendus **171**, 1106 (1920).

TABLE I—*Continued.*

	$^5F_5$ $333_5°$ 33370.06 1.39*B*	$339_2°$ 33943.98	$341_4°$ 34121.60 1.5*C*	$342_3°$ 34228.54	$343_1°$ 34342.37 1.56*A*	$343_3°$ 34353.99 0.71*C*	$344_2°$ 34485.83 0.82*C*	$346_4°$ 34632.59 0.89*C*	$347_1°$ 34719.32 0.15*B*
D_0					4*Z* +05				5*rM*?*H*?*A*?*KZ*−01
D_1		—			1 +06		5*rKz* 00		5*A*?*KZ*−03
S_2		2 +01	5*Kz* +08	—		3 +02	3 −02	2 +06	
D_2		—		2*dz* +02	2 −01	3*z* −01	4*K*= +06		3 00
D_3		2*z* +03	3*z* +03	0 +05		2*Z* +04	2*y* +01	5*K*?*z* +01*C*	
D_4	5*z* −04		0 −04	2*z* +03		—		3 −06	
09_0					3*Z* −04				—
12_4	0 −04		1 −02	2 −02		3*z* −01		3*z* −04	
13_1		0 +09			2 −02		2 −04		0 +13
13_3		3 −02	0 −15	2 −03		0*u* −15	4*z* −04	—	
13_2		—		2*u* +12	—	0 +02	—		3 +26
14_2		—		3*z* 00	0*u* +3	—	2 +01		0*u* −04
15_5	—		0*u* +17					0 +01	
15_3		0 00	2*u* −03	—		—	—	—	
16_4	0 00		0*u* 00	2*u* −13		—		0*uf* +18	
17_6	—								
17_4	1 +07		1*u* +03	2 00*C*		2 −07		0 −04	
17_3		2 −04*C*	—	0*u* −3		1*u* +07*C*	2 −03	0*u* +2	
18_1		—			—		1 +02		—
18_2		—		—	2 −07	—	1 +03		4 +04
$18_2'$		1 −01		—	1*u* −04	—	2 −03		3 +04
18_3		4 00	2*u* +08*C*	1*u* +02		2*u* +19*C*	2 −04	2*u* +06	
19_2		3*u* −02		1 −03		1*u* −20*C*	3 +12		3 −08
19_4	—		2*u* +10	2 −09		3*u* −07*C*		—	
19_5	2 +01		2 −02					3*u* +12*C*	
19_6	3 −06								
$19_5'$	2 +04		2*d* +18					—	
19_3		—	2 −03	—		?2 −40	4 +02	—	
20_1		—			1*u* +08		(*C* +44)		—
20_2		—		—	3 +04*C*	—	—		(*C* −38)
21_0					—				—
22_4	.4 −03		3 −02	2 −01		2 00		—	
22_5	.1 +25*c*		.4 +18					1 −02	
23_3		2 +15	2.0 +08	.1 +01	—	.1 +01	—	—	
28_5									
43_1									
44_2		—		—	—	—	—		—
45_0					—				.5 00
46_1		—			—		1 +03		2 −01
46_2		—	—	—		—	—	—	—
47_4	1 +04		2 −19*C*	—		—		—	
48_2		—		?1 +33	2 −09*C*	—	1 −04		3 +33
49_5	3 −02		1*u* +03					—	
49_3		—	0*u* +22	—		—	—	1*u* +05	
51_4	1*u* −05		2 00	0*u* +30		—		—	
52_{23}		—	—	—		—	—	—	—
53_1		—				—	—		—
55_4	3*z* −06*C*		—	—		—		—	
55_{34}	—		3 +15*C*			—		0*E* −01	
$?58_{56}$	—		—					—	
	$333_5°$	$339_2°$	$341_4°$	$342_3°$	$343_1°$	$343_3°$	$344_2°$	$346_4°$	$347_1°$

Thompson's[12] raies ultimes, King's[13] furnace lines, or the underwater spark lines of Hulburt,[14] Meggers,[15] and Allin and Ireton.[16] They were especially useful in the early part of the analysis. King's method yields less information here than usual on account of the low volatility of tungsten. In the light of the present classification, Hulburt's and Meggers' underwater spark lines are evidently the only such lines with much physical significance.

The revised Rowland[17] and Miss Moore[18] lists give 9 sure, and 11 other possible, tungsten absorption lines in the spectrum of the sun's disk, and 3 unquestioned and 6 questioned tungsten

[12] K. Thompson, plate kindly taken at the University of Michigan upon our request.

[13] A. S. King, Astrophys. J. **75**, 379 (1932).

[14] E. O. Hulburt, Phys. Rev. **24**, 129 (1924).

[15] W. F. Meggers, unpublished work kindly placed at our disposal.

[16] E. J. Allin, Trans. Roy. Soc. Canada **21**, Sec. 3, 231 (1927); E. J. Allin and H. J. C. Ireton, *ibid.* **21**, Sec. 3, 127 (1927).

[17] C. E. St. John, C. E. Moore, L. M. Ware, E. F. Adams, and H. F. Babcock, *Revision of Rowland's Preliminary Table of Solar Spectrum Wave-Lengths* (Carnegie Institution of Washington, 1928) publication no. 396; cf. H. N. Russell Astrophys. J. **70**, 11 (1929).

[18] C. E. Moore, *A Multiplet Table of Astrophysical Interest* (Princeton University Observatory, 1933); *Atomic Lines in the Sunspot Spectrum* (Princeton University Observatory, 1933).

TABLE I—*Continued.*

$351_4°$ 35116.73 1.2*B*	$353_2°$ 35311.46 1.0*C*	$354_2°$ 35499.10 1.0*C*	$357_2°$ 35731.92 1.5*C*	$359_2°$ 35943.17 1.4*C*	$360_4°$ 36082.27 1.24*B*	$361_1°$ 36190.42 1.62*A*	$362_2°$ 36275.08 1.27*B*	$366_2°$ 36673.67 1.50*B*	
	3 +09		5*rKz* +06			4*rZ* +02		4*Kz* −05	D_0
3*K* +08	2 +03	—	6*rKz* +03*C*	—	64*Kz* +02	4*rA*?*z* +02		5*AKZ* +07	D_1
—	—	4*z* +08	2 −02	1 −01		5*rKz* 00		5*z* 00	S_2
5*Kz* +08	—	2*z* +14*C*	—	1 +05	5*Kz* +02			1 +07	D_2
2 +02		—		2*z* −03	—		5*K*?*z* 00		D_4
3= −03		2*z* +01		2*z* +02	—	—	2*z* +02		09_0
	1 −03		2 −02			1 00		1*z* 00	12_4
2 −03	3*z* −02*C*	2= −04	3 −04	—	0 −13			3*z* −01	13_2
	3= 00	—	1= +02	0*u* −32		3*Z* 00		1*u* 00	13_2
	2 00	—	—	0 +04		3 −02		—	14_2
2*z* 00*C*		—		3 −03			1 −02		15_3
0 +01	—	—	2 00	0 −10	—			—	15_3
—		3 −01		—	—		—		16_4
							0*u* −01		17_6
0*u* +1		0*u* −10*c*		—	0 +14		—		17_4
—	2 00	0*z* +13	—	—	0 −11			0 +16	17_2
	—		2*u* +11*C*			0 +04		—	18_4
	0*u* −13	—	1 00	1 +18		1*u* −44		—	18_2
	1 +35	0*u* −12	1 +02	0 +01		—		—	$18_2'$
1 −04	1 +11	2 +02	4 −08	2*u* −04	—			4*z* −01*C*	18_2
	1 −11	2 +25*C*	1 +21	0*u* −01		2 +01		—	19_2
2 +12		2 −10*C*		0*u* 00	—		1*u* −07		19_4
2 −05					2 +01		—		19_5
							4 +02		19_6
4 −10					—		0*u* −1		$19_4'$
—	0*u* +26	0*u* 0	4 −01	4 −11	—			1 00	19_2
	—		3 −01		—	1*u* +18		2 −00*C*	20_4
	—	—	2 −04	1 −10	—	3 00		2*C* +13	20_2
						—			21_6
2 −03	—	—		—	1 +01		1 −04		22_4
—					—		1 00		22_6
2 +12	—	2 −22	2 +01	1 −02	—			—	23_2
									28_6
									43_1
									44_2
									45_0
	—		.4 −03			.1 +24		.0 +03	46_1
—	—	—	—	—	—			—	46_2
							—		47_4
—	—	—	—	—	—	1 +14		—	48_2
					—		1 +10		49_5
2 +02	—	—	—	1 −04	1 +05			—	49_2
1 +15				—	—		2*u* −01		51_4
—	—	—	—	—	—	—		—	52_{22}
	—	—	—	—		—		0 +22*C*	53_1
—		—		—	—		—		55_4
—					—		—		55_6
—					—		0 +04		$?58_5$
$351_4°$	$353_2°$	$354_2°$	$357_2°$	$359_2°$	$360_4°$	$361_1°$	$362_2°$	$366_2°$	

lines in the sunspot spectrum. On the disk, sure identifications have been made of at least one line for each of the lowest 6 levels (none for any higher even levels), and in the spot spectrum 5 lines, 2 unquestioned and 3 questioned ones, arise from $d^5s\ ^7S_3$, and the rest, 1 unquestioned and 3 questioned ones, from various $d^4s^2\ ^5D$ levels.

(c) Previous Publications of Levels

Incidental to his Zeeman effect work, Jack[19] tried to find series in tungsten with the aid of Preston's rule. He allowed a tolerance of about 2 cm^{-1}, and all his differences are meaningless. Paulson[20] made a rectangular array in which two differences, D_2-D_1 and 239_2-214_1, are real. In 1925 Laporte[21] published a preliminary extract from an array of about 70 levels which was the forerunner of our Table I. Most of the material that now comprises our final report has been communicated privately to several workers, and some of it has been published with our permission.[22,23] The most important general papers on

[19] R. Jack, Diss. Göttingen (1908); Ann. der Physik **28**, 1032 (1909).

[20] E. Paulson, Diss. Lund. (1914).

[21] O. Laporte, Naturwiss. **13**, 627 (1925).

[22] Bacher and Goudsmit, *Atomic Energy States* (McGraw-Hill, 1932). We have rejected six levels of this tentative list.

[23] C. E. Moore, *Term Designations for Excitation Potentials* (Princeton University Observatory, 1934).

TABLE I—*Continued.*

	$368_2°$ 36874.31 1.50*A*	$369_2°$ 36904.11 1.57*B*	$371_4°$ 37146.29 1.1*C*	$372_6°$ 37297.5	$373_5°$ 37309.13 1.25*B*	$374_2°$ 37466.26 1.28*B*	$376_3°$ 37674.04 1.13*A*	$377_1°$ 37773.94	$380_4°$ 38001.10 1.1*C*
D_0								0 +40	
D_1		3 −06				0 −11		4r*z* −02	
S_2	8r*MH*?*A*?*KZ*−03	7r*MHAKZ*−07	4*A*? +02			6r*MHA*?*KZ* 00	5r*MH*?*A*?ζ 03		—
D_2	5*Kz* +06	3 +07				2 00	4*z* +02	2 00	
D_3	3*K* +08	1 +10	5*Kz* +04			3 +07*c*	6*K*= −10		3*z* +01
D_4	3 +12		2*z* +04		2*fGKdz*−17		2 +02		3 +03
09_2								0 +18	
12_4	—		3ζ +01		3*z* 00		2*z* +02		0 −28
13_1		0 +19				2*z* +14*C*		—	
13_3	2 00	—	0 −03			2*z* −02	4 −01		1*z* −07
13_2	0 −05	—				0 −12	—	2 00	
14_2	2 00	2 −01				2 −01*C*	0 −05	—	
15_5			—	0 −2	3 −02				—
15_3	3 −04	3 −02	3*z* −03			2= −03*c*	—		—
16_4	1 −04*C*		—		2 −02		2 −02		3= −05
17_6				—	0 +06				
17_4	—		—		0 +15		—		—
17_3	0 −01	—	0 −13			0 −14	—		—
18_1		—				—		0 +02	
18_2	0*u* +3	—				—	0 +05	—	
$18_2'$	—	—				—	0*u* +15	0 −09	
18_3	—	0*u* −11	—			0 −18	—		—
19_2	1 +49	0*u* 0	—			0 +09	0 00	1 00	
19_4	2 −11		0*u* +05		1*u* −19		0*u* −06		—
19_5			2 −01*C*	—	—				0 −21
19_6				2*u* +2*C*	2 +21				
$19_5'$			0 −01	0*u* +1	—				2 −33
19_3	2 00	1 −14	—			—	0*u* +1		0 00
20_1		1 +02				—		—	
20_2	3 −01	—				2*u* +17	2*d* +07	1 −01	
21_0								—	
22_4	1 −21		3 −02		2*u* +15		—		1 −12
22_5			—	2 +2	1 +01				—
23_3	—	—	—			—	—		—
28_5									—
43_1									
44_2									
45_0									
46_1		—							
46_3	—	—							
47_4	—		—		—		—		—
48_2	.3 −01	—				—	—	—	
49_5			—	—	—				—
49_3	—	—	1 −07			—	—		1 +03
51_4	?1*d* +43		—		2 −02		1 −07		—
52_{23}	—	—	—			2*u* −21*C*	—	—	—
53_1	—	—				—		1*u* +17	
55_4	—		—		0*u* +5		—		—
55_6			—	0*u* −3	—				—
75_5			—	—	—				—
	$368_2°$	$369_2°$	$371_4°$	$372_6°$	$373_5°$	$374_2°$	$376_3°$	$377_1°$	$380_4°$

the spectrum that have appeared recently[24] are the extensive work of Catalán and Poggio,[25] who listed 42 real levels not previously published, of which 29 had been independently placed on our list. We gave up our intensive search for levels several years ago, supposing that the law of diminishing returns made further search useless. Laun[26] has reported several levels, including the

[24] Although this paper does not purport to cover more than the extranuclear structure of the atom, it should be recorded in this section that N. S. Grace and K. R. More, Phys. Rev. **45**, 166 (1934), studied the hyperfine structure of a few lines associated with the $d^4s^2\ ^5D$ (but none associated with d^5s^7S) and found separations into three components with a total spread of about 0.1 cm^{-1}, which they reconciled with the level scheme by ascribing to each of the ^5D levels among the various isotopes, the following spread with respect to the rest of the levels of the spectrum: Isotope 182, most stable; Isotope 183, nuclear angular momentum $I=\frac{1}{2}$, levels doubled and components approximately coincident with isotopes 182 and 184, respectively. (This might have been tested by an intensity study of a D_0 line.) Isotope 184, about 0.05 or 0.06 cm^{-1} less stable than 182. Isotope 186, about 0.09 to 0.11 cm^{-1} less stable than 182.

[25] M. A. Catalán and F. Poggio, Ann. Soc. Espan. Fisica y Quimica **32**, 255 (1934); Zeeman Verhandelingen (1935), p. 387; F. Poggio, Ann. Soc. Espan. Fisica y Quimica **33**, 171 (1935). We have rejected 13 Catalán-Poggio levels.

[26] D. D. Laun, Phys. Rev. **48**, 572 (1935); J. Research Nat. Bur. Stand. **21**, 207 (1938). Laun's report included some levels that were already in Catalán and Poggio's or our array, and some that we have rejected; of the Laun levels that we have incorporated in our list, we have altered several J values.

TABLE I—*Continued.*

$380_2°$ 38052.98 1.11*B*	$382_6°$ 38203.03	$382_3°$ 38206.32	$382_4°$ 38259.34	$?384_1°$ 38429.82	$387_4°$ 38748.43	$390_2°$ 39030.23	$391_1°$ 39183.17 1.01*C*	$393_3°$ 39360.98 1.13*C*	
				—			1*MAZ* −14		D_0
				—		2 −34	3*A*? −25		D_1
3*MAKZ*−06		3 −03	5*MsAKz*−06		5*Mz* −07	4*rMz* −01			S_2
4*M* +01		4*MuA*?*Kz*−06		2*M*? −17		4 −04	2 −03		D_2
5 −23		3 +02	3 +02		6*H*?*A*?*z*−04	4*A*?*z* −05			D_3
2 +01		3 +03	3*Kdz* +02		1*A*?*K*? −09*c*			5*z* −03	D_4
				0 +01			—		09_0
2 +09		4*fz* −03*C*	2 −02		—			3*z* +02	12_4
		—		2*z* +28*C*		2*z* +02	1 +05		13_1
2= −01			0*z* −06	—		3*z* −02			13_3
(*Cz* +42)		2 +07		1*z* +39*C*		3*z* +01	3*z* +03*C*		13_2
3*z* 00		0 +27		—		—	—		14_2
	—		0 +04		3*z* −01			2*z* 00	15_3
1 00		2 −02	3*z* −01		1 +17*C*	3*z* −01			15_5
2 00		0*u* −39	0*u* +16		0 +16			—	16_4
	2 00							1 −03	17_6
—		2 −01	1 00		—			1*z* −04	17_4
0*u* +07		0*u* +26	—		0 +04	0 +08			17_2
				—		0 +10	—		18_1
0 −03		0*u* +07		—		0*u* −21	2 00		18_3
0 +08		0 00		0 +05		—	—		$18_2'$
—		—	3 +01		—	0 −04	—		18_2
0 +1		0 +16		—		—	—		19_2
—		2 −03	—		—			0*f* −01	19_4
	0 +09		0*u* −01*C*		3 −04			—	19_5
	0*z* −01							0*u* −30	19_6
	1 00		0 −07		0 −08			0 +07	$19_4'$
—		0 −01	1 +02		—	3 +02			19_3
				0*u* +06		3 −02	—		20_1
1 +01		—		—		—	—		20_2
				—			—		21_0
—		—	—		2 −01			0*u* −05	22_4
	—		—		—			1*u* +11	22_5
—		1 −04	—		2*u* −12*C*	1*u* +04*C*			23_2
	—		—		.1 +10			.3*u* +12	28_5
									43_1
									44_2
									45_0
									46_1
									46_2
—		—	—						47_4
—		.2 −06	—		—			—	48_2
	—		—						49_5
—		—	—		.2 −02*C*	—			49_3
—		—	—		—			1 −06	51_4
—		—	—	—	—	—	—		52_{23}
				2 +12*C*					53_1
—		—	—		—			0*u* +07	55_4
	—		2 00*C*		—			0*u* −16	55_5
	—		—		—			—	$?58_5$
$380_3°$	$382_5°$	$382_5°$	$382_4°$	$?384_1°$	$387_4°$	$390_2°$	$391_1°$	$393_5°$	

important low odd level 214_2 that led to our identification of the $5d^46s6p$ triads.

(d) Zeeman Effect

The early Zeeman effect measurements of Jack[19] are by far the best that have been published. Perhaps the most striking proof of their excellence, in harmony with their almost complete self-consistency within about 1 percent as shown by our analysis, is the ready explainability of the asymmetries of all six of the classified lines among his seven asymmetric pattern measurements.[27] Beining's[28] lines, on the other hand, although each one as published shows an utterly complete self-consistency to 0.001 g-value unit, are inconsistent among themselves by as much as 25 percent, as is evident from work[21] referred to by that author! We were able to use a few of Beining's data after applying an empirical correction factor:

$$g_{\text{Beining}} = g_{\text{accepted}} \cdot (0.7375 + 1.25 \times 10^{-5}\nu).$$

Catalán and Poggio[25] give g values for 95 levels, if we include Laporte's[21] g values and omit levels we have rejected. They use the same experimen-

[27] J. E. Mack and O. Laporte, Phys. Rev. **51**, 291 (1937).

[28] H. Beining, Zeits. f. Physik **42**, 146 (1927). We have estimated intensity trends from Beining's interpretations, and corrected several evident misprints in this paper.

TABLE I—*Continued.*

	$396_0°$ 39613.98 1.20*C*	$396_1°$ 39636.56 1.44*C*	$396_2°$ 39646.35 1.46*B*	$397_2°$ 39707.02 1.00*C*	$397_4°$ 39719.90 1.17*B*	$400_2°$ 40011.44 1.0*C*	$402_4°$ 40233.91 1.53*A*	$402_2°$ 40269.29 1.03*B*	$404_4°$ 40411.05 1.58*A*
D_0		0 +01							.7 +08
D_1		3*MAz* −22		0 +24		2*Mz* −18			3*M*?*z* −19
S_2			4*MzA*?=−04	2*A*? −10*C*	4*Msz* −06	2 −21	4*MAz* −17	3*A* −08	
D_2		2 −01	—	2 −03		3*z* −26		?1 −11	3*Mz* −19
D_3			3 −03	2*M*?*A*?−06	2 −01	3*z* 00	2 −01	—	
D_4	4*z* +03		3 +01		3 00		3 +02	4 −13*c*	
09_0		3*Z* 00							?3*Z* +01
12_4	—		3*z* +03		—		0 +04	—	
13_1		0 +25*C*		—		—			2 +22*C*
13_3			2*z* −04*C*	4*z* +03	0 −41	—	—	—	
13_2		2 +01*C*	—	3*z* +02		4*z* +10		4*fz* +07	—
14_2		3*z* −02	0 −08	1*z* −04		—		3*z* +01	2*z* +10*C*
15_5	2*z* +01				0 +51		0 −09		
15_3			1*d*= −53*C*	1*z* −02	2*z* +04	2*ζ* −02	2*z* 00	1 −01	
16_4	2 +02		0 −11		1 00*C*		2 +05	0 −09	
17_6	0 −24								
17_4	2*z* +03		0 +08		2*z* +02		1 +02	—	
17_2			—	(*C* +37)	0 +13	0 −01	—	—	
18_1		—		0 −08		2 −01			0*u* +15
18_2		—	—	0 +10*C*		—		3*z* −01	6*dY* +09*C*
$18_{2'}$		1 −01	2 00	0*f* +04		—		3*z* 00	2 00
18_2			—	—	0*u* +35	2 −04	3 −01*C*	1 −04	
19_2		—	2*f* +02	—		1 +02		0 −01	3 00
19_4	1 +01		0*f* +01		—		0*u* −05	4*Kz* +23*C*	
19_5	—				—		—		
19_6	0 +12								
$19_{6'}$					0*u* −19				
19_2			0 +10	0*u* −10*C*	0*u* +07	0*f* +15	—	—	
20_1		3 +01		—		—			0 −06
20_2		—	0 +12	0*u* +25*C*		—		—	?2 +42
21_0		—							—
22_4	2 −05		2 +01		—		0*u* +11	0 +17	
22_5	1*f* −01				0*u* +12		—		
23_2			1 00	—	1*u* +15	—	—	—	
28_5	—				—		—		
43_1									
44_2									
45_0									
46_1									
46_2									
47_4									
48_2									
49_5	—				—				
49_3				—	—				
51_4	—		?1 +44		—		—	—	
52_{23}		—	—	—	—	—	—	—	—
53_1		—		—		—			—
55_4	—		—		—		—	.1*u* +06*C*	
55_5	—				—		2*u* +24*C*		
?58_5	—				—		—		
	$396_0°$	$396_1°$	$396_2°$	$397_2°$	$397_4°$	$400_2°$	$402_4°$	$402_2°$	$404_4°$

tal data and the same general methods of reducing unresolved patterns[29] as we. Our agreement is on the whole very good. In all except 15 of the 92 of these levels for which we had already independently calculated g values, their values and ours agree within 10 percent, and in most cases the agreement is considerably better.

We have had access to Ellingson's[30] new Zeeman effect data from plates taken at Wisconsin. Just as this report is about to be submitted for publication, Professor Harrison has very kindly sent us some remarkable Zeeman effect plates taken in very strong fields with the new M.I.T. magnet.[31] Preliminary g data[32] from these plates indicate values appreciably more self-consistent than Jack's, justifying a general reconsideration of the g values, which is under way.[30] A few tentative results of Ellingson's or our investigations of the Wisconsin or M.I.T. plates are incorporated in our tables with no attempt to differentiate them from the older work by means of any distinctive symbols.

[29] A. G. Shenstone and H. A. Blair, Phil. Mag. **8**, 765 (1929).

[30] E. Ellingson, in preparation.

[31] F. C. Bitter and G. R. Harrison, Phys. Rev. **56**, 15 (1940).

[32] J. H. Roberson and J. E. Mack, Phys. Rev. **55**, 1126 (1939); **57**, 1074 (1940); J. H. Roberson, J. E. Mack, and G. R. Harrison, Phys. Rev. **58**, 895 (1940).

TABLE I—*Continued.*

$404_5°$ 40476.37 1.04*B*	$405_4°$ 40582.99	$406_3°$ 40665.84 0.96*C*	$407_1°$ 40770.74 1.28*C*	$408_2°$ 40868.31 1.26*B*	$409_5°$ 40911.92 1.03*C*	$409_3°$ 40923.77 1.32*B*	$411_2°$ 41104.46 1.5*C*	?$411_0°$ 41127.28 0/0	
			.7*MZ* −03						D_3
			2*M* −18	1*z* −12			2 −37	2*M* +03	D_1
	4*MAy* −19*C*	—		—		3*M* −22	—		S_2
		3*MA* −29	1*A*? −30	3*MAz* −24		0 +01	3*z* −28*C*		D_2
	2 −07	3 −02		5*rAz* 00		4*rz* −01	3 00		D_3
4*A*?*Kz* +01	—	2 +02			—	2 −02			D_4
			—						06_0
1*z* +04	2 +05	2*z* +01			0 +21	3*z* +05*C*			12_4
			3*z* 00	3*z* +08*C*			0 −06	—	13_1
	1 +08	—		2 00		3= +04	0 −02		13_3
		—	2*z* +10	3*A*?*z* +08		—	1 +10		13_7
		—	2*z* −01	2 +17*C*		1 −01	2*z* −07*C*		14_2
—	—				2 +01				15_5
	2*z* +04*c*	—		0 +13		2*z* +01	—		15_3
—	1 +07	—			1*z* −04	—			16_4
					0 −07				17_6
1 +03					2= *y* +03	0 −09			17_4
0 +10	1*z* −27	—		—		0*u* +10	—		17_3
	—	2 −06	1 −01	(*C* +32)			—	1 −02	18_1
		?*ou* −44	1 −03	2*z* −01		—	0 −02		18_2
		—	2= −18*C*	—		0*z* −10	1 00		$18_2'$
	—	1 +05		1 −04		0 +03	—		18_3
		0 +13*C*	2 00	0 +08		4= +09*C*	—		19_2
2 −05	1 −07	—			—	—			19_4
3 −02*C*	—				3 −05				19_5
—					0 −05				19_6
—					—				$19_5'$
	—	2 00		1 +02		—	2 00		19_3
			0 +10	1 −01			1 00	—	20_1
		—	0 −07	0 +09		0 00	0 +12		20_2
			0 0						21_0
0 +08	—	1 00			1*u* +02	2 00			22_4
—	—				—				22_3
	1*u* −02*C*	0*u* +2		—		—	0 −05*C*		23_3
1 +02	—				—				28_3
									43_1
									44_2
									45_3
									46_1
									46_2
									47_4
									48_2
									49_3
									49_2
.2 +15	1 −25	—			—	—			51_4
	—	—	—	—		—	—		52_{23}
			—	—			—		53_1
—	—	—			—	—			55_4
—	1 +25				—				55_3
—	—				—				?58_5
$404_5°$	$405_4°$	$406_3°$	$407_1°$	$408_2°$	$409_5°$	$409_3°$	$411_2°$	?$411_0°$	

The unusual magnetic interaction of the levels of 214_1 and 214_2 has been pointed out:[32] In moderately strong magnetic fields their sublevels of the same M value repel one another in such a way as to give rise to extremely asymmetric Zeeman effect patterns. Harrison's plates show several other similar but less marked interactions. Further work is being done on this phenomenon.[33]

3. INTERPRETATION

(a) Low Even Levels

The actual distribution of the levels of W I can be seen from Fig. 1. The low even levels belong to the configurations $5d^46s^2$, $5d^56s$, and possibly $5d^6$. The levels arising from these configurations are well known to be:

d^4s^2 or d^6: $^5D\ ^3PPDFFGH\ ^1SSDDFGGI$,
d^5s: $^{7,5}S\ ^{5,3}PDFG\ ^{3,1}SPDDDFFGGHI$.

Immediate results to be read from Fig. 1 or from the observed values are that the lowest six levels are $5d^46s^2\ ^5D_{01234}$ and $5d^56s\ ^7S_3$ and that in certain obvious respects these six levels, like the lowest levels of most spectra, exhibit strong resemblances to LS coupling properties. There might still exist some doubt as to which of the two $J=3$ levels is $^7S_3$ and which $^5D_3$, or more cor-

[33] J. H. Roberson, in preparation.

TABLE I—*Continued.*

	411₄° 41198.05 1.22*B*	414₆° 41417.43 1.23*A*	414₃° 41499.37 1.11*A*	415₂° 41583.16 1.06*B*	416₃° 41694.28 1.28*A*	417₂° 41734.07 1.1*C*	418₄° 41871.91 1.11*C*	419₂° 41978.60 0.8*C*	422₃° 42251.45 1.32*B*
D_0									
D_1				2*Mz* −25		.9*Mz* −05		.8*Mz* +03	
S_2	3*MA*?*z*−14		0 +02	2 −30	3*M*? −23	0 +49*c*	2 −17	0 +41	—
D_2			1 −29	3*MA*?= −20	2 −14	2*z*? −23		0/*A*? +22	2 −30
D_3	4*rAz* +02		0 +28	1 −08	—	3*z* −12	2 −17	2 −28	3*Mz* −26
D_4	3 −07		4*MZ* 00		5*rz* −09		1 −01		5*rMz* −01
09_0									
12_4	3 −06		1 +04		—		0*u* +14		—
13_1				1*z* +02		0 +36		—	
13_3	1 +06		1 00	2*z* +01	—	3*z* +01	—	1 00	—
13_7			—	0 +07	—	3*dz* +07		2*z* −01*c*	—
14_2			3*z* +04	1 +01	3*fz* +04	—		3*z* +04	—
15_4	2*z* +11*C*	3*z* +04					—		—
15_2	—		0 −02	0 +28	—	0 −18*C*	0 +35	3*z* +02	—
16_4	—		1*z* −02		—		—		—
17_6		3*z* −02							
17_4	1*z* +04		0 −15		1*z* −02		3*z* −20*C*		1*z* +03*c*
17_3	0 +28		—	?1*uz* +36	—	1 00	—	—	—
18_1				2*z* +01		1 −02*c*		1*z* −04	
18_2			3*z* 00	(*Cz* −38)	2*z* +01	1*z* 00		—	2*z* +01
$18_2'$			1 −01	1*z*? −02	3 +03	—		2 +01	3*z* +02
18_3	2 −03		2*z* −04*c*	2*z* −05	1*f* −04	—	3*z* 00	3*z* −09	—
19_2			2*z* 00	0*u* −07	—	—		?0 −37	3*z* −01
19_4	0*u* +17		2*z* −04		2*z* −02		3= −01		2*z* −04
19_5	1 −01	0 +23					0 +22		
19_6		2= −06							
$19_5'$	3*z* −01	0*u* +05					2*z* +01		
19_3	—		—	—	1 −02	3*z* −01	3*z* 00	—	2*z* +01
20_1				0 +04		0*u* +04		—	
20_2			0*u* +02*c*	—	0 −12	2*c* +06		0*u* −14	(*Cz* +37)
21_0									
22_4	0*u* −2		2 +01		—		0 +16		1*f* +03
22_5	—	—					—		
23_3	—		0*u* +13	0 −43	—	0*u* 00	1 +13	—	2 −01
28_6	—	2 +02							
43_1									
44_2									
45_0									
46_1									
46_2									
47_4									
48_2									
49_5									
49_3									
51_4	—		—						
52_{23}	—		—	—	—	—	—	—	?.0 +37
53_1				—		—		—	
55_4	—		—		—		—		—
55_5	—	—					—		
?58_5	—	—					—		
	411₄°	414₆°	414₃°	415₂°	416₃°	417₂°	418₄°	419₂°	422₃°

rectly, what linear combination of the pure eigenfunctions represents the actual levels; but in view of the *g* values it appears safe to assert that the lower is almost purely $^7S_3$, and the higher, $^5D_3$. This is the assignment published by one of us[21] in the first paper on W I. We shall now investigate whether any even levels beyond the lowest six can be assigned, in the usual approximate sense, to configurations and, if so, whether a hint may be obtained as to other quantum numbers.

As was pointed out above, the number of known even levels is much smaller than the large number that the theory predicts for d^4s^2 (i.e., 34) and d^5s (i.e., 74). In composing a table of the levels to be expected, one is therefore first faced with the difficulty of deciding upon an approximate order in which they follow one another. Theoretical reasoning to the usual approximations as to the order of the levels is not of very great value here because different choices of the parameters would array the levels in different orders. We have here taken as a starting point in our study that order of the terms of a configuration which has been found to be correct in the Cr I spectrum.[34] Since this chromium order will serve only as a guide of the crudest sort or, in

[34] C. C. Kiess, Bur. Stand. J. Research **5**, 775 (1930); J. Research Nat. Bur. Stand. **15**, 79 (1935).

TABLE I—*Continued.*

$422_1°$ 42262.26 1.5*C*	$424_2°$ 42449.56	$425_3°$ 42514.14 1.22*B*	$425_1°$ 42573.36 1.3*C*	$426_3°$ 42601.12 1.12*C*	$428_5°$ 42865.93 1.11*B*	$429_4°$ 42910.70 1.18*A*	$430_4°$ 43034.09	?$430_5°$ 43053.82 0/0	
.8 +09			.6 +28						D_0
.9*M* +12*C*	.9*u*/*z* +09		.8*M* +10	1*MAz* −27*C*		0 +05	—	.8*M* +09	D_1
	—	—		2*Mz* −20					S_2
2 −27	1*Az* −19	0 −47	2*Mz* −14	2 −21		3*Mz* −19	?0*d* +44		D_2
	4*Mz* +05	—							D_3
		1 −49		2 −33*C*	1*u* −17	2*A*? −11	3*Az*? −13		D_4
3*A* +01			3*A*? −02						00_5
		3*z* 00		0 +20	2*z* +13	2 +12	—		12_4
1/*z* 00	0 +49		—					0 −05*C*	13_1
	—	3= −02		—		2 00	0 +36		13_3
1 +02	—	0 +11	—	3*z* +07					13_2
1 +06	—	3*z* −02*C*	—	—					14_2
					0 −07	4*Kz* +05	—		15_5
	—	0 +23		3=? +02		2*z* 00	—		15_3
		0 +06		2*Az* 00	2 +07	2 +04*C*	3/*z* +08*C*		16_4
					—				17_5
		—		—	—	—	—		17_4
	—								
	—	1= −10		1 −01		—	1 +03		17_3
	—		0 −04					—	18_1
1*uz* −02	2*z* 00	2*z* −24	—	—					18_2
2/*z* 00	0*z* −13	—	—	2*z* +03					$18_2'$
	—	—		0 −11		0 −24	—		18_3
1 −03	0 −03	—	0 +04	—					19_7
		1ζ −07		2*z* −10	2*z* 00	1 −03	3*z* −02		19_4
					—	2*z* −03	1*uz* +02		19_5
					—				19_6
					1 00	3*z* −03	4*z* −06		$19_5'$
	1 −01	0 −18		3 00		3*z* −03	—		19_3
—	0 +09		1 00					2*Z* 00	20_1
2 −02	0*u* +39	2 −06	0 00*C*	0 +02					20_2
—			—						21_6
		—		0 +09	—	2*f* −04	0*u* +25*C*		22_4
					0 −14	0 +30	—		22_5
	0 −19	0*u* +22		1*z* −22*C*		—	—		23_3
					1 −04	2 −03*C*	2 +06		28_5
									43_1
									44_2
									45_9
									46_1
									46_3
									47_4
									48_2
									49_5
									49_3
									51_4
—	—	—	—	—					52_{33}
—	—		—					—	53_1
		—		—	—	—	—		55_4
					—	—	—		55_2
					—	—	—		$75S_5$
$422_1°$	$424_2°$	$425_3°$	$425_1°$	$426_3°$	$428_5°$	$429_4°$	$430_4°$	?$430_5°$	

other words, since no detailed feature typical of Cr I will play a role in what follows, it seems that this is not too objectionable a procedure. However, any attempt to extrapolate W from Cr and Mo must reckon with two strong tendencies revealed by the $d^4s^2\ {}^5D$ and $d^5s\ {}^7S$ assignments already made: first, levels of d^4s^2 are relatively much lower in W, i.e., the configuration d^5s has lost its extra stability with respect to d^4s^2, of which it had about 8000 cm^{-1} in Cr and 11000 cm^{-1} in Mo; second, (LS) separations are enormously increased, which is a natural consequence of the increase in atomic number. (Compare the following over-all separations of the $d^5s^2\ {}^5D$: Cr 557 cm^{-1}, Mo 1380 cm^{-1}, W 6219 cm^{-1}.) In order to trace these two tendencies separately, though crudely, one might draw to scale on one strip of paper those levels of Cr I[35] that belong to d^4s^2, and on another, those that belong to d^5s; then (contrary to the actual case of Cr but in agreement with the assignments in W I) place $d^5s\ {}^7S$ in the midst of the levels of $d^4s^2\ {}^5D$; and finally, imagine the levels in each term to spread to per-

[35] We have chosen Cr I because relatively little information is available upon the analogous configurations: in Mn II, C. W. Curtis, Phys. Rev. **53**, 474 (1938); in Fe III, P. Swings and B. Edlén, Astrophys. J. **88**, 618 (1938), and in Mo I, W. F. Meggers and C. C. Kiess, J. Opt. Soc. Am. **12**, 417 (1926), M. A. Catalán and P. de Magariage, Ann. Soc. Espan. Fisica y Quimica **31**, 707 (1933).

TABLE I—*Continued.*

	?4314° 43185.41 1.3C	4321° 43217.27 1.3C	4322° 43227.64 1.3C	4324° 43250.97 1.14B	4335° 43330.81	4347° 43411.46 1.20A	4345° 43478.59 1.3C	4352° 43514.67 0.9C	4374° 43720.86
D_0		.8M? −11							
D_1		.8 +08	.8M? −21					.8 +09	
S_2	—		.8 +02	.7s +08			—	—	—
D_2		1 −06C	0 +02				.9MA? +01	.8M? −17C	
D_3	3fMz +15		2 −25	2M? −15			0 −06	?0 −56	0 +26
D_4	0 00			3M −20	—		—		1d −49
09_0		—							
12_4	—			—	—		—		—
13_1		—	—					2 +04	
13_3	0 −12		3fz +03	3f +03			2 −03	1 +04	0 +19
13_7		2z +03	0 +03				1 00	1 −10	
14_7		1 +23	2z −02				—	2z −03	
15_5	1 −08C			1z −02	4z 00C				2z +02
15_7	—		0 −04C	3z −01			1z 00	2z −01	4z +01C
16_4	—			—	—		—		3 +04
17_6					—	2z +04			
17_4	—			—	—		—		0 +01
17_3	—		0 +07	1z −02			—	4z +08C	—
18_1		—	(C −37)					2z −03	
18_2		1 −03	0z −32				2z −04	2z −04	
$18_2'$		—	—				—	0 +05	
18_3	—		1 −05	3z −03			1 +05	—	2z −06C
19_2		0 −10	0 −19				3z 00	—	
19_4	1 −16			—	0 −08		—		—
19_6	—			2f −01	—				1d=y −04C
19_6					—	3Z −05			—
$19_5'$	—			0 −09	0 +12				2z −03
19_3	—		1 −02	1u +01			(C +32)	0 −03	
20_1		2 −06	—					?0 −44	
20_2		0 −27	—				0 +20	3z +29C	
21_0		—							
22_4	—			—	0u −06		?0 −33		—
22_5	—			—	—				—
23_3	—		—	—			—	—	—
28_5	—			1 +05	(C +31)				—
43_1									
44_2									
45_0									
46_1									
46_2									
47_4									
48_7									
49_5									
49_3									
51_4									
52_{23}							—	—	—
53_1		—	—					—	
55_4	—			—	—		—		—
55_5	—			—	—				—
$?58_6$	—			2u −23C	1 +14				—
	?4314°	4321°	4322°	4324°	4335°	4347°	4345°	4352°	4374°

haps ten times the total separation of the corresponding Cr I term. In this way one would be led to realize that the dozen or so even levels, which follow ^7S and ^5D, i.e., up to perhaps 18000 cm^{-1}, are all d^4s^2 with the exception of $d^5s\ ^5S_2$, which, evidently having lost its LS character almost completely, is somewhere among them; and that the other d^5s terms, such as $^5G_{23456}$, are not among these earlier even levels. To what extent can we now identify in the energy diagram the terms $^3P\ ^3H\ ^3F\ ^3G$..... (listed here according to the order in which they occur in Cr I) which, according to theory,[2] are next in line? The levels $^3P_0$ and $^3H_6$ are immediately identified with 09_0 and 17_6, for their unique J values make them independent of coupling. The other $J=6$ level, 19_6, we identify with $d^5s\ ^5G_6$. The reason for this choice rather than the opposite one is that (LS) separations within d^5s terms are expected to be small in comparison with those of d^4s^2, and within a few hundred cm^{-1} of 19_6 there are enough levels with proper J values and g values not violently discrepant to constitute the whole ^5G term, while the nearest $J=5$ level to 17_6 is almost 2000 cm^{-1} distant.

These and further identifications are summarized in Fig. 2a in which the interpreted levels have been plotted to scale as in Fig. 1.

TABLE I—*Continued.*

$437_5°$ 43741.33 1.09*C*	$?437_6°$ 43790.0 0/0	$438_3°$ 43850.77 1.17*B*	$438_1°$ 43892.60 1.05*B*	$439_4°$ 43924.17 1.2*C*	$439_3°$ 43975.20 1.15*C*	$439_4°$ 43985.36 1.24*C*	$440_2°$ 44020.48 1.2*C*	$443_1°$ 44353.42 1.02*C*	
			.7*uf*uM +2					.8 +2	D_0
	.6 +47		.7 +20		.9u*M* +10			.3 0	D_1
		——			5 +47*c*	.6 +02	.4 +5		S_2
		.9u*MAz*+04	.8 00		.9u*Mz* +06		.9*M* +51	.7*A* +04	D_2
		3*Mz* −16			1*M*?*z* −20	——	——		D_3
——		4*MAz* +04*C*		——		2 −26	1 −40		D_4
			3*A* −03					0 +09	09_0
——		——		——		3 +06	1 +03		12_4
	2 −02	——	1 +02		——	3*A* +09	——	3 −04	13_1
		——			——				13_2
		——	0 +15		——		2 +07	2*z* +06	13_2
		——	——		——		1 −01	——	14_2
——		——		——	——	2 +04			15_3
		——			——	1 −03	3*Az* −04		15_3
2*z* +08		——		——		——	——		16_4
——									17_6
				2*z* +11					17_4
1*uf* +03		1 00		.0u +33		3*z* +01	——		17_3
		——			0 −15*C*	0 +26*C*	——		17_3
	0 −14		——		2 −05*C*			0 −14	18_1
		——	0 +08		——		3*z* −01	3*z* −01	18_2
		——	1*z* 00		1*z* +01		1 −03	——	$18_2'$
		——			2*z* −02	2*z* −05	——		18_2
		——	0*z* +09		1*z* −01		——	2*z* 00	19_2
4*z* −02		3*z* 00		——		——	3*z* −05*C*		19_4
?0*z* −35				2*z* +05		2*z* −04			19_5
									19_5
1*z* −01				2*z* 00*c*					$19_5'$
1= +02				——		2*z* −03*C*			19_2
		0 −11			1*z* +02	2 −01	1= −02		20_1
	——	1 +04	——		0 +15			——	20_2
					2*f* −17		?2*z* +47	——	
			2*Z* +2					——	21_0
——		——		2 −02		——	1*u* −09		22_4
0*u* 00				——		0*u* +17			22_5
		0 +02			——	——	——		23_5
——				2 −03*C*		0*u* −4			28_5
									43_1
									44_2
									45_0
									46_1
									46_3
									47_4
									48_2
									49_2
									49_3
									51_4
									52_{23}
	——		——		——				53_1
——		——		——		——	——		55_4
——				——		——			55_5
——				——		——			$?58_5$
$437_5°$	$?437_6°$	$438_3°$	$438_1°$	$439_4°$	$439_3°$	$439_4°$	$440_2°$	$443_1°$	

By means of inclined lines connecting levels we have indicated to what extent we believe the levels to be groupable with some justification into multiplets. Where a connecting line branches out into two such lines, a pair of levels lie sufficiently close together to destroy through interaction any decided individuality. Such a pair should, of course, be used twice. Levels 18_2, $18'_2$, and 19_2 account for $d^5s\ {}^5G_2$ and ${}^5S_2$ and for $d^4s^2\ {}^3D_2$. The ordinarily prominent g value ($g=2$) that one would expect in $d^5s\ {}^5S_2$ with ideal (LS) coupling is offset in the g-sum by the uncommonly small g value of ${}^5G_2$ ($g=\frac{1}{3}$). The g value of 20_1 strongly indicates $d^5s\ {}^5P_1$. Probably 21_0 (and perhaps 22_4) must be assigned to $d^5s\ {}^5D$, though $d^4s^2\ {}^1S$ is a possibility. Thus 20_2 and one $J=3$ level (say 17_3) are the only even levels below 21,000 cm^{-1} left unaccounted for. Since all the d^4s^2 $J=5$ levels have been accounted for, 22_5 must be ${}^5F_5$ (or possibly a ${}^3G_5$) of d^5s.

We do not attempt any further identifications among the low even levels, for there is little theoretical or empirical indication of the most likely levels to follow.

We have made an exhaustive search in this neighborhood, and believe it highly probable that all the levels below 22,000 cm^{-1} *have been found.*

TABLE I—*Continued.*

	$443_2°$ 44367.45 1.1*C*	$443_6°$ 44390.33 1.28*B*	$444_3°$ 44446.95 1.38*A*	$445_1°$ 44546.69 1.3*C*	$445_3°$ 44596.27 1.11*C*	$447_1°$ 44737.18 1.1*C*	$449_6°$ 44923.78 1.23*A*	$449_4°$ 44940.47 1.20*A*	$449_7°$ 44970.72 1.20*A*
D_0						.7 −70			
D_1	.0 −33*C*				.6 −2	.4 +3			
S_2	.6 +06		.3*m* −1		.0*f* +22			.4 −3	
D_2	.7 +48		.8*M*? −02		.7 +02	.8*M*? +06			
D_3	—		2*Mz* −14		1 −19			.7 −08	
D_4			2*A* −22	2*Mz* −22				—	
09_0						3*M* −08*c*			
12_4			—	2 +01				—	
13_1	3*z* 00				2 +02	4*f* −02			
13_3	—		—		1 +02			4*z* +10	
13_2	2 +04		2*z* +01*C*		—	—			
14_2	1 +01		—		2*z* +01	—			
15_5		0 +14*C*		2*z* +04*C*			—	—	
15_3	2 +04		3*z* +02		—			2*z* +05	
16_4			0 +18	1 00*c*				2= −04*C*	
17_6		3*z* +08		3*z* −28			2 +11		2*z* +04
17_4			—	0 +28				1*u* +05	
17_3	—		0 −03		2*z* −03			—	
18_1	0 −15*C*				1 −01	0*uf* +03			
18_2	—		0 −40*C*		2 00*C*	0 −18			
$18_2'$	0 −06		—		2 00	2*z* +08			
18_3	3*f* −04		2= +01		1*z* −05			—	
19_2	—		1 +06		1*z* −02	—			
19_4			2*z* +01	2*z* +23*C*				1*z* 00	
19_5		3*f* +17*C*		—			2*z* 00	3*z* +02*C*	
19_6		2= −01		4*fz* −04			4= 00		3*Z* −04
$19_6'$		2*z* −01		—			3*fK*?*z* +01	3*z* 00	
19_2	0 −08		2= −01		—			—	
20_1	0 −15				—	1*u* 00*C*			
20_2	1*u* +03		—		—	—			
21_0						—			
22_4			1 −02	2 −06				2 −02	
22_5		1 −21*C*		—			—	—	
23_3	—		—		0 −22*C*			2 −01	
28_5		1*u* +13		4 +01			—	2*u* +01	
43_1									
44_2									
45_6									
46_1									
46_3									
47_4									
48_2									
49_5									
49_3									
51_4									
52_{23}									
53_1									
55_4			—	—	—			—	
55_5		—		—			—	—	
758_5		1*u* +06		2 −06			—	—	
	$443_2°$	$443_6°$	$444_3°$	$445_5°$	$445_2°$	$447_1°$	$449_6°$	$449_4°$	$449_7°$

(b) High Even Levels, Series, and Ionization Potential

The apparent thinning out of the even levels from here upward is to be regarded as not real but only caused by incomplete wave-length material. As in most arc spectra, among levels of the same parity as the ground level (i.e., in this case, even) it becomes increasingly difficult in this region to establish higher levels because combinations involving them are generally faint. Of course the still higher "third set" levels again show strong combinations, this time downward to low odd levels.

The occurrence of series is the only circumstance that runs counter to the general tendency toward increasing level density and hopeless complexity with increasing energy. Among complex spectra tungsten is especially fortunately situated for the discovery of series, for a reason that we shall now outline.

If many levels of about equal probability are associated with a single value of the current principal quantum number n, the search for series is subject to all the difficulties inherent in the study of a complex spectrum. On the other hand, the identity of, say, only one or two S terms may be harder to establish than that of one or two

TABLE I—*Continued.*

$450_2°$ 45014.54 1.3C	$450_2°$ 45019.02	$451_4°$ 45116.70 1.2C	$452_4°$ 45262.51 1.1C	$?453_1°$ 45374.07	$454_2°$ 45422.24 0.63	$454_5°$ 45451.58 1.16B	$455_3°$ 45551.32 1.30A	$456_2°$ 45677.66 1.24A	
	.2 −2			.4 +2	.5M? 0				D_0
—	.4 0	.7 +08	—	—	.4 +3		.5 0	—	D_1
.7M? +03	.8M 00			—	.7 −06		.1s −4	.8M −02	S_2
.6 +03	.8M? −03C	1.0Mz +26C	.8M +03		.9M −14C		.9Mz +01	.5 +07	D_2
—		2 −25	0 +08			—	0 +27	—	D_4
				—					09_0
1 −01		2 00	2 +01			—	—	0u −3	12_4
	—			3z −08	0 +26				13_1
0 +30	—	—	—		—		1 +02	2 −01	13_2
0 +38C	2 +03C			0 +21	1 +09		2 −01	4z +02	13_2
2z +01	2 −03			0 +47	1 −06c		—	3z +07	14_2
		—	0 +12			1 +04			15_3
2z +02	1z −02	—	5K?z +10C		0f +22C		2 +11	—	15_2
—		—	—			—	0 +03	0 +08	16_4
									17_6
1z +02		—	1 00			3/z +04	—	—	17_4
1 00	0 +29	—	3z −05C		2dz −05		—	2= −02	17_3
	(C −39)			1 −06	1 +06				18_1
1z 00	—			3z −07	0 −02		—	—	18_2
2z 00	2 −27C			3A?z −09C	3=? 00C		2z 00	(C −36)	$18_2'$
—	4fz −15C	1 +01	1 00		1 −01		2z −09	2= −05	18_2
0 +03	1 −04			0 +02	—		2z +05C	—	19_2
0 +02		—	—			1z −01	3z −07C	3z +03	19_4
		—	—			—			19_5
						2z −02C			19_6
		2z +02C	0z +26			—			$19_6'$
0 +14	—	3z +02	2z +14C		2z −02		—	0 +02C	19_2
	0 +03C			—	—				20_1
1Z +02	—			—	2 −03		0 −10	1 +39	20_2
				0 +35					21_6
1 −06		2 −02	0 −07c			—	—	2z −07	22_4
		0u 00	—			2z 00			22_5
0 −10	—	2 −01	0 +07		—	—	—	—	23_2
		0u +29	—			0u −12			28_5
									43_1
									44_2
									45_0
									46_1
									46_2
									47_4
									48_2
									49_5
									49_2
									51_4
									52_{22}
									53_1
—		—	—			—	—	—	55_4
		—	—			—			55_5
		—	—			—			$?58_5$
$450_3°$	$450_2°$	$451_4°$	$452_4°$	$?453_1°$	$454_2°$	$454_5°$	$455_3°$	$456_2°$	

multiplet terms of predictable spread. The latter may be considered the optimum conditions for the discovery of series in complex spectra.

In a configuration of z equivalent electrons, l^z, there are usually several terms of the highest multiplicity; but if $z=2l+1$, there is only a term ^{2l+2}S, and if $z=2l+1\pm1$, there is only a term ^{2l+1}l. (Here we are neglecting the cases $z\leqslant 2$ and $z\geqslant 4l$, for we are considering complex spectra.) If one or two s-electrons are added, i.e., in the configurations $l^{2l}ns$ and $l^{2l}s\cdot ns$, the situation is similar, but two terms of different multiplicity are of comparable importance. Thus, in $l^{2l}s\cdot ns$ the important terms are ^{2l+3}l and ^{2l+1}l.

In the long periods ($l=2$), so long as s^2 plays an important part, the above optimum conditions occur in the sixth and eighth columns.[36] In W I in particular, $d^4s\cdot s\ ^7D$, ^5D series might be expected to be prominent. Actually, we have identified all the members of $5d^46s\cdot 7s\ ^7D$, ^5D and searched unsuccessfully[37] for higher members of

[36] Albertson (reference 1) has remarked somewhat similarly on the dependence of the prominence of series upon z for the special case of the rare earths, $z=3$.

[37] It is possible that 53_1 is in reality $5d^46s8s\ ^7D_1$, which would lead to an ionization potential near the lower limit of the range given in the next paragraph; but our failure to find any of the remaining members of the septet in spite of the close predictability of the separations argues against this supposition.

TABLE I—*Continued.*

	$457_5°$ 45789.71 1.19*B*	$458_4°$ 45869.00 1.36*A*	$459_2°$ 45902.45 0.5*C*	$460_2°$ 46067.97 1.46*B*	$461_1°$ 46104.55	$462_2°$ 46291.61 0.3*C*	$463_2°$ 46327.71 0.8*C*	$463_3°$ 46385.44 1.4*C*	$465_3°$ 46506.35 1.38*A*
D_0					.0 +05				
D_1			.7 +5		.4 −5	.6*M* +1	.3 +2		
S_2		.5 +6	.6 −3	.6 +06		.7*M*? +2*C*	—	—	
D_2			.7*D* +03	.4*f* −2	.3 0	.6 −1	.0*f* 0	.9*M* −07	
D_3		1.0*Mz* +08	.7*fM* −03	.9*uMu* −07		—	.8*A* +12	.9*M*? +04	
D_4	0 +01	1*MAz* −12*C*		2 −23				.8 −03	1.0*Mz* −08*C*
09_0					2 −10				
12_4	3 +03	0 −01						2 −01	—
13_1			—		1 +03	—	0 +34		
13_3		3 +03*c*	0 −04	3 +01*C*		—	0 −15	—	
13_7			1 +06	1 00	0 −05	—	—	0 −24	
14_7			—	—	—	1 +02	—	3 −03	
15_5	4*z* +08	—							—
15_7		—	—	0 +21		—	1*u* +08	2*z* +01	
16_4	1 00	—		0 −10*C*				0 −12	0 +05
17_6	—								—
17_4	3*z* −05	3*z* −13*C*		0 +20				—	—
17_3		—	(*Cz* −41)	1*z* 00		—	0 −24	?1 −48	
18_1			0 +13		0*u* −07	—	—		
18_2			0 −05	—	—	2*z* −04	1 +04	—	
$18_2'$			—	1 −01	0 +08	3*z* +02	—	—	
18_3		—	—	3*A*?*z* −01*C*		—	—	0 +04	
19_2			2*z* +08	1 +01	—	0 −03*C*	—	2*z* −01	
19_4	2 −03	—		—				2*z* −03	3*z* +02
19_5	—	2*z* +06						—	—
19_6	2*uz* −06								3*Az* −03
$19_5'$	—	—							—
19_3		—	1 −04	0 −33		—	—	2*z* −03	
20_1			2 −06		1 00	1 −04	—		
20_2			0 00	—	—	0 +16	—	—	
21_0					—				
22_4	—	2 +05		—				0 +01	1*z* −03
22_5	—	0 +11							—
23_2		3*r* −12	—	1 −06		0*u* −38	2*z* 00	0 −16	
28_5	0*u* +09	—							—
43_1									
44_2									
45_0									
46_1									
46_2									
47_4									
48_2									
49_5									
49_3									
51_4									
52_{23}									
53_1									
55_4	—								
55_5	—								
?58_5	—	—							—
	$457_5°$	$458_4°$	$459_2°$	$460_2°$	$461_1°$	$462_2°$	$463_2°$	$463_3°$	$465_3°$

this series and for members of the $5d^5 \cdot ns\ ^7S$, ^5S series. The intervals and g values in the D series may be studied in Fig. 3 and Table III. The distributions of the intervals are quite similar; and in particular the distribution in $5d^46s7s\ ^7D$ is remarkably like that in the limit term W II $5d^46s\ ^6D$. The sagging of the middle levels of $5d^46s\ ^6D\ 7s\ ^5D$ compared with those of $5d^46s7s\ ^7D$ might have been expected from a qualitative consideration of the Landé interval rule. The over-all separations of $d^4s^2\ ^5D$, $d^4s \cdot s\ ^7D$, and $d^4s \cdot s\ ^5D$ may be predicted,[38] in an LS coupling approximation, to have the relative values

$$\tfrac{14}{15}\Delta\nu(d^4s^2\ ^5D) = \Delta\nu(d^4s \cdot s\ ^7D) = \Delta\nu(d^4s \cdot s\ ^5D).$$

The interpretation of these higher levels opens the way for the spectroscopic determination of the ionization potential. The application of a Rydberg formula to $5d^46s(^6D)ns^5D_0$ for $n=6, 7$ yields a limit of 66,299 cm^{-1}, which is brought by a Ritz correction of (-2.8 ± 1) percent to 64.4 $\times 10^3$ cm^{-1}. The 2.8 percent correction, estimated from other spectra, is not so reliable as similar estimates in other parts of the periodic table because of the paucity of data in the neighborhood of tungsten. Since the limit $5d^46s\ ^6D_{\frac{1}{2}}$ is, according

[38] O. Laporte, *Handbuch der Astrophysik* (Berlin, Springer, 1930), Vol. 3, Part 2, p. 644.

TABLE I—*Continued.*

$466_4°$ 46625.03 1.14*B*	$466_6°$ 46672.15 1.18*B*	?$467_7°$ 46755.26	$468_2°$ 46806.40 1.1*C*	$468_5°$ 46854.76 1.21*B*	$469_4°$ 46931.81 1.0*C*	$470_2°$ 47079.36 1.3*C*	$473_2°$ 47337.76 0.9*C*	$473_8°$ 47361.69 1.3*C*	
			—			.4 +5	—		D_0
—			—		.7 +7	—	—	—	D_1
			.6 −3			.6M? −4	.6 −2	.3 −1	S_2
.4 +2			.7 −2		.9 +15	.8p′ −12	.6 +2	.7 −3	D_2
.9Mz −01				.8 −04	.8Mz +04*C*			.7d −14	D_3
2 00*C*				—	2 −02			1u −08	D_4
			—			3 +01	1 −03		09_3
0u +26			1 −04		3 +05*C*	1 +02	2 −04	2 −02	12_4
			3z −01			3 −01	—	—	13_1
—	4z +05		3 +04			—	2 −03	—	13_2
1 +03			3f +02	?0 +46	2 +02	—	3 +02	1u +02	14_7
—				0 +07	—	—		2 +02	15_5
	0 −03	1 −10*C*		—					15_2
0 +01				—	0 −41			—	16_4
0 +10			0 +32		—	—	0 −03	1 00	17_6
			0 −06			0 +25	—		17_4
			—			2z 00	—	—	17_3
			—			0 +23	—	—	18_1
0 +08			0 −02		—	—	0 +36	2z −05	18_2
0 +03			0f −20	3z 00	—	—	2z −01	—	$18_2'$
—	3z −03			1z +02	1 +01*c*			—	19_2
	3= 00	5z 00		3z −02					19_4
3z −04	0 +16			2z +02	—				19_5
—			—		2 +04*C*	—	—	3z +07	19_6
			—			—	2z 00		$19_6'$
			—			—	0 +08*C*	—	19_8
—				1 +19	—			0 +00*C*	20_1
—	—			0 −12	—				20_2
0 −13			—		1 −07	1 −05	1u −04	3 −03	21_0
(C +37)	—			0 +31	—				22_4
									22_8
									23_8
									28_8
									43_1
									44_2
									45_0
									46_1
									46_3
									47_4
									48_2
									49_5
									49_2
									51_4
									52_{23}
									53_1
									55_4
									55_5
—	1 −03		—	—	—				?58_5
$466_4°$	$466_6°$	?$467_7°$	$468_2°$	$468_5°$	$469_4°$	$470_2°$	$473_2°$	$473_8°$	

to Laun,[26] the normal level of W II, we have[37, 39, 40] for the ionization energy:

W I $5d^4 6s^2\ {}^5D_0$ = W II $5d^4 6s\ {}^6D_{\frac{1}{2}}$
= (7.94±0.1) volts.

Russell's[41] estimate of 6.7×10^4 cm^{-1} = 8.1 volts was obtained from our data at an earlier stage by considering S_3, 46_3 as members of a $d^5ns\ {}^7S_3$ series and subtracting two percent as a probable Ritz correction.

(c) Odd Levels

In the past there has been no successful attempt to assign quantum numbers other than J to the odd levels.[42, 43] We are essaying the in-

[39] We ought to mention, but we give no weight to, the possibility that a whole series member has been missed in the difficult region 34×10^3 to 42×10^3 cm^{-1}, which would bring the ionization energy down to 6.4 volts. This region has been searched without result.

[40] Of course the ±1 percent and ±0.1 volt recorded here represent only a crude guess as to our error.

[41] H. N. Russell, Astrophys. J. **70**, 11 (1929).

[42] Laporte, reference 21, misidentified the levels 214_1, 239_2, and 261_3 as a ^5P term.

[43] A. T. Williams, Comptes rendus **199**, 1201 (1934) made the following attempts at assignment of L and S by comparison with Cr and Mo, without benefit of g value:

$214_1\ {}^5P$	$347_1\ {}^5F$	$382_4\ {}^7P$
$239_2\ {}^5P$	$361_1\ {}^5D$	$387_4\ {}^5F$
$261_3\ {}^7P$	$368_3\ {}^7P$	$396_3\ {}^7P$
$262_2\ {}^7P$	$369_2\ {}^7P$	$397_2\ {}^5P$
$278_4\ {}^7P$	$376_3\ {}^7P$	$402_3\ {}^7P$.

TABLE I—*Continued.*

	474₃° 47483.70 1.29*B*	475₆° 47541.49 1.23*C*	475₂° 47593.37 1.2*C*	476₄° 47689.29 1.4*C*	478₅° 47850.76	479₄° 47968.55 1.23*B*	481₅° 48138.33 1.2*C*	481₅° 48170.53	482₂° 48244.24 1.4*C*
D_0									.6 −6
D_1	—		—	—		—		—	—
S_2			—						
D_2	.6 −4		.5*uf* −21	.6 −10		.5 +24		1*f* +1 .7*M*? 0*C*	.6*M* +3 .7 +2
D_3	.6 −02		.5 +10	.5 +33	.6 +06	—	.9*M* +11	.8*u* +11	
09_0									
12_4	3/*H* −12		0 +18	—	3/*z* 00	3 +02	—	—	
13_1									2 −08
13_3	2 +17		1*u* −04	—		3 −02		3 −08	—
13_2	0 −10*C*		—					2 +05	3 +03
14_2	0 −21		—					2 −07	2 00
15_5		—		—	6*rKz* −14*C*	?1 +44*c*	1 −03		
15_3	0*u* −34		2*f* +09	—		2 −02		2 +06	1 +03
16_4	—		2 +08	0*f* +22	—	2 +03	3 +08	—	
17_6					1 −37		—		
17_4	0 +35		?0 +52	2 +05	—	—	2 −01	—	
17_3	0 +02		(*C* −45)	—		—		—	0 −06
18_1									0 +24
18_2	1 −03		2*z* +25*C*					—	—
$18_2'$	1 +01		0 −01					—	—
18_3	2= −09*C*		1 +01			—		—	0 −21
19_2	—		0 +18					—	—
19_4	2*z* −07		0 +21	—	—	3*z* +03	0 +26	—	
19_5		0 +01		3*z* −03	—	1*z* 00	—		
19_6		3= 00			2 +03		2*z* −02		
$19_6'$		3*z* −01		—	0 +12	0 −07	1*z* 00		
19_3	0 +14		0 +26*C*	—		—		—	—
20_1									2A?*z* −01
20_2	2*z* −01		1 +01					—	3*z* −01*C*
21_0									
22_4	0*z* −17		0 −18	3/= −02	0 −10	—	—	—	
22_5		—		0 +09	0 +06	—	1 00		
23_3	(*Cz* +37)		2 00	—		—		—	—
28_5		0*u* −16		1 +02	—	0 +07	0 +01		
43_1									
44_2									
45_0									
46_1									
46_3									
47_4									
48_2									
49_5									
49_3									
51_4									
52_{23}									
53_1									
55_4									
55_5									
?58_5									
	474₃°	475₆°	475₂°	476₄°	478₅°	479₄°	481₅°	481₅°	482₂°

terpretation of individual odd levels in the region of low energy; for the rest of the levels we shall offer only a brief statistical discussion.

Even a casual glance at an energy plot of the odd levels in columns according to J value (Fig. 1) shows in the region 20,000–30,000 cm^{-1} the stepped structure that is characteristic of multiplets. Although there is hardly a semblance of Landé interval ratios, it is evident, from a qualitative study of the energies, g values, and intensities, that the levels form the pair of triads $5d^46s(^6D)6p\ ^{7,5}FDP$. Every one of the multiplets overlaps all the other five, except for the gap between the adjacent levels $^7P_4=278_4$ and $^5P_1=281_1$; and there are levels extraneous to the multiplet within each multiplet interval, except at the bottom of the ^7F. In view of this complexity the following, though probably without general significance, is a striking fact: except for the case of $^7P_4$ and $^7D_4$, the levels of each J value in the triad are ordered in energy according to S and L: $^7FDP\ ^5FDP$. Ambiguities in LS assignment, offering further possible exceptions to this regularity, occur in the three cases of 261_3 and 274_3 ($^7D_3$ and $^7P_3$), 263_2 and 276_2 ($^5F_2$ and an extraneous level, mentioned below), and 314_4 and

TABLE I—*Continued.*

$483_2°$ 48318.80 1.4*C*	$483_3°$ 48326.40	$486_4°$ 48676.18 1.20*B*	$490_3°$ 49072.09 1.26*C*	$491_4°$ 49147.95	$491_2°$ 49151.84	$491_5°$ 49187.87 1.25*B*	$492_2°$ 49270.22	$494_3°$ 49417.90	
A −6					*5f* −4	— —			D_5
—	—	—	—	—	—		—	—	D_1
6f +2	—	—	—		—		*8* +1	—	S_2
5 −1	*7* −16	—	*Sf* +68	2*u* 0	*6* 0		*6* +3	*0* 0	D_2
	8uM +47	*8uM* −02	*6* −2	3*f* −2		*7M* +10		*7M* 0	D_4
	—	—	—	—		*3MA?z* −14		—	09_3
2 −05					—		—		12_4
2 −15	—	*3Az* −24	2 −05	2 −05	1 +01		—	2 −06	13_1
2 +02*C*	2 −03		1 +03		1 +02		0 +33	—	13_3
1 +03	2 −03		1 +01		—		2 −07	1 00	13_2
	—					3 00			14_2
0 +27*C*	?2 −11	—	—	—	—		0 +18*C*	2 −09	15_5
	—	—	—	—		*1d* +04		—	15_3
									16_4
	—	1 −10*C*	—	—		—			17_6
2 +08*C*	1 +06	2 −17	2 00	3*z* −04	—	1 +09	1 +01*C*	1 +03	17_4
0 +37					0 +12		2 −01	*1d* 00	17_3
—	—	—	—		—		—	—	18_1
2*z* +06*C*	—	—	—	—	—		0 +04	—	18_2
1*f* +06	—	—	2*z* +01	—	—		—	—	$18_2'$
—	—	—	—	—	—		0 −21	—	19_2
	0 −23	2*AKz* −15	0 −01*C*	1 −03*c*		—		0 −04*C*	19_4
		—		—		2= +29*C*			19_5
		—		1 +01		2*z* +03			19_6
—	0 +31	0 +11	0 −10	0 +25*C*	—	1 +05	0 +04	0 +12	19_7
—					—		—		20_1
—	0*u* +07		0 +16		—		—	—	20_2
			—						21_0
	0 +26*C*	0 +15	—	—		2 −03		—	22_4
		—		3*z* −10*C*		—			22_5
—	—	2*z* +21*C*	1 −03	—	0 +06		0 +11	1*A*= −03	23_3
		1 +20*C*		—		—			28_3
									43_1
									44_2
									45_3
									46_1
									46_2
									47_4
									48_2
									49_5
									49_3
									51_4
									$52_{??}$
									53_1
									55_4
									55_5
									?58_3
$483_2°$	$483_3°$	$486_4°$	$490_3°$	$491_4°$	$491_2°$	$491_5°$	$492_2°$	$494_3°$	

328_4 ($^5F_4$ and $^5D_4$). Among all the levels of the two triads there is (if ?285_6 is real) no level missing, and but one extraneous level, *viz.*, the uninterpreted 276_2. The g sum for the seven $J=2$ levels is so low that, clearly, the interloper must be one of the predicted levels discussed in the next paragraph: Σg_{obs} (seven levels including 276_2) $=10.4$, Σg_{calc} (six ideal LS-coupling levels $^{7,5}FDP$) $=10\frac{1}{6}$.

A short distance above these triads is a close group of four adjacent levels 343_3, 344_2, 346_4, 347_1, with exceptionally small g values. This can only be interpreted as an indication of levels arising from the addition of a p electron to ionic levels with large L and small S, e.g., $5d^46s(^4HGF\ldots\ldots)6p\,^5I_4\,^5H_3\,^5G_2\,^5F_1$ ($g_{\text{ideal } LS}=0.60, 0.50, 0.33, 0.00$, respectively).

There is no indication that any of the six levels arising from $5d^5(^6S)6p$ are low; they would all have large g values in either (L) (S) or (LS ion) (electron) coupling.

Upon the suggestion of Professor H. N. Russell a table has been compiled which gives additional qualitative support to the above assignments of L and S values. At the top and at the left-hand side the odd and even levels were listed respec-

TABLE I—*Continued.*

	494_1° 49443.72	495_2° 49514.34 1.3*C*	495_2° 49517.26	496_4° 49636.58	497_2° 49700.02 1.9*C*	497_4° 49788.60	499_2° 49966.04	501_3° 50137.52 1.11*B*	501_3° 50185.68
D_0	—								
D_1	.5 0		.5 +5		.5 −4				
S_2		—	—	—	—	—	—		—
D_2	.2*f* −63	.6 +3	.3 +3		.5 −3		—		—
D_3		.5 −2	—	—	.6*Mu* −4	.7*M* −1	—		.4 +6
D_4		.8*Mu* −27		—		.7*f*′*M* −76	.7*M* +1	.3 −4	.6 +02
09_2	0 −33								
12_4		0 −34		—		0 +02	—	2*M*?*z* −30	1 −16
13_1	—		—		0 −05				
13_3		—	2 −02	3 −08	—	3 −20*C*	—		0 +01
13_2	1 +08*C*	—	2 −05		—		—		1 −02
14_2	—	0 −27	2 +02*C*		—		3 −14		(*C* −42)
15_3				1 −04		—		2 −07	
15_2		2 −05	—	3*z* −06	0*u* +22*C*	—	2 −01		—
16_4		—		00 +16		2 −09	0 −31	0 −33*C*	1 +01
17_6								—	
17_4		2 −05*C*		(*C* −53)		—	0 +04	?3 −55	—
17_3		—	3 +03*C*	—	—	—	2 00		—
18_1	1 −01		1 +03		0 +07				
18_2	0 +06	3*z* −02	1 +03		—		1 +04		1 +02
18_2′	—	1 +02	0 +33*C*		2*z* −02		2*K* +07		—
18_3		0 −01	0 +24*C*	—	—	—	—		2 +02
19_2	4*y* +03*C*	0 +37	0 +29		(*C* −42)		—		—
19_4		—		0 +28		—	—	—	1 +02
19_5				0 +13		—		2*z* +04	
19_6								—	
19_5′				1 +04		0*f* −12*C*		2*z* +04	
19_3		0 −04*c*	0 +12	2*z* +05	—	—	0 +09		—
20_1	1 −06		—		—				
20_2	0 +03	—	2*f* +02		—		0 +35		—
21_6	—								
22_4		0 +30*C*		0 −11		1 −05	1 −04	?0*A* −42	—
22_5				1*z* −02		1 +01*c*		—	
23_2		—	—	—	—	(*C* +33)	—		0 −14
28_5				—		0 +20		1*u* −02	
43_1									
44_2									
45_5									
46_1									
46_2									
47_4									
48_2									
49_5									
49_3									
51_4									
52_{23}									
53_1									
55_4									
55_5									
?58_5									
	494_1°	495_2°	495_2°	496_4°	497_2°	497_4°	499_2°	501_3°	501_3°

tively, not according to their position, but according to their L and S values, as if W I obeyed LS coupling. In the body of the table intensities were put, as taken from Table I. They clearly showed intensity gradations according to the old qualitative intensity rules for LS multiplets. Because all the data for the compilation of such a table are at the reader's disposal in Table I, it is not included here.

In an attempt towards further interpretation of odd levels, $N_J(\nu)$ was plotted as a function of ν, where $N_J(\nu)$ is the number of odd levels of a definite J with energy less than ν. The broken curves thus obtained were compared with the same curves derived from the odd levels of Ti I, Cr I, and Fe I, whose spectra are supposed to be rather exhaustively classified. No definite statistical information could, however, be derived from these curves since the $N_J(\nu)$ plots seem, to a considerable extent, to be independent of the number of optically involved electrons.

In view of the fact that the $N_J(\nu)$ curves for W I lie reasonably close to those for Ti I, Cr I and Fe I, one may merely conclude that in the regions investigated, the spectrum W I is now classified with a comparable degree of completion.

TABLE I—*Continued.*

$502_4°$ 50284.57 1.03*B*	$504_7°$ 50494.68	$507_3°$ 50718.85	$508_2°$ 50800.43 1.0*C*	$508_5°$ 50806.08	$508_4°$ 50894.05	$509_4°$ 50909.40 1.2*C*	$510_{34}°$ 51072.17	$511_{22}°$ 51182.48	
	—	—						—	D_0
	—	—	—		—	.0*f* +1	—	—	D_1
	—	—	—				—	.3*f* +2	S_2
.4 +6	.0 −17	.8 +6	.7 +8		.5 +4	.9 +2	—	.0*f* +29	D_3
.6 −4			.4 0	—	.5 0	—	—	—	D_4
0 +07			0 +21	1 −22	2 −17	0 −06	—	?3*Ms* +10*C*	09_0 12_4
	0*f* −02	0 +23						—	13_1
2*z* −11	0 +12	0 −14	—		0 +04	0 +07	—	0 −17	13_3
	—	—	?0*uA* +60				—	—	13_2
	—	—	2*f* +19*C*				—	2 −09	14_2
2 −01				2 −09	2*f* +34*C*	1 +31	—		15_5
—	3 −28	—	0 00		1 00	0 +10	—	—	15_3
—			—	2 −03	2 +32*C*	—	1 −02	—	16_4
				1 −02					17_6
2 +05			2 +03	3 +02	1 +09	0 +27	2 −03	—	17_4
—	—	2 −03	—		—	2 +01	1 −03	0 +11	17_3
	0 −08	(*C* +36)						—	18_1
	1 −12	0 −16	0*u* −23				—	—	18_2
	—	2 +03	(*C* +55)				?2 +03	0 −01*C*	$18_{2'}$
?0 +48	0 +38	—	1 +01		—	1 −01	1 +07	0 +09	18_5
	2 +25*C*	2*f* +05	1 +02				—	—	19_2
3*z* +13*C*			—	—	—	—	3 +18*C*	—	19_4
—				—	—	—	?2 +11*C*		19_5
				2 +03					19_6
—				—	—	0*uf* +23	—		$19_{6'}$
—	—	—	—		—	—	—	—	19_3
	0 +10	0 +07							20_1
	—	0 +19	—				—	—	20_2
									21_0
—			—	—	—	—	—	—	22_4
—				2*z* +01	0 −02	—	?0 +03		22_5
0 +27*C*	—	—	2 −02		—	2*z* +05	3=? −34*C*	—	23_6
—				—	0 −11	1 −02	—		28_3
									43_1
									44_2
									45_0
									46_1
									46_3
									47_4
									48_2
									49_5
									49_2
									51_4
									52_{33}
									53_1
									55_4
									55_5
									?58_3
$502_4°$	$504_2°$	$507_3°$	$508_2°$	$508_5°$	$508_4°$	$509_4°$	$510_{34}°$	$511_{22}°$	

4. DESCRIPTION OF TABLE I, LEVEL AND TRANSITION ARRAY, AND TABLE II, LINE LIST

(A)

Table I, the rectangular array, serves at the same time as a list of all the known energy levels[44] of W I with their properties and as a compilation of the transitions among these levels with all their pertinent data (except that on the Zeeman effect for the individual lines).

[44] Notation as to the discoverer of each level has been omitted from the already bulky Fig. 1 and Table I. Interested readers may search the papers referred to in Section 2c.

At the head of each row and each column occurs the description of a level: each row in the body of the table is headed by the description of an even level, and each column by that of an odd level. The description of each level consists of the following items, respectively:

(1) The approximate structural symbol (only if the structure is approximately known, of course). Where symbols are bracketed together they are indifferently interchangeable, e.g., it would have had as much meaning to give the level 17_3 the structural symbol $5d^56s\ {}^5G_3$ or $5d^46s^2\ {}^3D_3$ as to leave its interpretation blank; cf. Sections 3a, 3c.

TABLE I—*Continued.*

	$512_5°$ 51290.71	$?516_3°$ 51600.38	$?516'_2°$ 51606.4	$516_2°$ 51693.82	$517_1°$ 51763.28	$518_4°$ 51856.06	$520_3°$ 52015.23	$520_4°$ 52059.72	$520_5°$ 520.8112
D_0									
D_1									
S_3		—	.4 +1.5	—		—	—	—	
D_2		.4 0	—	—	—		—		
D_3		.4 −4	.0f 0	—		—	—	0 −01	
D_4	—	.7 +4				.7 +4	—	—	.9 +4
09_0					.8 +25				
12_4	2? +34	—				0 +25	2 +13	1 −11	0 +05
13_1			0 +06	—	—				
13_3		—	—	0 +18		0u +07	2 −32	—	
13_2		2A −16c	0 −05	—	—		0 −41		
14_2		—	—	0 −03	1u +01		—		
15_5	2 −03					—		—	0 +36
15_3		—	0 +36C	2 00		2 −01	—	—	
16_4	—	1u +05				—	—	—	3 −06
17_6	2 +02								1 −06
17_4	—	2 +10				2 −02	—	1 −04	1 +11
17_2		—	—	2 00		3 00	—	1 +03	
18_1			—	—	0 −09				
18_2		—	—	—	0 +02		1 +03		
$18_2'$		—	—	0 −15	—		0 +03		
18_3		—	0 +04	3 +11C		—		2 −01	
19_2		2 +10	0 −19	—	—		0u +43		
19_4	2 −04	—				—	—	?2 00	1 00
19_5	—					—		2A? +01	?0 −50
19_6	1d +04								—
$19_5'$	—					2 −02		—	—
19_3		—	—	—		—	4 +14	—	
20_1			—	—	—				
20_2		2 +29C	—	—	—		—		
21_0					—				
22_4	—	—				0 +12	—	—	0 −02
22_5	—					0u +06		—	1 +07
23_3		—	—	—		—	—	—	
28_5	—					0 +36		—	—
43_1									
44_2									
45_0									
46_1									
46_3									
47_4									
48_2									
49_5									
49_3									
51_4									
52_{23}									
53_1									
55_4									
55_5									
$?58_5$									
	$512_5°$	$?516_3°$	$?516_2°$	$516'_2°$	$517_1°$	$518_4°$	$520_3°$	$520_4°$	$520_5°$

(2) The name. If the existence of the level is doubtful, the name is preceded by a question mark. The name of each of the lowest six levels is the approximate structural symbol, abbreviated to a capital letter and subscript. The name of each of the other levels consists of the first two (for even levels) or three (for odd levels) digits in its excitation energy value, and its J value as a subscript.[45] In cases of doubtful J, both J values are used. The additional symbol "°" is used to distinguish an odd level in this table, but not in the rest of the paper, for a three-digit-and-subscript name is sufficient. In a few instances it is necessary to distinguish one of a pair of otherwise identical level symbols by a prime.

(3) The energy, measured in cm^{-1} from the most stable level, D_0.

(4) The tentative Zeeman effect g value, followed by one of the letters A, B, C, indicating its reliability. The uncertainty of g for "A" levels is about 0.01; for "B" levels, between 0.01 and 0.1; and for "C" levels, greater than 0.1.

At each appropriate row-column intersection

[45] This system has the advantages of showing the level's parity and approximate energy without requiring any more digits than if the levels were numbered serially, while at the same time the list can be supplemented to almost any probable future requirement, with no more emergency symbols than an occasional prime.

TABLE I—*Continued.*

?521₂° 52152.54	522₃° 52255.75	523₅° 52395.48	524₄° 52436.40	525₂° 52503.43	527₅° 52774.04	529₂° 52943.38	530₁° 53042.02	531₄° 53118.29	
				—					D_0
									D_1
—	—		?.2*f* +7	—		—			S_2
—	—			—		—	.0 +4		D_2
—	—		—	—		—		—	D_3
	—	.5 +2	.3 −1		.3 −1	—	.4 +4	—	D_4
									$^3D_0$
	.8 +06	.9*Mz* +08	.8*M*?*A* +04		.7*A* +08	.9 +20		.3 +1	$^1D_2$
2 −15				—			—		$^1S_1$
—	—		0 −03	—		0 +01		—	$^1D_2$
—	2 −15*C*			0 +02		0 −05	—		$^1D_2$
—	0 +47			0*f* +14		—	2*u* +40		$^3F_2$
—	1*u*/*A*? −04*C*	—	0 −04		0 −26	—		0 +36	$^3D_3$
	2*f* 00*C*	2 −04	0*f* −38	—	1 +03	2 +05		1 −35	$^3F_3$
		—	—		—			—	$^3F_4$
	—	1 −04	—		—	—		2 −02	$^3F_4$
2 +07	2 +01		1 −17	1 +38		—			$^3F_2$
—				—			—		$^1F_3$
—	—			2 00		0 −09	0 −08		$^1D_2$
									$^3F_2'$
1 00	2 +01		—	—		—	—		$^3F_3$
—	—		—	1 −06		—		2 +01	$^3F_3$
2 +10*c*	—		—	1 00		—	1 +12		$^3D_2$
	—	—	—		3 00*C*	—		—	$^3F_4$
		1 00	—		—			3 +04*C*	$^3D_3$
		1 +04			1 −01				$^3D_3$
		1*A* +04	0 −34		3 00			2 +01	$^3F_3'$
—	—		—	—		—		—	$^3D_3$
—				—			—		$^3D_1$
—	—			0 +22*C*		0 +42	2 −06		$^3D_2$
							—		$^3D_0$
	0 00*C*	—	0 +01		0*u*/*f* −42	—		—	$^1F_2$
		—	0 +21		—	—		—	$^1D_2$
—	—		—	—	—	2*z* −13*C*		0*u* +25	$^3D_2$
		(*C* +48)	—		—			0 +22*C*	$^3D_3$
							—		$^3D_3$
									$^3D_1$
									$^3D_2$
									$^3P_0$
									$^3P_1$
									$^3P_2$
									$^1S_0$
									$^5D_4$
									$^5D_3$
									$^5D_2$
									$^5D_1$
									$^5D_0$
?521₂°	522₃°	523₅°	524₄°	525₂°	527₅°	529₂°	530₁°	531₄°	

the properties of a transition are recorded, as follows:

(1) The intensity and sometimes one or more of the symbols *f*, *r*, *G*, *M*, *H*, *A*, *K*, *y*, *Z*, *z*, *ζ*, =, etc., from Table II, below, showing the character of the line. In order to give some degree of consistency to the intensities in Table I, we have divided the intensities from certain of the newer investigations ($\nu > 40{,}000$ and $\nu < 11{,}340$) by 10. Lines not given arc intensities in the first column of Table II are here given the arbitrary intensity 0. Almost all these zeros are for lines recorded only by Exner and Haschek or by M.I.T. This arbitrary zero usually, but not always, signifies low intensity. For further discussion of the intensities, see the discussion of them in connection with Table II.

(2) The discrepancy, ν_{observed} minus $\nu_{\text{calculated}}$ (to be read with a decimal point before the first digit if no decimal point is given) between the observed wave number given in Table II and that calculated by applying the Ritz combination principle to the energy values given above and to the left in Table I. This item is identical with the last column of Table II.

(3) If appropriate, one or more of the following: *c* or *C*. The same observed line fits more than one allowed transition. In case the criteria at

TABLE I—*Continued.*

	$5315°$ 53194.22 1.3C		$5324°$ 53238.39		$5334°$ 53345.60		$5332°$ 53390.44		$5362°$ 53669.42		?$5372°$ 53748.90		$5386°$ 53862.73		$5392°$ 53949.38		$5436°$ 54310.20	
D_0																		
D_1																		
S_2																		
D_2																		
D_3			.0	+2	.4	+8	—		—		.0*f*	−2			—			
D_4	.5	−1	—		—		—						—				.2*f*	+6
09_0																		
12_4	—		.6	+07	.5	+1	.0	+04					.5	−1			.5*u*	0
13_1									.4*y*	−01	.1*uf*	0			1	−19		
13_2			0	00	1*u*	−27	.0*f*	−09	.2*f*	−1	.6	−12*C*			2	−35		
13_2							—		1	00*C*	0*f*	+19			4	+10		
14_2							0	+05	0	00	—				—			
15_5	2*M*?	+04	1*f*	−24									2	−15			—	
15_3			3*z*	+29*C*	0	+36	0	+08			—				2	+07		
16_4	1*A*?*z*	−06	—		1	−26	—										—	
17_6	2	−01											0	+02*C*			1	−18
17_4	2	+49	—		1	−11	1	−06					2*A*?	−07*C*			0	+02
17_3			2	−03	0	−42	—		—		—				—			
18_1									1	−07	1	+03*C*			2	−04		
18_2							0	+03	—		2	+03			—			
$18_2'$							1	00	—		—				11	−04		
18_3	—		2	+03	—		1	−02*C*	—		—				—			
19_2							—		3	+11*C*	—				—			
19_4	—		—		—		—						1*u*	−02			—	
19_5	—		—		0	−20*C*							2	+02			—	
19_6	—												1	+01			2	+04
$19_3'$	2	+01	—		—								3	+01			—	
19_3			1	+01	3	−11*c*	0	−09	—		—				—			
20_1									1	−05	3	−13			—			
20_2							4	−09*C*	0*u*	−42	—				—			
21_6																		
22_4	—		0	+30	—		—						1	−01			2	+14*C*
22_5	—		—		0*u*	+14							—				—	
23_2			0	+18	0	+04	—		—		—				—			
28_5	—		—		—								—				—	
43_1									—		—				—			
44_2																		
45_0																		
46_1																		
46_2																		
47_4																		
48_2																		
49_5																		
49_3																		
51_4																		
52_{23}																		
53_1																		
55_4																		
55_5																		
?58_5																		
	$5315°$		$5324°$		$5334°$		$5332°$		$5362°$		?$5372°$		$5386°$		$5392°$		$5436°$	

hand do not make one assignment much more probable than the other "*C*" is placed after the discrepancy at each intersection. In case they do, for the more probable assignment "*c*" is placed after the discrepancy, and for the less probable assignment "*C*" replaces the intensity and the whole set of symbols for the transition is enclosed in parentheses ( ), corresponding to the parentheses about the assignment of the same line in Table II.

? (before the intensity). Doubtful assignment. (A question mark in any other position refers only to the symbol immediately before it.)

— (alone). Transition allowed by the Laporte rule and the *J*-selection rule, for which no line has been observed.

(B)

Table II, the list of classified lines of the neutral tungsten atom, incorporates all the available information regarding each line, except for the omission of the details of the Zeeman effect patterns and all but one of the many intensity estimates. The data are given in five principal columns, as follows:

(1) *I*, arc intensity and special excitation data. (In the extreme ultraviolet, $\nu > 40{,}000$ cm^{-1}, two columns I_{LM} and I_T are devoted to these data,

TABLE I—*Continued.*

545_3° 54556.56	547_6° 54733.16	548_9° 54859.13	549_2° 54911.54	550_3° 55009.13	550_7° 55032.65	550_8'° 55043.26	?550_7'° 55084.09	553_2° 55389.28	
									D_0
									D_1
									S_2
—									D_2
—		—	—	—		—		—	D_4
.6 +02		.0*f* −32*C*	.6*z* +19	.7 +3	.5*s* −2	.8 00	.0*f* +08	—	09_0 12_4
.6 −10		—	.8*f* −04		.5 +1		.6 +1	.5 0	13_1 13_4
—		.6 00	—		—		.6 −04	.7*A* +08	13_2
—	2*MZ* +01	—	—	0 +17	0*f* 00	0 −2	—	.5 +07	14_3 15_5
0 +15		—	0 −08		0*u* −34		—	—	15_3
—		—	—	—		—		0 −18	16_4
	1 −15			—		—			17_6
—		0 +39*C*	0 +37	—		—		0 −21	17_4
—		0 +18	0 +03		0 +19		—	—	17_3
					—		0 −11		18_1
3*C* +14		—	—		—		—	0 +09	18_2
—		—	—		—		—	—	$18_2'$
1 −14		1*A* −03	—		2 00		—	1*u* −03	18_3
—		2 +02	—		—		—	—	19_2
—		1 +01	—	2 00*C*		0 −16		2 −02	19_4
	1*u* −02			2 +03		1 00			19_5
				4 +17		—			19_5
	?2 +15			—		1 +01			$19_5'$
—		—	1*d* +05*C*		—		—	—	19_3
					—		—		20_1
0 +01		—	1*f* −10		(*C* +28)		—	1 +26	20_2
									21_0
0 −15	—	—	—	—		—		—	22_4
	—			—		—			22_5
—		1 +42*C*	—		—		—	—	23_3
	—			—		—			28_5
					—		3*C* +11		43_1
—		—	—		—		—	—	44_2
									45_0
									46_1
									46_2
									47_4
									48_2
									49_3
									49_2
									51_4
									52_{23}
									53_1
									55_4
									55_5
									?58_3
545_3°	547_6°	548_9°	549_2°	550_3°	550_7°	550_8'°	?550_7'°	553_2°	

as noted below.) A key to the symbols used in this column is given below.

(2) λ, wave-length in air, in Angstrom units.

(3) ν, vacuum wave number, in cm^{-1} (followed in the regions $\nu 18174$ to $\nu 14313$ and $\nu 11333$ to $\nu 10915$, by certain observational discrepancy values discussed below).

(4) Classification.

(5) Discrepancy, $\nu_{observed} - \nu_{calculated}$. (A decimal point belonging before the first digit has been omitted.)

For brevity, only one value is given in each column for each line except as noted in this paragraph and the next. Rather than weighing the data from various sources, we have followed the simple practice of using the most recent arc intensity and wave-length data in each case (see the second paragraph below), except in connection with the M.I.T. list, which unfortunately became available to us only after Tables I and II were in nearly their final form. While the full use of this list would have enhanced the self-consistency of these tables appreciably both in intensity and in wave number values, a sampling study shows that it would have changed the term values so slightly as scarcely to justify the required alteration. For $\nu < 40{,}000$ cm^{-1}, therefore, we have made use of the M.I.T. list only for lines

TABLE I—*Continued.*

	$554_5°$ 55492.08		$555_3°$ 55545.91		?$556_7°$ 55619.70		$557_5°$ 55795.55		$558_7°$ 55835.12		$559_{34}°$ 55955.41		$559_5°$ 55987.86		$561_3°$ 56108.50		$561_{34}°$ 56174.64	
D_0																		
D_1																		
S_2																		
D_2																		
D_3																		
D_4	—		—				—				—		.0	+2	—		—	
09_7																		
12_4	—		—				.3*u*	+2			.5	−4	.0	+1	.5	−4	—	
13_1					.4*z*	−21												
13_3			.3	−1	.4*z*	+1			.6*u*	+1	.3	+1			.3	−3	.0	+1
13_2			.7	+3	—				.6	−4	—				.5	+1	?.0*f*	−2
14_2			.3*f*	+3	—				.3	0	—				.7	+02	—	
15_5	.2	0					.9*M*?	+01			?.0	+36	.6	+07			—	
15_4			.3	+1	—				.5	+13	.3	0			—		.5	+08
16_4	0	−11		—			0	+25			0	+02		—	—		—	
17_6	2	+29*C*					0	+43					1	−32				
17_4	2	−30	1	−11							—		—		—		—	
17_3			—		—				—		—				—		0	+34
18_1					0	+25			0	+23*C*								
18_2			—		—				0	−23	?0	−06			—		—	
$18_2'$			0	+03	—				—		—				—		—	
18_3			—		—				—		—				0	−02	1	−35
19_2			—		2	00			0	+27	—				0	−24*C*	—	
19_1	1	00	—				2	−09			—		1*f*	−07	—		1	−27
19_5	2	−20					—				?1	−08	—				—	
19_6	3	+03					0	−31*e*					—					
$19_5'$	1	+03*C*					0	+01			—		—				—	
19_3			—		—				—		3	−08			—		—	
20_1					0	−07*C*			—									
20_2			0	+09	—				—		—				—		?0	+24*e*
21_9																		
22_4	—		—				?0	+55			—		—		1	+12	—	
22_5	1	+17					—				—		—				—	
23_2			—		—				—		—				—		—	
28_5	—						—				—		—				—	
43_1					—													
44_2			—		—				2.0	+02*C*	—				—		—	
45_2																		
46_1																		
46_2															—		—	
47_4																		
48_2																		
49_5																		
49_3																		
51_4																		
52_{23}																		
53_1																		
54_4																		
55_3																		
?58_5																		
	$554_5°$		$555_3°$		?$566_7°$		$557_5°$		$558_7°$		$559_{34}°$		$559_5°$		$561_3°$		$561_{34}°$	

not found on previous lists, and lines for which the M.I.T. wave-length yields a wave number different by more than 0.5 cm^{-1} from the value that would previously have been used (a circumstance that occurs only for a few Exner-Haschek lines, e.g., ν24836). In the region $\nu > 40{,}000$ cm^{-1}, on the other hand, the M.I.T. list has been used as much as possible, and two intensity columns are listed, I_L for intensities from data original with this investigation and I_T for those from the M.I.T. list. Our list (from which only the classified lines are set down here) includes many lines not found elsewhere but it is incomplete with respect to certain lines which we erroneously supposed to be spark lines, and it is inferior to the M.I.T. list in wave number self-consistency.

Because of a falling off in the self-consistency of some of the lists near their ends, an auxiliary column immediately following the wave number column is used to compare the observed wave number values in certain regions of overlap; in particular, values are recorded for $\nu_{\text{Belke}} - \nu_{\text{Kiess–Meggers}}$ in the region ν18,174 to ν14,313 and for $\nu_{\text{Kiess–Meggers}} - \nu_{\text{Kiess}}$ in the region ν11,333 to ν10,915.

A chronological list (starting with the oldest) of the sources of the arc intensity and wave-length data compiled in Table II, with the wave

TABLE I—*Concluded.*

562₄° 56255.64	?564₂° 56484.40	565₆° 56526.58	567₂° 56717.16	568₄° 56831.70	571₅° 57143.49	575₅° 57560.75	?579₆° 57919.11	580₂° 58091.6	
									D_0
									D_1
									S_2
									D_2
									D_3
									D_4
.3 0	—		—	.4 −0	—	—		—	00_0
4*f* +3	.5*h* −1		.4 −4	.5 +2				—	12_4 13_1
	.3 −4		—					—	13_2
	.1 −4		—					.2 −6	14_2
.7 +05		—		.4*V'* +6	.8 −09	—	—		15_5
.4*s* +15	.5 00*c*		.2 −3	.3 +3				.4*u* +1	15_3
—	.4 −09			.6 −2*c*	.8*M* +36*C*	.4 −13		—	16_4
		1*MuA* −30			.6 −06	.7 +05	.8 −06		17_6
0 +27	—		—	0 −06	.7 −3	.6 +05		.5 −04	17_4
—	0 +05*C*		0 −27	—				.6 −09	17_3
	—		—					—	18_1 18_2
	—		—					0 −14	$18_2'$
—	—		0 +−1	0*u* +20				—	18_3
	0 +10		0 +28					—	19_2
—	—		—	0 +28	2 −22	0 −34		—	19_4
1 −12		2 −27		—	0 −14	—	—		19_5
	—				—	—	2*f* −27		19_6
—		1 −13		—	—	0 −02	0 +26		$19_5'$
—	—		0 −01	—				—	19_3
	—		2 −06					—	20_1 20_2
									21_0
—	—		0*u* −27*C*	—	—	1*d* −18*C*		—	22_4
2 −47		0 +36		0 +05	—	—	—		22_5
—	—		—	0 +36*C*	—			0 −24	23_3
—		—		—	—	—	0 −07*C*		28_4
	—		—					—	43_1 44_2
—	—								45_5 46_1
			—	—				—	46_3
						—		—	47_4
									48_2 49_3
								—	49_2
									51_4
									52_{23}
									53_1
									55_4
									55_5
									$?58_5$
562₄°	?564₂°	565₆°	567₂°	568₄°	571₅°	575₅°	?579₆°	580₂°	

number ranges covered, is given below:

Exner and Haschek[5]	*vv*44,434 − 14,779
Belke[6]	44,231 − 14,313
Kiess and Meggers[7]	18,174 − 10,915
Kiess[7]	11,333 − 9,541
This investigation[9]	49,488 − 39,938
Massachusetts Institute of Technology[10]	49,832 − 10,915.

The symbols used in the intensity column to designate the character of the lines or the source of the data are as follows:

A—underwater spark absorption line, Allin or Allin and Ireton.[16]

B—data from the arc line list of Belke.[6]

d—partly resolved pair.

E—data from the arc line list of Exner and Haschek.[5]

f—intensity greater in spark than in arc.

G—raie ultime, de Gramont.[11]

H—underwater spark absorption line, Hulburt.[14]

K—furnace lines, King.[13] *vv*44,958 − 33,923.

L—data from the arc line list of this investigation.[9, 18]

M—underwater spark absorption lines, Meggers.[15] *vv*35,308 − 17,750.

m—probably an arc line masked by a spark line.

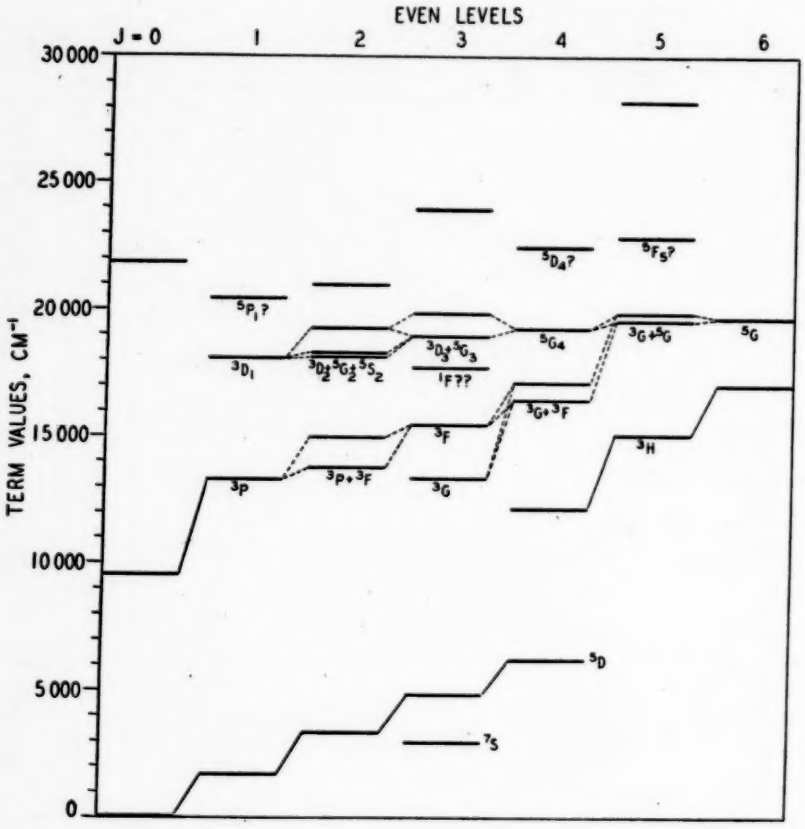

FIG. 2a. Interpreted low even levels. Except for the low ^7S and the quintets above 18,000 cm^{-1}, which belong to $5d^56s$, all these interpreted levels belong to $5d^46s^2$.

n—possibly a molecular band.

r—reversed.

ρ—shows a red shift in the spark with respect to its position in the arc.

ρ′—diffuse on the red side.

S—solar spectrum line.[17,18]

s—especially sharp.

T—data from the arc line list of M.I.T.

u—especially diffuse.

v—shows a violet shift in the spark with respect to its position in the arc.

v′—diffuse on the violet side.

y—Zeeman-effect pattern seriously inconsistent with our assignment of *J* and *g* values.

z—incompletely resolved Zeeman-effect pattern not requiring any of the symbols =, *y*, or *ζ* (i.e., usually an unresolved triplet).

Z—completely resolved weak-field Zeeman-effect pattern.

ζ—asymmetric, completely resolved Zeeman-effect pattern.

= incompletely resolved Zeeman-effect pattern indicating $\Delta J=0$.

– (after intensity value) the intensity value given is for a line not resolved in the list being used in this region, but resolved by the investigation indicated by the letter to the right; the wave number given here comes from that investigation.

Where the first symbol in the intensity column is a letter, the line is not found in the list principally used in that region. Where the first symbol is a number followed by a hyphen and a letter, the intensity is that of a blend, recorded as a single line on the list principally used and resolved by another observer. In either case the wave number given is that of the observer indicated by the letter (*B*, *E*, *L*, or *T*). When the first symbol is a number followed immediately by a letter referring to an observer, only the symbol immediately following the letter is associated with the observer referred to (e.g., a number after *M* refers to the intensity given by Meggers for the line in the underwater spark spectrum) except for a few instances where a number or letter is followed by the letter *T*, in which case the wavelength and wave number are taken from the M.I.T. tables because of an exceptionally large difference between it and the previous values.

Parentheses about a classification and its corresponding discrepancy indicate an assignment that is possible but improbable relative to another assignment made for the same line.

5. NOTES ON CERTAIN LEVELS AND LINES

This section is devoted to a few isolated notes on certain levels and lines. The conclusions that depend upon (published) Zeeman-effect work, i.e., those concerning the reality or the J values of certain levels, are subject to verification in the course of a reinvestigation of the Zeeman effect, now in progress. Because of this reinvestigation we have omitted any discussion of the discrepancies between our classification and the results of Zeeman-effect studies ("y" lines, Tables I and II) insofar as in our opinion they do not affect the validity of our conclusions but arise from trivial causes such as masking or fortuitous wave number coincidences.

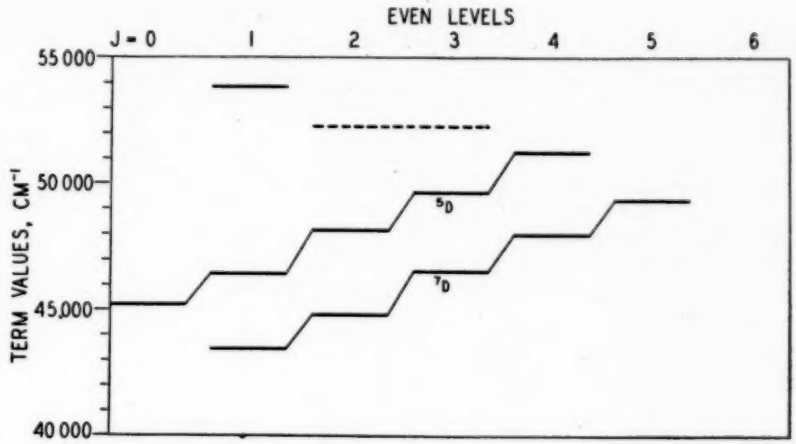

FIG. 2b. Interpreted high even levels. These belong to $5d^46s(^6D)7s$.

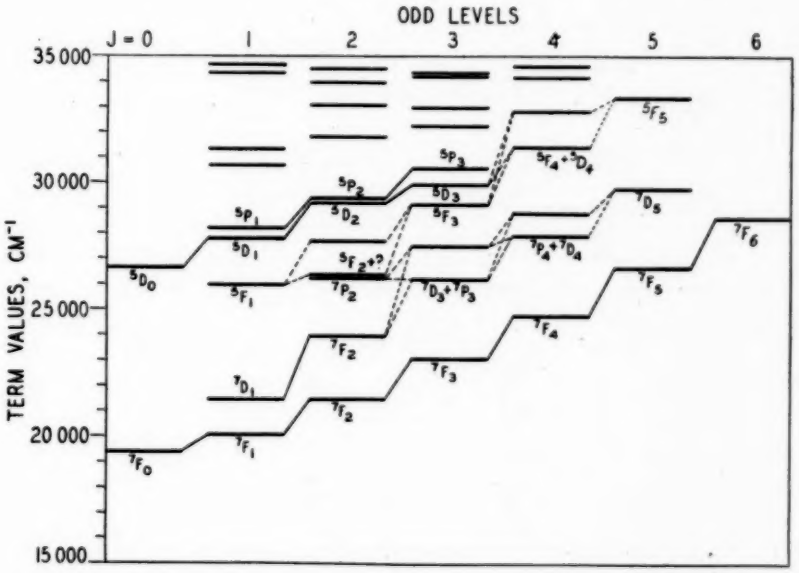

FIG. 2c. Interpreted high odd levels. These belong to $5d^46s(^6D)7p$.

(A) $5d^46s^2\ ^5D$ and $5d^56s\ ^7S$

In the underwater spark, the sun, and the conditions for de Gramont's raies ultimes, ^7S show a considerably greater intensity sum than any other level. This is satisfactorily accounted for by a consideration of the factor $(2J+1)\exp-[h\nu/kT]$, which is shown in the following tabulation to be appreciably greater for $^7S_3$ than for any other level in the atom, throughout a wide temperature range that undoubtedly covers the temperatures encountered in these investigations:

	1000°K	2000°K	4000°K	8000°K
$^5D_0$	1.0	1.0	1.0	1.0
$^5D_1$	0.27	0.90	1.6	2.2
$^7S_3$	0.10	0.84	2.4	4.1
$^5D_4$	0.0012	0.10	0.96	2.3

Moreover, d^5s is the only low configuration that combines with both d^4sp and d^5p in one-electron transitions. Not so easy to understand is the preference of ^7S for combination with lower odd levels than ^5D in the underwater spark, as shown in Table IV; one might have expected that the tendency of levels with large spin vectors to be low, which would lead to such a preference, would be more than offset by the contrary tendency of d^4sp levels to be lower than those based on d^5. Table IV is principally an extract from Table I, showing all the surely absorbed and unambiguously classified Meggers underwater spark lines;

TABLE II. Classified lines of neutral tungsten, W I.

Intensity (See text)		λ_{air}	ν_{vac}	Assignment	$\nu_{obs}-\nu_{calc}$
	4	2008.64	49768.8	D_4-559_4	+2
	3	2010.74	49716.9	D_2-530_1	+4
2*f*	8	2020.13	49485.8	S_2-524_4	+7
	6*f*	2043.55	48918.7	D_2-537_2	−2
4		2054.56	48656.6	$S_2-?516'_2$	+1.5
3		2060.50	48516.4	D_2-533_4	+8
	10	2065.09	48408.6	D_2-532_4	+2
4	5	2070.81	48274.9	$D_2-?516_3$	0
2*f*		2078.70	48091.5	D_4-543_5	+6
5	8	2081.39	48029.4	D_1-497_2	−4
	21*f*	2084.48	47958.2	S_2-509_4	+1
3		2088.88	47857.2	D_2-511_{23}	+2
5		2089.31	47847.5	D_1-495_2	+5
	10	2092.54	47773.5	D_1-494_1	0
	10	2098.25	47643.6	D_4-538_5	+2
5*f*		2105.43	47481.2	D_1-491_2	−4
	5*f*	2116.638	47229.72	D_2-520_4	−01
5		2128.13	46974.8	D_4-531_5	−1
	4*f*	2137.15	46776.4	$D_2-?516'_2$	0
4		2137.45	46770.0	$D_2-?516_3$	−4
4		2143.05	46647.8	D_1-483_2	−6
6		2146.47	46573.4	D_1-482_2	−6
3		2147.34	46554.6	D_4-527_5	−1
5		2155.69	46374.2	D_2-497_2	−3
	f	2156.688	46352.78	D_2-511_{32}	+29
3		2163.02	46217.0	D_4-524_4	−1
3		2165.19	46192.1	D_2-495_2	+3
6		2164.33	46189.1	D_2-495_2	+3
5		2164.93	46176.4	D_4-523_5	+2
2	*f*	2167.687	46117.59	D_2-494_1	−63
	10	2168.298	46104.60	D_0-461	+05
9	15	2169.48	46079.6	D_2-509_4	+2
5		2170.19	46064.5	D_2-508_4	+4
7		2174.59	45971.2	D_2-508_3	+8
8		2175.84	45944.8	D_2-492_2	+1
8		2178.46	45889.5	D_2-507_2	+6
	4	2189.197	45664.52	D_2-504_2	−17
7		2190.51	45637.2	D_4-518_4	+4
4		2199.28	45455.2	D_2-502_4	+6
4		2201.49	45409.6	D_1-470_2	+5
7		2202.85	45381.5	$D_4-?516_3$	+4
4		2203.20	45374.3	D_0-453_1	+2
4		2204.08	45356.3	D_2-501_3	+6
6*f*	12	2221.85	44993.5	D_2-483_2	+2
7*M*2		2223.56	44958.5	D_2-497_4	−1
6*M*2	8	2225.54	44919.0	D_2-482_2	+3
6*M*5*u*	10	2227.98	44869.6	D_2-497_2	−4
1*f*		2229.20	44845.1	D_2-481_3	+1
7		2234.59	44747.0	D_0-447_1	−2
5		2237.23	44684.2	D_2-495_2	−2
5		2237.70	44674.8	D_4-508_4	0
4		2237.96	44669.7	12_4-568_4	0
3	6	2238.56	44657.6	D_1-463_2	+2
6*M*3		2240.38	44621.4	D_1-462_2	+1
	12	2242.06	44587.9	D_2-494_3	0
4		2242.41	44581.1	D_4-508_3	0
6	10	2249.5	44440.5	D_2-492_2	+3
4	10	2249.84	44433.8	D_1-461_1	−5
8		2253.91	44353.6	D_0-443_1	+2
6	3	2255.52	44321.9	D_2-491_2	0
	2*u*	2255.72	44318.0	D_2-491_4	0
8*f*	12	2259.555	44242.78	D_2-490_3	+68
7	15	2260.07	44232.7	D_1-459_2	+5
6		2263.90	44157.8	D_2-474_3	−4
3		2267.22	44093.3	12_4-562_4	0
6		2268.68	44064.9	D_4-502_4	−4
3		2270.16	44036.1	D_2-473_3	−1
6		2271.40	44012.1	D_2-473_2	−2
7	10	2273.00	43981.2	S_2-469_4	+7
6	10	2273.76	43966.40	D_4-501_3	+02
5		2274.81	43946.1	12_4-561_2	−14
3		2276.28	43917.8	D_4-501_5	−4
7*u*f*u*M5	20	2277.58	43892.8	D_0-438_1	+2
	4*f*	2281.04	43826.0	12_4-559_5	+1
5		2282.76	43793.1	12_4-559_{24}	−4
6 / 5	*M*5?	2284.82 / 2284.90	43753.5 / 43752.0	D_2-470_2 / D_1-454_2	−4 / 0
7*M*10	10	2285.17	43746.8	D_4-499_3	+1
3*u*		2291.09	43633.8	12_4-557_5	+2
7*f*v*M*4	20	2294.544	43568.18	D_4-497_4	−1.12
4	4	2297.38	43514.4	09_0-530_1	+4
7	3	2298.340	43496.25	D_2-483_3	−16
5	8	2298.74	43488.7	D_2-483_2	−1
5	4	2299.02	43483.4	13_2-568_4	+2
6		2299.31	43480.6	D_2-468_2	−3
7	8	2302.67	43414.5	D_2-482_2	+2
4		2305.12	43368.2	17_4-567_3	−4
2		2306.17	43348.5	D_1-450_2	−2
7*M*10?	12	2306.60	43340.5	S_2-462_2; D_2-481_3	+2 / 0
8*f*'*M*15*u*	12	2309.036	43294.77	D_4-495_2	−27
8*M*10?	8	2313.188	43217.06	D_0-432_1	−11
7*M*12		2316.26	43159.8	D_4-494_3	0
5	2	2317.39	43138.8	D_2-479_4	+24
5	2*u*	2317.55	43135.8	$13_2-?564_2$	−1
6	8	2318.58	43116.6	S_2-460_3	+06
2		2318.67	43114.8	14_2-580_2	−6
4	5	2321.24	43067.2	D_1-447_1	+3
9*M*10	12	2321.634	43059.87	D_2-463_2	−07
	2*f*	2324.74	43002.2	D_2-463_2	0
7*M*10	10	2326.562	42968.67	D_4-491_5	+10
6	10	2326.71	42966.0	D_2-462_2	−1
6		2327.52	42950.9	S_2-459_2	−3
3	*f*	2328.72	42928.8	D_4-491_4	+2
6		2328.88	42925.8	D_1-445_2	−2
5	4	2329.29	42918.3	S_2-458_4	+6
4*f*	2*f*	2329.88	42907.4	13_2-562_4	+3
8*M*1	15	2331.303	42881.30	$12_4-550'_5$	00
6	5	2332.50	42859.2	D_2-476_4	−10
6		2332.86	42842.6	D_4-490_2	−2
7	7	2333.14	42847.5	12_4-550_5	+3
5	4	2334.30	42826.2	13_2-561_{24}	+1
3		2336.87	42779.1	D_2-461_1	0
5	8	2337.743	42763.17	D_2-475_2	−21
3		2337.93	42759.7	13_2-561_3	+03
6*z*	10	2338.476	42749.77	12_4-549_2	+19
3		2340.86	42706.3	$13_2-?564_2$	−4
	12	2341.374	42696.85	D_1-443_2; 12_4-548_2	−33 / −32
3	3	2342.12	42683.2	D_1-443_1	0
6	5	2343.744	42653.69	D_2-474_3	−02
4*u*		2344.95	42631.7	15_2-580_3	+1
3	4	2346.31	42607.0	13_3-559_{24}	+1
5	5	2346.69	42600.1	S_2-455_2	0
7*f*	10	2347.967	42576.98	D_2-459_2	+03
6	8	2348.151	42573.64	D_0-425_1	+28
7		2350.48	42531.4	D_2-473_3	−3
6	5	2351.78	42508.0	D_2-473_2	+2
6*u*	8	2352.96	42486.7	13_2-558_2	+1
4	3	2353.81	42471.3	S_2-454_2	+3
8*u*M15	12	2354.611	42456.86	D_4-486_4	−02
	f	2357.93	42397.1	13_2-561_{24}?	+2
6	10	2358.072	42394.62	12_4-545_3	+02
8*M*15	15	2360.433	42352.14	D_2-456_2	−02
5	6	2361.62	42330.9	13_2-561_3	+1
4*z*		2362.65	42312.4	$13_1-?556_2$	−2
9*u*M20	15	2363.06	42305.03	D_1-439_2	+10
4*z*	8	2364.95	42271.3	$13_2-?556_2$	+1
8	12	2365.448	42262.35	D_0-422_1	+09
8*f*	12	2366.182	42249.25	D_2-470_2	−12
8	12	2366.952	42235.50	09_0-517_1	+25
1*z*		2367.52	42225.4	D_2-455_2	−4
7	10	2367.68	42222.53	D_1-438_1	+20
3		2369.10	42197.3	13_2-555_3	−1
7	10	2370.881	42165.52	S_2-451_4	+09
5	8	2371.85	42148.2	12_4-543_3	0
6	4	2373.43	42120.2	$Dt-?437_0$	+5
8*M*5*u*	12	2374.144	42107.57	D_4-483_2	+47
9	12	2374.460	42101.97	D_2-469_4	+15
7	10	2374.758	42096.68	D_2-454_2	+06

TABLE II—*Continued.*

Intensity (See text)		λ_{air}	ν_{vac}	Assignment	$\nu_{obs}-\nu_{calc}$
8	10	2376.069	42073.46	15_5-571_5	−09
4	4	2376.39	42067.7	S_3-450_2	0
6		2377.00	42057.0	13_2-557_5	−4
5	4	2377.92	42040.7	13_3-553_3	0
4		2380.85	41988.9	S_3-449_4	−3
7	8	2381.57	41976.2	D_3-468_2	−2
8	15	2382.986	41951.34	D_4-481_3	+11
9*M*10	12	2384.817	41919.14	D_4-481_5	+11
	12	2389.072	41844.49	D_1-435_2	+09
4	4	2391.89	41795.2	D_3-466_4	+2
	8	2392.927	41777.08	$13_1-?550'_2$	+08
7	10	2393.42	41768.5	13_1-555_3	+3
4*s'*	4	2393.77	41762.4	15_5-568_4	+6
6	6	2395.30	41735.7	$13_3-?550'_2$	+1
5*s*	6	2395.89	41725.54	13_1-550_2	−2
5		2397.21	41700.7	12_4-538_5	−1
8*M*6	12	2397.723	41693.52	D_2-450_2	00
7*M*4	8?	2397.979	41689.07	D_2-450_3	+03
5	3	2398.27	41684.0	13_3-550_2	
	1*f*	2400.505	41645.22	S_3-445_2	+22
6	12	2401.294	41631.52	D_4-478_3	+06
7*fA*	15	2502.441	41611.65	13_2-553_3	+08
8	10	2405.256	41562.97	13_2-549_3	−04
8 *M*10?		2405.592	41557.16	D_1-432_2	−21
9	15	2405.688	41555.49	D_3-463_3	+04
8	10	2406.175	41547.08	D_1-432_1	+08
1		2408.45	41507.8	$14_3-?564_3$	−4
8*A*	10	2409.031	41497.84	D_2-463_2	+12
3*m*		2409.16	41495.6	S_3-444_3	−1
5	7	2410.529	41470.32	D_4-476_4	+33
6	9	2313.778	41416.24	S_3-443_2	+06
8*M*5?	12	2414.040	41411.74	D_3-447_1	+06
8*M*10	15	2415.679	41383.64	$D_1-?430_0$	+09
5	9	2416.232	41374.17	D_4-475_2	+10
3		2416.36	41371.9	15_2-568_4	+2
6	10	2420.200	41306.34	$13_2-?550'_2$	−04
7	2*f*	2422.285	41270.79	D_3-445_2	+02
6	7	2422.659	41264.42	D_4-474_3	+02
2		2423.10	41257.0	15_3-567_3	−2
9*u*M5*u*	20	2424.216	41237.91	D_3-460_2	−07
5	6	2424.770	41228.49	12_4-533_3	+04
6	7*d*	2425.980	41207.93	13_2-545_3	−10
7	10	2427.287	41185.75	15_5-562_4	+05
5		2427.41	41183.7	12_4-533_4	+1
7	10	2429.843	41142.43	D_2-443_2	+48
7	10	2430.438	41132.35	14_2-561_3	+02
4	4	2430.617	41129.32	16_4-575_5	−13
8*M*2?	10	2431.084	41121.43	D_2-444_3	−02
6	9	2433.45	41081.42	13_2-548_2	00
6	7	2433.743	41076.50	12_4-532_4	+07
7*fM*4	12	2433.984	41072.43	D_3-459_2	−03
4		2434.14	41069.7	S_3-440_3	+5
10*M*2*s*	30	2435.962	41029.09	D_3-458_4	+08
6	8	2436.258	41034.11	S_3-439_4	+02
7*A*	12	2436.623	41027.96	D_2-443_1	+04
5	6	2436.835	41024.40	S_3-439_2; $15_3-?564_3$	+47, 00
5	4	2439.204	40984.55	17_4-580_3	−04
	3	2440.88	40956.4	12_4-531_4	+1
6	5	2443.172	40917.99	15_5-559_5	+07
8	15	2443.615	40910.57	$17_6-?579_6$	−06
8*M*5*u*	18	2444.056	40903.19	D_1-425_1	+10
5	5*d*	2445.246	40885.83	15_5-559_{34}?	+36
3		2446.70	40859.3	14_2-558_2	0
5	8	2447.374	40847.74	D_3-456_3	+07
4*s*	3	2450.494	40795.75	15_3-562_4	+15
9	12	2451.342	40781.62	12_4-529_3	+20
9*u*S	15*f*	2451.477	40779.38	D_1-424_2	+09
7*M*5*Z*	12*f*	2451.998	40770.71	D_3-407_1	−03
9 *M*5*d*	15	2454.713	40725.62	15_5-557_5	+01
9 *M*5*d*	15	2454.971	40721.34	D_3-455_3	+01
5	5	2455.370	40714.72	15_3-561_{34}	+08
8*M*5	12	2455.501	40712.55	D_4-469_4; 16_4-571_5	+04, +36
9*M*6	15	2456.531	40695.49	D_2-40_0	+51
9*u*M8	18	2459.295	40649.76	D_2-439_2	+06
8	12	2460.162	40635.42	D_4-468_5	−04
7*A*	12	2461.572	40612.16	12_4-527_3	+08
9*u*M8*s*		2459.315	40649.45	D_3-439_2	−25
9*M*3	15	2462.788	40592.11	D_1-422_1; D_3-454_2	+12, −14
3	3*f*	2464.128	40570.04	14_2-555_3	+30
8	15	2464.307	40567.10	D_2-438_1	00
7	1*f*	2465.204	40552.32	17_5-575_5	+05
9*u*M6*A*	15	2466.848	40525.31	D_3-438_5	+04
3		2468.67	40495.4	15_3-559_{34}	0
0	10	2471.209	40453.79	17_4-575_5	+05
1*uf*		2471.94	40441.8	$13_1-?537_2$	0
8*M*10	15	2472.508	40432.55	D_3-452_4	+03
2		2473.14	40422.1	15_5-554_5	0
5	4	2473.692	40413.18	14_2-533_3	+07
7	7	2473.818	40411.13	D_0-404_1	+08
9*M*15	20	2474.149	40405.72	D_4-466_4	−01
6	6	2474.484	40400.25	$13_3-?537_2$; 16_4-568_4	−12, −2
6	10	2475.091	40390.35	17_3-580_3	−09
5	7	2476.017	40375.25	15_3-558_2	+13
4	5	2476.810	40362.32	13_1-536_2	−01
4		2476.82	40362.2	13_1-536_2	−1
8*M*6*s*	10	2480.126	40308.36	D_1-419_2	+03
7*s*	10	2480.654	40299.78	S_3-432_4	+08
10*M*8*s*	25	2481.443	40286.97	D_3-451_4; D_4-465_5	+26, −08
8	10	2482.098	40276.34	S_3-432_2	−03
8*M*2?*A*	10	2482.212	40274.48	12_4-524_4	+04
9*M*5*s*	20	2484.735	40233.60	12_4-523_5	+08
8*M*10?	15	2487.492	40189.00	D_3-435_2; D_3-450_3	−17, −03
6	10	2487.766	40184.58	D_3-450_3	+03
4	3	2487.940	40181.77	13_2-539_2	+10
8	10	2488.910	40166.11	D_4-463_3	−03
9*M*8*A*?	8	2489.718	40153.08	D_3-434_2	−01
6	9	2490.843	40134.95	17_5-571_5	−06
7	12	2492.367	40110.40	D_3-449_4	−08
8	10	2493.393	40093.90	12_4-522_3	+11
3		2493.88	40086.0	15_3-555_3	+1
9*M*9*s*	20	2495.264	40063.85	D_1-417_2	+05
	4*f*	2495.722	40056.48	14_2-550_2	00
4	4	2495.938	40053.01	$16_4-?564_3$	−09
	10*f*	2496.638	40041.79	13_3-533_3	−12
7		2496.98	40036.2	17_4-571_5	−3
1*u*		2499.447	39996.80	13_3-533_4	−27
L		2500.93	39973.1	$15_3-550'_5$	−2
Tf		2501.036	39971.38	$13_2-?537_2$	+19
E		2501.781	39959.48	S_3-429_4	+05
ET		2503.042	39939.36	15_3-550_5	+17
E		2504.31	39919.21	12_4-520_5	+05
E		2504.55	39915.38	09_4-494_1	−33
2*s*		2504.718	39912.64	D_1-415_2	−25
E		2505.37	39902.16	D_3-432_3	+02
1		2505.658	39897.65	12_4-520_4	−11
1		2506.032	39891.71	D_2-432_1; 13_2-536_2	−06, 00
T		2506.148	39889.86	13_3-532_4	00
1		2508.455	39853.18	12_4-520_3	+13
2		2508.754	39848.44	D_4-460_3	−23
E		2511.11	39810.98	18_2-580_3	−14
1		2513.948	39766.09	D_3-445_2	−19
E		2516.57	39724.63	17_4-568_4	−06
E		2518.49	39694.35	12_4-518_4	+25
2*M*4*s*		2520.468	39663.23	15_3-547_6	+01
1*M*10*As*		2521.336	39649.58	S_3-426_3; D_4-458_4	−27, −12
ET		2522.15	39636.57	D_3-396_1	+01
2*M*15*s*		2523.421	39616.82	D_3-444_3	−14
E		2524.82	39594.86	13_3-529_3	+01
Eu		2526.26	39572.31	15_3-550_2	−34
E		2526.38	39570.42	D_4-457_5	+01

TABLE II—*Continued.*

Intensity (See text)	λ_{air}	ν_{vac}	Assignment	$\nu_{obs}-\nu_{calc}$
E	2529.34	39524.13	16_4-559_{34}	+02
1*M*5*uA*	2529.745	39517.80	17_6-565_6	−30
2*M*	2533.641	39457.04	$D_1-?411_0$	+03
E	2534.00	39451.46	15_3-549_3	−08
2	2535.13	39433.82	D_1-411_2	−37
E	2539.00	39364.50	16_4-557_5	+25
E	2541.08	39332.29	D_4-455_3	+27
2*M*10*z*	2545.358	39275.42	D_2-426_3	−20
2*M*20*z*	2547.155	39247.72	D_2-425_1	−14
1*z*	2550.39	39197.92	D_1-408_2	−12
E	2551.02	39188.17	D_2-425_3	−47
1*M*30*AZ*	2551.360	39183.03	D_0-391_1	−14
E	2552.49	39165.62	13_2-529_3	−05
E	2553.58	39148.90	17_4-562_4	+27
1*M*5*u*?*z*	2553.839	39145.01	D_3-439_2	−20
2*A*	2554.878	39129.09	12_4-512_5	+34
1*Az*	2555.218	39123.87	D_2-424_2	−19
2*M*2	2556.760	39100.29	D_1-407_1	−18
E	2556.99	39096.71	15_3-545_3	+15
E	2557.57	39087.84	13_2-524_4	−03
E	2559.35	39060.67	16_4-554_5	−11
E	2560.49	39043.29	D_4-452_4	+08
E	2561.51	39027.74	S_3-419_2	+41
3*M*8*z*	2561.980	39020.62	D_3-438_3; 12_4-511_{32}?	−16; +10
E	2562.30	39015.71	17_3-567_3	−27
1	2564.713	38979.06	17_6-559_5	−32
E	2566.11	38957.80	16_4-553_3	−18
2	2567.517	38936.49	D_2-422_1	−27
2	2568.232	38925.65	D_2-422_3	−30
2	2568.574	38920.47	S_3-418_4	−17
2	2570.113	38897.15	D_4-451_4	−25
E	2570.51	38891.13	D_3-437_4	+26
E	2572.42	38862.27	$09_0-?483_1$	+23
2	2573.545	38845.30	$13_1-?521_2$	−15
2	2577.045	38792.54	15_5-538_5	−25
E	2577.38	38787.50	17_6-557_5	+43
E	2577.66	38783.29	S_3-417_2; $17_3-?564_3$	+49; +05
E	2580.05	38747.38	12_4-509_4	−06
3 / 3*z* } *M*30*d*	2580.355 / 2580.501	38742.78 / 38740.59	S_3-416_2 / D_1-404_1	−23 / −19
2	2581.079	38731.92	12_4-508_4	−17
E	2581.48	38725.92	13_2-525_2	+20
E	2583.66	38693.25	14_2-536_2	00
E	2584.27	38684.12	D_3-435_2	?−56
2	2585.454	38666.38	13_3-520_3	−32
EfA?	2586.33	38653.32	D_2-419_2	+22
E	2586.65	38648.54	D_3-434_2	−06
1	2586.959	38643.88	12_4-508_5	−22
E	2587.31	38638.68	12_4-508_2	+21
2	2587.782	38631.59	S_3-415_2	−30
E	2593.39	38548.12	S_3-414_2	+02
Eu	2596.11	38507.60	13_3-518_4	+07
E	2596.66	38499.45	15_3-539_2	+07
E	2597.71	38483.89	13_2-522_3; 17_6-554_5	−15; +29
E	2598.39	38473.82	17_3-561_{34}	+34
1	2600.763	38438.79	17_4-555_3	−11
2*M*5*u*?	2601.979	38420.83	D_3-432_4	−15
ET	2602.419	38414.32	14_2-533_3	+05
2*z*	2602.825	38408.34	D_2-417_2	−23
2	2603.567	38397.40	D_3-432_2	−25
E	2604.42	38384.77	17_4-554_5	−30
2	2605.518	38368.64	D_2-416_3	−14
3*EfM*1*z*	2606.406	38355.57	$D_3-?431_4$	+15
E	2607.10	38345.47	13_3-516_2	+18
2*M*3*z*	2607.398	38340.99	D_1-400_2	−18
2*M*2*z*	2608.338	38327.17	D_4-445_5	−22
E	2609.90	38304.19	19_4-575_5	−34
E	2610.23	38299.37	$13_1-?516'_2$	+06
E	2611.41	38282.06	17_4-553_3	−21
2*Ef*	2612.210	38270.36	$19_6-?579_6$	−27
3*M*10 = / 3*M*8*z* } *A*	2613.090 / 2613.830	38257.46 / 38246.64	D_2-415_2 / S_3-411_4	−20 / −14
E	2614.48	38237.11	13_2-520_3	−41
2*A*	2615.144	38227.43	D_4-444_2	−22
E	2616.37	38209.50	15_3-536_2	+08
Ed	2616.71	38204.54	D_3-430_4	?+44
1	2618.833	38173.58	D_2-414_2	−29
1*Ef*	2619.201	38168.21	15_5-532_4	−24
2*M*10*u*?	2622.217	38124.32	15_5-531_5	+04
E	2622.33	38122.68	12_4-502_4	+07
E	2624.35	38093.35	$19'_5-?579_6$	+26
3*M*5*z*	2625.232	38080.52	D_2-429_4	−19
1*u*	2626.272	38065.45	14_2-530_1	+40
E	2627.43	38048.71	15_5-531_4	+36
E	2628.24	38036.99	D_1-397_2	+24
1	2629.166	38023.56	12_4-501_3	−16
2*M*2?*z*	2632.510	37975.26	12_4-501_5	−30
3*M*2	2632.717	37972.28	S_3-409_3	−22
3*M*10*Az*	2633.147	37966.07	D_1-396_1	−22
E	2635.60	37930.80	15_3-533_3	+36
2	2638.639	37887.05	19_4-571_5	−22
E	2638.71	37885.96	15_3-533_4	+36
Eu	2640.70	37857.42	18_3-568_4	+20
E	2642.02	37838.52	18_2-559_{34}?	−06
E	2642.35	37833.78	13_3-511_{32}	−17
E	2642.71	37828.64	$13_2-?516'_2$	−05
2*A*	2643.142	37822.51	$13_2-?516_3$	−16
E	2644.37	37804.90	17_4-549_2	+37
1	2644.626	37801.28	D_4-440_3	−40
3*z*	2646.209	37778.68	D_2-411_2; 15_3-532_4	−28; +29
E	2646.51	37774.34	D_0-377_1	+40
2	2646.752	37770.92	D_3-426_2	−21
2	2647.111	37765.81	D_4-439_4	−25
E	2648.04	37752.51	17_4-548_2; 18_1-558_2	+39; +23
E	2648.73	37742.69	19_4-567_3	+01
E	2649.29	37734.71	$19'_6-575_5$	−02
1	2650.006	37724.55	17_6-547_6	−15
E	2650.46	37718.06	18_2-558_2	−23
E	2651.46	37703.84	15_3-527_5	−26
1	2654.694	37657.94	15_3-531_4	−35
4*M*20*Az*	2656.558	37631.51	S_3-405_4; D_4-438_3	−19; +04
E	2656.90	37626.66	12_4-497_4	+02
4*M*10*z*	2657.398	37619.62	D_3-424_2	+05
ET	2658.194	37608.35	19_5-571_5	−14
ET	2658.906	37598.28	D_2-409_3	+01
E	2660.50	37575.76	19_4-568_4	+28
E	2661.55	37560.94	13_3-509_4	+07
E	2662.64	37545.56	13_2-508_4	+04
3*M*10*Az*	2662.853	37542.57	D_3-408_2	−24
E	2663.24	37537.11	$18_1-?556_2$	+25
Ef	2663.93	37527.40	14_2-525_2	+14
3*A*?	2664.977	37512.65	D_1-391	−25
1*Ld*	2665.800	37501.07	D_4-437_4	−49
E	2668.45	37463.85	19_2-567_3	+28
1*A*?	2669.796	37444.94	D_2-407_1	−30
3*M*6*z*	2671.489	37421.20	D_3-422_3	−26
E	2672.15	37411.99	13_1-507_2	+26
E	2675.14	37370.18	13_3-507_2	−11
E	2675.41	37366.42	15_3-524_4	−04
2	2675.893	37359.62	D_1-390_2	−34
E	2676.44	37352.04	12_4-495_3	−34
3*M*5*A*	2677.296	37340.05	D_2-406_3	−31
E	2677.90	37331.68	17_3-550_2	+19
3*AT*	2678.883	37317.94	S_3-402_3	−08
2	2680.060	37301.54	17_6-543_5	−18
E	2680.37	37297.14	19_5-568_4	+44
4*M*20*Az*	2681.431	37282.47	S_3-402_4	−17
E	2681.60	37280.05	14_2-522_3	+47
E	2682.14	37272.54	18_2-553_3	+09
E	2682.65	37265.46	18_2-555_3	+03
E	2685.14	37230.91	$19_2-?564_3$	+10
E	2686.62	37210.41	17_3-549_3	+03
E	2687.14	37203.21	17_4-543_5	+02
1	2687.389	37199.81	18_3-561_{34}	−35

TABLE II—*Continued.*

Intensity (See text)	λ_{air}	ν_{vac}	Assignment	$\nu_{obs}-\nu_{calc}$
Ef	2688.27	37187.57	13_1-504_2	−02
E	2690.40	37158.15	17_3-548_3	+18
2	2691.113	37148.33	D_3-419_2	−28
E	2691.26	37146.27	13_3-504_2	+12
E	2692.15	37134.00	18_3-561_3	−02
3M8z	2695.683	37085.36	D_2-404_1	−19
2	2697.531	37059.96	S_2-400_2	−21
2	2698.857	37041.75	D_3-418_4	−17
3M7 = *3M4z* *Eu* } *A*	2699.607	37031.47	D_4-432_4	−20
	2700.022	37025.77	12_4-491_5	−14
	2700.20	37023.32	13_2-508_2	?+60
E	2701.06	37011.54	15_5-520_5	+36
E	2701.82	37001.14	18_1-?550′$_2$	−11
2	2702.537	36991.31	19_5-565_6	−27
Ef	2703.60	36976.78	15_3-524_4	+38
E	2704.38	36966.11	D_4-?431$_4$	00
?1	2706.022	36943.68	D_2-402_3	−11
?2z	2706.590	36945.93	13_3-502_4	−11
1	2707.894	36918.15	19_4-561_{24}	−27
1	2708.195	36914.04	16_4-533_4	−26
3z	2708.935	36903.96	D_3-417_2	−12
E	2710.00	36889.48	19_3-567_3	−01
E	2712.56	36854.67	17_6-538_3; 19_2-561_3	+02 −24
ET	2713.847	36837.16	13_3-501_3	+01
3Az	2715.506	36814.66	D_4-430_4	−13
1*uEfA*?	2716.905	36795.71	15_3-522_3	−04
1*u*	2717.540	36787.12	14_3-517_1	+01
4M20zz	2718.911	36768.57	S_3-397_4	−06
1z } *A*	2719.333	36762.86	16_4-531_5	−06
2 } *A*	2719.867	36755.65	S_3-397_2; 17_4-538_5	−10 −07
1	2720.056	36753.09	D_3-415_2	−08
1*Ef*	2721.650	36731.57	19_4-559_5	−07
1	2722.469	36720.52	19_5-562_4	−12
T	2722.683	36717.62	14_2-516_2	−03
1	2723.959	36700.43	$19'_5-565_6$	−13
4M10z = } *A*	2724.359	36695.04	S_3-396_3	−04
2	2724.637	36691.29	D_4-429_4	−11
3y	2725.054	36685.68	D_2-400_2	−26
E	2726.24	36669.66	D_3-414_3	+28
1*u*	2727.970	36646.46	D_4-428_5	−17
E	2732.79	36581.80	19_3-558_2	+27
2	2733.193	36576.44	09_6-461_1	−10
2	2735.976	36539.24	19_4-557_5	−09
2	2738.008	36512.13	16_4-529_3	+05
3	2743.437	36439.87	13_3-497_4; 18_2-545_3	−20 +14
1	2744.909	36420.33	19_5-559_{34}?	−08
1*u*	2745.328	36414.77	18_3-553_3	−03
1	2745.843	36407.95	13_2-501_3	−02
2	2746.740	36396.05	15_3-518_4	−01
E	2746.98	36392.88	13_1-497_2	−05
2	2747.839	36381.49	D_3-397_2; D_4-426_3	−02 −33
4rAz	2748.853	36368.08	D_3-411_4	+02
2	2749.002	36366.11	19_2-?556$_2$	00
1	2750.767	36342.77	16_4-527_5	+03
2	2753.170	36311.05	D_3-396_1	−01
E	2754.44	36294.35	D_3-425_2	−49
3	2754.922	36287.97	13_3-496_4	−08
2	2755.270	36283.37	17_4-533_3	−06
3	2755.947	36274.47	D_3-411_2	00
1	2758.685	36238.48	17_4-533_4	−11
1	2758.880	36235.86	19_4-554_3	00
2	2759.039	36233.82	15_3-516_2	00
2	2760.035	36220.74	15_5-512_5	−03
2	2761.142	36206.22	14_2-511_{32}	−09
4rZ	2762.346	36190.44	D_6-361_1	+02
2	2762.705	36185.75	17_6-531_5	−01
2	2764.007	36168.71	13_3-495_2	−02
E	2765.68	36146.76	15_3-?516′$_2$; 19_6-557_5	+36 −31
2	2766.735	36133.04	19_4-553_3	−02
3	2767.147	36127.66	19_3-559_{24}	−08
4rz	2768.988	36103.65	D_1-377_1	−02
4rz	2769.746	36093.77	D_2-409_2	−01
2	2770.211	36087.70	17_4-531_5	+49
4rzM1?	2770.883	36078.95	S_2-390_2	+01
2	2771.624	36069.31	13_3-494_3	−06
2	2772.481	36058.17	18_3-550_2	00
5rzA	2774.007	36038.32	D_3-408_2	00
5rzM3	2774.483	36032.14	D_4-422_3	−01
2	2776.091	36011.26	17_4-531_4	−02
E	2779.31	35969.54	$19'_5-557_5$	+01
2	2779.729	35964.14	16_4-523_5	−04
2	2780.290	35956.88	19_5-554_5	−20
1*A*	2785.889	35884.62	18_3-548_3	−03
2	2786.520	35876.50	18_1-539_2	−04
2	2787.986	35857.64	D_2-391_1	−03
3	2789.076	35843.63	19_6-554_5	+03
1	2789.376	35839.77	15_5-509_4	+31
3	2789.683	35835.83	D_3-406_3	−02
2*Ef*	2790.569	35824.45	14_2-508_3; 15_5-508_4; 16_4-522_3	+19 +34 00
3	2791.960	35806.61	12_4-479_4	+02
1	2792.216	35803.32	13_2-491_2	+01
2	2792.528	35799.32	13_2-491_4	−05
5M3	2792.702	35797.09	S_2-387_4	−07
T	2792.796	35795.88	D_1-374_2	−11
E	2793.50	35786.88	$19_4-550'_5$	−16
2	2796.152	35752.91	D_3-405_4; 19_4-550_5	−07 00
2	2797.202	35739.50	13_2-495_2	−05
2	2797.473	35736.03	15_5-508_5	−09
2	2797.630	35734.03	20_2-567_3	−06
2	2798.454	35723.51	13_3-490_3	−05
4	2799.929	35704.69	D_2-390_2	−04
3Efz	2801.175	35688.80	12_4-478_5	00
1	2801.956	35678.86	$18'_2-539_2$	−04
1	2802.959	35666.09	13_2-494_1; 18_1-?537$_2$; $19'_5-554_5$	+08 +03 +03
1	2804.021	35652.60	D_4-418_4	−01
3	2804.244	35649.76	16_4-520_5	−06
E	2804.70	35644.02	17_3-533_4	−42
2	2805.633	35632.10	18_2-?537$_2$	+03
2	2807.725	35605.56	19_2-548_2	+02
1	2807.933	35602.92	19_4-548_2	+01
1	2809.228	35586.51	18_1-536_2	−07
1	2809.589	35581.94	18_3-545_3	−14
2	2813.126	35537.20	17_3-532_4	−03
1	2815.419	35508.26	$19_5-550'_5$	00
E	2816.64	35492.84	13_2-492_2	+33
5rz	2818.068	35474.89	D_4-416_2	−09
2	2818.126	35474.16	19_3-550_5	+03
E	2820.10	35449.30	15_3-509_4	+10
1	2821.317	35434.05	15_3-508_4	00
E	2821.51	35431.59	12_4-475_3	+18
2	2823.718	35403.91	D_3-402_4	−01
1	2826.093	35374.15	13_2-491_2	+02
1*Eu*	2827.159	35360.82	19_4-550_5	+17
E	2828.79	35340.43	15_3-508_3	00
3Az	2829.833	35327.41	13_3-486_4	−24
3Ef/H	2830.296	35321.62	12_4-474_3	−12
5M7sAK4z	2831.387	35308.01	S_3-382_4	−06
1	2832.479	35294.41	13_2-490_3	+03
1	2832.959	35288.43	17_4-523_5	−04
4M2Z	2833.634	35280.03	D_4-414_3	00
T	2834.146	35273.64	18_2-533_3	+03
3	2835.644	35255.02	S_3-382_3	−03
3	2837.353	35233.78	D_3-369_2	−06
1	2838.681	35217.31	$19'_5-550'_5$	+07
2	2838.897	35214.62	15_5-502_4	−01
3M4	2839.343	35209.09	09_6-447_1; 14_2-501_3	−08 −42
1*u*	2840.104	35199.65	12_4-473_3	−08
1*u*	2840.226	35198.14	19_6-547_5	−02
E	2840.74	35191.81	20_1-?556$_2$; 20_2-561_{34}?	−07 +24

TABLE II—*Continued.*

Intensity (See text)	λ_{air}	ν_{vac}	Assignment	$\nu_{obs}-\nu_{calc}$
3s	2841.574	35181.45	D_3-400_2	00
1u	2842.569	35169.13	$16_4-?516_3$	+05
1	2847.359	35109.96	$18'_2-533_3$	00
2M2?	2847.831	35104.15	$D_2-?384_1$	−17
3M3AK2Z	2848.029	35101.71	S_3-380_3	−06
1Ed	2849.474	35083.92	19_3-549_3; 22_4-575_5	+05 −18
1	2850.394	35072.58	17_6-520_5	−06
2	2850.806	35067.51	15_5-501_5	−07
3	2853.501	35034.40	15_3-504_2	−28
2	2855.354	35011.66	13_1-483_2	−05
4K1s	2856.033	35003.35	D_1-366_2	−05
3	2857.144	34989.73	14_2-499_2	−14
3	2858.047	34978.68	D_4-411_4	−07
1	2858.428	34974.22	17_4-520_5	+11
2	2858.747	34970.12	13_3-483_2	−15
1	2860.174	34952.67	17_4-520_4	−04
2	2861.451	34937.07	13_1-482_2	−08
E	2862.43	34925.11	18_2-530_1	−08
?2	2863.893	34907.29	$19'_5-547_5$	+15
2	2865.320	34889.90	D_3-397_4	−01
4M5uK1 −s A	2866.071	34880.76	D_3-382_3	−06
2	2866.383	34876.97	D_3-397_2	−06
E	2870.54	34826.46	18_2-529_3	−09
E	2870.62	34825.50	09_0-443_1	+09
3	2870.914	34821.92	13_3-481_3	−08
3	2871.376	34816.33	D_3-396_3	−03
1	2872.504	34802.65	17_3-525_3	+38
2	2875.216	34769.83	12_4-469_4	−02
2	2876.936	34749.03	17_4-518_4	−02
1	2878.081	34735.07	17_3-524_4	−17
4M3	2878.721	34727.49	D_3-380_3	+01
5rM10K1 HA	2879.110	34722.80	S_3-376_3	−03
5rM2?K3s HA	2879.400	34719.31	D_0-347_1	−01
2	2880.632	34704.45	D_4-409_3	−02
3	2884.181	34661.76	19_5-543_5	+04
1	2885.921	34640.85	16_4-510_{34}	−02
3	2887.660	34620.00	13_3-479_4	−02
1Eu	2888.788	34606.49	19_4-538_5	−02
1	2892.121	34566.60	15_5-496_4	−04
E	2892.44	34562.73	20_2-555_3	+09
2	2893.125	34554.60	17_3-522_3	+01
2	2893.622	34548.66	13_3-483_3	−03
2	2894.255	34541.11	13_3-483_3; 14_3-495_2	+02 +02
E	2894.52	34537.90	14_3-495_3	−27
4rs A	2896.010	34520.17	D_1-361_1	+02
6rM7HK4Z A	2896.445	34514.99	S_2-374_2	00
2	2897.197	34506.03	15_3-499_3	−01
2	2898.252	34493.47	$17_4-?516_3$	+10
3	2900.515	34466.56	13_3-482_3	+03
2	2900.809	34463.07	12_4-466_4; 16_4-508_4	00 +32
2	2901.787	34451.45	$17_3-?521_3$	+07
2	2902.041	34448.44	D_2-377_1	00
2	2902.200	34446.56	D_4-406_3	+02
1	2902.606	34441.73	14_2-494_3	00
3	2904.783	34415.94	18_3-533_3; 19_2-536_2	−02 +11
1	2905.598	34406.27	20_2-553_3	+26
2	2906.731	34392.87	13_2-481_3	+05
2	2907.260	34386.60	18_2-525_2	00
2	2908.264	34374.73	16_4-508_5	−03
3A	2909.125	34364.56	09_0-438_1	−03
1	2909.632	34358.59	17_3-520_4	+03
4s	2910.481	34348.56	D_2-376_3	+02
4Z	2911.001	34342.42	D_0-343_1	+05
2	2912.245	34327.75	19_5-538_5	+02
2	2915.112	34293.98	14_2-492_2	−07
2	2916.109	34282.27	17_6-512_5	+02
2	2917.669	34263.94	18_3-532_4	+03
4A?K1s	2918.253	34257.08	D_4-404_5	+01
1u	2919.300	34244.80	13_3-475_3	−04
Eu	2919.69	34240.24	15_3-497_3; 22_4-567_3	+22 −27
2	2921.121	34223.47	12_4-463_3	−01
1	2921.906	34214.26	19_4-538_5	+01
4s A	2923.100	34200.29	D_3-390_3	+05
4 A	2923.548	34195.04	S_3-371_4	+02
3s	2925.132	34176.52	15_3-496_4	−06
E	2926.44	34161.29	23_3-580_3	−24
3	2926.984	34154.90	17_3-518_4	00
2	2927.933	34143.82	18_3-531_4	+01
2	2928.196	34140.76	D_2-374_2	00
2	2928.661	34135.34	13_3-474_3	+17
3	2930.155	34117.93	15_5-491_5	00
1	2932.047	34095.93	14_2-490_3	+01
5rK2s	2934.994	34061.71	D_1-357_2	+06
2	2935.632	34054.29	15_3-495_3	−05
4	2936.014	34049.86	D_4-402_3	−13
3	2937.149	34036.70	$19'_5-538_5$	−01
1	2937.673	34030.64	13_1-473_2	−03
3	2939.055	34014.63	D_4-402_4; 20_3-550_2	+02 +28
2	2939.185	34013.14	13_3-473_3	−02
2	2940.954	33992.66	17_3-516_2	00
2	2941.255	33989.19	13_3-473_2	−04
E	2942.14	33978.93	22_3-568_4	+05
2	2942.459	33975.28	$18'_2-522_3$	+01
2	2943.338	33965.13	17_4-510_{24}	−03
2	2943.972	33957.81	15_3-494_3	−09
7rM20HAK10Z	2944.410	33952.77	S_3-369_2	−07
1Ef	2946.527	33928.37	20_2-549_3	−10
8rM20K8Z HA	2946.992	33923.01	S_3-368_3	−03
6s	2947.393	33918.40	D_3-387_4	−04
1	2949.130	33898.43	18_2-520_3	+03
1	2951.418	33872.06	$18'_2-?521_2$	00
E	2951.79	33867.88	$24'_4-?58_5$	+28
E	2956.81	33810.40	15_2-492_2; 19_5-533_4	+18 −20
E	2957.54	33802.06	17_4-509_4	+27
1	2957.931	33797.58	17_6-508_5	00
1	2958.730	33788.45	19_2-530_1	+12
1	2958.846	33787.13	17_4-508_4	+09
3	2960.146	33772.28	13_1-470_2	+01
1	2961.715	33754.39	16_4-501_3	+01
E	2963.44	33734.78	$18'_2-520_3$	+03
1	2963.783	33730.85	13_3-470_2	+02
5AK2Z	2964.520	33722.47	S_3-366_2	+07
E	2965.88	33707.03	12_4-458_4	−01
E	2965.98	33705.89	13_3-474_3; 16_4-501_5	−10 −33
3	2966.578	33699.07	17_4-508_5	+02
2	2967.073	33693.45	17_4-508_3	+03
E	2968.23	33680.35	$18_1-?517_1$	−09
E	2968.78	33674.12	22_5-565_5	+36
E	2971.22	22646.47	$18_2-?517_1$	+02
3	2971.675	33641.28	D_1-353_2	+09
1	2972.497	33631.97	22_4-561_3	+12
3	2972.919	33627.18	12_4-457_5	+03
3	2976.802	33583.33	13_3-469_4; 19_5-531_4	+05 +04
3	2977.104	33578.68	D_2-369_2	+07
E	2977.67	33573.50	20_2-545_3	+01
E	2978.63	33562.68	19_3-533_3	−09
5K3s	2979.860	33548.87	D_2-368_3	+06
E	2981.14	33534.43	16_4-499_3	−31
1	2981.636	33528.89	18_3-525_2	−06
3	2982.620	33517.82	$18_1-?516_{12}$; 19_4-527_5; 19_3-533_4	+28 00 −11
Eu	2982.8	33515.4	12_4-456_3	−3
3	2984.154	33500.60	D_4-397_4	00
1	2985.668	33483.61	$18_2-?516_{12}$	+06
E	2985.86	33481.43	17_3-511_{23}	+11
1	2987.968	33457.83	13_3-468_2	−04
3	2990.512	33429.37	D_3-382_4	+02
3	2990.719	33427.06	D_4-396_3	+01
E	2991.96	33413.19	$18'_2-516_2$	−15

TABLE II—*Continued.*

Intensity (See text)	λ_{air}	ν_{vac}	Assignment	$\nu_{obs}-\nu_{calc}$
1	2992.181	33410.73	19_3-532_4	+01
2	2992.932	33402.35	22_5-562_4	−47
4s	2993.616	33394.71	D_4-396_5	+03
3	2995.264	33376.35	D_3-382_3	+02
1	2995.745	33370.98	17_3-510_{24}	−03
2	2995.994	33368.21	19_5-531_5	+01
2	2996.982	33357.21	16_4-497_4	−09
2	2997.612	33350.20	14_2-483_3	+01
5s	2997.794	33348.17	D_2-366_2	00
1	2998.290	33342.66	14_2-483_2	+03
3	3000.243	33320.95	$20_1-?537_2$	−13
E	3000.38	33319.45	22_4-557_5?	+55
3	3001.983	33301.64	13_2-470_2	−01
3	3002.827	33292.28	$19'_5-531_4$	+01
2	3004.23	33276.76	13_3-466_4	+26
EH				
2	3005.012	33268.07	14_2-482_2	00
1	3006.660	33249.84	19_2-525_2	00
1	3007.410	33241.55	20_1-536_2	−05
5	3009.085	33222.76	D_3-380_3	−23
2	3010.426	33208.25	17_3-509_4	+01
EH	3010.68	33205.44	16_4-496_4	+16
2	3011.682	33194.29	14_2-481_3	−07
2	3013.206	33177.61	17_4-502_4	+05
3s	3013.796	33171.12	D_3-380_4	+01
5s	3016.475	33141.65	D_4-393_5	−03
6rK4s	3017.447	33130.98	S_3-360_4	−02
1	3017.942	33125.55	19_4-527_5	−01
2	3020.220	33100.56	12_4-452_4	+01
2	3021.620	33085.23	18_3-520_4	−01
1	3023.162	33068.36	15_5-481_5	−03
5K4Z A	3024.931	33049.02	D_1-347_1	−03
3 A	3025.268	33045.33	09_0-425_1	−02
3	3026.683	33029.89	17_4-501_5	.?−55
3s	3026.794	33028.68	13_2-468_2	−01
E	3027.50	33020.96	13_1-463_2	+34
2	3027.804	33017.66	17_3-507_2	00
E	3031.35	32979.03	13_3-463_2	−15
2	3033.585	32954.74	12_4-451_4	00
3	3034.204	32948.02	$19'_5-527_5$	00
E	3038.45	32901.99	$18'_2-511_{32}$; 23_3-568_4	−01 +36
1	3038.720	32899.05	15_5-497_4; $19_2-?521_2$	?+44 +10
?2	3041.749	32866.29	15_3-483_3	−11
5rK2s	3041.876	32864.92	D_2-361_1	00
1	3042.287	32860.48	19_5-523_5	00
E	3042.42	32859.07	15_3-483_2; 17_4-499_3	+27 +04
1	3043.020	32852.57	12_4-450_3	−01
6K1 =	3043.819	32843.95	D_3-376_3	−10
1	3045.585	32824.90	19_4-520_5	00
5rK3s	3046.452	32815.56	D_1-344_2	00
?2	3047.572	32803.50	19_4-520_4	00
1	3048.131	32797.49	13_1-461_1	+03
2	3048.667	32791.72	$18'_2-510_{24}$?	+03
1	3049.360	32784.27	15_3-482_2	+03
6rK5s	3049.694	32780.68	S_3-357_2; 15_3-478_3	+03 −14
EH	3051.43	32762.07	19_2-520_3	+43
1Ed	3051.935	32756.61	16_4-491_5	+04
1	3052.827	32747.04	19_6-523_5	+04
3A	3054.020	32734.25	09_0-422_1	00
3	3055.401	32719.45	13_3-460_3; 18_3-516_2	+01 +11
2	3056.229	32710.59	15_3-481_3	+06
EH	3058.53	32685.93	20_2-536_2	−42
EH	3058.77	32683.37	18_2-508_3	−23
1	3059.825	32672.16	D_1-343_1	+06
1	3062.893	32639.43	22_5-554_5	+17
3	3063.183	32636.34	D_3-374_2; 18_1-507_2	+07 +36
E	3063.59	32631.96	$18_2-?516_{21}$	+04
1	3064.938	32617.66	D_2-359_3	−01
E	3065.65	32610.04	$19'_5-524_4$	−34
E	3065.89	32607.49	13_2-463_3	−24

Intensity (See text)	λ_{air}	ν_{vac}	Assignment	$\nu_{obs}-\nu_{calc}$
E	3066.42	32601.86	18_2-507_2	−13
1A	3069.470	32569.50	19_5-523_5	+04
E	3070.94	32553.88	13_3-459_2	−04
E	3071.72	32545.62	19_3-520_5?	−50
1K1−? A	3073.287	32529.04	D_4-387_4; 17_4-496_4	−09 −53
2 A	3073.695	32524.73	19_3-520_4	+01
3	3074.094	32520.50	13_3-458_4; $18'_3-508_3$	+03 +55
1	3075.227	32508.53	15_3-479_4	−02
E	3075.34	32507.32	14_2-474_2	−21
2	3081.875	32438.40	$18'_2-507_2$	+06
E	3084.41	32411.76	18_1-504_2	−08
2	3084.834	32407.28	17_4-495_5; 20_2-533_3	−05 −09
2	3084.918	32406.40	D_2-357_2	−02
E	3085.61	32399.16	21_4-53_1	+01
2	3086.981	32384.74	12_4-445_5	+01
1	3087.650	32377.73	18_2-504_2	−12
2	3089.193	32361.56	14_2-473_2	−03
2	3089.321	32360.22	S_3-353_2	+03
E	3090.05	32352.62	$19_2-?516'_2$	−19
2	3090.593	32346.89	$19_2-?516_3$	+10
2	3092.293	32329.12	13_3-456_3	−01
E	3092.52	32326.79	13_2-461_1	−05
5K1s	3093.515	32316.34	D_3-371_4	+04
1	3094.034	32310.92	17_4-494_3	+03
1	3096.013	32290.26	13_2-460_3	00
E	3096.45	32285.66	230_3-55_4	−18
2	3098.449	32264.88	17_3-499_3	00
E	3103.91	32208.09	18_2-511_{32}	+09
1	3104.422	32202.81	13_3-455_3	+02
4	3105.879	32187.70	19_3-520_3	+14
4s	3107.233	32173.68	D_2-354_3	+08
3K1	3108.019	32165.54	S_3-351_4	+08
2Ef	3111.122	32133.46	15_3-475_3	+09
1	3111.961	32124.80	13_2-459_2	+06
E	3112.87	32115.41	13_1-454_2	+26
1	3114.583	32097.76	18_3-510_{24}	+07
1	3116.215	32080.95	17_4-491_5	+09
E	3116.33	32079.76	22_4-545_3	−15
1	3116.869	32074.22	D_3-369_2	+10
1	3117.389	32068.87	18_2-501_3	+02
3s	3117.580	32066.90	13_1-453_1	−08
1	3118.360	32058.89	20_3-530_1	−06
3K2	3119.773	32044.40	D_3-368_3	+08
3K1?s	3120.192	32040.06	D_4-382_4	+02
2	3120.738	32034.45	19_4-512_5	−04
2	3121.170	32030.02	$19'_5-518_4$	−02
EH	3121.82	32023.36	15_3-474_3	−34
3	3125.363	31987.05	D_4-382_3	+03
EH	3127.94	31960.73	20_2-539_3	+42
1	3130.465	31934.91	18_2-509_4	−01
1EH	3133.724	31901.71	15_3-473_3	+02
4s	3133.895	31899.97	13_2-456_3	+02
3	3136.076	31877.78	15_3-473_2	+02
2	3137.641	31861.89	15_5-469_4	+02
1	3137.921	31859.05	12_4-440_3	+03
1	3138.886	31849.25	18_2-449_3	+04
1	3139.430	31843.74	D_3-366_2	+07
2	3140.420	31833.69	D_4-380_3; 22_4-543_5	+01 +14
3	3140.758	31830.27	14_2-468_2	+04
1	3141.183	31825.96	18_2-508_2	+01
3	3141.430	31823.46	12_4-439_4	+06
3	3142.154	31816.13	17_3-495_2; 19_4-510_{24}	+03 +18
E	3145.20	31785.28	15_5-468_5	?+46
3	3145.545	31781.83	D_4-380_4	+03
2	3146.359	31773.60	13_2-455_3	−01
1Ed	3152.000	31716.74	17_3-494_3	00
3	3152.958	31707.11	16_4-481_5	+08
2K1	3155.095	31685.63	$18'_2-499_3$	+07
2	3155.518	31681.38	S_3-346_4	+06
E	3157.02	31666.31	13_3-450_3	+30

TABLE II—*Continued.*

Intensity (See text)	λ_{air}	ν_{vac}	Assignment	$\nu_{obs}-\nu_{calc}$
1	3159.185	31644.62	13_3-454_2	+09
1*Ed*	3159.420	31642.27	19_4-512_5	+04
E	3161.92	31617.25	18_1-497_2	+07
4z	3163.419	31602.26	15_5-466_6	+05
E	3163.99	31596.57	13_2-453_1	+21
4z	3164.442	31592.04	13_3-449_4	+10
1	3166.744	31569.07	17_4-486_4; 17_3-492_2	−10 +01
1	3168.975	31546.86	19_2-508_3	+02
2	3169.938	31537.28	16_4-479_4; 19_5-510_{24}	+03 ?+11
3	3170.212	31534.54	S_3-344_2	−02
*EK*1?	3171.62	31520.58	18_3-504_8; 20_2-525_2	+38 +22
4*K*1?z	3176.602	31471.11	D_1-331_2	−02
2*Ef*	3177.187	31465.31	19_2-507_2	+08
2	3178.254	31454.76	D_4-376_3	+02
3z	3179.064	31446.75	17_3-491_4	−04
1	3180.307	31434.45	18_1-495_2	+03
4*Ef*	3180.750	31430.07	13_1-447_1	−02
2z	3181.819	31419.52	$18'_2-497_2$	−02
3	3182.860	31409.24	14_2-463_3	−03
3	3183.518	31402.74	S_3-343_2	+02
1	3183.750	31400.46	18_2-495_2	+03
3z	3184.051	31397.49	18_2-495_2	−02
3	3184.423	31393.82	D_2-347_1	00
1	3185.210	31386.07	22_4-538_6	−01
2	3186.746	31370.93	17_3-490_3	00
1	3187.769	31360.97	18_1-494_1	−01
3*Ef*	3189.239	31346.42	15_3-468_2	+02
E	3191.22	31326.95	18_2-494_1	+06
1*K*3*Z*	3191.577	31323.45	D_0-313_1	+04
1	3192.392	31315.46	14_2-462_2	+02
E	3192.89	31310.57	18_3-502_4	?+48
2	3195.071	31289.20	13_1-445_2	+02
Ef	3198.24	31258.21	16_4-476_4	+22
5*K*1z	3198.843	31252.30	D_3-360_4	+02
1	3199.308	31247.76	13_3-445_2	+02
2	3199.966	31241.34	13_2-450_2; 19_2-504_2	+03 +25
E	3200.40	31237.11	13_2-450_3; $18'_2-495_2$	+38 +33
1	3200.729	31233.89	$18'_2-495_3$	+02
2	3203.054	31211.22	18_3-501_3	+02
2	3205.503	31187.37	18_1-492_2	−01
5*K*2z	3207.248	31170.41	S_3-341_4	+08
1	3207.799	31165.06	15_3-466_4	+03
2	3208.098	31162.15	16_4-475_3	+08
4*K*1 =	3208.279	31160.39	D_2-344_2	+06
2	3208.566	31157.61	19_6-508_5	+03
1	3213.142	31113.23	D_4-359_3	+05
2*EfGK*5?z	3215.578	31089.66	D_4-373_5	−17
Euf	3216.20	31083.61	$19'_5-509_4$	+23
E	3217.70	31069.12	18_1-491_2	+12
3z	3218.612	31060.36	13_1-443_2	00
3	3220.070	31046.29	13_1-443_1	−04
2	3221.625	31031.31	17_4-481_5	−01
3z	3221.919	31028.48	D_2-343_3; 19_4-502_4	−01 +13
2	3223.126	31016.86	D_2-343_1	−01
2	3225.636	30992.72	S_3-339_2	+01
E	3225.94	30989.78	$18'_2-492_2$	+04
2	3227.498	30974.85	17_3-486_4	−17
2	3232.135	30930.41	16_4-473_3	+02
1	3232.232	30929.48	19_4-501_3; 17_4-548_3	+02 +42
2	3232.489	30927.03	D_4-371_4	+04
2z	3232.654	30925.45	15_3-463_3	+01
2*Ed*z	3234.996	30903.06	D_2-342_2	+02
3*Z*	3237.091	30883.05	09_0-404_1	+01
1*Eu*	3238.692	30867.79	15_3-463_2	+08
1	3241.409	30841.91	17_4-478_5	−37
3*K*1z	3242.026	30836.05	$21_{42}-52_{23}$	00
E	3249.83	30762.04	22_4-532_4	+30
2 =	3251.219	30748.86	12_4-429_4	+12
4z	3254.353	30719.25	15_5-457_5	+08
2z	3255.959	30704.10	12_4-428_5	+13
3z	3256.227	30701.56	14_2-456_3	+07
2	3258.137	30683.57	D_0-306_1	+12
2z	3259.659	30669.25	D_3-354_3; 13_2-444_3	+14 +01
3	3261.160	30655.13	D_4-368_2	+12
3*A*	3263.099	30636.92	13_3-439_4	+09
1	3264.337	30625.30	17_3-483_3	+06
2	3265.145	30617.72	17_3-483_2; $20_2-?516_{12}$; $24?_4-55_5$	+08 +29 +15
E	3266.16	30608.18	15_3-460_2	+21
2z	3266.762	30602.56	19_5-501_5	+04
2	3268 128	30589.78	13_2-443_2	+04
1	3268.582	30585.53	13_1-438_1	+02
2	3268.924	30582.33	17_4-476_4	+05
2z	3269.626	30575.77	13_2-443_1	+06
2	3270.269	30569.75	$24?_4-55_4$	+02
E	3273.13	30543.02	17_3-482_2; 18_3-495_2	−06 +24
E	3273.47	30539.85	18_3-495_3	−01
Eu	3278.51	30492.92	22_5-553_4	+14
E	3279.16	30486.88	17_4-475_2	?+52
2	3279.588	30482.89	$13_1-?437_0$	−02
1	3283.561	30446.01	14_2-454_2; $(19_2-497_2$	−06 −42)
E	3284.28	30439.36	12_4-426_2	+20
E	3285.99	30423.53	16_4-468_5	+07
E	3288.71	30398.37	14_2-453_1	+47
1	3290.513	30381.68	15_5-454_5	+04
E	3290.63	30380.64	19_4-496_4	+28
E	3291.02	30377.04	17_4-474_3	+35
E	3291.51	30372.52	13_3-437_4	+19
3z	3293.711	30352.18	12_4-425_3	00
2z	3298.128	30311.54	$19'_5-501_5$	+04
Euf	3299.71	30296.97	22_4-527_5	−42
E	3300.35	30291.10	20_1-507_2	+10
5*K*5z	3300.819	30286.82	D_3-351_4	+08
E	3303.31	30263.96	19_2-495_2	+29
E	3303.62	30261.12	19_3-495_3	+37
2	3305.565	30243.34	13_2-440_2	+07
E	3306.33	30236.33	18_1-483_2	+37
2	3309.475	30207.62	13_1-435_2	+04
E	3311.11	30192.69	15_5-452_4	+12
4*K*5*Z*	3311.389	30190.16	S_3-331_2; 19_2-494_1	+03 +03
1	3314.021	30166.18	13_3-435_2	+04
E	3314.52	30161.64	18_1-482_2; 19_4-494_3	+24 −04
3z	3316.091	30147.34	D_1-318_2	00
E	3317.07	30138.46	19_3-499_3	+09
2	3317.997	30130.03	13_3-434_3	−03
E	3319.65	30115.04	13_2-438_1	+15
3*Z*	3320.364	30108.55	09_0-396_1	00
E	3321.12	30101.71	19_5-496_4	+13
2z	3321.569	30097.63	18_2-490_3	+01
2	3322.253	30091.43	15_3-455_2	+11
E	3324.06	30075.10	16_4-465_5	+05
E	3324.96	30066.96	20_1-504_2	+10
5*K*1?z	3326.194	30055.78	D_4-362_5	00
2	3327.629	30042.82	14_2-450_2	−03
2z	3328.121	30038.38	14_2-450_3; $18'_2-483_2$	+01 −06
E	3330.56	30016.42	19_2-492_2	−21
5*K*3 =	3331.678	30006.31	S_3-329_3	+02
Ef	3336.55	29962.46	15_3-454_2; $19'_5-497_4$	+22 −12
E	3336.85	29959.76	22_4-524_4	+01
E	3337.49	29954.02	16_4-463_3	−12
3*Ef*	3343.247	29902.47	13_2-432_4	+03
1	3344.446	29891.76	$(17_3-475_3$; 19_4-491_4	−45) +03
3*Ef*z	3345.858	29879.14	13_3-432_2	+03
E	3346.10	29876.97	S_3-328_4	+13

TABLE II—*Continued.*

Intensity (See text)	λ_{air}	ν_{vac}	Assignment	$\nu_{obs}-\nu_{calc}$
E	3350.61	29836.76	$13_3-?431_4$	−12
E	3352.00	29824.39	17_4-469_4	−41
E	3352.96	29815.86	$\{D_2-331_2$;	−04
			$\{19_4-490_2$	−01
1	3353.552	29810.60	$19'_5-496_4$	+04
2*z*	3353.736	29808.96	19_3-496_4	+05
5*K*1?*z*	3354.451	29802.61	$\{D_2-346_4$;	+01
			$\{15_2-452_4$	+10
E	3356.71	29782.56	17_3-474_3	+02
E	3357.10	29779.10	22_4-522_3	00
E	3360.76	29746.68	$\{13_1-?430_3$;	−05
			$\{17_6-?467_7$	−10
E	3361.87	29736.86	13_2-435_2	−10
E	3361.97	29735.97	20_2-507_2	+19
2*z*	3363.341	29723.84	D_4-359_2	−03
Eu	3364.90	29710.09	12_4-418_4	+14
1	3365.941	29700.88	13_2-434_3	00
E	3367.21	29689.71	19_3-495_2	+12
E	3367.56	29686.63	$\{19_3-495_3$;	−04
			$\{28_5-?579_6$	−07
E	3367.64	29685.92	13_3-430_4	+36
E	3370.17	29663.64	17_4-466_4	−03
1	3370.520	29660.53	17_3-473_3	00
2*y* =	3371.052	29655.85	D_3-344_2	+01
2 =	3371.358	29653.16	$\{D_1-313_1$;	+02
			$\{19_5-491_3$	+29
E	3373.24	29636.57	$\{16_4-460_3$;	−10
			$\{17_3-473_2$	−03
3*K*2*z*	3373.756	29632.08	D_2-329_3	+02
2*z*	3375.120	29620.11	14_2-445_2	+01
E	3376.90	29604.45	22_4-520_5	−02
E	3378.51	29590.35	19_3-494_3	+12
E	3379.26	29583.79	22_5-524_4	+21
2	3381.735	29562.17	13_3-429_4	00
1*y*	3382.097	29559.00	15_3-450_2	−02
2*z*	3382.606	29554.56	15_3-450_3	+02
2*z*	3384.340	29539.42	19_6-491_5	+03
2*A*	3386.102	29524.04	D_3-343_3	+04
E	3386.79	29518.03	17_4-466_4	+01
2*z*	3391.102	29480.52	15_3-449_4	+05
2*z*	3391.531	29476.79	$\{15_5-445_5$;	+04
			$\{18_2-475_3$	+25
E	3394.62	29449.96	13_2-432_2	+03
E	3395.47	29442.59	19_2-492_2	+04
2*z*	3395.817	29439.59	13_2-432_1	+03
2*AK*2*z*	3398.099	29419.81	19_4-486_4	−15
E	3398.59	29415.57	23_3-533_4	+04
ET	3400.51	29398.97	D_3-342_3	+05
1	3401.396	29391.29	14_2-443_2	+01
E	3402.76	29379.53	22_4-518_4	+12
1	3404.229	29366.84	18_2-474_3	−03
1	3404.802	29361.90	$19'_5-491_5$	+05
1	3405.276	29357.81	16_4-457_5	00
1*Ef*	3406.834	29344.38	18_3-483_2	+06
1	3407.639	29337.45	12_4-414_3	+04
1	3409.442	29321.94	$19'_5-491_4$	+01
E	3409.61	29320.53	$\{15_5-443_6$;	+14
			$\{19_3-491_4$	+25
E	3410.50	29312.88	$18'_2-475_3$	−01
E	3411.01	29308.50	23_3-532_4	+18
3*z*	3412.969	29291.64	D_3-341_4	+03
3 =	3413.539	29286.75	S_2-322_3	+02
E	3415.54	29269.55	18_3-482_2	−21
E	3418.24	29246.44	16_4-456_3	+08
E	3418.49	29244.32	19_2-490_2	−10
1	3419.288	29237.52	$23_{03}-52_{23}$	00
1	3420.358	29228.37	22_5-520_5	+07
1	3423.302	29203.23	$18'_3-474_3$	+01
Eu	3425.03	29188.47	23_3-531_4	+25
3 =	3427.720	29165.59	13_3-425_3	−02
1	3430.269	29143.91	$26l_3-55_4$	−01
E	3430.38	29142.96	13_1-424_3	+49
E	3433.08	29120.05	16_4-455_3	+03
2*z*	3433.791	29114.02	D_3-339_2	+03
E	3434.79	29105.56	17_3-468_2	+32
ET	3438.966	29069.95	19_4-483_3	−23
1	3441.975	29044.80	14_2-440_3	−01
3y =	3443.014	29036.03	12_4-411_4	−06
1	3445.411	29015.84	20_1-494_1	−06
2*z*	3445.726	29013.18	$\{D_1-306_1$;	00
			$\{23_3-529_3$	−13
ET	3446.900	29003.30	22_5-518_4	+06
E	3447.68	28996.77	18_1-470_2	+25
3*z*	3448.842	28986.97	15_3-444_3	+02
E	3449.28	28983.32	20_2-499_3	+35
2	3451.752	28962.53	18_2-470_2	00
E	3451.91	28961.16	17_4-460_3	+20
1*Efz*	3452.630	28955.17	13_1-422_1	+01
E	3456.35	28923.97	17_3-466_4	+10
2	3457.372	28915.46	15_5-439_4	+04
3*z*	3457.726	28912.50	D_2-322_3	00
2	3458.325	28907.49	15_3-443_2	+04
E	3459.00	28901.82	$09_9-?384_1$	+01
2	3459.527	28897.45	D_4-351_4	+02
E	3461.33	28882.37	19_4-481_5	+26
3*A*?	3463.252	28866.36	S_2-318_2	+02
E	3465.38	28848.62	19_3-486_4	+11
3*z*	3468.405	28823.48	13_3-426_3	+07
E	3471.34	28799.11	$18'_2-470_2$	+23
3*z*	3475.836	28761.86	$\{12_4-409_3$;	+05
			$\{17_4-458_4$	−13
E	3477.25	28750.17	12_4-409_5	+21
E	3478.90	28736.54	13_2-425_3	+11
E	3480.48	28723.50	18_1-468_2	−06
3*z*	3481.828	28712.36	19_4-479_4	+03
E	3482.79	28704.45	266_5-55_5	−01
1	3485.295	28683.80	17_3-463_3	?−48
3*z*	3485.507	28682.05	17_4-457_5	−05
2*z*	3489.293	28650.94	15_5-437_4	+02
1	3491.836	28630.07	13_3-419_2	00
E	3492.29	28626.31	17_3-463_2	−24
1	3493.198	28618.90	18_3-475_3	+01
3*Az*	3500.287	28560.94	15_3-440_3	−04
2*z*	3503.044	28538.47	14_2-435_2	−03
2*Ef*	3503.567	28534.21	20_2-495_2	+02
1	3504.658	28525.33	15_3-439_4	−03
2 =	3506.649	28509.13	$\{16_4-449_4$;	−04
			$\{18_3-474_3$	−09
2*z*	3507.294	28503.89	12_4-406_3	+01
E	3507.89	28499.04	19_3-483_3	+31
3*z*	3508.746	28492.10	D_2-318_2	−01
2*z*	3509.025	28489.83	19_6-481_5	−02
1	3509.674	28484.57	13_2-422_1	+02
5*z*	3510.041	28481.58	S_3-314_4	−02
E	3512.62	28460.68	20_3-494_1	+03
1*z*	3515.971	28433.55	19_5-479_4	00
E	3516.74	28427.34	13_1-417_2	+36
2	3517.516	28421.06	12_4-405_4	+05
3	3518.485	28413.23	D_4-346_4	−06
2*z*	3521.717	28387.16	18_2-473_3	−05
3*z*	3521.916	28385.55	13_3-417_2	+01
1*z*	3524.243	28366.81	17_3-460_3	00
E	3524.64	28363.64	18_3-473_2	+36
3*Efz*	3527.004	28344.61	17_4-454_5	+04
E	3527.59	28339.93	19_2-475_3	+18
E	3527.91	28337.36	19_4-475_3	+21
1*z*	3530.761	28314.45	12_4-404_5	+04
1*z*	3531.027	28312.31	$19'_5-481_5$	00
E	3531.08	28311.85	D_3-331_2	?+44
1*z*	3535.551	28276.09	13_1-415_2	+02
4*z*	3537.455	28260.87	$\{15_5-433_5$;	00
			$\{15_3-437_4$	+01
2*z*	3538.634	28251.45	14_2-432_2	−02
E	3539.30	28246.11	09_9-377_1	+18
E	3539.90	28241.33	14_2-432_1	+23
2*z*	3540.741	28234.64	13_2-415_2	+01
2*z*	3541.648	28227.41	19_4-474_3	−07
ET	3542.655	28219.38	22_5-510_{24}?	+03
1	3543.719	28210.92	18_2-463_3	+04
2	3544.801	28202.31	19_6-478_5	+03

TABLE II—*Continued.*

Intensity (See text)	λ_{air}	ν_{vac}	Assignment	$\nu_{obs}-\nu_{calc}$
2s	3544.981	28200.88	$\begin{cases}13_2-419_2; \\ (17_3-459_2\end{cases}$	$\begin{matrix}-01 \\ -41)\end{matrix}$
6K2Z	3545.234	28198.86	D_0-281_1	+02
1s	3547.480	28181.01	15_5-432_4	−02½
2s	3548.269	28174.74	18_2-462_2	−04
1	3550.694	28155.50	17_4-452_4	00
3s	3550.850	28154.26	19_5-476_4	−03
1	3551.282	28150.84	13_3-414_2	00
E	3552.34	28142.46	$19'_5-479_4$	−07
3s	3554.220	28127.57	D_3-329_3	00
1	3555.760	28115.39	$\begin{cases}15_5-?431_4; \\ 16_4-445_5\end{cases}$	$\begin{matrix}-08 \\ 00\end{matrix}$
E	3559.08	28089.18	20_2-490_3	+16
2s	3559.714	28084.16	19_2-473_2	−01
E	3561.26	28071.99	12_4-402_4	+04
2s	3563.457	28054.66	15_3-435_2	−01
E	3565.17	28041.21	22_5-508_4	−02
E	3567.25	28024.86	$19'_5-478_5$	+12
Eu	3567.66	28021.64	18_1-461_1	−07
1s	3568.045	28018.59	15_3-434_2	00
E	3568.40	28015.83	16_4-444_3	+18
3s	3568.993	28011.15	$18'_2-462_2$	+02
2s	3569.233	28009.27	D_4-342_3	+03
E	3569.59	28006.50	19_5-475_6	+01
6	3570.662	27998.05	$\begin{cases}D_2-313_1; \\ D_3-328_4\end{cases}$	$\begin{matrix}+14 \\ -07\end{matrix}$
2 =	3573.415	27976.48	17_3-456_2	−02
2s	3575.230	27962.28	17_6-499_7	+04
3Eds	3575.979	27956.43	13_2-417_2	+07
2s	3576.384	27953.25	22_5-508_5	+01
?2	3581.233	27915.41	17_6-449_6	+11
1s	3582.242	27907.55	17_6-450_5	+02
E	3582.92	27902.26	D_4-341_4	−04
3 =	3584.109	27893.01	19_6-475_6	−01
1	3589.699	27849.58	13_3-411_4	+06
4K1s	3590.830	27840.81	15_3-429_4	+05
1u	3591.771	27833.51	17_4-449_4	+05
E	3591.98	27831.90	18_3-468_2	−02
E	3592.98	27824.15	$18'_2-461_1$	+08
E	3593.55	27819.74	18_1-459_2	+13
2A?s	3593.979	27816.41	20_1-482_2	−01
T	3595.386	27805.52	13_2-415_2	+07
E	3596.45	27797.31	13_1-411_2	−06
E	3596.63	27795.92	15_5-428_5	−07
3s	3597.271	27790.96	18_3-432_4	+03
1	3597.721	27787.48	$18'_2-460_3$	−01
E	3597.97	27785.57	18_2-459_2	−05
3Z	3598.885	27778.50	D_0-277_1	+04
E	3600.30	27767.60	$\begin{cases}15_2-432_2; \\ 19_3-475_3\end{cases}$	$\begin{matrix}-04 \\ +26\end{matrix}$
E	3601.84	27755.73	13_3-411_2	−20
3s	3606.074	27723.11	D_1-293_2	00
2Eds	3606.344	27721.03	17_3-454_2	−05
3s	3607.070	27715.46	$19'_5-475_6$	00
EA	3614.24	27660.45	22_4-501_5	?−42
E	3614.80	27656.17	19_3-474_3	+14
E	3615.52	27650.66	18_3-466_4	+08
8rK10Z	3617.522	27635.39	S_3-305_3	+05
E	3619.78	27618.13	$26?_2-53_1$	00
3s	3622.352	27598.54	19_4-468_5	00
3 =	3625.408	27575.28	13_3-409_3	+04
3s	3627.246	27561.30	$\begin{cases}13_1-408_2; \\ 17_3-452_4\end{cases}$	$\begin{matrix}+08 \\ -05\end{matrix}$
Ef	3628.39	27552.61	19_2-468_2	−20
3s	3630.324	27537.93	$\begin{cases}14_2-425_3; \\ 17_6-445_5\end{cases}$	$\begin{matrix}+02 \\ -28\end{matrix}$
3s	3630.830	27534.09	19_3-473_3	+07
5s	3631.959	27525.54	D_1-291_2	−03
2	3632.719	27519.78	13_3-408_2	00
1	3636.740	27489.35	22_4-499_3	−04
3s	3637.393	27484.42	12_4-396_3	+03
1	3637.942	27480.27	$26?_2-53_1$	−32
3s	3640.144	27463.65	13_1-407_1	+08
2s	3641.862	27450.70	15_3-429_4	00
E	3642.81	27443.58	278_4-55_4	+11
E	3643.29	27439.96	17_4-445_5	+28
E	3647.13	27411.00	18_3-463_3	+04
3Ais	3647.531	27408.03	D_3-322_3	+02
1	3649.023	27396.82	$\begin{cases}(18'_2-456_3; \\ 19_5-469_4\end{cases}$	$\begin{matrix}-36) \\ +01\end{matrix}$
3s	3651.008	27381.93	17_6-443_6	+08
E	3652.75	27368.84	19_4-466_4	+03
3s	3654.204	27357.98	D_2-306_1	+03
Eu	3656.15	27343.40	20_2-483_3	+07
1	3656.680	27339.49	18_1-454_2	+06
1	3658.368	27326.85	13_2-411_2	+10
1s	3659.315	27319.78	19_5-468_5	+02
E	3659.53	27318.15	17_3-450_2	+29
1	3660.171	27313.38	17_3-450_3	00
1	3660.369	27311.90	22_4-497_4	−05
2s	3660.609	27310.11	16_4-437_5	+08
E	3661.24	27305.39	18_2-454_2	−02
1	3663.150	27291.17	18_1-453_1	−06
3	3663.360	27289.60	16_4-437_4	+04
1	3663.824	27286.15	14_2-422_1	+06
2s	3665.881	27270.84	$18'_2-455_3$	00
3s	3667.183	27261.16	$\begin{cases}D_2-305_3; \\ 20_2-482_2\end{cases}$	$\begin{matrix}+05 \\ -01\end{matrix}$
3s	3667.719	27257.17	18_2-453_1	−07
3s	3668.664	27250.15	19_4-465_5	+02
1	3670.771	27234.51	13_3-405_4	+02
ET	3672.95	27218.35	266_0-53_1	+05
3s	3674.584	27206.26	19_6-468_5	−02
3s	3675.559	27199.04	12_4-393_5	+02
E	3680.87	27159.82	22_4-496_4	−11
5s	3682.101	27150.72	D_4-333_5	−04
3 =	3683.316	27141.76	$\begin{cases}18'_2-454_2; \\ 23_3-510_{34}\end{cases}$	$\begin{matrix}00 \\ -34\end{matrix}$
3 =	3683.399	27141.14	15_2-426_3	+02
3s	3683.945	27137.12	19_5-466_6	−03
2s	3684.663	27131.84	19_2-463_3	−01
2s	3685.023	27129.19	19_4-463_3	−03
5s	3688.069	27106.78	$19_6-?467_7$	00
2	3688.423	27104.18	$\begin{cases}13_1-404_1; \\ 19_3-469_4\end{cases}$	$\begin{matrix}+22 \\ +04\end{matrix}$
3s A	3689.877	27093.50	$\begin{cases}18'_2-453_1; \\ 18_3-460_3\end{cases}$	$\begin{matrix}-09 \\ +01\end{matrix}$
3s A	3690.261	27090.68	13_2-408_2	+08
E	3695.21	27054.37	15_3-425_3	+23
E	3697.45	27037.99	$\begin{cases}19_2-462_2; \\ 22_4-495_3\end{cases}$	$\begin{matrix}-03 \\ -30\end{matrix}$
2s	3698.715	27028.76	$19'_5-468_5$	+02
3 =	3699.411	27023.67	19_6-466_6	00
3s	3702.316	27002.47	14_2-419_2	+04
2s	3703.596	26993.13	13_2-407_1	+10
2s	3705.485	26979.38	23_3-509_4	+05
6K1?Z	3707.929	26961.59	S_3-299_3	+06
1	3711.481	26935.79	$\begin{cases}(18_1-450_2; \\ 22_5-497_4\end{cases}$	$\begin{matrix}-39) \\ +01\end{matrix}$
2s	3714.238	26915.80	17_6-439_5	+11
2	3715.046	26909.94	20_1-473_2	00
1s	3716.735	26897.71	18_2-450_3	00
2s	3717.099	26895.08	17_3-445_2	−03
3s	3719.412	26878.36	17_4-439_4	+01
2 =	3720.522	26870.34	23_3-508_3	−02
3Ais	3722.254	26857.84	19_6-465_5	−03
E	3723.85	26846.29	$19'_5-466_6$	+16
Eu	3727.85	26817.49	17_4-439_5	+33
1	3728.285	26814.39	19_2-460_3	+01
3s	3730.429	26798.97	$19'_5-466_4$	−04
1s	3732.552	26783.74	22_5-496_4	−02
E	3737.85	26745.76	17_3-446_3	−03
E	3738.13	26743.76	17_4-438_3	00
2	3738.899	26738.27	$\begin{cases}D_4-329_3; \\ 18'_2-450_2\end{cases}$	$\begin{matrix}+01 \\ -27\end{matrix}$
2s	3739.488	26734.06	$18'_2-450_3$	00
3Efs	3741.714	26718.15	14_2-416_2	+04
2	3742.689	26711.19	22_4-491_5	−03
2 =	3743.820	26703.13	18_3-456_3	−05
Euf	3750.67	26654.37	18_1-447_2	+03

TABLE II—*Continued.*

Intensity (See text)	λ_{air}	ν_{vac}	Assignment	$\nu_{obs}-\nu_{calc}$
2s	3751.432	26648.94	19_3-459_2	+08
1u*Ef*	3753.487	26634.35	17_4-437_5	+03
Eu	3754.15	26629.67	214_3-48_2	00
E	3754.87	26624.56	214_1-48_2	+03
E	3755.49	26620.17	18_2-447_1	−18
E	3756.38	26613.86	17_4-437_4	+01
1	3756.878	26610.31	20_3-475_3	+01
3	3757.093	26608.79	D_4-328_4; 230_3-49_2	−02 +03
1	3757.345	26607.00	14_2-415_2	+01
3*Ef*z	3757.929	26602.87	D_2-314_4; 16_4-430_4	−01 +08
4*Ef*z	3760.133	26587.27	D_2-299_3	−03
2	3760.644	26583.66	287_4-55_5	00
2s	3761.623	26576.75	18_3-455_3	−09
2s	3764.316	26557.74	19_3-463_3	−03
1s	3767.419	26535.86	287_4-55_4	+04
2	3767.846	26532.86	19_4-457_5	−03
5*K*2*Z*	3768.448	26528.62	D_1-281_1	+05
3s	3769.213	26523.24	14_2-414_3	+04
3*y*	3769.869	26518.62	15_3-419_2	+02
1	3770.608	26513.42	18_1-445_2	−01
2s	3772.430	26500.62	20_3-474_2	−01
4*Ef*z	3773.707	26491.65	13_3-402_3	+07
2	3775.447	26479.44	16_4-429_4; 18_2-445_2	+04 00
2s	3778.684	26456.76	$18'_2-447_1$	+08
1	3779.971	26447.75	18_3-454_2	−01
5*Ef*K3z	3780.770	26442.16	S_3-293_2	+05
2	3781.836	26434.70	16_4-428_5	+07
3s	3783.731	26421.47	19_4-456_3	+03
E	3785.05	26412.26	15_3-418_4	+35
2s	3786.375	26403.02	17_6-434_7	+04
E	3790.98	26370.96	13_3-397_4	−41
4s	3792.768	26358.52	13_3-397_2	+03
E	3793.31	26354.77	20_2-473_2; 23_3-502_4	+08 +27
3s	3794.349	26347.53	15_5-414_6	+04
2s	3796.290	26334.06	19_5-458_4	+06
E	3796.92	26329.72	13_1-396_1; 18_2-444_3	+25 −40
2	3798.926	26315.79	$18'_2-445_2$	00
2s	3801.527	26297.78	13_3-396_3; 19_2-455_3	−04 +05
3s	3801.925	26295.03	19_4-455_3; 22_5-491_4	−07 −10
1	3802.938	26288.03	18_3-452_4	00
E	3803.45	26284.46	17_3-439_4; 18_1-443_2	+26 −15
E	3804.98	26273.89	15_3-417_2; 17_3-439_2	−18 −15
E	3805.48	26270.44	18_1-443_1	−14
E	3807.65	26255.47	23_3-501_3	−14
5Z	3809.239	26244.55	S_3-291_2	−02
E	3809.90	26239.97	19_3-460_3	−33
3s	3810.395	26236.58	18_2-443_1	−01
4s	3810.804	26233.77	13_2-400_2	+04
E	3815.76	26199.68	22_4-486_4	+15
1s	3816.393	26195.35	19_4-454_5	−01
6*Z*	3817.489	26187.83	S_3-291_3	00
2*As*	3820.115	26169.82	16_4-426_3	00
1	3824.148	26142.23	18_3-451_4	+01
2us	3824.392	26140.57	19_6-457_5	−06
2s	3826.198	26128.22	14_2-411_2; 15_5-411_4	−07 +11
E	3826.90	26123.44	15_3-415	+28
E	3827.33	26120.50	19_2-453_1	+02
3 =	3829.133	26108.20	D_1-277_1	+01
2	3830.723	26097.36	12_4-382_4	−02
Eu	3830.98	26095.62	261_3-52_{21}	+02
E	3832.26	26086.91	$18'_2-443_2$	−06
E	3832.85	26082.90	16_4-425_3	+06
1	3834.047	26074.74	19_3-459_2	−04
5*Ef*Z	3835.058	26067.86	D_2-293_2	−02
2	3836.966	26054.90	262_2-52_{21}	−13
4*Ef*z	3838.514	26044.39	12_4-382_3; 18_3-450_2	+03 −15
ET	3839.257	26039.35	15_3-414_3	−02
2*Ef*	3842.307	26018.68	D_4-322_3	−02
5*Ef*Z	3846.225	25992.17	D_1-276_2	00
3*Ef*K1?Z	3847.501	25983.56	D_3-259_1	−01
1	3852.834	25947.59	14_3-409_2	−01
3s	3855.548	25929.33	13_2-397_2	+02
1	3857.293	25917.60	263_2-52_{23}	+11
3s	3859.298	25904.14	18_2-440_3	−01
2	3861.060	25892.31	14_2-408_2; 18_1-439_2	+17 −05
2	3861.240	25891.11	12_4-380_3	+09
1	3863.475	25876.13	13_1-391_1	+05
3 =	3864.335	25870.37	D_2-291_2	+03
1	3865.324	25863.75	20_1-462_2	−04
2	3866.054	25858.86	13_2-396_1; $(23_3-497_4$	+01 +33)
E	3867.38	25850.01	19_3-456_2; 22_4-483_3	+02 +26
5*Ef*K4?Z	3867.986	25845.95	S_2-287_4	+01
2	3868.579	25841.99	15_5-409_5	+01
E	3869.05	25838.86	12_4-380_4	−28
4s	3872.835	25813.59	D_2-291_2; 17_3-453_2	−01 +08
2s	3874.414	25803.08	19_6-454_5; $328_4-?58_5$	−02 +29
2s	3875.691	25794.57	14_2-407_1	−01
E	3878.51	25775.85	18_2-438_1	+08
1	3880.081	25765.39	19_2-450_2	−04
E	3880.74	25760.98	19_2-450_3	+03
ET	3881.141	25758.34	19_4-450_3	+02
5*Ef*K?s	3881.402	25756.62	D_3-305_3	00
1	3883.837	25740.47	$18'_2-440_3$	−03
2s	3886.451	25723.16	13_1-390_2	+02
E	3888.89	25707.02	$18_1-?437_0$	−14
1s	3890.750	25694.73	$18'_2-439_2$	+01
E	3891.26	25691.35	239_2-49_3	−02
1s	3892.338	25684.25	19_4-449_4	00
3s	3892.729	25681.68	13_3-390_2	−02
1	3893.478	25676.73	20_1-461_1	00
1s	3901.835	25621.74	18_3-445_2	−05
1*y*	3903.301	25612.12	$18'_2-438_1$	00
1s	3903.987	25607.62	297_5-55_5	+02
2s	3905.980	25594.55	19_3-454_2	−02
Eu	3911.30	25559.76	297_5-55_4	00
1s	3912.824	25549.79	17_3-432_4	−02
E	3916.39	25526.55	17_3-432_2	+07
2s	3918.603	25512.10	12_4-376_3	+02
1*A* =	3922.339	25487.80	23_3-494_3	−03
2	3924.377	25474.57	20_1-459_2	−06
2 =	3924.699	25472.48	18_3-444_3	+01
2s	3926.040	25463.78	15_3-409_2	+01
Es	3930.21	25436.75	$19'_5-452_4$	+26
2s	3930.485	25434.98	14_2-404_1; 19_3-452_4	+10 +14
2s	3930.976	25431.80	18_1-435_2	−03
E	3934.59	25408.44	15_3-408_2	+13
3s	3935.048	25405.49	13_2-391_1; 19_5-449_4	+03 +02
2s	3936.239	25397.80	18_2-435_2	−04
3*Ef*	3936.993	25392.93	18_3-443_2	−04
2s	3937.637	25388.78	19_5-449_6	00
E	3939.93	25374.01	22_4-478_5	−10
2s	3941.837	25361.73	18_2-434_2	−04
1s	3944.803	25342.66	19_2-445_2	−02
E	3945.18	25340.26	23_3-492_2	+11
1	3946.313	25332.96	17_3-430_4	+03
3s	3947.991	25322.20	19_4-449_7	−04
E	3950.10	25308.70	20_2-462_2	+16
3s	3952.529	25293.13	14_2-402_2	+01
2s	3952.909	25290.70	19_4-445_5; $19'_5-451_4$	+23 +02
3s	3953.166	25289.05	19_3-451_4	+02
1	3953.720	25285.51	22_5-481_5	00

TABLE II—*Continued.*

Intensity (See text)	λ_{air}	ν_{vac}	Assignment	$\nu_{obs}-\nu_{calc}$
4 =	3955.317	25275.30	19_6-449_6	00
3s	3958.884	25252.53	13_2-390_2	+01
E	3961.75	25234.24	$18'_2-435_2$	+05
E	3963.70	25221.83	23_2-491_2	+06
2	3965.003	25213.56	D_4-344_4	+01
3Ef =	3965.150	25212.62	22_4-476_4	−02
1	3968.173	25193.42	19_2-444_2	+06
2s	3968.594	25190.74	19_4-444_3	+01
E =	3969.18	25187.01	19_3-450_3	+14
E	3972.83	25163.88	15_5-402_4	−09
E	3973.30	25160.90	200_1-45_0	−02
3s	3975.470	25147.17	12_4-373_5	00
1s	3975.897	25144.47	17_4-422_3; $(18_1-432_2$	+03 −37)
1	3976.289	25141.99	23_3-490_3	−03
2s	3979.293	25123.01	$13_1-?384_1$; 15_3-405_4	+28 +04
E	3980.32	25116.54	22_4-475_3	−18
3s	3980.649	25114.45	$19'_5-449_4$	00
Es	3981.28	25110.49	18_2-432_2	−32
1	3982.876	25100.41	18_2-432_1	−03
2s	3982.969	25099.83	19_2-443_1	00
3EfK1?s	3983.294	25097.77	$19'_5-449_6$	+01
1s	3988.017	25068.05	16_4-414_3	−02
2s	3991.232	25047.86	214_2-46_3	+02
1s	3993.913	25031.05	230_3-48_2	−09
2s	3997.142	25010.83	18_3-439_4	−05
Es	3997.35	25009.50	214_2-46_1	−04
Es	3997.77	25006.88	22_4-474_3	−17
2 =	3998.165	25004.43	214_1-46_1	+03
2s	3998.762	25000.70	18_3-439_2	−02
E	3999.19	24998.00	22_5-478_5	+06
3s	4001.379	24984.34	12_4-371_4	+01
3Z	4005.408	24959.21	D_1-266_0	−03
8GK10Z	4008.769	24938.30	S_3-278_4	+01
2s	4010.384	24928.25	230_3-47_4	−01
E	4011.81	24919.38	20_2-459_2	00
Es	4013.20	24910.75	13_3-382_4	−06
1	4014.943	24899.95	17_3-426_3	−01
4Ef?	4015.229	24898.17	19_6-445_5	−04
1	4016.114	24892.68	274_4-49_3	+03
E	4017.34	24885.10	22_4-473_5; 28_5-531_4	+06 +22
4Z	4019.238	24873.34	D_2-281_1	00
3	4022.123	24855.50	19_5-443_6; 200_1-44_2	+17 +02
ET	4025.19	24836.56	22_5-476_4	+09
3Z	4028.798	24814.32	09_0-343_1	−04
1 =	4029.030	24812.88	17_3-425_2	−10
1	4029.615	24809.28	15_2-402_3	−01
E	4031.66	24796.67	274_3-52_{33}	+01
2s	4035.368	24773.91	15_3-402_4	00
3s	4036.870	24764.70	19_4-440_3; 17_4-418_4	−06 −20
2s	4039.869	24746.32	18_3-437_4; 23_3-486_3; 305_3-55_4	−06 +21 −10
2 =	4040.600	24741.84	19_6-443_6	−01
1s	4042.402	24730.81	14_2-397_2	−04
1s	4043.909	24721.60	19_2-439_2	−01
5K1?Z	4045.615	24711.16	S_3-276_2	−01
2 =	4046.716	24704.44	13_3-380_3	−01
2	4047.948	24696.93	D_1-263_2	−02
1	4048.266	24694.98	20_2-456_2	+39
E	4052.35	24670.10	14_2-396_2	−08
3s	4053.948	24660.37	14_2-396_1	−02
1s	4055.243	24652.50	13_3-380_4; $13_3-?384_1$	−07 +39
E	4055.64	24650.09	15_3-397_4	+15
Es	4057.45	24639.10	19_2-438_1	+09
2 =	4060.716	24619.27	19_3-444_3	−01
3s	4064.799	24594.55	19_4-438_3	00
E	4065.35	24591.23	20_1-450_3; 247_4-49_5	+03 −05
1s	4066.005	24587.25	17_4-416_3	−02
E	4069.17	24568.15	20_2-455_3	−10
2s	4069.804	24564.30	$19'_5-443_5$	−01
4	4070.618	24559.38	D_1-262_3	−03
2	4071.939	24551.42	15_3-400_3	−02
2s	4073.161	24544.05	15_5-396_5	+01
E	4073.88	24539.70	19_3-443_2	−08
6Ep'K5 =	4074.374	24536.75	S_3-274_3	−03
1	4079.794	24504.16	18_3-434_3	+05
E	4082.07	24490.48	18_1-425_1	−04
4s	4082.972	24485.09	19_4-437_5	−02
1s	4083.722	24480.58	16_4-409_5	−04
4s	4088.340	24452.94	D_2-277_1	−02
2s	4088.778	24450.32	19_6-439_4	−04
2s	4089.392	24446.64	266_5-51_4	−03
2	4090.646	24439.14	20_2-454_2	−03
2	4092.398	24428.68	13_2-382_3	+07
3s	4095.710	24408.93	17_6-414_6	−02
2s	4097.673	24397.07	18_2-425_3	−24
E	4098.52	24392.21	17_4-414_3	−15
2s	4099.029	24389.22	19_5-439_5	+05
1	4101.855	24378.30	22_4-468_5	+19
5Ep'fK1?s	4102.713	24367.27	D_4-305_3	−04
E	4107.83	24336.94	D_2-276_2	00
2s	4108.538	24332.73	18_2-424_2	00
4 =	4109.758	24325.50	13_3-376_2	−01
2s	4110.573	24320.67	$18'_2-426_3$	+03
4Z	4111.819	24313.31	D_1-259_1	+01
1u	4112.487	24309.36	D_3-291_3; 20_1-447_1	+25 00
2s	4115.588	24291.04	15_5-393_5	00
3s	4118.060	24276.46	18_2-432_4	−03
2s	4118.189	24275.69	$(13_2-380_3$; 19_6-439_5	+42) 00
2s	4120.863	24259.94	15_2-397_4	+04
1s	4122.025	24253.11	18_3-432_2	−05
1s	4123.064	24247.00	15_2-397_2	−02
3s	4126.808	24225.00	19_2-434_3	00
Es	4130.05	24205.98	19_5-437_5	?−35
1y =	4132.216	24193.29	19_3-440_3	−02
1Ldy =	4133.492	24185.82	19_5-437_4	−04
Es	4136.38	24168.95	$18'_2-424_2$	−13
5Ef?	4137.475	24162.55	D_2-274_2	00
2s	4138.030	24159.31	13_1-374_2; 19_3-439_4	+14 −03
2	4138.308	24157.68	19_3-439_4	−01
1 =	4139.325	24151.75	16_4-405_4	+07
1s	4140.044	24147.55	19_3-439_2	+02
1us	4140.410	24145.41	18_2-422_1	−02
2s	4142.261	24134.63	18_2-422_3	+01
2s	4145.168	24117.71	13_2-374_2	−02
2s	4145.953	24113.14	12_4-362_5	+02
1s	4149.445	24092.84	19_6-437_5	−01
1y	4149.749	24091.08	17_4-411_4	+04
E	4152.60	24074.51	19_4-433_5	−08
2Z	4154.678	24062.51	193_0-43_1	00
1	4159.793	24032.91	17_3-417_2	00
1s	4160.039	24031.49	20_3-450_3	+02
1s	4160.353	24029.67	22_4-465_5	−03
E	4161.52	24022.99	19_3-438_3	−11
E	4165.18	24001.82	22_5-468_5	−12
2	4166.151	23996.23	13_2-377_1	00
2Ef	4168.664	23981.78	$18'_2-422_1$	00
E	4170.04	23973.86	19_2-432_2	−19
3s	4170.538	23970.99	$18'_2-422_2$	+02
5s	4171.189	23967.25	D_3-287_4	+03
E	4171.83	23963.58	19_2-432_1	−10
E	4176.03	23939.48	20_1-443_2	−15
E	4176.64	23935.98	18_3-429_4	−24
1	4177.835	23929.13	$19_4-?431_4$	−16
1 =	4180.245	23915.33	$19'_5-437_5$	+02
E	4181.39	23908.80	22_4-463_3	+01
E	4182.34	23903.37	17_6-409_5	−07
E	4182.88	23900.29	314_4-55_4	+13
1s	4183.674	23895.72	18_1-419_2	−04
2s	4183.834	23894.81	19_3-437_4	−03

TABLE II—*Continued.*

Intensity (See text)	λ_{air}	ν_{vac}	Assignment	$\nu_{obs}-\nu_{calc}$
1us	4186.016	23882.36	17_3-415_2	?+36
E	4193.82	23837.90	16_4-402_3	−09
E	4197.56	23816.67	17_4-409_3	−09
2y=	4199.631	23804.94	17_4-409_5	+03
2	4200 031	23802.66	16_4-402_4	+05
E	4200.90	23797.73	13_3-371_4	−03
2s	4203.825	23781.19	12_4-359_3	−02
3s	4204.415	23777.85	19_4-430_4	−02
1u	4205.560	23771.38	214_1-45_0	00
3s	4207.056	23762.93	19_6-434_7	−05
2Ef	4215.387	23715.96	19_5-432_4	−01
2	4218.561	23698.13	$18'_2-419_2$	+01
5s	4219.383	23693.51	D_4-299_3	+01
E	4220.29	23688.43	13_2-374_2	−12
E	4220.55	23686.97	19_3-435_2	−03
3s	4222.061	23678.48	15_5-387_4	−01
2	4224.768	23663.30	23_3-475_2	00
1	4226.348	23654.45	19_4-429_4	−03
1	4226.922	23651.24	18_1-417_2; $(19_3-434_2$	−02 +32)
E	4231.34	23626.53	18_3-426_3	−11
E	4231.97	23623.01	28_5-518_4	+36
1s	4233.006	23617.24	18_2-417_2	00
2s	4234.358	23609.71	19_4-428_5	00
E	4236.60	23597.21	13_1-369_2	+19
2s	4240.150	23577.46	18_2-416_3	+01
3s	4241.451	23570.22	15_2-390_2	−01
4K1?s	4244.374	23554.00	D_4-297_5; $(23_3-474_3$	+03 +37)
E	4245.54	23547.53	20_1-439_2	+15
2	4249.464	23525.78	13_2-368_2	00
E	4250.85	23518.12	21_0-453_1	+35
E	4253.24	23504.91	$19'_5-433_5$	+12
2s	4254.066	23500.33	18_1-415_2	+01
1us	4254.29	23499.11	19_5-430_4	+02
E	4254.64	23497.17	17_3-411_4	+28
1s	4258.532	23475.69	17_4-405_4	−27
5=	4259.362	23471.11	214_2-44_2	−03
1	4259.942	23467.92	17_6-404_5	+03
3s	4260.299	23465.95	$(18_2-415_2$; 214_1-44_2	−38) +01
5=	4263.318	23449.33	230_3-46_3	+02
3	4266.547	23431.59	23_3-473_3	−03
E	4267.77	23424.86	$19'_5-432_4$	−09
1u	4268.054	23423.31	19_3-432_4	+01
5EfK2Z	4269.399	23415.94	S_3-263_2	−01
3	4269.784	23413.83	$18'_2-416_3$	+03
1u	4270.910	23407.65	23_3-473_2	−04
1	4272.314	23399.95	19_3-432_2	−02
2=	4273.694	23392.40	22_4-458_4	+05
3Ef/Z	4274.554	23387.69	200_1-43_1	+06
1u	4275.153	23384.41	20_2-443_2	+03
3s	4275.497	23382.54	18_2-414_2	00
2s	4276.752	23375.67	19_5-429_4	−03
E	4277.89	23369.46	17_4-404_5	+10
1s	4278.416	23366.58	13_1-366_2	00
Es	4282.41	23344.80	19_4-426_2	−10
2s	4283.813	23337.15	12_4-354_3	+01
3s	4286.021	23325.13	13_3-366_2	−01
E	4287.00	23319.81	19_2-425_1	+04
1y?	4290.152	23302.66	$18'_2-415_2$	−02
1	4292.743	23288.60	15_3-387_4; 16_4-397_4; 263_2-49_3	−17 00 −13
6rGK15s	4294.623	23278.41	S_3-262_2	00
1	4298.420	23257.85	19_4-425_3	−07
6GK4Z	4302.123	23237.83	S_3-261_3	−01
E	4303.49	23230.42	14_2-382_3	+27
Eu	4304.92	23222.71	17_3-409_3	+10
1	4305.634	23218.88	$18'_2-414_3$	−01
E	4306.36	23214.94	16_4-396_3	−11
1=	4306.886	23212.13	247_4-47_4	−02
4s	4307.645	23208.01	$19'_5-430_4$	−06
2s	4308.963	23200.94	22_4-456_3	−07
E	4309.89	23195.94	19_2-424_2	−03
T	4311.10	23189.44	15_3-382_4	+04
2	4312.354	23182.70	16_4-396_5	+02
1	4318.587	23149.24	23_3-470_2	−05
1	4322.754	23126.92	17_4-402_4	+02
E	4328.44	23096.55	13_2-368_3	−05
E	4330.34	23086.41	20_1-435_2	?−44
3s	4330 670	23084.65	$19'_5-429_4$	−03
3s	4330.979	23083.00	19_3-429_4	−03
3s	4332.140	23076.81	14_2-380_3	00
T	4335.357	23059.69	D_3-278_4	+12
L	4338.230	23044.42	$18_1-?411_0$	−02
1	4339.080	23039.91	$19'_5-428_5$	00
2s	4339.463	23037.88	20_2-440_3	?+47
E	4343.53	23016.29	22_5-458_4	+11
1	4344.977	23008.64	19_2-422_1	−03
3s	4345.846	23004.03	18_3-419_2	−09
1	4346.294	23001.67	23_3-469_4	−07
3s	4347.014	22997.85	19_2-422_3	−01
2s	4347.517	22995.19	19_4-422_3	−04
2Efs	4348.129	22991.96	20_2-439_2	−17
E	4348.95	22987.61	18_2-411_2	−02
2	4353.304	22964.62	17_3-406_3	−06
3=	4355.179	22954.74	12_4-351_4	−03
3s	4361.822	22919.78	D_4-291_3	−02
4s	4364.795	22904.17	D_3-262_3	−01
3s	4366.080	22897.43	18_3-418_4	00
1Eu	4366.359	22895.96	13_2-366_2	00
1	4368.773	22883.33	13_1-361_1	00
1	4371.738	22867.74	20_2-438_3	+04
3s	4372.539	22863.60	D_2-261_3	−01
3	4378.501	22832.42	D_3-276_2	−03
1	4380.130	22823.98	$18'_2-411_2$	00
3s	4384.868	22799.33	15_3-382_4	−01
2	4386.780	22789.39	20_1-432_1	−06
E	4387.47	22785.79	18_1-408_2; 22_4-452_4	+32 −07
3	4389.851	22773.45	19_2-426_2	00
2s	4394.092	22751.47	18_3-408_2	−01
2	4395.089	22746.30	15_3-382_3	−02
E	4397.55	22733.57	13_2-360_4	−13
E	4399.28	22724.64	19_2-419_2	?−37
1Ef	4400.222	22719.76	18_2-416_3	−04
E	4404.48	22697.82	14_2-376_3	−05
E	4405.06	22694.83	23_3-466_4	−13
1	4406.404	22687.89	18_1-407_1	−01
E	4406.72	22686.29	19_2-425_3	−18
3=	4408.285	22678.22	266_5-49_5	+05
1	4408.720	22675.97	28_5-509_4	−02
E	4411.73	22660.53	28_5-508_4	−11
4Ef	4412.206	22658.06	D_2-259_1; D_3-274_3	−01 00
1	4413.020	22653.88	18_2-407_1	−03
Es	4415.10	22643.19	$18'_2-409_2$	−10
2	4415.719	22640.03	22_4-451_4	−02
2Z	4418.458	22626.00	$20_1-?430_0$	00
1	4419.264	22621.88	19_3-424_2	−01
3=	4420.474	22615.68	19_4-418_4	−01
2s	4421.015	22612.91	17_4-397_4	+02
2s	4421.852	22608.63	18_3-415_2	−05
E	4422.51	22605.26	17_6-396_5	−24
2s	4423.785	22598.76	22_5-454_5	00
1	4424.914	22592.98	15_3-380_3	00
Eu	4433.63	22548.57	18_2-406_3	?−44
E	4435.43	22539.42	17_4-396_3	+08
1	4435.745	22537.83	22_4-450_3	−06
3s	4436.912	22531.89	20_2-435_2; 239_2-46_3	+29 −03
2s	4438.300	22524.85	18_3-414_3; $(313_1-53_1$	−04 +46)
2s	4441.820	22507.00	17_4-396_5	+03
E	4444.05	22495.72	20_2-434_3	+20
E	4444.45	22493.70	239_2-46_1	+08
2=	4445.161	22490.08	14_2-374_2; $18'_2-407_1$	−01 −18
3s	4449.018	22470.59	12_4-346_4	−04

TABLE II—*Continued.*

Intensity (See text)	λ_{air}	ν_{vac}	Assignment	$\nu_{obs}-\nu_{calc}$
2	4450.361	22463.80	22_4-449_4	−02
E	4452.06	22455.21	23_3-463_3	−16
2*s*	4455.471	22438.04	19_4-416_3	−02
2	4458.100	22424.81	13_1-357_2	−02
2*s*	4458.304	22423.79	19_2-422_3	+01
3*Z*	4460.507	22412.71	13_2-361_1	00
2*s*	4463.507	22397.64	23_3-463_2	00
3	4466.357	22383.35	13_3-357_2	−04
Eu	4470.79	22361.16	23_3-462_2	−38
Eu	4471.85	22355.86	$362_5-?58_5$	+04
1	4472.528	22352.47	17_6-393_5	−03
E	4475.60	22337.13	19_3-418_4	+22
Eu	4477.13	22329.50	19_2-415_2	−07
Eu	4477.36	22328.36	18_1-404_1	+15
Ef	4477.83	22326.01	287_4-51_4	+14
E	4479.58	22317.29	16_4-387_4	+16
E	4480.99	22310.27	17_3-400_2	−01
6*LdK*2*Z*	4484.197	22294.31	D_1-239_2; 18_2-404_1	00 +09
Eu	4490.33	22263.88	22_5-451_4	00
1*s*	4492.334	22253.93	17_4-393_5	−04
2*s*	4493.978	22245.78	19_2-414_3	00
2*s*	4494.518	22243.11	19_4-414_3	−04
3	4495.315	22239.17	15_5-373_5	−02
E	4496.27	22233.93	20_2-432_1	−27
E	4497.69	22227.41	$15_5-?372_6$	−2
2	4498.474	22223.54	18_3-411_4	−03
3*s*	4504.865	22192.02	12_4-343_3	−01
Eu	4510.33	22165.14	13_2-359_3	−32
3*s*	4512.913	22152.45	18_2-402_3	−01
2=	4513.305	22150.53	13_2-354_3	−04
1	4514.320	22145.54	20_1-425_1	00
1	4515.890	22137.84	23_3-460_2	−06
2	4517.375	22130.57	$18'_2-404_1$	00
2	4529.777	22069.98	22_4-445_5	−06
2	4530.479	22066.56	12_4-342_2	−02
2*s*	4534.726	22045.90	$19'_5-418_4$	+01
3*s*	4535.065	22044.24	19_2-418_4	00
2*Z*	4536.668	22036.46	21_0-438_1	+2
E	4539.68	22021.83	20_1-424_2	+09
E	4540.29	22018.87	17_3-397_4	+13
2	4542.900	22006.23	15_3-374_2; $(17_3-397_2$	−03 +37
1	4543.290	22004.34	13_1-353_2	−03
3	4543.524	22003.20	214_2-43_1	−03
1	4544.585	21998.06	214_1-43_1	−03
3*s*	4546.498	21988.81	$18'_2-402_3$	00
1	4550.332	21970.28	22_4-444_3	−02
3*s*	4551.860	21962.91	13_3-353_2; 333_5-55_4	−02 −06
1	4552.540	21959.62	12_4-341_4	−02
1	4553.661	21954.23	13_2-357_2	+02
E	4554.68	21949.32	18_3-409_2	+03
Eu	4556.20	21942.00	19_4-411_4	+17
3*r*	4556.859	21938.81	23_3-458_4	−12
2	4558.984	21928.59	18_1-400_2	−01
2	4559.121	21927.93	14_2-369_2	−01
3*s*	4563.602	21906.39	19_3-417_2	−01
1*u*	4564.084	21904.09	28_5-501_5	−02
2	4565.325	21898.14	14_2-368_2	00
1	4566.229	21893.79	18_3-408_2	−04
E	4568.55	21882.66	19_5-414_4	+23
4*K*?*Z*	4570.665	21872.54	230_3-44_2	−01
1	4571.910	21866.59	19_3-416_3	−02
Eu	4579.95	21828.20	16_4-382_4	+16
3*Z*	4586.856	21795.34	09_0-313_1	−06
4*s*	4588.766	21786.27	261_3-47_4	−07
Eu	4591.22	21774.63	16_4-382_3	−39
2=	4592.429	21768.89	19_5-414_4	−06
2	4592.584	21768.17	13_3-351_4	−03
4*s*	4599.972	21733.20	247_4-46_3	00
E	4608.83	21691.41	18_3-406_3	+05
3*s*	4609.928	21686.26	15_3-371_4	−03
4=	4613.328	21670.27	D_4-278_4; 19_2-409_3	+01 +09
1	4614.869	21663.04	19_5-411_4	−01
E	4623.18	21624.10	18_1-397_2	−08
2	4623.696	21621.68	16_4-380_3	00
E	4624.47	21618.07	20_2-426_2	+02
E	4625.17	21614.80	19_2-408_2	+08
Eu	4630.17	21591.46	$19'_5-414_5$	+05
E	4630.42	21590.29	18_2-397_2; 20_2-425_1	+10 00
3*s*	4634.830	21569.75	16_4-380_4	−05
E	4637.92	21555.39	28_5-497_4	+20
1*u*	4640.318	21544.24	22_4-440_2	−09
1	4641.812	21537.30	D_3-263_2; 22_5-443_6	+07 −21
3=	4642.579	21533.75	13_2-353_2	00
2	4643.169	21531.01	20_2-425_2	−06
2	4646.159	21517.15	19_2-407_1	00
Eu	4657.04	21466.88	20_2-424_2	+39
3	4657.450	21464.99	278_4-49_5	−03
6*Z*	4659.886	21453.77	D_0-214_1	−03
2	4661.248	21447.50	22_4-439_4	−02
3	4661.990	21444.09	15_3-369_2	−02
Ef	4665.80	21426.58	$18'_2-397_2$	+04
3	4668.480	21414.27	15_3-368_3	−04
E	4668.90	21412.36	13_1-347_1; 19_2-406_3	+13 +13
2	4671.663	21399.68	D_3-262_2	−01
3	4676.647	21376.87	19_3-409_3	−05
3*s*	4677.710	21372.02	$19'_5-411_4$	−01
2	4679.058	21365.87	$18'_2-396_3$	00
6*K*?*Z*	4680.539	21359.11	D_3-261_3	−01
1	4681.203	21356.07	$18'_2-396_1$	−01
E	4682.57	21349.82	297_5-51_4	+01
E	4686.37	21332.51	23_3-452_4	+07
E	4687.11	21329.15	17_3-390_2	+08
1	4687.654	21326.68	19_4-405_4	−09
Eu	4692.14	21306.29	20_1-417_2	+04
5*K*?*s*	4693.748	21298.99	266_5-47_4	−05
1	4694.677	21294.77	18_3-402_2	−04
2	4698.120	21279.17	20_2-422_1	−02
2	4698.647	21276.79	19_2-411_2	00
3*s*	4700.422	21268.75	D_4-274_2; 20_2-422_3	00 +37
E	4701.61	21263.39	19_6-409_5	−05
3	4702.486	21259.42	18_3-402_4; 341_4-55_5	−01 +15
2	4706.184	21242.72	16_4-376_2	−02
2	4711.199	21220.10	19_4-404_5	−05
3	4712.504	21214.23	14_2-361_1	−02
Eu	4713.43	21210.08	299_2-51_4	−20
E	4713.88	21208.06	12_4-333_5	−04
1	4714.528	21205.12	15_5-362_5	−02
2	4716.878	21194.55	17_6-382_4	00
2	4718.643	21186.62	23_3-451_4	−01
2	4720.409	21178.70	13_1-344_2	−04
3	4725.148	21157.46	19_2-404_1	00
E	4725.61	21155.38	09_0-306_1	−06
			20_1-415_2	+04
1	4726.293	21152.33	17_4-382_4	00
4*y*	4729.664	21137.26	13_3-344_2	−04
Eu	4730.68	21132.71	22_5-439_4	+17
2	4738.173	21099.30	17_4-382_3	−01
E	4741.53	21084.37	23_3-450_3	−10
E	4745.58	21066.34	18_2-391_1	00
E	4749.88	21047.31	17_3-387_4	+04
1	4751.378	21040.66	19_2-408_2	+02
2	4752.222	21036.92	18_3-400_2	−04
2	4752.598	21035.26	13_1-343_1	−02
E	4757.02	21015.69	19_2-402_3	−01
4*K*1*s*	4757.565	21013.30	S_3-239_2; 19_4-402_3	−01 +23
3	4757.790	21012.30	15_5-360_4	−03
2	4758.225	21010.39	23_3-449_4	−01
Eu	4759.37	21005.31	13_3-343_6	−15
E	4760.21	21001.61	22_4-434_3	−33
Eu	4761.62	20995.39	20_2-419_2	−14

TABLE II—*Continued.*

Intensity (See text)	λ_{air}	ν_{vac}	Assignment	$\nu_{obs}-\nu_{calc}$
Eu	4765.65	20977.64	19_4-402_3	−05
E	4768.06	20967.04	14_3-359_3	+04
E	4770.76	20955.18	239_3-44_3	+02
E	4772.51	20947.49	18_1-390_3	+10
3	4773.911	20941.35	13_2-347_1; 19_3-404_3	+26 −02
Eu	4780.34	20913.19	18_2-390_2	−21
Eu	4785.99	20888.51	22_3-437_3	00
2	4787.943	20879.98	13_3-342_3	−03
2	4788.442	20877.80	16_4-373_3	−03
E	4792.82	20858.71	287_4-49_2	−03
Eu	4793.88	20854.10	22_4-433_3	−06
2	4797.548	20838.17	19_3-406_3	00
2	4807.369	20795.61	12_4-329_3	+01
E	4812.62	20772.92	13_3-341_4	−15
1	4816.108	20757.87	19_2-400_2	+02
E	4816.82	20754.81	$?285_3-49_3$	+04
E	4817.69	20751.06	20_2-417_2	+06
E	4818.34	20748.27	346_4-55_3	−01
Eu	4818.92	20745.77	18_3-397_4	+35
E	4826.99	20711.09	20_2-416_3	−12
T	4828.084	20706.38	331_2-53_1	−03
1	4835.031	20676.64	20_1-411_2	00
E	4837.52	20665.98	12_4-328_4; 23_3-445_2	−17 −22
6K8Z	4843.829	20639.08	D_2-239_2	00
E	4844.32	20636.98	13_1-339_2	+09
3	4854.095	20595.43	13_2-339_2	−02
E	4858.61	20576.30	13_2-343_3	+02
Eu	4863.01	20557.69	22_4-430_4; 287_4-49_3	+25 −24
E	4867.98	20536.66	305_3-51_4	+19
Eu	4872.81	20516.32	20_2-414_3; $(291_3-49_3$	+02 −53)
Eu	4875.40	20505.42	17_3-382_3	+26
E	4880.72	20483.07	15_3-359_3	−10
6K5?z	4886.922	20457.08	D_4-266_3	−03
2*u*	4888.386	20450.95	13_2-342_3	+12
1	4890.295	20442.97	16_4-368_3; 28_3-486_4	−04 +20
1	4890.892	20440.48	20_1-408_2	−01
2*Ef*	4892.442	20434.01	22_4-429_4	−04
T	4896.784	20415.88	276_2-48_2	−01
2*Ef*	4902.332	20392.78	19_2-396_2	+02
Ef	4902.97	20390.14	19_4-396_3	+01
1	4910.763	20357.77	19_4-396_3	+01
Eu	4912.18	20351.89	17_3-380_3	+07
E	4914.32	20343.02	20_1-407_1	+10
2	4916.193	20335.29	14_2-353_2	00
Eu	4922.92	20307.49	261_3-46_3	+10
EuT	4924.565	20300.71	17_5-373_3	+06
2	4931.561	20271.92	15_3-357_2	00
Eu	4932.77	20266.96	262_3-46_3	+14
Eu	4933.77	20262.85	293_2-49_3	+28
E	4948.57	20202.27	17_4-373_3	+15
Ef	4953.07	20183.92	19_3-400_2	+15
E	4961.55	20149.39	$18'_2-?384_1$	−13
T	4967.670	20124.56	22_4-426_3	+09
T	4968.424	20121.51	20_2-411_2	+12
Ef	4972.57	20104.75	19_4-393_3	−01
Eu	4976.33	20089.56	18_2-382_3	+07
E	4977.22	20085.97	278_4-47_4	+08
5K3Z	4982.613	20064.22	D_0-200_1	−04
E	4984.11	20058.17	22_4-429_4	+30
E	4984.72	20055.71	18_3-390_2	00
2*z*	4986.943	20046.79	15_3-351_4; $322_3-52_{2?}$	00 +08
E	4995.37	20012.97	22_3-428_3	−14
E	5002.82	19983.17	20_1-404_1	−06
6K?z	5006.169	19969.81	D_4-261_3	00
E	5007.22	19965.62	19_4-396_3	+12
E	5013.48	19940.70	20_2-409_2	00
E	5014.63	19936.12	18_2-380_3	−03
6K?z	5015.334	19933.31	D_3-247_4	00
E	5017.21	19925.84	$18'_2-382_3$	00
T	5019.511	19920.72	23_3-438_3	+02
T	5022.484	19904.93	28_3-481_3	+01
Eu	5025.32	19893.69	$19'_3-397_4$	−19
Eu	5025.67	19892.30	19_3-397_4	+07
T	5027.435	19885.33	20_2-408_2	+09
Eu	5028.97	19879.25	19_3-397_3; 281_3-48_2	−10 −24
2	5040.369	19834.31	13_1-331_2	00
Eu	5041.82	19828.60	266_3-46_1	−09
E	5044.32	19818.78	19_3-396_3	+10
E	5052.27	19787.60	20_2-407_1	−07
8K3Z	5053.300	19783.55	D_1-214_1	+02
5K?z	5054.615	19778.40	D_1-214_2	+01
1*Ef*	5055.528	19774.83	22_4-422_3	+03
T	5056.103	19772.58	$18'_2-380_3$	+08
E	5058.05	19764.96	17_3-374_2	−04
Eu	5063.65	19743.11	14_2-347_1; 299_3-49_3	−04 +01
T	5065.677	19735.21	28_3-479_4	+07
6K1?z	5069.148	19721.70	D_2-230_3	+01
Eu	5071.59	19712.20	19_4-393_3	−30
E	5077.02	19691.12	18_1-377_1	+02
T	5085.900	19656.74	15_3-351_4	+01
2	5105.489	19581.32	297_3-49_3	+01
E	5110.36	19562.66	15_3-346_4	+01
E	5111.77	19557.26	18_2-376_3	+05
E	5117.59	19535.03	$19'_3-393_3$	+07
2	5124.240	19509.67	14_2-344_2	+01
E	5128.53	19493.37	$18'_2-377_1$	−09
2	5130.123	19487.30	239_2-43_1	−01
1	5138.403	19455.90	28_3-476_4	+02
E	5141.28	19445.00	17_3-371_4	−13
2	5145.774	19428.40	20_2-404_1	?+42
E	5154.43	19395.41	22_4-418_4	+16
Eu	5154.88	19393.71	$18'_2-376_2$	+15
Eu	5162.1	19366.5	14_2-343_1	+3
Eu	5162.7	19364.2	13_2-331_2	+5
Eu	5177.78	19307.92	28_3-475_4	−16
3	5183.974	19284.87	18_3-382_4	+01
Eu	5188.89	19266.59	17_4-362_3	−01
3*z*	5192.725	19252.37	14_2-342_3	00
1*u*	5195.63	19241.61	259_2-45_3	00
3	5203.258	19213.39	19_3-387_4	−04
3	5204.516	19208.75	20_1-396_1	+01
3	5206.189	19202.58	19_3-390_2	+02
Eu	5212.35	19179.87	13_2-329_2	+02
2*Ef*	5212.804	19178.22	287_4-47_4	−02
E	5214.18	19173.14	17_3-368_3	−01
6K3Z	5224.680	19134.62	D_3-239_2	+03
3*z*	5242.989	19067.79	16_4-354_3	−01
Eu	5247.38	19051.83	15_3-341_4	+17
2	5255.409	19022.73	22_4-414_3	+01
2*z*	5259.356	19008.46	274_3-46_3	+01
E	5268.52	18975.40	17_4-360_4	+14
E	5269.28	18972.67	17_3-366_2	+16
E	5274.78	18952.89	19_2-382_3	+16
2	5275.555	18950.09	19_4-382_3	−03
E	5278.55	18939.35	291_3-48_3	+12
E	5283.29	18922.33	$19'_3-387_4$	−08
E	5285.51	18914.39	21_3-407_1	0
Eu	5317.8	18799.5	19_3-380_3	+1
2	5318.880	18795.73	276_2-46_1	−03
Eu	5329.8	18757.2	18_2-368_3	+3
1*u*	5337.360	18730.66	261_3-44_2	+03
Eu	5339.2	18724.2	19_3-382_4; 20_2-397_2	−1 +25
Eu	5339.9	18721.2	22_4-411_4	−2
2	5348.947	18690.08	262_3-44_2	+02
2	5350.440	18684.87	293_2-48_2	−08
1	5351.903	18679.76	277_1-46_1	+02
1*Z*	5354.463	18670.83	09_3-281_3; 23_3-426_3	00 −22
E	5355.24	18668.14	19_3-382_4	+09
E	5356.69	18663.40	20_2-396_3	+12
2*u*	5357.120	18661.57	15_3-341_4	−03

TABLE II—*Continued.*

Intensity (See text)	λ_{air}	ν_{vac}	Assignment	$\nu_{obs}-\nu_{calc}$
E	5368.60	18621.66	28_5-468_5	+31
E	5372.85	18606.93	278_4-46_2	−01
3	5374.163	18602.39	20_1-390_2	−02
Eu	5379.40	18584.29	23_3-425_3	+22
2*s*	5388.023	18554.54	19_6-382_6	−01
E	5388.60	18552.57	263_2-44_2	+05
1	5391.088	18543.99	D_4-247_4	−01
1	5397.970	18520.35	19_2-377_1	00
E	5398.27	18519.30	23_3-424_3	−19
E	5400.96	18510.09	13_1-318_2	?−43
E	5406.35	18491.64	18_3-374_3	−18
E	5408.59	18483.98	15_3-339_2	00
Eu	5413.04	18468.79	13_2-318_2	−29
E	5413.89	18465.89	19_5-380_4	−21
E	5415.59	18460.09	13_2-322_3	−20
2	5419.400	18447.12	22_4-409_3	00
1*u*	5422.88	18435.29	22_4-409_5	+02
E	5423.48	18433.25	$19'_5-382_4$	−07
1	5423.935	18431.69	19_3-382_4	+02
E	5427.25	18420.45	19_2-376_3	00
Eu	5428.04	18417.76	19_4-376_3	−06
3*s*	5435.063	18393.96	D_1-200_1	−03
Eu	5435.64	18391.99	17_4-354_3; $(28_5-466_4$	−10 +37)
E	5438.89	18381.00	17_3-360_4	−11
E	5439.59	18378.64	19_3-382_3	−01
Eu	5451.82	18337.42	$19'_5-382_6$	00
2	5456.593	18321.37	23_3-422_3	−01
Eu	5464.5	18294.9	328_4-51_4	−1
E	5475.09	18259.47	281_1-46_1	+11
5*Z*	5477.802	18250.45	09_0-277_1	00
1	5486.018	18223.10	314_4-49_3	+02
2*s*	5487.786	18217.24	D_3-230_3	+04
T	5489.134	18212.76	19_2-374_2	+09
6*K*?*s*	5492.331	18202.16	297_5-47_4	−02
Euf	5492.54	18201.47	16_4-346_4	+18
1	5496.245	18189.19	22_4-406_3	00
2	5500.62	18174.75+.31	$19'_5-380_4$	−33
2	5503.53	18165.13+.27	14_2-331_2; $(299_3-48_2$; $(329_3-51_4$	−10 −40) −39)
7*K*?	5514.77	18128.09+.20	D_2-214_1	−21
T	5521.008	18107.62+.04	18_1-361_1	+04
Eu	5528.05	18084.56	13_2-314_4	+23
Ou	5528.5	18083.1	372_6-55_5	−3
1	5531.54	18073.15+.43	18_2-361_1	−44
1	5537.80	18052.72+.20	19_4-373_5	−19
Eu	5546.5	18024.4	373_5-55_4	+5
Eu	5548.9	18016.6	13_1-313_1	+3
Eu	5551.0	18009.8	17_4-351_4	+1
Eu	5553.2	18002.6	$20_1-?384_1$	+6
E	5554.08	17999.80	22_4-404_5	+08
E	5559.78	17981.34	14_2-329_3	−05
E	5571.98	17941.97	23_3-418_4	+13
Eu	5575.85	17929.52	18_3-369_2	−11
Eu	5578.28	17921.71	314_4-49_3	00
Eu	5588.13	17890.12	19_4-371_4	+05
Eu	5601.8	17846.5	19_3-376_2	+1
1*s*	5604.32	17838.45	318_2-49_3	+11
1	5608.07	17826.52	18_3-359_3	+18
Eu	5615.16	17804.00	23_3-417_2	00
Es	5617.03	17798.07	17_3-354_3	+13
2*Bu*	5617.33	17797.11	16_4-342_3	−13
E	5618.69	17792.81	22_4-402_3	+17
1−*T*	5629.647	17758.19	15_3-328_4	+02
Eu	5629.93	17757.37	22_4-402_4	+11
1*Bu*	5631.30	17752.97+.03	333_5-51_4	−05
2*K*?	5631.94	17750.95−.09	12_4-299_3	+11
2	5642.12	17718.93+.25	D_1-193_0	−18
4*s*	5648.42	17699.18+.09	18_3-366_2; 287_4-46_3	−01 −11
Eu	5651.25	17690.30	16_4-341_4	00
E	5654.12	17681.32	15_3-331_2	−08
E	5660.110	17662.70	$18'_2-359_3$	+01
2	5660.67	17660.86−.25	19_6-373_5	+21
E	5663.30	17652.66	23_3-415_2	−43
Eu	5664.0	17650.5	19_2-369_2	0
2*Bu*	5664.40	17649.23+.19	18_1-357_3; $19_6-?372_6$	+11 +2
1	5673.41	17621.21−.47	19_2-368_3	+49
2	5674.45	17617.98+.10	19_4-368_3	−11
1	5675.38	17615.09+.01	18_2-357_2	00
*B*2	5676.608	17611.28	12_4-297_5; 19_5-371_4	−03 −01
*B*2	5676.924	17610.30	17_3-353_3	00
Eu	5690.13	17569.43	23_3-414_3	+13
Eu	5694.55	17555.79	28_5-457_5	+09
2	5697.86	17545.59 .14	13_2-313_1	−11
E	5704.38	17525.54	17_4-346_4	−04
1*Eu*	5715.35	17491.91	305_3-48_2	+19
Eu	5722.0	17471.6	$19'_5-?372_6$	+1
2*Bu*	5723.19	17467.95+.37	259_1+43_1	−37
1	5728.60	17451.46	$18'_2-357_2$	+02
4*s*	5735.11	17431.62+.05	274_3-44_2	−07
2*Eu*	5739.59	17418.02	322_3-49_3	+07
2*Bu*	5747.26	17394.78−.03	306_1-48_2	−10
2	5749.22	17388.86−.05	305_3-47_4	+02
1*Eu*	5753.41	17376.19	13_1-306_1	−17
2*Bu*	5756.16	17367.89+.24	15_2-328_4	−22
2*Bu*	5759.66	17357.34+.03	291_3-46_3	−06
1−*T*	5771.988	17320.26	$19'_5-371_4$	−01
1*Eu*	5791.36	17262.33	291_2-46_1	−03
2	5793.02	17257.39−.07	276_2-44_2	+09
2	5796.54	17246.91+.12	17_4-343_3	−07
1	5799.53	17238.02	13_3-305_3	−06
4	5804.86	17222.17+.05	262_2-43_1	00
Eu	5806.10	17218.50	$18'_2-354_3$	−12
2*Eu*	5806.25	17218.05	28_5-454_5	−12
Eu	5814.2	17194.5	18_2-353_2	−13
E	5821.03	17174.34	23_3-411_5; 366_2-53_1	−05 +22
2	5822.60	17169.71+.04	22_4-396_3	+01
1	5832.32	17141.10	277_1-44_2	−18
2	5833.62	17137.28+.13	22_4-396_5	−05
2	5838.99	17121.53+.09	17_4-342_5; 382_4-55_5	00 00
2	5845.28	17103.08+.08	293_2-46_3	−04
2	5851.59	17084.64+.08	263_2-43_1	−03
1	5854.45	17076.30	19_3-369_2	−14
1	5856.64	17069.92+.09	20_2-380_3	+01
2	5864.64	17046.64+.05	19_3-368_3	00
1*Eu*	5869.91	17031.33	$18'_2-353_2$	+35
1*Eu*	5871.58	17026.49	281_1-45_0	+15
1*Eu*?	5874.24	17018.79	19_4-362_5	−07
1*Eu*	5875.68	17014.62	17_4-341_4	+03
2	5880.21	17001.48−.02	341_4-51_4	00
2*Bu*	5891.59	16968.65−.10	18_3-359_3	−04
E	5901.99	16938.76	16_4-333_5	00
2	5902.66	16936.84−.03	19_2-361_1	+01
1−*Eu*	5904.5	16931.6	17_3-346_4	+2
1	5913.51	16905.74	13_2-306_1	00
Eu	5917.33	16894.84	342_3-51_4	+30
Eu	5921.03	16884.28	22_4-393_5	−05
Eu	5921.28	16883.58	28_5-451_4	+29
Eu	5927.03	16867.20	22_5-397_4	+12
1	5934.49	16846.00	19_3-366_2	00
1*Eu*	5940.90	16827.82	D_4-230_3; 328_4-49_3	−07 −02
Eu	5942.7	16822.7	266_0-43_1	+3
4	5947.56	16808.98−.07	13_2-305_3	+08
1	5953.97	16790.86	20_2-377_1	−01
2	5956.18	16784.64 .00	17_3-344_2	−03
Eu	5958.6	16777.8	15_3-322_3	−2
1*Ef*	5964.53	16761.15	22_5-396_3	−01
4	5965.88	16757.36+.06	18_3-357_2	−08
2	5972.46	16738.89−.15	D_2-200_1	+13
Eu	5973.5	16736.0	23_3-406_3	+2
2	5978.91	16720.84+.08	281_1-44_2	−06
2*Bu*	5983.84	16707.07+.03	28_5-449_4	+01
2*ud-Eu*	5986.98	16698.30	329_3-49_3	−09

TABLE II—*Continued.*

Intensity (See text)	λ_{air}	ν_{vac}	Assignment	$\nu_{obs}-\nu_{calc}$
2*dBu*	5989.59	16691.04	20_2-376_2	+07
Eu	5990.11	16689.57	19_2-359_2	−01
Eu	5991.05	16686.95	19_4-359_2	00
1*Eu*	6003.30	16652.90	17_3-343_3; 23_3-405_4	+07 −02
1	6009.68	16635.23	12_4-287_4	−02
4	6012.79	16626.62 −.08	19_4-362_3	+02
Eu	6015.7	16618.6	D_3-214_2	−1
4	6021.52	16602.53 −.06	18_2-347_1	+04
2	6028.32	16583.78 −.08	299_3-46_3	+08
1*Eu*	6035.52	16564.00	13_3-299_2	−27
2*Bu*	6041.62	16547.28 −.05	19_5-360_4	+01
3	6043.33	16542.60 −.04	314_4-47_4	+02
Eu	6049.0	16527.1	17_3-342_3	−3
2	6049.90	16524.64 −.07	18_3-354_2	+02
1*Eu*	6055.90	16508.27	22_5-393_5	+11
2*Bu*	6065.05	16483.36 −.14	20_2-374_2	+17
1	6066.82	16478.54	19_2-357_2	+21
1	6067.64	16476.31	20_1-369_2	+02
Eu	6077.7	16449.0	$19'_5-362_3$	−0
3	6081.46	16438.88 −.07	$18'_2-347_1$	+04
1	6094.76	16403.01	18_1-344_2	+02
1	6107.41	16369.02	18_2-344_2	+03
2	6111.67	16357.62 −.07	15_3-318_2	+01
2	6115.55	16347.24 −.05	14_2-313_1	00
1	6119.35	16337.09	18_2-353_2	+11
4	6128.28	16313.29 −.04	28_5-445_5	+01
2	6143.91	16271.77 −.15	22_4-387_4	−01
1	6147.18	16263.12	17_4-333_5	+07
1*Eu*	6148.22	16260.38	318_2-48_2	−34
2	6153.75	16245.76 +.03	19_2-354_3; 20_1-366_2	+25 −09
2	6154.88	16242.78 .00	17_3-339_3; 19_4-354_3	−04 −10
2	6161.45	16225.47 +.05	18_2-343_1	−07
2	6169.11	16205.32 +.02	$18'_2-344_2$	−03
1*Eu*	6187.54	16157.05	28_5-443_6	+13
1	6193.23	16142.21	18_3-351_4	−04
2*u-B*	6195.986	16135.03	13_2-299_2	−06
4	6203.54	16115.39 +.05	19_3-359_2	−11
1*u*	6219.50	16074.02	377_1-53_1	+17
1*Eu*	6224.41	16061.85	$18'_2-343_1$	−04
1	6225.80	16057.76	19_2-353_2	−11
Eu	6240.59	16019.73	393_5-55_5	−16
1	6245.74	16006.50	351_4-51_4	+15
3	6254.33	15984.50 +.05	333_5-49_5	−02
2*u*	6258.93	15972.75	15_3-314_4	−12
Eu	6259.19	15972.12	393_5-55_4	+07
4	6285.89	15904.24 −.04	19_2-357_2	−01
3	6291.04	15891.23	20_2-369_2	−01
4	6292.02	15888.75 −.07	13_1-291_2	00
2	6303.18	15860.63 −.17	19_4-351_4	+12
1	6308.47	15847.33	13_3-291_2	+02
Eu	6324.7	15806.7	16_4-322_3	0
1*Eu*	6331.38	15789.98	23_3-397_4	+15
Eu	6335.2	15780.5	291_3-44_2	−1
1*Eu*	6342.31	15762.78	20_1-361_1	+18
Eu	6346.8	15751.6	28_5-439_4	−4
Eu	6352.49	15737.54	322_3-47_4	+09
1*Eu*	6359.15	15721.05	17_4-328_4	−05
1	6361.07	15716.28	23_3-396_2	00
1	6364.77	15707.14	14_2-306_1	−14
2	6371.43	15690.73 −.11	20_2-366_2; 28_5-439_5	+13 −03
Eu	6378.5	15673.3	277_1-43_1	−1
Eu	6379.3	15671.4	19_3-354_3	−03
1	6382.51	15663.49	$18'_2-339_2$	−01
2*Eu*	6384.68	15658.17	18_3-346_4	+06
2	6402.07	15615.63 −.02	13_2-293_2	−04
4	6404.22	15610.39 −.02	14_2-305_3	−05
2	6416.02	15581.68	19_5-351_4	−05
2*u-Eu*	6435.52	15534.57	341_4-49_3	+22
1	6439.72	15524.33	22_4-380_4	−12
2	6445.13	15511.31 −.02	18_3-344_2	−04
Eu	6456.49	15484.05	19_3-353_2	+26
3	6464.16	15465.65	19_2-347_1	−08
1*Eu*	6474.78	15440.27	17_3-331_2	+03
2	6484.09	15418.11 −.03	13_2-291_2; ?384_1-53_1	−02 +12
2*u*	6500.29	15379.70	18_3-343_3; $432_4-?58_3$	+19 −23
2	6508.01	15361.46 −.09	13_2-291_2	+07
3	6532.40	15304.09 −.05	20_1-357_2	−01
1*Eu*	6534.05	15300.23	$433_5-?58_3$	+14
4	6538.16	15290.61 +.04	$19'_5-351_4$	−10
2	6552.84	15256.34	17_3-329_2	−04
1*Eu*	6553.81	15254.08	18_3-342_3	+02
2	6554.24	15253.08	281_1-43_1	+03
1*Eu*	6562.88	15233.01	341_4-49_3	+03
3	6563.16	15232.36 −.16	19_2-344_2	+12
3	6573.96	15207.35 .00	20_2-361_1	00
2*Eu*	6600.06	15147.20	18_3-341_4; 328_4-47_4; 402_4-55_5	+08 −14 +24
2	6607.17	15130.90 +.03	17_4-322_3	−09
2*Eu*	6609.06	15126.58 −.01	15_3-305_3	−03
3*Eu*	6611.63	15120.70	329_3-48_2	−07
1*Eu*	6620.60	15100.20	19_2-343_3; 23_3-390_2	−20 +04
3*Eu*	6621.69	15097.71	19_4-343_3; 19_5-346_4; $(28_5-433_5$	−07 +12 +31)
1*u*	6636.60	15063.80	314_4-46_3; 402_3-55_4	+17 +06
1*u*	6654.45	15023.41	346_4-49_3	+05
1	6657.02	15017.61	28_5-432_4	+05
1*u*	6664.16	15001.50	16_4-314_4	−07
1	6675.99	14974.92	19_2-342_3	−03
2	6677.19	14972.23	19_4-342_3	−09
4	6678.41	14969.50 −.04	18_3-339_2	00
1	6682.65	14960.00	20_2-359_2	−10
5*Eu*	6693.11	14936.63 −.07	14_2-299_3; 331_2-48_2	00 −30
2	6713.30	14891.70 −.04	13_1-281_1	−05
2*Eu*	6725.19	14865.48	19_4-341_4	+10
2*Eu*	6733.06	14847.99	362_5-51_4	−01
2*Eu*	6740.03	14832.63	22_4-373_5	+15
2*Eu*	6746.58	14818.24	23_3-387_4; 374_2-52_{33}	−12 −21
2	6754.56	14800.74	28_5-430_4	+06
1	6755.75	14798.13	405_4-55_5	+25
2	6778.34	14748.81	20_2-357_2	−04
2	6799.35	14703.25	15_4-297_5	−08
3*Eu*	6805.31	14690.37 .00	19_2-339_2	−02
2	6811.38	14677.26	$18'_2-329_3$; 28_5-429_4	+18 −03
3	6814.93	14669.62	22_4-371_4	−02
4	6820.25	14658.18 −.11	19_2-344_2	+02
2	6828.43	14640.63	318_2-46_1	+04
1	6832.23	14632.48	28_5-428_5	−04
1	6844.88	14605.43	333_5-47_4	+04
2	6853.73	14586.58	19_5-341_4	−02
2	6874.93	14541.61	306_1-45_0	−12
2	6876.05	14539.24	351_4-49_3	+02
2	6877.60	14535.96	19_2-343_3	?−40
3	6908.31	14471.34 −.04	13_1-277_1	−03
1	6915.49	14456.32	22_5-373_5	+01
1	6917.21	14452.73	15_3-299_2	−07
2	6920.98	14444.83	$22_5-?372_6$	+2
4	6934.29	14417.12 +.04	14_2-293_2	−08
1	6943.72	14397.54	22_4-368_3	−12
3	6964.14	14355.34 +.01	13_1-276_2	−01
4	6984.28	14313.93 −.04	13_2-276_2	+02
2*d*	6993.15	14295.76	$19'_5-341_4$	+18
2	6994.06	14293.90	19_3-341_4	−03
1	7002.73	14276.21	23_3-382_3	−04
1*d*	7016.01	14249.20	368_2-51_4	?+43
1*u*	7020.23	14240.63	$443_6-?58_3$	+06
1	7058.79	14162.84	14_2-291_2	−05
2	7098.23	14084.15	$445_5-?58_3$	−06

TABLE II—*Continued.*

Intensity (See text)	λ_{air}	ν_{vac}	Assignment	$\nu_{obs}-\nu_{calc}$
1	7111.20	14058.45	$(20_1-344_2$; $293_2-43_1)$	(+44) −06
1	7127.07	14027.15	12_4-261_3	00
3	7140.51	14000.74	13_2-277_1	−01
2	7162.64	13957.49	$18'_2-322_3$	−03
1	7179.88	13923.99	357_2-49_3	−04
1H	7184.71	13914.63	20_1-343_1	+08
1	7191.33	13901.81	313_1-45_0	+04
1	7198.62	13887.73	19_2-331_2	−08
2	7200.16	13884.76	13_2-276_2	+03
2	7216.32	13853.66	18_3-328_4; 341_4-47_4	+03 −19
1	7218.16	13850.12	342_3-48_2	?+33
2	7226.02	13835.07	19_3-333_5	+01
2	7237.08	13813.93	373_5-51_4	−02
1	7245.23	13798.39	22_4-362_5	−04
2	7278.21	13735.87	15_3-291_2; $(20_2-347_1$; 343_1-48_2	+03 −38) −09
3	7285.82	13721.52	19_6-333_5	−06
1H	7291.83	13710.20	13_2-274_3	−14
1	7295.15	13703.96	19_2-329_3	−01
3	7296.57	13701.30	19_4-329_3	−04
1	7347.88	13605.63	22_4-360_4	+01
1	7355.00	13592.46	344_2-48_2	−04
1	7365.15	13573.73	360_4-49_3	+05
2	7381.27	13544.08	$19'_5-333_5$	+04
1	7384.04	13539.00	329_3-46_2	+06
3	7385.08	13537.09	$18'_2-318_2$	−04
1	7389.00	13529.92	$15_5-?285_6$	+05
1	7448.26	13422.26	22_5-362_5	00
3	7483.34	13359.34	20_2-343_1; 347_1-48_2	+04 +33
2	7504.07	13322.45	13_1-266_0	+03
3	7508.98	13313.74	19_3-331_2	+01
3	7537.42	13263.50	18_3-322_3	−02
2	7550.46	13240.58	18_1-313_1	+01
3	7569.87	13206.63	18_2-313_1	+05
2	7582.85	13184.04	28_5-414_6	+02
3	7614.07	13129.98	19_3-329_3	+09
1	7630.24	13102.14	318_2-44_2	+01
1	7643.40	13079.59	362_5-49_3	+10
2	7654.78	13060.15	13_1-263_2	+02
?3	7664.86	13042.96	$18'_2-313_1$	+03
1	7679.15	13018.70	13_3-263_2	+01
3	7688.93	13002.14	$19'_5-328_4$	+05
1	7689.96	13000.40	19_2-328_4	−04
1	7699.42	12984.41	19_2-322_3	00
2	7700.96	12981.82	19_4-322_3	+04
1	7736.16	12922.75	13_1-262_2	+16
1	7758.58	12885.42	17_3-305_3	−03
2	7761.13	12881.19	13_3-262_2	+04
3	7784.11	12843.15	18_3-318_2	+02
2	7808.95	12802.29	14_2-277_1	00
2	7863.45	12713.57	20_1-331_2	−01
2	7867.01	12707.82	16_4-291_3	+02
2	7880.34	12686.33	14_2-276_2	+06
1	7883.17	12681.76	322_3-44_2	+02
2	7886.45	12676.49	13_1-259_1	+01
2	7909.19	12640.05	22_4-351_4	−03
3	7940.92	12589.54	13_2-263_2	+03
1	7955.43	12566.57	18_2-306_1	−05
2	7957.05	12564.02	19_2-318_2	00
1	7991.67	12509.59	371_4-49_3	−07
4	8017.17	12469.81	18_2-305_3	+03
1	8043.11	12429.51	15_3-278_4	−05
1	8054.87	12411.44	13_2-261_3	+04
3	8055.61	12410.31	19_3-322_3	−02
2	8060.35	12403.01	$18'_2-306_1$	+04
3	8123.78	12306.16	$18'_2-305_3$	+03
1	8165.71	12242.98	28_5-404_5	+02
?2	8210.20	12176.64	19_4-314_4	−01
1H	8222.52	12158.38	20_2-331_2	+05
1	8311.60	12028.08	15_3-274_3	+03
1	8321.98	12013.08	23_3-359_3	−02
2	8338.02	11989.96	19_3-318_2	+02
1	8348.77	11974.53	20_2-329_3	+04
1	8350.25	11972.40	344_2-46_1	+03
1	8359.81	11958.72	$466_6-?58_5$	−03
2	8382.88	11925.80	09_0-214_1	+01
2	8402.53	11897.90	19_5-314_4	+03
1	8409.50	11888.05	361_1-48_2	+14
2	8417.08	11877.34	22_4-343_3	00
2	8470.92	11801.86	23_3-357_3	+01
3	8475.15	11795.96	18_2-299_3	−01
1	8486.81	11779.75	22_5-346_4	−02
1	8499.60	11762.04	393_5-51_4	−06
2	8506.95	11751.88	22_4-342_3	−01
2	8516.37	11738.87	347_1-46_1	−01
1	8577.75	11654.88	380_4-49_3	+03
3	8585.07	11644.93	22_4-341_4	−02
3	8594.38	11632.31	$18'_2-299_3$; $43_1-?550'_2$	−01 +11
3	8613.22	11606.88	$19'_5-314_4$	+03
2	8614.49	11605.17	19_3-314_4	−03
2	8641.56	11568.81	23_3-354_3	−22
1	8710.56	11477.17	396_3-51_4	?+44
2	8740.44	11437.93	17_3-291_3	−01
2	8746.59	11429.89	19_2-306_1	+03
1	8776.45	11391.00	14_2-263_2	−05
1	8777.45	11389.70	20_1-318_2	−09
1	8821.12	11333.32 −.39	19_2-305_3	+30
2	8823.27	11330.56 −.15	19_4-305_3	+17
15	8865.43	11276.67 −.08	18_3-293_2	+12
4	8871.50	11268.96 −.18	22_5-341_4	+18
4	8883.71	11253.47 +.06	14_2-262_2	−04
7	8915.70	11213.10 −.16	14_2-261_3	+16
3	8922.93	11204.01	368_3-48_2	−01
2	8936.67	11186.78	23_4-351_4	+12
3	8984.13	11127.69 − 09	28_5-393_3	+12
4	8996.04	11112.95	18_1-291_2; $18'_2-293_2$	−05 +05
1	9023.80	11078.77	18_2-291_2	−24
0	9041.53	11057.04	16_4-274_3	+29
5	9069.98	11022.36	18_2-291_2	+09
5	9082.15	11007.59	14_2-259_1	+19
4	9139.69	10938.29	18_3-299_3	−03
20	9158.86	10915.40 −.02	$18'_2-291_2$; 44_2-558_2	+04 +02
2	9165.49	10907.50	15_3-263_2; 387_4-49_3	+28 −02
1	9175.47	10895.64	20_1-313_1	+05
4	9177.37	10893.38	22_4-333_5	−03
2	9206.67	10858.71	$18'_2-291_3$	+09
2	9227.14	10834.62	20_2-318_2	+08
4	9282.67	10769.81	15_3-262_2	+13
3H	9291.96	10759.04	19_3-305_3	+10
3	9317.78	10729.23	15_3-261_3	+12
4	9320.37	10726.25	357_2-46_1	−03
3	9378.88	10659.33	19_2-299_3	+12
25	9381.29	10656.59	19_4-299_3	+01
2	9389.87	10646.86	404_5-51_4	+15
1	9485.21	10539.84	405_4-51_4	−25
1	9505.37	10517.49	$(19_4-297_5$; $22_5-333_5)$	(+44) +25
1	9507.51	10515.12	28_5-387_4	+10
5	9515.89	10505.86	347_1-45_0	00
25	9538.45	10481.01	22_4-329_3	+10
1	9590.68	10423.93	23_3-343_3	+01
4	9595.25	10418.97	18_3-293_2	+07
2	9667.99	10340.58	20_2-313_1	+24
1	9707.53	10298.46	23_3-342_3	−01
1	9736.31	10268.02	361_1-46_1	+24
4	9747.98	10255.73	20_1-306_1	+10
8	9764.48	10238.40	19_5-297_5	+13
7	9780.72	10221.40	18_2-291_2	+04
20	9809.30	10191.61	23_3-241_4	+08
10	9813.74	10187.00	13_2-239_2	+13
10	9835.20	10164.73	18_3-291_3	+16
4	9859.30	10139.93	19_2-293_2	+14

TABLE II—*Concluded.*

Intensity (See text)	λ_{air}	ν_{vac}	Assignment	$\nu_{obs}-\nu_{calc}$	Intensity (See text)	λ_{air}	ν_{vac}	Assignment	$\nu_{obs}-\nu_{calc}$
12	9873.87	10124.97	19_4-297_5	+18	0	10217.38	9784.56	366_2-461	+03
3	9912.76	10085.24	19_3-299_3	+11	4	10241.63	9761.40	22_4-322_3	+05
18	9915.78	10082.17	18_2-281_1	+16	0	10306.04	9700.39	20_2-306_1	+01
0	9963.75	10033.63	422_3-523	?+37	3	10347.27	9661.75	18_3-277_1	+12
2	9983.22	10014.06	23_3-339_2	+15	2	10409.77	9603.71	20_2-305	+17
2*un*	10021.50	9975.81	22_3-328_4	?+52	1*ud*	10450.97	9565.85	19_3-293_2	+14
4*u*	10050.31	9947.21	$19'_3-297_5$	−04	0	10477.97	9541.20	19_4-287_4	+21
1	10079.52	9918.39	$18'_2-281_1$	+03					
3	10115.52	9883.08	19_4-291_3	+20					
2	10126.93	9871.95	382_3-482	−06					

but instead of each level having its own column, each column after the heavy line represents all the odd levels in an interval of 1000 cm^{-1}, and the numbers in the body of the array show the number of underwater spark lines belonging to the levels in that interval. The symbols in the first column represent the initial states of all the lines, and the numbers in the first row represent energy values in thousands of wave number units. In the face of the general tendency of the numbers to cluster on the diagonal from upper left to lower right on account of the spectrum selectivity of the apparatus, the preponderance of low levels among the $^7S_3$ combinations is striking.

(B)

Level *21*$_0$. The reality of this level tends to be confirmed by the following Zeeman-effect patterns:

21_0-404_1 (0) 1.66
21_0-438_1 (0) 1.05.

266$_0$. The reality of this level tends to be confirmed by the following Zeeman-effect pattern:

D_1-266_0 (0) 1.55.

359$_3$ *and* *360*$_3$. Here is a remarkable example of two neighboring levels with the same J, mutually almost exclusive in their combinations.

371$_4$. The J value of this level is verified by the following conclusions from Zeeman-effect blends:

D_3-371 implies g_3 (impossible) or $g_4=0.9$
15_3-371 implies $g_3=0.29$ or $g_4=0.99$.

387$_4$. The J value of this level is evident from its combinations. Catalan and Poggio's conclusion that $J=3$ was a necessary consequence of accepting Beining's pattern for S_3-387, but

TABLE III. Observed (tentative) g values of the $5d^46s(^6D)ns$ levels of W I.

	$^7D_1$	$^7D_2$	$^7D_3$	$^7D_4$	$^7D_5$	$^5D_1$	$^5D_2$	$^5D_3$	$^5D_4$
IDEAL *LS*	3.00	2.00	1.75	1.65	1.60	1.50	1.50	1.50	1.50
$5d^46s^2$		(e x c l u d e d)				1.51	1.48	1.50	1.49
$5d^46s7s$	2.83	1.9	1.74	1.68	1.7		1.55	1.66	1.4

TABLE IV. Upper state statistics of Meggers' underwater spark lines (doubtful and ambiguous cases omitted).

	36	40	45	50	55	57 ·10^3 cm^{-1}
D_0	1	1 1				
D_1	1	2 3 2 2	1			
S_3	2 2 3 2	3 1 1				
D_2	2	3 1 2 3 1	2 1 1			
D_3		3 3 1	6 1 2			
D_4		1 1 2 1	1 3 3 5			
09_0		1				
12_4				1		
15_5					1	
16_4						1
17_6					1	

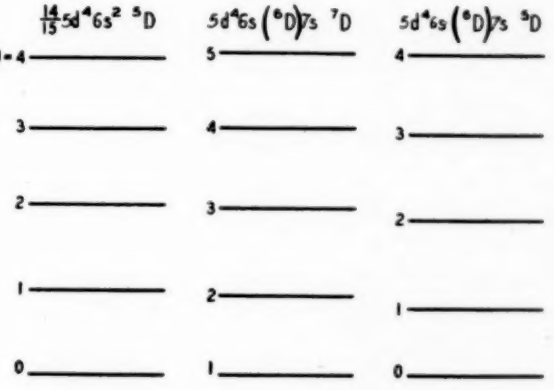

FIG. 3. Relative separations arising from W III $5d^4\,^5D$ plus s electrons. The relative separations within the $5d^46s7s\,^7D$ (center column) are, within one part in a thousand, equal to those of W II $5d^46s\,^6D$, although the absolute separations of the latter are greater by 4.1 percent.

Beining has evidently misread a difficult and unusual pattern.

404$_5$. The J value of this level is verified by the following conclusions from Zeeman-effect blends:

D_4-404 implies g_4 (impossible) or $g_5=1.00$
12_4-404 implies $g_4=1.61$ or $g_5=1.09$.

430$_4$. The J value of this level was determined by independent Zeeman-effect studies. The numerical coicidence with 19_6 is evidently fortuitous.

?430$_0$. The reality of this level tends to be confirmed by the apparently simple nature of the Zeeman-effect pattern of $20_1-?430_0$.

434$_3$. The J value of this level had to be determined from the consistency of Zeeman-effect blends:

15_3-434 implies $g_2=1.02$ or $g_3=1.47$
18_2-434 implies $g_2=1.70$ or $g_3=1.24$
19_2-434 implies $g_2=1.24$ or $g_3=1.20$.

?467$_7$. The reality of this level tends to be confirmed by the Zeeman-effect pattern of $19_6-?467_7$ on Harrison's plates, which is a wide blend showing large J values with g(smaller J)$>$ g(larger J).

497$_2$. There is a possibility that this level has an energy about 0.4 cm^{-1} lower than shown and $J=3$, or that the level listed and the lower one constitute a real pair.

55$_5$. The J value of this level may be 4. Though it shows no $J=3$ combinations, its only $J=6$ combination, 372_6-55_5, is weak and in bad wave number disagreement.

?58$_5$. The J value of this level may be 6. Though it shows no $J=7$ combinations, its only unambiguous $J=4$ combination, $247_4-?58_5$, is weak and in bad wave number disagreement.

(C) νν23044.52, 23043.96

Belke's λ4338.278 intensity 1*r*, was the only line listed as reversed in the arc which we were unable to classify. A careful re-examination shows it to be a pair, with the vacuum wave numbers given here.

Poggio[25] uses, probably in some cases correctly, several lines that we have omitted on the grounds that a comparison of the arc and spark intensities shows them to be probably not attributable to the neutral atom: e.g., "13_2-504_2."

(D)

Table V is a list of all the unclassified lines that appear, on account of their intensity or their occurrence under special conditions, to give evidence of important undiscovered structural properties of the atom. Since all the solar lines, arc reversals, and raies ultimes are classified, we have selected for inclusion in the table only those unclassified lines that have been reported in the underwater spark or furnace spectrum, or have

TABLE V. Important-appearing unclassified lines of the tungsten arc spectrum.

Intensity						Wave-length				
	arc		spark	under-water spark	fur-nace	this paper		Wave number	Assignment	Zeeman effect J values (tentative)
B	K	T	T				T			
2		10	5	M20		2533.641	0.633	39457.04	$D_1-?411_6$	1, 0
2		15	8	M1		2560.139	.119	39048.69		1, 0
3		10	—	M1		2606.406	.386	38355.57	$D_2-?431_4$	
2		9	12	M2?		2847.831	.823	35104.15	$D_2-?384_1$	
1		8 1d	9 18n	H		2852.37	.909 .10	35048.25	Ta ?0.355	
5		12d	10d			3221.220	.212	31035.21		1, 0
3		12	10		1−	3281.944	.939	30461.00		2, 1
5		12	201			3495.250	.246	28602.11		7, 6
5		12	7			3688.069	.069	27106.78	$19_6-?467_7$	large
4		12	10			4000.702	.694	24998.00		
4		40	3			5071.739	.733	19711.62		5, 4
	5					9161.43	—	10912.33		
	7					9531.13	—	10489.06		
	5					9757.39	—	10245.83		
	15					10002.65	—	9994.60		

a Belke or Kiess intensity greater than 3. The list consists of 15 lines. There are 29 unclassified lines with intensity 3, not counting the region $\nu > 40{,}000$ cm^{-1}.

6. ACKNOWLEDGMENTS

We wish to acknowledge our grateful indebtedness not only to those workers whose assistance has already been mentioned, especially Doctors Russell, Meggers, and Kiess, but also to the federal Works Progress Administration for support, and to the following students and helpers, who have aided us materially, especially in the search for levels: G. Caine, M. Fromer, N. Geier, H. R. Kratz, D. D. Laun, L. T. Mack, I. Milbauer, W. Wetzel, and J. Winnig.

PHYSICAL REVIEW VOLUME 63, NUMBERS 7 AND 8 APRIL 1 AND 15, 1943

The Small Angle Scattering of Electrons by Aluminum

BOWEN C. DEES AND BERNARD HAMERMESH
Physics Department, New York University, University Heights, New York, New York

(Received January 11, 1943)

The angular distribution of scattering of 46.4-kev electrons scattered by an aluminum foil 1.3×10^{-5} cm thick has been studied in the angular range between 0° and 10°. The values obtained for the mean projected angle of scattering have been compared with the values predicted by the theoretical treatment of Goudsmit and Saunderson, and agreement between experiment and theory has been found. The type of scattering has been investigated and it has been found that the scattering observed in this experiment was mainly plural.

INTRODUCTION

MOST of the previous experiments on multiple electron scattering have been concerned with electrons of several Mev energy.[1–4] There has been very little work done on electrons having energies of less than 100 kev.[5] With this in mind, a study of the scattering of 46.4-kev electrons in thin aluminum foils was undertaken.

For the values of the energy, thickness, atomic number, and angular range used, various criteria for single scattering show that the scattering should be non-single.[6,7]

The problem of incoherent multiple scattering has been treated theoretically by E. J. Williams,[8] and by Goudsmit and Saunderson.[9] Both treatments refer to and give values for the mean of the projected angle which is usually dealt with in non-stereoscopic cloud-chamber work. A given projected angle α corresponds to an infinite slit, perpendicular to the plane of projection, placed so that the line perpendicular to it drawn from the scattering center makes an angle α with the direction of the incident beam. If a collecting chamber provided with such a slit could be set at such a given angle, the intensity of the scattered current at that angle could be measured; this intensity will be called the slit intensity.

The mean projected angle of scattering $\langle\alpha\rangle_{Av}$ is defined by

$$\langle\alpha\rangle_{Av}=\frac{\int_0^\infty \alpha F(\alpha)d\alpha}{\int_0^\infty F(\alpha)d\alpha},$$

where $F(\alpha)$ is the relative slit intensity.

Goudsmit and Saunderson treat the problem of non-single scattering by using a special property of the Legendre polynomials which makes possible the determination of the angular

---

[1] W. A. Fowler and J. Oppenheimer, Phys. Rev. **54**, 320 (1938).
[2] C. W. Sheppard and W. A. Fowler, Phys. Rev. **57**, 273 (1940).
[3] Oleson, Chao, and Crane, Phys. Rev. **60**, 378 (1941).
[4] L. A. Kulchitsky and G. D. Latyshev, Phys. Rev. **61**, 254 (1942).
[5] E. Kruppke, Ann. d. Physik **30.7**, 577 (1937).
[6] G. Wentzel, Ann. d. Physik **69**, 335 (1922).
[7] C. T. Chase and R. T. Cox, Phys. Rev. **58**, 243 (1940).
[8] E. J. Williams, Proc. Roy. Soc. **169**, 531 (1939); Phys. Rev. **58**, 292 (1940).
[9] S. Goudsmit and J. L. Saunderson, Phys. Rev. **57**, 24 (1940); Phys. Rev. **58**, 36 (1940).

distribution of the scattered electrons. They have given, furthermore, a formula for determining the mean of the sine of the projected angle:

$$\langle \sin \alpha \rangle_{Av} = \frac{4}{\pi}\left\{\frac{1}{2} - \sum_{n=1}^{\infty} \frac{G_{2n}}{(4n^2-1)}\right\}$$

where $G_l = \exp\{-2\mu l(l+1)[\log_e \xi - (\frac{1}{2}+\frac{1}{3}+\frac{1}{4}+\ldots+1/l)]\}$

$$\mu = \pi\{Ze^2w/(mc^2)(w^2-1)\}^2 Nt$$

and $$\xi = 150(w^2-1)^{\frac{1}{2}}/Z^{\frac{1}{3}}.$$

The symbols have the following meanings:

Z = atomic number; e = electronic charge; m = electronic mass; c = velocity of light; w = energy of electrons in units of m_0c^2; N = number of scattering centers per cc; t = thickness of foil.

Goudsmit and Saunderson also give a factor for converting $\langle \sin \alpha \rangle_{Av}$ to $\langle \alpha \rangle_{Av}$ which was the quantity most suitable for comparison with experimental results.

The theoretical treatment given by Williams assumes a scattering distribution which is Gaussian for small angles. Criteria which he gives show that his results are not applicable in certain cases of thin foils, and consideration of these criteria led to the conclusion that his results are inapplicable to the conditions of this experiment.

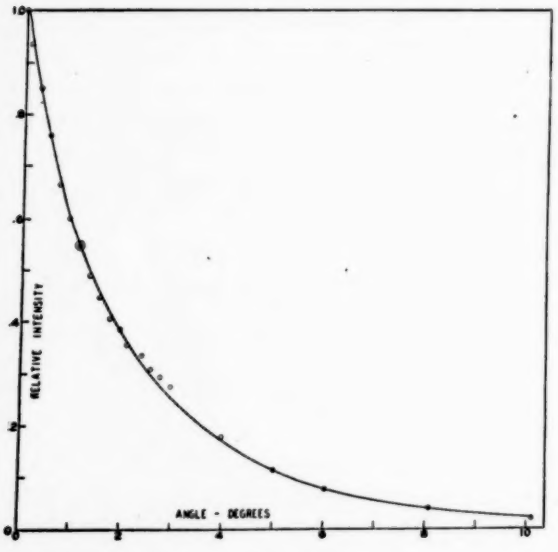

FIG. 1. Graph of relative pinhole intensity *versus* angle of scattering for electrons incident normally on the foil.

APPARATUS

The source of electrons was a heated filament and the electrons were accelerated by a high potential V equal to 46.4 kev, this value being chosen so that $\beta = 0.4$ in order to simplify calculations. This voltage V was maintained by a transformer and electron-tube rectifier with a very large condenser, which virtually eliminated any ripple. The beam of accelerated electrons then struck a thin aluminum foil at an angle of incidence of either 0° or ±45°. A collecting chamber set on the movable floor of the scattering chamber could be adjusted to any angle below 90° by means of controls in an adjacent control room.

The current from the plate of the collecting chamber was amplified by a d.c. amplifier of the Barth type, described by Penick,[10] and the amplified current was measured by a shunted Leeds and Northrup type R galvanometer. Currents as low as 10^{-5} μa could be measured accurately. The angular position of the collecting chamber could be determined quite accurately by means of a gear mechanism located inside the vacuum system. This gear mechanism operated a mirror system so constructed as to reflect a beam of light into a telescope in the control room every time the collecting chamber was rotated 0.2°.

The apparatus used consisted, in the main, of apparatus used by Chase and Cox in their work on the single scattering of electrons.[7] A number of modifications were necessary in order to allow manipulation of the apparatus from the control room and to increase the angular resolving power of the collecting chamber.

The foil was prepared by evaporating aluminum from a tungsten filament onto a collodion film, the evaporation chamber being kept at a pressure below 5×10^{-5} mm of mercury. The thickness of the foil was determined by assuming that all of the aluminum was evaporated and that the fraction deposited per unit area on the collodion was $1/4\pi r^2$ where r was the distance from the filament to the collodion. Small sections of several foils were mounted on tantalum holders. After it had been subjected to careful microscopic examination, a foil of suitable thickness

[10] D. B. Penick, Rev. Sci. Inst. **6**, 115 (1935).

(1.3×10^{-5} cm) was chosen and mounted in the mechanism used for adjusting the position of the foil in the beam.

RESULTS

After checking voltages and adjusting the electron gun current to a constant value, the electron beam was aligned by means of field coils so arranged that by changing the current through them the electron beam could be deflected in either the horizontal or vertical direction. The incident current was measured by moving the collecting chamber to the position of maximum deflection of the galvanometer. The foil was then lowered into position, and the reading corresponding to maximum scattered current was taken. (The foil could be lowered into position without disturbing in any way the adjustment of the apparatus.) The collecting chamber was rotated to a standard reference position (or angle) which was known as the "master point," and readings were taken of the scattered current for that position.

Readings of current were then taken for various angular positions of the collecting chamber, the chamber being moved between readings in steps of 0.2° or multiples thereof. The angular range for each "run" was between +10° and −10°. Readings were taken frequently of the galvanometer zero, thus eliminating any error due to galvanometer drift. A number of readings of current for the master point were interspersed at frequent regular intervals so as to make possible the detection of systematic changes in the electron beam. As will be pointed out presently, these readings were necessary for correlating the data.

Before and after taking a set of data, the sensitivity of the amplifier-galvanometer system was determined to guard against changes in the input resistance or other elements of the amplifier due to change of humidity or temperature. This precaution was felt to be necessary because the temperature of the high voltage room—where the electrometer tube and input resistance of the amplifier circuit were installed—was found to rise as much as 10°C during some runs.

Data from five complete runs—two for normal incidence and three for 45° incidence—have been analyzed and will be considered here.

The readings of current for the master point—run 1, normal incidence—were averaged, and each individual master point reading was multiplied by a factor which made that particular value equal to the average value. The readings which lay between two master point readings were corrected by factors intermediate between the correction factors for the two master point readings.

The same process was applied to the data of run 2, normal incidence, but here a further correction factor was necessary to correlate the data of runs 1 and 2. The correction factor in this case was constant and was obtained by finding the ratio

$$(I_m)_{\text{run 1}}/(I_m)_{\text{run 2}},$$

where $(I_m)_{\text{run 1}}$ is the average value of current for the master point for run 1 and $(I_m)_{\text{run 2}}$ is the average value of current for the master point for run 2.

Weighting each of these runs equally, averaging the values of scattered currents, and reducing all currents to relative values (maximum current = unity) leads to the data used for plotting the curve of Fig. 1. A similar process was applied to the three runs taken at 45° incidence; this led to Fig. 2.

Since the diaphragm openings in the collector are small, scarcely larger than a pinhole, the angular distribution plotted from these data will

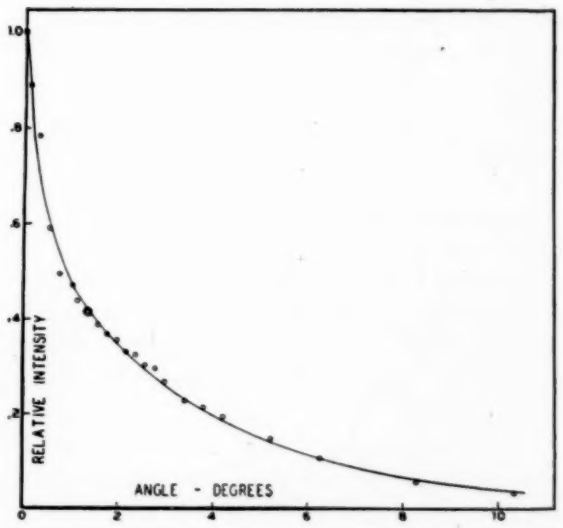

FIG. 2. Graph of relative pinhole intensity *versus* angle of scattering for electrons incident at 45° on the foil.

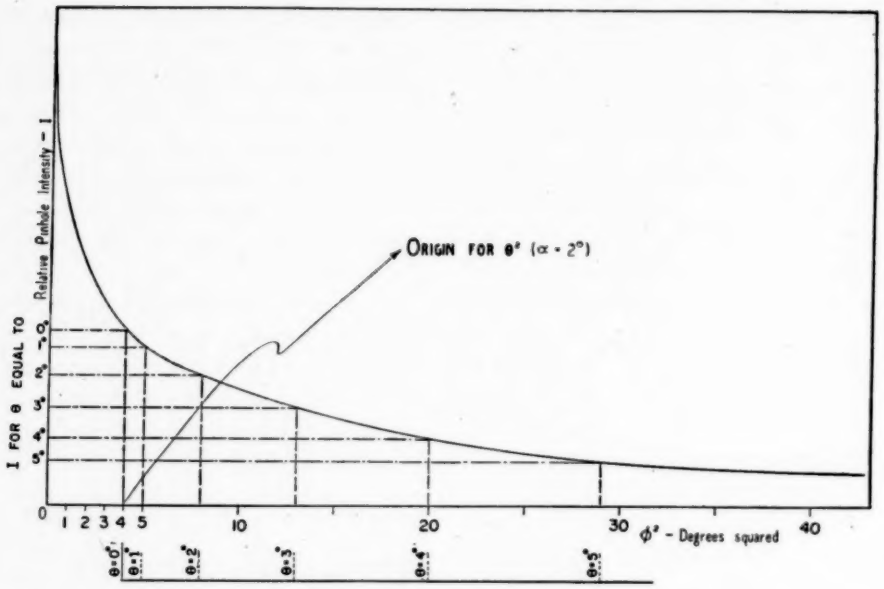

FIG. 3a. Illustrating how the derived curves were obtained by construction. This diagram shows the steps necessary in obtaining points for plotting the derived curve for $\alpha=2°$.

henceforth be called the "pinhole distribution." In the curves plotted from these data—Figs. 1 and 2—the double circles represent the master points.

There is available no theoretical treatment of what is here called the pinhole distribution. However, the integral of the pinhole distribution curve of Fig. 1 is proportional to the current to an infinite slit placed at 0°. If such a slit were placed at any angle α the current to the slit would be proportional to the integral of the curve of intensity obtained by moving a pinhole collecting chamber along the slit. Given the pinhole curves of Figs. 1 and 2 therefore, it is possible to obtain also slit intensity curves which can be used to find the average value of the angle of scattering, $\langle\alpha\rangle_{Av}$, and this value can be compared with results obtained theoretically.

A method of graphical construction was used in obtaining the desired slit intensity curves from the experimentally determined pinhole distribution curves. The method involved the following considerations:

Let the scattered electrons be considered incident on a spherical surface having the scattering foil at its center. The small portion of the spherical surface covered in the experiment may be treated as plane, and rectangular coordinates

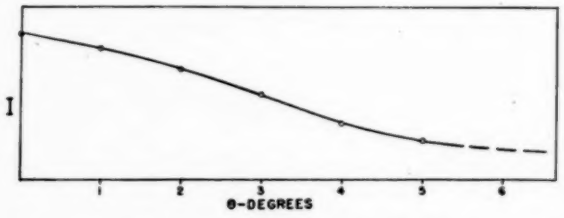

FIG. 3b. The derived curve obtained by plotting the relative pinhole intensities obtained from 3a against θ. The area under this curve was measured with a planimeter to obtain the data for plotting the desired slit intensity curves.

α and θ may be used. The point at which an undeviated electron would strike the surface is taken as the origin of coordinates, and the coordinates are measured in degrees.

Let the current of scattered electrons to the element $d\alpha d\theta$ at the point (α, θ) be denoted by $f(d\alpha d\theta)$. The function f will be an even function of ϕ, where $\phi^2=\alpha^2+\theta^2$, and it may therefore be written $f(\phi^2)$. The current to a slit of width $d\alpha$ of infinite length parallel to the θ-axis at a distance α will be an even function of α and we may therefore write $F(\alpha)=G(\alpha^2)$; $F(\alpha)$ has been mentioned above and is known as the relative slit intensity. Then

$$G(\alpha^2)=\int_{-\infty}^{+\infty} f(\alpha^2+\theta^2)d\theta.$$

The pinhole distribution curve shown in Fig. 1 is the graph of $f(\phi^2)$ against ϕ. When $\alpha=0$, we have

$$G(\theta^2)=\int_{-\infty}^{+\infty} f(\theta^2)d\theta.$$

Thus the area under the curve of Fig. 1 is proportional to $G(0^2)$. The integration may be performed graphically. (In practice a planimeter was used.)

Values of $G(\alpha^2)$ for values of α other than zero may be found as follows: Let the measurements made with the pinhole collector be plotted not against ϕ, as in Fig. 1, but against ϕ^2, as shown in Fig. 3a. Then $f(\alpha^2+\theta^2)$ plotted against θ^2 with any fixed value of α is described by the same graph when the origin is displaced a distance α^2 on the axis of abscissas, for

$$f(0+\theta^2)=f\{\alpha_1^2+(\theta^2-\alpha_1^2)\}.$$

Thus, for $\alpha=1°$, the origin for θ^2 is at $\phi^2=(1°)^2$ and for $\alpha=2°$ the origin for θ^2 is at $\phi^2=(2°)^2$, and so on. For each of a series of values of α, the values of $f(\alpha^2+\theta^2)$ are thus found for different values of θ, and are plotted again against θ as abscissa.

Figure 3b shows such a plot for $\alpha=2°$. The area under this curve is then proportional to $F[(2°)^2]$ and, graphically determined, furnishes one point for the graph of Fig. 4, in which $G(\alpha^2)=F(\alpha)$ is plotted against α. (One such "derived" curve must be plotted and measured for each of the points of Fig. 4.) This curve is the desired slit intensity curve for the case of normal incidence. The curve of Fig. 5 is determined in the same way from Fig. 2 and represents the slit intensity for the case of 45° incidence.

The experimental points (found as just mentioned) are shown in Figs. 4 and 5 as open circles. The last experimental point obtainable

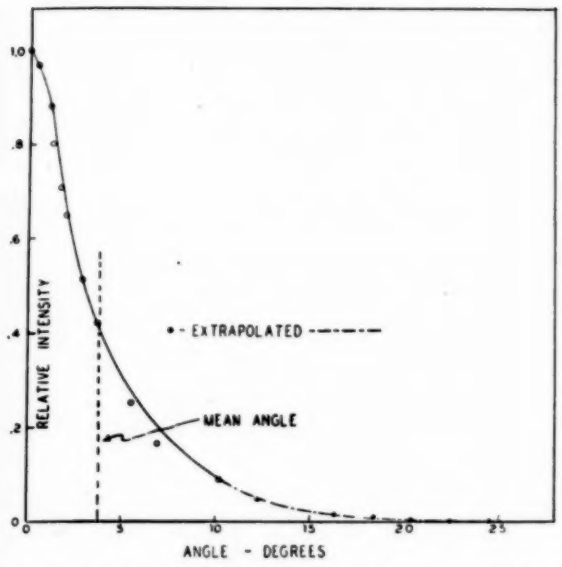

FIG. 4. Graph of relative slit intensity *versus* angle of scattering for electrons incident normally on the foil.

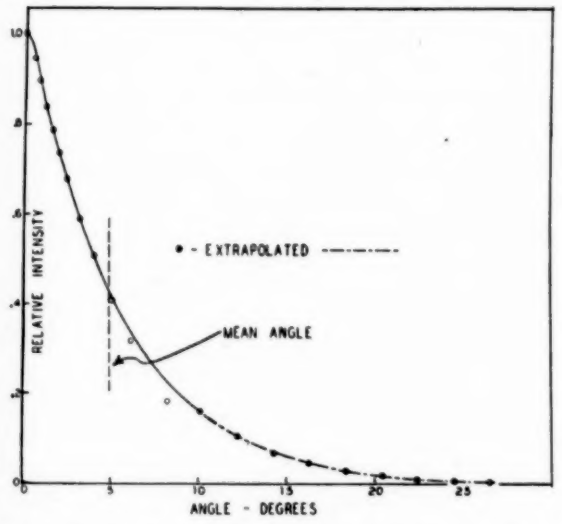

FIG. 5. Graph of relative slit intensity *versus* angle of scattering for electrons incident at 45° on the foil.

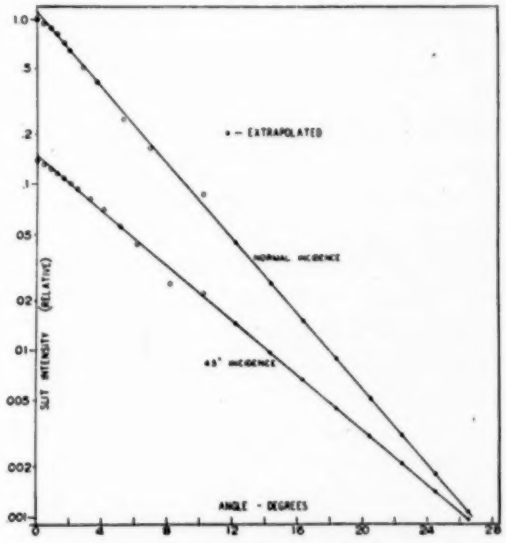

FIG. 6. Graph of log of relative slit intensity *versus* angle of scattering.

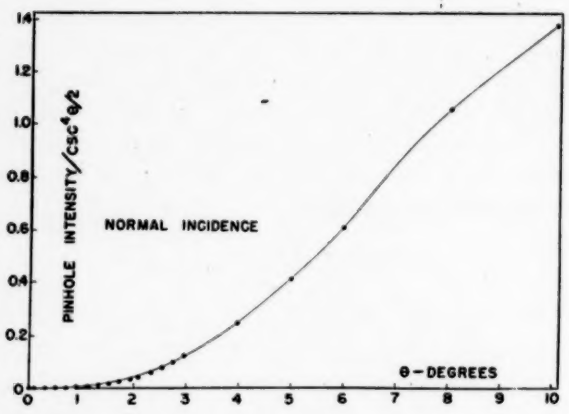

FIG. 7. Graph of relative pinhole intensity divided by $\csc^4 \theta/2$ *versus* angle. The fact that this curve does not level off shows that the scattering in this experiment was non-single.

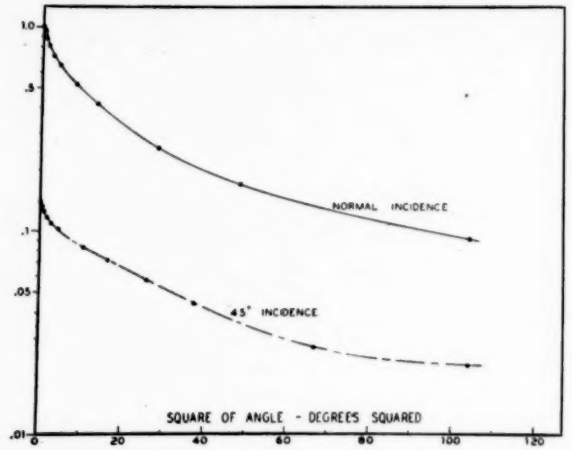

FIG. 8. Graph of log of slit intensity *versus* square of angle of scattering. The fact that these curves are not straight lines shows that the scattering was not strictly multiple.

is seen to lie at a considerable distance above the angle axis. For comparison with theory it is necessary to extrapolate in some manner so that the resulting curve can be used for obtaining an experimental value of the quantity defined above. Obviously, a straight line extrapolation would not be correct, for the intensity must actually have a finite value even for 180°, and a straight line extrapolation would cross the angle axis only a few degrees from the origin. Any method of extrapolation would have to be chosen rather arbitrarily, but the method actually used was considered justifiable because of the following circumstance: If the logarithm of slit intensity is plotted against angle, the resulting points all lie very close to a straight line. This fact is easily seen from Fig. 6 where the experimental points are again represented by open circles. If, now, the straight line found from the experimental points is extended, values of slit intensity can be read from it at intervals, and these values can then be plotted on the slit distribution curve corresponding to the condition of incidence considered. Points obtained by this method are shown in Figs. 4 and 5 as solid circles.

The mean projected angle of scattering was found experimentally in each case by cutting from sheet metal a lamina the exact shape of the slit distribution curve. Comparison of the equation defining the mean projected angle with the expression defining center of mass shows that there is a direct correspondence between $\langle\alpha\rangle_{Av}$ and the center of mass of the body. Consequently, the problem of determining $\langle\alpha\rangle_{Av}$ reduces simply to the problem of finding the center of mass of the sheet-metal lamina. This determination was made by balancing the lamina on a sharp-edged fulcrum which was accurately perpendicular to the angle axis; this defined a line containing the center of mass, and hence also the angle $\langle\alpha\rangle_{Av}$, since the value of $\langle\alpha\rangle_{Av}$ must correspond to the perpendicular distance from the intensity axis to the center of mass.

The value of $\langle\alpha\rangle_{Av}$ for the slit distribution curve corresponding to normal incidence was found to be 3.82°. The value of $\langle\alpha\rangle_{Av}$ for the case of 45° incidence was 5.29°.

For comparison with theory a total of nineteen terms of the series given by Goudsmit and Saunderson involving G_l was used in each of the two cases. The resulting value of $\langle\sin\alpha\rangle_{Av}$ for the case of normal incidence was 0.072. From the conversion factor given by Goudsmit and Saunderson, it was possible to obtain a theoretical value of $\langle\alpha\rangle_{Av}$ from $\langle\sin\alpha\rangle_{Av}$. The theoretical value found was 4.08°, a value differing from the experimental value of 3.82° by less than 7 percent.

The values of the G_l's corresponding to the case of 45° incidence were calculated, and the value of $\langle\sin\alpha\rangle_{Av}$ for this case was found using them. The calculations were identical with those for the case of normal incidence except for the factor involving foil thickness: The foil thickness was t for the case of normal incidence,

but was $\sqrt{2}\times t$ for the case of oblique incidence. The value of $\langle\alpha\rangle_{Av}$ thus calculated was 5.13°, a value differing by only 3.1 percent from the experimental value of 5.29°.

In order to determine empirically the type of scattering that was being dealt with, i.e., multiple, plural, or single, Figs. 7 and 8 were plotted. To see whether single scattering played any considerable part in this experiment, the relative pinhole intensity divided by the quantity $csc^4(\theta/2)$ has been plotted against angle in Fig. 7. (The data used were those obtained for normal incidence.) If the scattering had become mainly single in the range shown, the curve should have leveled off, for any single scattering to be expected in this case would have approximated the Rutherford law of scattering. The curve here has obviously not levelled off, so apparently any effect due to single scattering is inconsequential in this range.

To see whether the scattering was purely multiple, in which case the scattering distribution should have been Gaussian, the logarithm of the relative intensity was plotted against the square of the angle in Fig. 8. For strictly multiple scattering this curve should be a straight line. The form of the curves of Fig. 8 shows that the scattering in this case was Gaussian over an extremely small range of angles at most.

It would seem, therefore, that in this experiment almost all of the scattering may be considered to be plural. This conclusion seems inescapable in view of the facts represented in Figs. 7 and 8.

ERRORS

The errors involved in this work were not large. The high voltage was stable and its value could be read directly on an accurately calibrated voltmeter which was accurate to within 2 percent. The angles could be read accurately to 0.20°, and it is believed that the final result could not be in error by more than 0.5 percent on account of inaccuracy of angular measurement. The exact foil thickness could not be determined with much certainty, but fortunately an error in the foil thickness causes only a much smaller error in the calculated value of the mean projected angle. This error should not have amounted to more than about 3 percent. Errors in the graphical constructions leading to the slit intensity curves were certainly not large, and repeated determinations of $\langle\alpha\rangle_{Av}$ with different metal laminas showed that the error introduced here was not likely to be more than about 1 percent.

CONCLUSION

In considering the problems of electron scattering, most investigators have given their attention either to the case of single scattering or to the case of multiple scattering, and apparently the region of plural scattering has not been considered very fully. Williams has stated that for certain conditions the transition from multiple to single scattering should be rather sharp, and that therefore the region of plural scattering could be considered small. Under the conditions of this experiment this is clearly not the case. In this experiment the scattering is plural over nearly the entire angular range.

Previous investigation[4] has shown that the theoretical treatment of Goudsmit and Saunderson represents quite accurately the scattering of very high energy electrons. This experiment has shown that their treatment is also valid for electrons having energies around 50 kev, inasmuch as the theoretical and experimental values of $\langle\alpha\rangle_{Av}$ agree within the limits of experimental error.

ACKNOWLEDGMENTS

The authors wish to thank Dr. R. T. Cox and Dr. C. T. Chase for their cooperation and helpfulness. Their suggestions and help were of the greatest value in carrying out this research.

The Structure of Liquid Carbon Tetrachloride

A. EISENSTEIN*
University of Missouri, Columbia, Missouri
(Received February 5, 1943)

X-ray diffraction patterns of liquid CCl_4 at 27°C have been obtained by both the photographic and G-M counter methods. The corrected patterns were subjected to a Fourier analysis to obtain the electron density distribution function for the liquid. In addition to showing the C−Cl and Cl−Cl distances within the molecule, the intermolecular distances and concentrations are indicated as well. The latent heat of vaporization has been calculated from the distribution function and found to be in reasonably good agreement with the measured value.

INTRODUCTION

CARBON tetrachloride has the distinction of having been among the first polyatomic molecules subjected to an early structural analysis by means of diffraction methods. X-ray and electron diffraction studies[1,2] of the vapor have shown the molecular structure to be tetrahedral, having a central carbon atom surrounded by four equidistant chlorine neighbors. The most recent electron diffraction investigations[3] give as the Cl−Cl distance 2.98A from which the C−Cl distance of 1.83A may be derived. A qualitative picture of the liquid structure has been obtained[4] by comparing the x-ray diffraction pattern of the liquid with a calculated pattern which assumes a mercury-like (close-packed) molecular distribution.

A determination of the liquid atomic structure as characterized by the atomic distribution function cannot in general be carried out with a high degree of accuracy for other than the monatomic liquids. This is due largely to the unknown natures of the exact molecular scattering factors whereas the monatomic scattering factors are well known.[5] Many polyatomic liquids have been investigated and approximate atomic distribution functions obtained by assuming (1) that the liquid is essentially monatomic,[6] which is justified in such cases where the scattering power of one type of atom is large compared to that of the other atoms (C_6H_6, H_2O, etc.) or (2) where the molecular scattering factor can be approximated by a sum of the individual atomic scattering factors.

The second method seems to offer the best approach to a structural analysis of carbon tetrachloride for the scattering power of the Cl atom is less than three times that of the C atom. Also, the tetrahedral molecular structure should show enough spherical symmetry to justify using the second approximation. Thus, an analysis based on the x-ray diffraction pattern of the liquid should result in an electron distribution function which shows, in addition to the interatomic Cl−Cl and C−Cl distances, the intermolecular concentrations and distances as well.

EXPERIMENTAL

The x-ray diffraction patterns used in this study were obtained by allowing a beam of

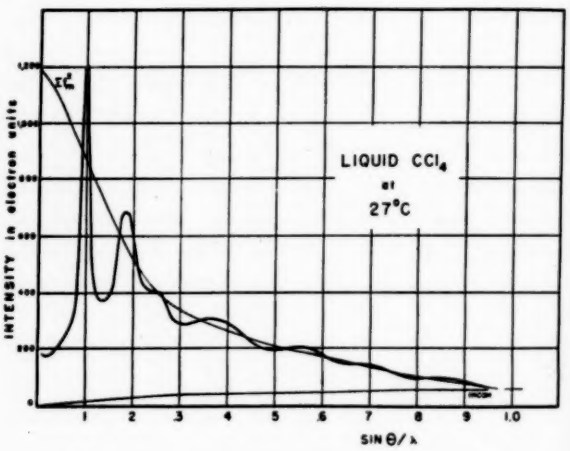

FIG. 1. Corrected x-ray diffraction pattern of liquid CCl_4 at 27°C.

* Now at the Radiation Laboratory, Massachusetts Institute of Technology, Cambridge, Massachusetts.
[1] P. Debye, L. Bewillogua, and F. Ehrhardt, Physik. Zeits. **30**, 84 (1929).
[2] R. Wierl, Ann. d. Physik **8**, 521 (1931).
[3] S. B. Hendricks, L. R. Maxwell, V. L. Mosley, and M. E. Jefferson, J. Chem. Phys. **1**, 549 (1933).
[4] H. Menke, Physik. Zeits. **33**, 593 (1932).
[5] A. H. Compton and S. K. Allison, *X-Rays in Theory and Experiment* (D. Van Nostrand, New York, 1935).
[6] J. Morgan and B. E. Warren, J. Chem. Phys. **6**, 66 (1938).

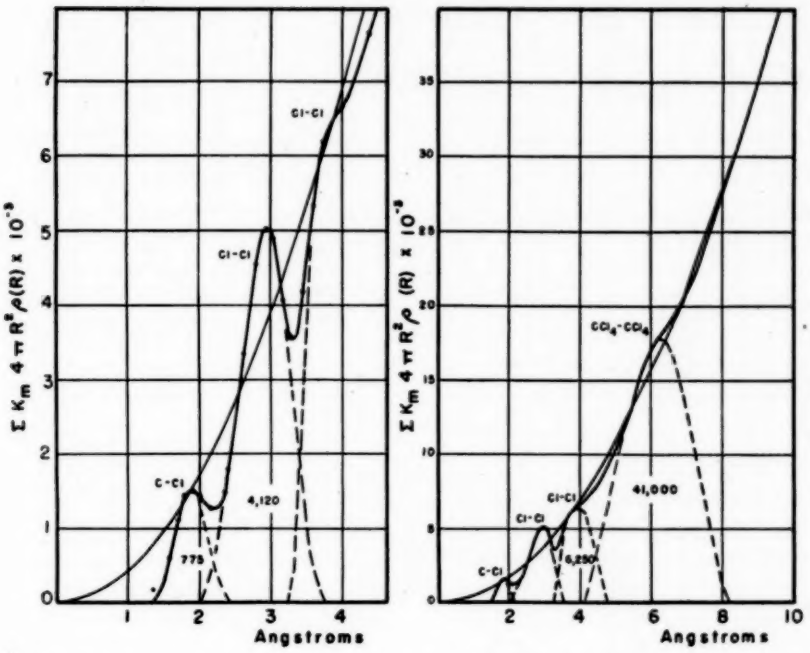

FIG. 2. Electron distribution function of liquid CCl_4 showing the interatomic C—Cl and Cl—Cl concentrations and distances, as well as the intermolecular CCl_4-CCl_4 structure.

monochromatic x-rays (rocksalt reflected) of 0.71A wave-length to fall upon a cylindrical sample of the liquid. The diffracted x-rays were recorded photographically or by means of a Geiger-Mueller counter. A Pyrex glass capillary having walls 0.02 mm thick and a diameter of 0.94 mm was filled with chemically pure CCl_4 and sealed off at atmospheric pressure for use as a sample. Suitable diffraction photographs were recorded in 22 hours by use of a camera of 5.377-cm radius and a high intensity x-ray tube.[7] These diffraction patterns of the liquid at 27°C have been investigated to a value of $\sin\theta/\lambda = 1.1$ and show seven diffraction maxima in this region.

The liquid small angle scattering was recorded with the G-M counter method. In this, the sample was held at the center of an evacuated camera which in turn was mounted at the center of an x-ray spectrometer, the general set-up being quite similar to that used for liquid argon.[8] Patterns obtained in this manner showed five distinct peaks; the sixth was obtained only with difficulty since the weak scattered intensity in this region presents a probable error in counting of nearly the same magnitude as this prominence. No attempt was made to find the seventh peak. When compared over the same regions, both methods of detecting the scattered x-rays yield very nearly the same diffraction pattern. Figure 1 shows the corrected x-ray diffraction pattern formed by combining the small angle pattern as obtained by the G-M counter method with the large angle pattern recorded photographically. The experimental pattern has been corrected for polarization and absorption in the sample, the incoherent scattering has been subtracted, and the intensity is plotted in terms of electron units per molecule.

As will be explained in detail in the next section, an attempt has been made to correlate the position of the first diffraction peak with the intermolecular distance. In order that this correlation may be checked in an approximate manner, the sample was heated to a temperature of about 240°C under a calculated pressure of 26 atmos. Under these conditions of pressure and temperature the position of the first peak was again observed by the G-M counter method.

[7] A. Eisenstein, Rev. Sci. Inst. **13**, 208 (1942).
[8] A. Eisenstein and N. S. Gingrich, Phys. Rev. **62**, 261 (1942).

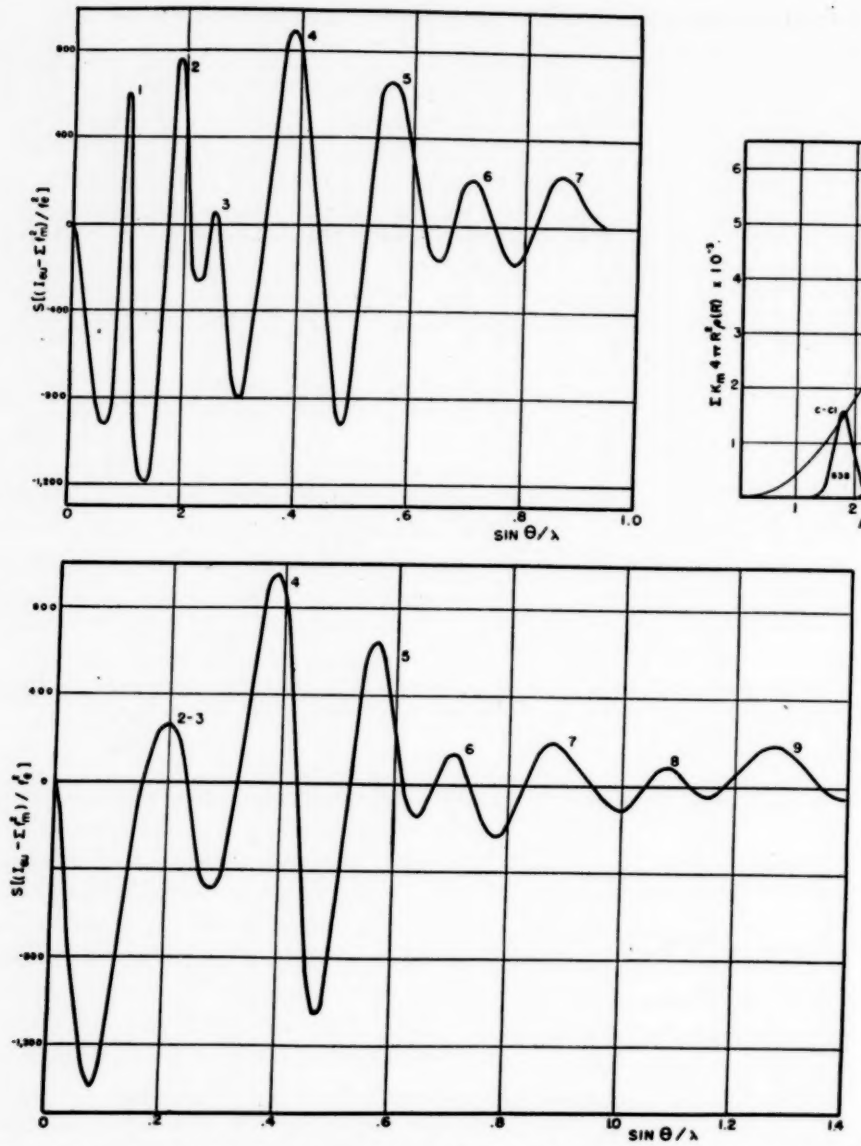

FIG. 3 (A—Upper left) Experimental intensity function. (B—Upper right) Idealized electron distribution. (C—Lower) Intensity function calculated from (B) using Eq. (2).

RESULTS

The fully corrected intensity function of Fig. 1 has been subjected to an analysis to obtain the electron density distribution function by the method[9] indicated below.

$$\sum K_m 4\pi R^2 \rho_m(R) = \sum K_m 4\pi R^2 \rho_0 + (2R/\pi) \times \int_0^\infty S[(I_{eu} - \sum f_m^2)/f_e^2] \sin SR dS. \quad (1)$$

$\sum$ denotes the summation over all the atoms of the molecule; $K_m = f_m/f_e$ or the effective number of electrons in the type m atom; f_m = atomic scattering factor of the type m atom; $f_e = \sum f_m / \sum Z_m$ or the average f per electron; Z_m = atomic number of type m atom; $\rho_m(R)$ = density of atoms of type m at a distance R from a given atom; ρ_0 = mean electron density of scattering matter; R = distance from the origin atom; $S = 4\pi \sin \theta/\lambda$; I_{eu} = intensity of unmodified scattering in electron units per molecule.

The harmonic analysis required to evaluate

[9] B. E. Warren, H. M. Krutter, and O. Morningstar, J. Am. Ceramic Soc. **19**, 202 (1936).

the integral was performed by means of a Coradi† analyzer. Figure 2 shows a plot of $\sum K_m 4\pi R^2 \rho_m(R)$ which represents a superimposed electron distribution function such as would be obtained by placing each atom in turn at the origin and summing over all the resulting electron distributions. On the right may be seen the complete distribution curve out to 10A while at the left an enlarged portion of this curve is shown to better illustrate the interatomic structure. The first electron concentration shows a maximum at 1.85A thus representing the C−Cl distance; the second concentration occurs at 2.95A which indicates the interatomic Cl−Cl separation. The manner in which the peaks are drawn in is somewhat arbitrary, especially for those prominences representing the intermolecular distances. Despite this, reasonable agreement has been obtained in comparing the peak areas with the calculated electron concentrations. For example, the measured area of the C−Cl peak $775e^2$ is to be compared to $2(K_C \times 4K_{Cl}) = 648e^2$ where $K_C = 4.60$ and $K_{Cl} = 17.34$. The Cl−Cl peak area of $4129e^2$ compares similarly to $4(K_{Cl} \times 3K_{Cl}) = 3610e^2$. In addition to this interatomic structure, a peak at 3.9A having an area of $6250e^2$ may be interpreted as representing a further Cl−Cl concentration, these Cl atoms belonging presumably to neighboring molecules. By use of the measured area of this peak the number of Cl neighbors surrounding each Cl atom at this distance may be calculated as follows: $8(K_{Cl} \times nK_{Cl}) = 6250$ from which n has the value 2.6 indicating 2 to 3 neighbors in adjacent molecules. The fourth peak at 6.2A represents a concentration which at this large distance is probably due to the molecules themselves, $CCl_4 - CCl_4$. Under this premise the number of molecular neighbors n may be obtained from $2(K_{CCl_4} \times nK_{CCl_4}) = 41{,}000e^2$ and has the value of 3.7 or approximately 4.

In the process of evaluating the integral of Eq. (1), the intensity function $S(I - \sum f_m^2)/f_e^2$ must be assumed to be negligible beyond a certain arbitrary point. Experience shows, however, that in most cases the experimental difficulty in evaluating this function at large scattering angles prohibits setting the vanishing point with a high degree of accuracy.[10] Certain considerations lead to the belief that this intensity function at large angles is determined chiefly by the atomic structure at small values of R or in this case by the C−Cl and Cl−Cl concentrations.

An attempt, based on these assumptions, has been made to calculate the above function for scattering angles to 180°. It has been measured experimentally to 103°, a plot of which is shown in Fig. 3A. An idealized interatomic structure has been chosen, the C−Cl and Cl−Cl peaks being represented by Gaussian error functions having the proper area and position of maxima. Beyond 3.6A the distribution represents that of a completely homogeneous liquid. This structure is shown in Fig. 3B and is used to calculate the intensity function by the use of Eq. (2), derivable from (1).

$$S(I - \sum f_m^2)/f_e^2 = \int_0^\infty (1/R)(\sum K_m 4\pi R^2 \rho_m(R) - \sum K_m 4\pi R^2 \rho_0) \sin SR dR. \quad (2)$$

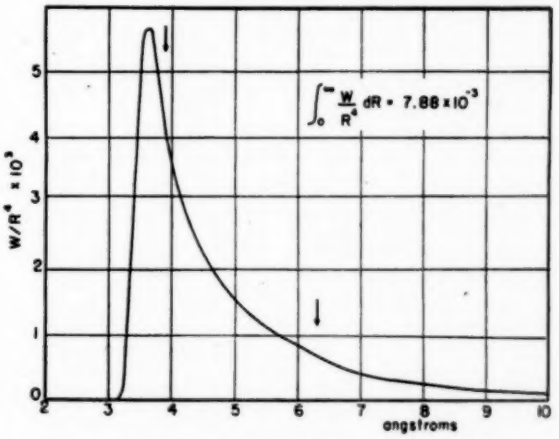

FIG. 4. The function W/R^4 *vs.* R used in evaluating the latent heat. Arrows indicate the intermolecular Cl−Cl and $CCl_4 - CCl_4$ distances.

The integral was again evaluated with the aid of the Coradi analyzer. Figure 3C shows this calculated function. A comparison of the measured and calculated curves may be most easily facilitated by numbering the maxima, each of which has its counterpart in the diffraction pattern. Peaks 4, 5, 6, and 7 are reproduced in

† The Coradi analyzer was made available for this work by the Aeronautics Department of the Massachusetts Institute of Technology.

[10] N. S. Gingrich, Phys. Rev. **59**, 290 (1941).

both instances with a noticeable fidelity. This is consistent with the basic assumption as to the origin of the scattering at large angle. Peaks 8 and 9 have also been obtained and their magnitudes indicate that the vanishing point chosen for the initial analysis is not truly valid, although probably justifiable.

At small angles the fine structure, peaks 1, 2, and 3, of the experimental function is not present in the calculated function. This is taken to indicate that this fine structure, particularly peak 1, arises directly from intermolecular interference. When the position of this first prominence ($\sin\theta/\lambda=0.10$) is substituted into Ehrenfest's diffraction equation[11] to calculate the recurring distance giving rise to this diffraction peak, the resulting value is 6.2A. By applying this approximate method of calculation to the position of the first diffraction peak from the liquid at 240°C and 26 atmos. the intermolecular distance is found to be 7.3A showing an increase proportional to $T^{\frac{1}{3}}$.

The relationship between the atomic distribution function and the latent heat of vaporization L, has been shown[12] to assume the form

$$L=RT-2\pi N\rho_0\int_0^\infty R^2V(R)(\rho(R)/\rho_0)dR, \quad (3)$$

where R is the gas constant, T the absolute temperature, N Avogadro's number, $V(R)$ the intermolecular potential, $\rho(R)$ the atomic distribution function, and ρ_0 the average molecular density. Heretofore, the application of this relationship has been made only to monatomic liquids, but since the molecular distribution function of CCl_4 is available from the curves of Fig. 2 by subtracting off the interatomic concentrations C−Cl and Cl−Cl, an attempt has been made to evaluate the latent heat. Only the van der Waals' attractive forces will be considered in this calculation in which the form $V(R)=-kR^{-6}$ is assumed. The proportionality constant k has been related to the molecular polarizibility α by the equation[13]

$$k=(3/8)hem^{\frac{1}{2}}\alpha^{\frac{1}{2}}N^{\frac{1}{2}}, \quad (4)$$

where N is the total number of electrons in the molecule and h, e, and m have their conventional significance. If one uses for the molecular polarizibility $\alpha=11.2\times10^{-24}$ cc, he finds the constant k assumes the value 12.6×10^{-10} erg A^6.

The integral of Eq. (3) has been evaluated graphically by plotting W divided by R^4 *vs.* R, where W, the probability function, equals $\rho(R)/\rho_0$. This curve is shown in Fig. 4, the arrows indicating the intermolecular Cl−Cl and CCl_4-CCl_4 distances. From this, the contribution to the intermolecular cohesive energy due to the neighboring Cl atoms of different molecules at 3.9A may be compared to that contributed by the remainder of the molecule. The fact that the maximum of this curve does not correspond exactly to this Cl−Cl distance is probably due to the neglected repulsive terms of the potential function. From the area under the curve, 7.88×10^{-3}, the latent heat of vaporization is found to be 6.24 kcal./mole as compared to the observed value 7.09 kcal./mole. The discrepancy between these values is of the same order of magnitude as that existing between the calculated and experimentally observed electron concentrations. These inconsistencies are believed to arise primarily from the basic assumptions involving the nature of the molecular scattering factor.

ACKNOWLEDGMENTS

Appreciation is herewith expressed to Dr. N. S. Gingrich for making available certain equipment obtained through grants in aid to research from the American Academy of Arts and Science, from the Elizabeth Thompson Science Fund, and the University of Missouri Research Council.

[11] P. Ehrenfest, Proc. Amst. Akad. Sci. **17**, 1184 (1915).
[12] J. H. Hildebrand and S. E. Wood, J. Chem. Phys. **1**, 817 (1933).
[13] J. G. Kirkwood, Physik. Zeits. **33**, 57 (1932).

Quantization of Molecules, Inter- and Intramolecular Forces[1]

KASIMIR FAJANS AND THEODORE BERLIN*
Department of Chemistry, University of Michigan, Ann Arbor, Michigan

(Received February 2, 1943)

In diatomic molecules (e.g., P_2) the distinction is made between the quantization of the electrons of the atomic cores (P^{5+}), which is assumed to be the same ($1^2 2^8$) as in the free atom (P), and of the valence electrons $3^{2.2}(P^{5+})II^2(P^{5+})3^{2.2}$. The latter can be quantized with respect to the field of both cores ("shared" II^2 electrons) and to the field of single cores ("unshared" $3^{2.2}$ electrons). The Pauli principle is applied separately to the quantization of the "shared" electrons and to the others. On this basis it is possible to interrelate the great difference in the strength of the external field (intermolecular forces) of N_2 and P_2 with the size of the atomic cores N^{5+} and P^{5+}. The comparison of the intramolecular binding strength in (AB) with that in $(AB)^+$ supports the conclusions: in N_2 all ten (not merely six) valence electrons, in HCl all eight (not two) participate in the binding of the cores N^{5+} and N^{5+}, H^+ and Cl^{7+}; the molecules of monohydrides of positively di- and trivalent elements, like those of positively monovalent elements, contain hydrogen as a more of less strongly deformed H^-.

1.

THE method of quantization of molecules proposed in communications II, III, V differs from other methods in that it attempts to picture the actual properties of the molecule without stressing its origin. In the Hund-Mulliken method of molecular orbitals N_2 is, for example, considered as intermediate between the state of two infinitely separated N atoms and their complete coalescence to an atom of Si. The comparison with the N atoms leads[2] to the formula of N_2:

$$KK(\sigma_g 2s)^2(\sigma_u 2s)^2(\pi_u 2p)^4(\sigma_g 2p)^2. \quad (1)$$

The formula (2) for the molecule P_2 is analogous[2] to (1), but the whole outer shell is characterized in (1) by the principal quantum number $n=2$, in (2) by $n=3$, corresponding to the state of the valence electrons in the free atoms.

$$KKLL(\sigma_g 3s)^2(\sigma_u 3s)^2(\sigma_g 3p)^2(\pi_u 3p)^4. \quad (2)$$

Our method should be able to express the great difference in the properties of P_2 and N_2. The latter behaves like a noble gas (b.p. 77°K). P_2 has a strong external field shown by its polymerization to P_4 which only partly dissociates at 2000°K. In III the quantum formula $KK1^2 2^8$ was proposed for N_2. An alternative way to write it is:

$$(N^{5+})I^2II^8(N^{5+}). \quad (3)$$

Formula (3) indicates that the two electrons with the principal quantum number $n=I$ and the eight with $n=II$ are common to both atomic cores N^{5+} or, more exactly, are quantized with respect to the field of both cores. With respect to quantization, the two cores in N_2 play a role similar to the nucleus Ne^{10+} in the neon atom.

2.

The exact quantitative meaning of the values of n in molecules is less evident than in atoms and for this reason roman numerals are used in formula (3) and later for the principal quantum number of electrons quantized with respect to more than one core. However, in atoms and molecules the main quantum number n can be considered as closely related to the energy of the electron or to its average distance from the nuclei. This can be explained by Fig. 1. In N_2 (C), the two electrons with $n=I$ can be considered as moving predominantly between the N^{5+} cores.[3] The distance between the center of the molecule and the nuclei is 0.55A; half of

* Horace H. Rackham Predoctoral Fellow, 1941–1942 and 1942–1943.

[1] Communication VI on "Electronic Structure of Molecules." The previous communications in J. Chem. Phys. 10 (1942) will be quoted by the corresponding roman numerals. I. K. Fajans and N. Bauer, p. 410; II. T. Berlin and K. Fajans, p. 691; III–V. K. Fajans, pp. 759–761.

[2] G. Herzberg, *Molecular Spectra and Molecular Structure* (Prentice-Hall, Inc., New York, 1939), p. 368.

[3] The radial electron density in number of electrons per A in the free atomic cores, pictured in Fig. 1, has been calculated by means of the wave functions of J. Slater, Phys. Rev. **34**, 1293 (1929); **36**, 57 (1930). In Na^+ and P^{5+} only the L shell at large distances from the nuclei are significant for the above considerations. Concerning H^-, see H. Bethe, Zeits. f. Physik **57**, 815 (1929).

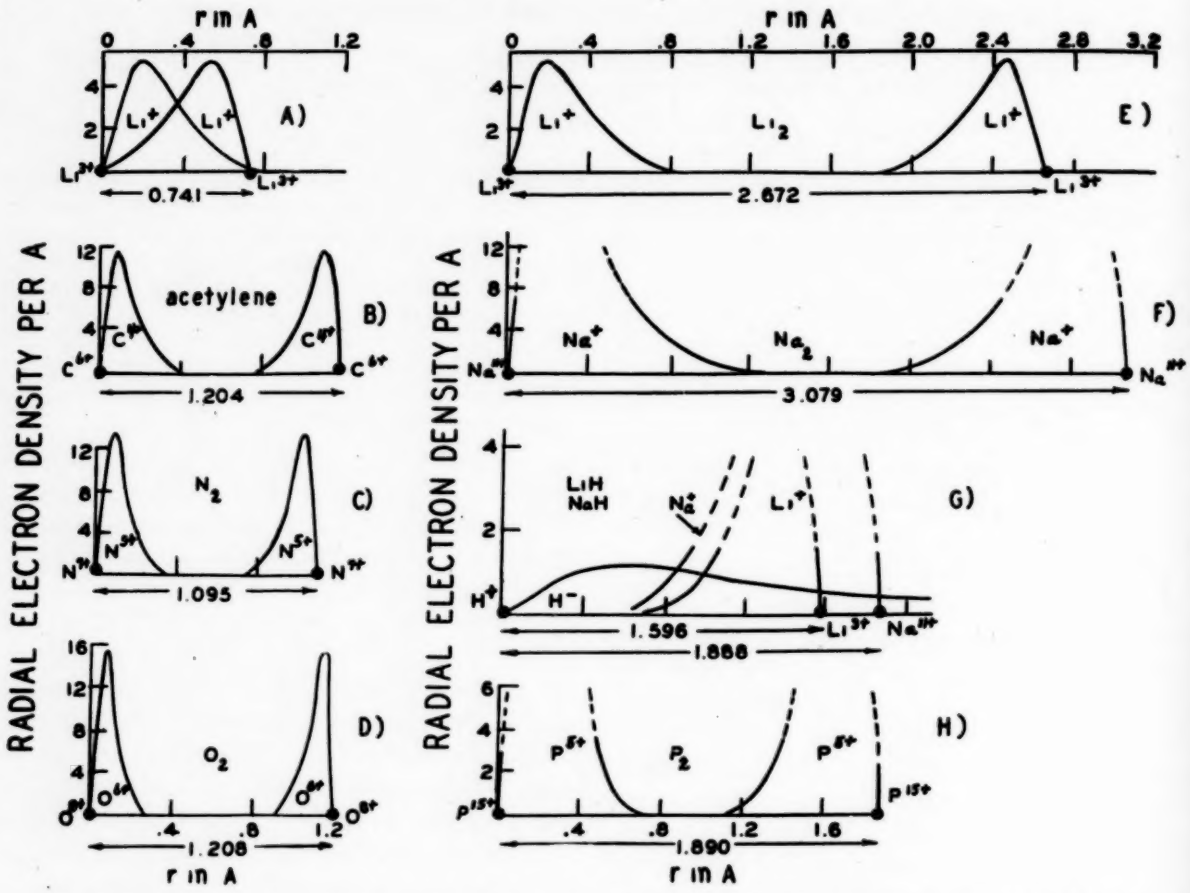

FIG. 1. Radial electron density in number of electrons per angstrom of gaseous atomic cores (in G also of H⁻) placed at the internuclear distance observed in the indicated molecules.

the distance between the centers of neighboring N_2 molecules in the close packed crystal lattice[4] is 2.00A. The latter value is an estimate of the "radius" of the outer shell II[8]. These eight electrons will participate in the binding only during the time their path lies between the cores.

Another example of the meaning of the principal quantum number in molecules is offered by comparing H_2, Li_2, Na_2. In Fig. 1A, two Li^+ cores ~~overlap extensively and there is little space~~ Are placed at the internuclear distance 0.74A of H_2 ($n=I$). The electronic shells of the cores overlap extensively and there is little space left for the binding electron pair. The actual, nearly four times larger, distance 2.67A in Li_2 (E) indicates a quantum effect and the formula $(Li^+)II^2(Li^+)$.[5]

See errata p 399

The internuclear distance in Na_2 (Fig. 1F) being only 15 percent larger than in Li_2 suggests that its formula is $(Na^+)II^2(Na^+)$, i.e., that $n \neq 3$ as could be assumed by a schematic application of the Pauli principle to molecules.[5] This last result and the value $n=I$ for two of the binding electrons in N_2 (outside the two K electron pairs) mean that an electron quantized with respect to the field of *two* cores can have a lower principal quantum number than the lowest it can assume when quantized with respect to only one of these cores. This is understandable since the strength of the field of two cores (N^{5+}) is intermediate between that of the single core and a nucleus (Ne^{10+}) with the same total charge.

We consider the symbols used in this paper for

[4] *Strukturbericht*, Vol. II (Akademische Verlagsgesellschaft, Leipzig, 1937), p. 14.

[5] The values calculated for the process $2X^+ + 2e^- = X_2$ on the basis of the Bohr model of H_2, with the cores considered as point charges, gave (II) for $n=2$ an internuclear distance of 2.33A and a binding energy of -7.5 ev. The experimental values for Na_2 (3.08A; -10.9 ev) correspond better, as will be explained in a detailed paper, to these values than to the values (5.35A; -3.9 ev) for point charges and $n=3$.

the quantum states of the molecules as provisional and subject to an extension including the angular momentum of the molecules. Thus, formula (3) does not imply that all eight electrons with $n=II$ have the same energy, but the notation is sufficient to indicate that in respect to the external field this electronic shell deviates little from that of a noble gas and the field of $(N^{5+})I^2(N^{5+})$ from that of a nucleus with a charge 8+.

3.

From Fig. 1, one can see that the electronic shells of the P^{5+} cores (H) would considerably overlap at the internuclear distance of the N^{5+} cores (C). Thus, $n=I$ appears to be improbable for P_2. If the lowest state of the valence electrons is $n=II$, the ten electrons of P_2 can not form a closed noble gas shell.[5a] Eight electrons quantized with respect to both cores could have $n=II$ and the two remaining $n=III$. However, the analogy (see V) between an electron pair and the oxygen ion O^- makes formula (4), analogous to (5), which could be expected for a P_2O_5 molecule, more probable.

$$3^{2.2}(P^{5+})II^2(P^{5+})3^{2.2} \qquad (4)$$

$$\begin{matrix} O^- \\ O^- \end{matrix}(P^{5+})O^-(P^{5+})\begin{matrix} O^- \\ O^- \end{matrix} \qquad (5)$$

In (4) the distinction is made between the II^2 electrons quantized with respect to both P^{5+} cores (analogous to the "shared" electrons in the G. N. Lewis theory) and the four 3^2 electron pairs. The latter are analogous to the "unshared" electrons but, from the point of view of charge distribution, they must be considered as moving part of the time between both cores. Attempting to assign to electrons within molecules definite quantum states, it appears logical to consider those four pairs as quantized with respect to single cores and to assign to them the value $n=III$ which they would have in the free P atom. In respect to motion, they differ from the II^8 electrons of N_2 in that they are considered as moving predominantly near the single cores.

Formulae (4) and (5) make it understandable that P_2 and P_2O_5 polymerize to P_4 and P_4O_{10}, respectively. In the single molecules 4/5 of the electron pairs or O^- are unshared. In the polymers the P^{5+} cores are tetrahedrally arranged and six of the ten electron pairs or O^- respectively are electrically bound by two cores (see V). On the other hand, in N_2 the field of the cores is practically completely screened by the outer II^8 electrons and cannot interact with electrons of other molecules.

4.

The distinction between quantization of electrons of diatomic molecules with respect to both or to single cores proves to be useful in considering the role the electrons play in the binding of the cores. The monohydrides can serve as an example.

According to the method of quantization proposed, hydrogen can be bonded in molecules only in two forms; either as a more or less

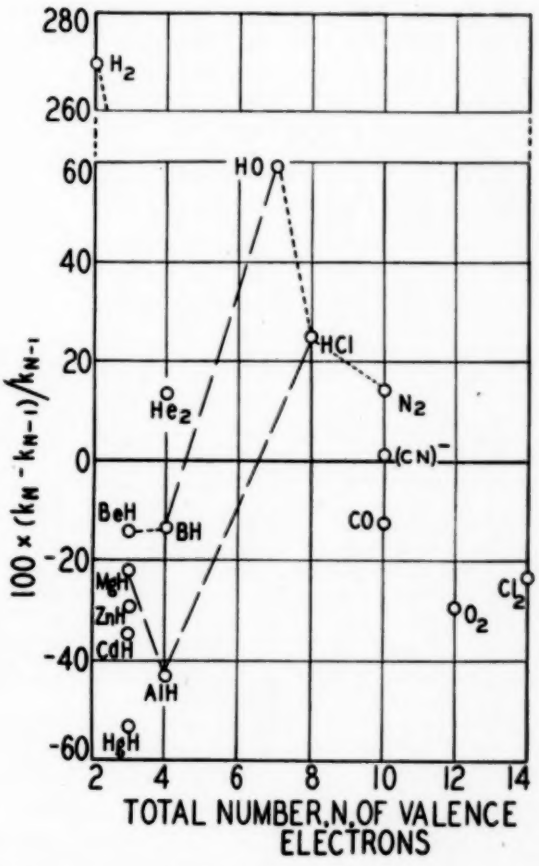

FIG. 2. Percent change in the force constant, k_{N-1}, on addition of the Nth electron to a particle with $N-1$ valence electrons.

[5a] Another reason against a closed eight electron shell is the larger deviation of the axial field of the P^{5+} cores, as compared with the N^{5+} cores, from central symmetry.

deformed[6] H^- (in combination with electropositive elements) or as a proton having a common shell with some other cores (of negative elements). It has been concluded (III, reference 4) from the discontinuity of the gradation of internuclear distances in monohydrides that the binding character of hydrogen changes, within the periods of the system, between BH and HC, AlH and HSi, TlH and HPb or near these places. Accordingly, one would formulate, e.g., HO as $(H^+)II^7(O^{6+})$, HCl as $(H^+)III^8(Cl^{7+})$ and the hydrides of the first three groups as $(M^+)(H^-)$, $n^1(M^{++})(H^-)$, $n^2(M^{3+})(H^-)$.[7]

5.

Figure 2 offers strong support for these formulations. It shows the relative change of the force constant k[8] caused by the addition of an electron to singly charged positive ions.

The binding in the monohydrides containing H^- is due to its attraction by the positive charge of the core, which in hydrides of divalent and trivalent elements, e.g., in $3^2(Al^{3+})(H^-)$, is partially screened by the electrons quantized with respect to these cores. In the ion $(AlH)^+$, which can be formulated as $3^1(Al^{3+})(H^-)$, one of these screening electrons is eliminated; the binding should become stronger. Figure 2 confirms this expectation, the value $100(k_N - k_{N-1})/k_{N-1}$ is negative for all listed monohydrides of divalent and trivalent elements, changing from -13.8 for BH to -53.5 for HgH.[9]

On the other side, the positive values of the ordinate for HO and HCl show that the seventh and eighth electrons increase the value of k, which proves that they take part in the binding of the cores, and the same is true for H_2, He_2, and N_2. That not only the Nth electron but all electrons common to both cores in H_2, HO, HCl, and N_2 participate in the binding is supported by the fact that the relative strengthening of the binding caused by addition of the Nth electron is the larger the smaller the value of N. This is shown in the figure by the line connecting N_2, HCl, and HO and its extrapolation to H_2.

Thus, not only in H_2 and N_2 (see III) but also in HCl all valence electrons participate in the binding of the cores (H^+ and Cl^{7+}, see I). This result cannot be brought into agreement with the usual formula H—Cl of the valence bond theory or with its electronic interpretation $H:\ddot{\underset{\cdot\cdot}{Cl}}:$, which assumes that only two electrons take part in the binding.

6.

As Fig. 2 shows, He_2 does not fit into the line connecting H_2, HO, HCl, and N_2. One would expect that the fourth electron of He_2 increases the k value of He_2^+ by about 180 percent, but in reality the increase is only 13 percent. This peculiar molecule He_2 has been found in the spectrum in spite of its instability with respect to two normal He atoms and on the basis of the Hund-Mulliken method it appears that its lowest observed state is not the ground state.[10] Our method suggests, for the lowest possible state of He_2 the formula $1^1(He^{2+})I^2(He^{2+})1^1$, for He_2^+ the formula $1^1(He^{2+})I^2(He^{2+})$. The formulae, in which the electrons quantized with respect to the single cores He^{2+} are unpaired, agree with the fact that the number of unpaired electrons is two in He_2 and one in He_2^+ (see reference 2, p. 488). The relatively small contribution of the fourth electron of He_2 to the binding strength indicates that its motion brings it infrequently between the cores, which is not surprising for an "unshared" electron.

[6] A strong tightening of H^- in the LiH and NaH molecules is indicated in Fig. 1G by the considerable overlapping which undisturbed electronic shells of ions would have at the actual internuclear distances of these molecules.

[7] E.g., BH would be $2^2(B^{3+})(H^-)$ or $2^2(B^{3+})(H^+)1^2$.

[8] The force constants k were derived from the frequencies at the minimum of the potential curves given by G. Herzberg (reference 2, see p. 105 and Table 36). The comparison of the internuclear distances of the ionized and neutral molecules leads throughout to the same result about the direction of the change in binding strength.

[9] The negative values for CO, O_2, and Cl_2 have a different reason and will be discussed, as well as the case of $(CN)^-$, in a paper to follow.

[10] See G. Herzberg, reference 2, p. 390 and F. L. Arnot and M. B. M'Ewen, Proc. Roy. Soc. **A171**, 106 (1939).

PHYSICAL REVIEW VOLUME 63, NUMBERS 7 AND 8 APRIL 1 AND 15, 1943

A Statistical Theory of Liquids. II

GEORGE JAFFÉ
Louisiana State University, Baton Rouge, Louisiana
(Received February 6, 1943)

In continuation of Part I, vapor pressure, surface tension, and the neighborhood of the critical point are discussed. Section IX deals with the vapor pressure law. A comparison with experimental data shows that the experimental values of the heat of vaporization are, on the average, 55 percent higher than the calculated values for the ten liquids studied. This suggests association in the liquid phase. However, even for the noble gases and mono-atomic metal vapors there remains a discrepancy, though of less degree. In Section X the previously established expression for the surface tension is developed. The "number of molecules per sq. cm of surface" can be defined by the aid of integrals involving the potential of molecular interaction. If, then, a "molar surface S^*," is defined as a surface containing one mole of the liquid, the equation of state for the surface phase assumes the form $\gamma S^* = RT$. The value for mercury can be calculated quantitatively from the potential as established in Part I. In the case of the other nine liquids the potential has to be "cut off" at a distance of the order σ_1. Eötvös' law follows as a limiting law for sufficiently high temperatures.—In Section XI the potential in the surface layer is supplemented for the case that the density in the vapor phase becomes comparable with that in the liquid phase. Then the proof of the coexistence of the two phases (Section IV) is extended to the neighborhood of the critical point. For that neighborhood the rule of Cailletet and Mathias is deduced. Finally the Kamerlingh Onnes constant is deduced from the special form of potential introduced in Section VII. It comes out 25 to 33 percent too low.

THE following three sections deal with the application of the previously developed theory[1] (Part I), to vapor pressure, to surface tension, and to the neighborhood of the critical point.

IX.[2] VAPOR PRESSURE

The vapor pressure law is contained in our formula (3.18).[2] This formula was deduced under the restriction that the radii of curvature of the liquid boundary are large compared with the range of molecular action. Under this assumption the surface term in (3.18) is insignificant. Neglecting it and making use of (3.07) and (3.08) we obtain

$$n_2/n_1 = \exp\left(-(u_2-u_1)/kT\right), \qquad (9.01)$$

where u_1 and u_2 are given by (2.14) and (2.15), respectively.

We shall introduce molar quantities and shall not treat here the density in the vapor phase ρ_2, as small compared with that in the liquid phase ρ_1. If we call Avogadro's number N_0, the potential energy of the two phases per mole becomes

$$U_1^* = N_0 u_1, \quad U_2^* = N_0 u_2. \qquad (9.02)$$

Furthermore, the ordinary molar heat of vaporization L^* (which still contains the external work), is given by

$$L^* = -(U_1^* - U_2^*) + Mp(v_2 - v_1), \qquad (9.03)$$

where M signifies the molecular weight, and where v_1, v_2 represent the specific volumes. For $v_1 \ll v_2$ this is equivalent to our previous equation (6.10).

If, finally, we assume that the molecular constitution is the same in the two phases the ratio n_2/n_1 will be equal to the ratio ρ_2/ρ_1 of the densities, and (9.01) assumes the form

$$\rho_2/\rho_1 = \exp\left[-(L^* - Mp(v_2 - v_1))/RT\right]. \qquad (9.04)$$

It was pointed out before (p. 467, Part I) that the relation (9.01) might have been obtained directly from Boltzmann's theorem. This relation (9.01) is based on the fundamental principles of statistical mechanics, and the only specific assumption involved in (9.04) is the equality of molecular constitution in the two phases.

In principle Eq. (9.04) could serve to calculate the pressure of the saturated vapor as a function of temperature. Once the potential of molecular interaction is known completely, the dependence on temperature of all quantities involved in (9.04) is calculable, and then, from the equation of state (3.20), the pressure in the vapor phase

[1] G. Jaffé, Phys. Rev. **62**, 463 (1942).
[2] Section numbers and the numbering of equations and tables are continued from Part I.

can be evaluated. However, the determination of the potential of molecular interaction carried through in Part I claims to be valid only for the neighborhood of the chosen standard temperature, and it is not the object of the present investigation to calculate the quantities involved over a wide range of temperatures. As stated before (p. 475, Part I) this may necessitate a refinement in the choice of the potential.

However, the density law (9.04) can be tested without reference to any particular law of molecular interaction. If ρ_1 and ρ_2 are known for any temperature, L^* can be calculated and compared with the empirical value of L^* for that temperature. Equation (9.04) should hold for all temperatures lower than the critical. If, however, the temperature is so low that $v_1 \ll v_2$ and that the vapor may be treated as an ideal gas, we obtain from (9.04)

$$L^* = RT(\log(\rho_1/\rho_2)+1). \qquad (9.05)$$

We have calculated, from (9.04) and (9.05), L^* for the ten liquids discussed in Part I and over the range of temperatures where independent determinations of L^* are available. In Table III the ratios $Q = L^*_{\text{exp}}/L^*_{\text{theor}}$ are indicated together with the range of temperatures.

TABLE III. Comparison of theoretical and empirical data. (L = molar heat of vaporization, K = Kamerlingh Onnes constant.)

1	2	3	4	5	6	7
Liquid	t°C	$Q = L^*_{\text{exp}}/L^*_{\text{th}}$	t°C	$Q = L^*_{\text{exp}}/L^*_{\text{th}}$	K_{exp}	K_{theor}
Mercury	357	1.26				
Bromine	58.8	1.50				
Carbon disulfide	46.3	1.44				
Acetone	56.5	1.58	100	1.59	4.10	2.89
Carbon tetrachloride	76.8	1.55	280	1.52	3.68	2.80
Chloroform	61.2	1.57				
Ethyl ether	34.6	1.61	180	1.45	3.83	2.77
Benzene	80.1	1.56	280	1.52	3.76	2.86
Ethyl alcohol	78.4	1.91	240	1.71	4.02	2.86
Water	100	1.57	220	1.59	5.42	2.92

It will be noticed that the ratios Q are considerably larger than 1 in all cases, but that they depend comparatively little on the temperature (though the values of L^* change considerably in some cases). There does not seem to be any other explanation for this discrepancy except the assumption that the molecular constitution in the two phases is not the same. Now, some of the 10 liquids are definitely known to be "associating" (water, ethyl alcohol). Most of the others, even mercury, show the well-known rise of the boiling point upon energetic drying[3] which, again, indicates a complex constitution in the liquid phase. This makes the suggested explanation plausible.

The assumption of equal molecular constitution in the two phases is most legitimate in the case of monatomic vapors. We have, therefore, extended the calculations to the noble gases and to some metals. In the former group Q rises from 1.30 in the case of neon to 1.46 in the case of xenon (for the respective boiling points). Helium, it is true yields $Q = 0.83$ but this must be accidental since classical statistical mechanics is not applicable to helium.[4]

For the 10 metals Na, K, Rb, Cs, Ag, Zn, Cd, Al, Pb, and Bi for which sufficiently reliable data are available Q rises from Al ($Q = 0.985$) to Bi ($Q = 1.35$) with an average value of 1.16.[5]

Thus, on the whole, the situation is more satisfactory for substances with monatomic vapors but it seems awkward to ascribe the remaining difference to molecular association, e.g., in the case of the inert gases. It should be pointed out, however, that this difficulty is not specific of our theory but would be the same in every theory which is based on classical statistical mechanics.

In performing the numerical calculations of Part I we made use of the empirical knowledge of the heat of vaporization at the ordinary boiling point. It might be mentioned that the systematic deviations recorded on p. 475, Part I could be reduced if the values of L^* calculated from (9.05) were used instead of the empirical values. We did not consider it worth while to repeat the lengthy calculations as there is very little gain if the error is thrown on the values of L^*.

X. SURFACE TENSION

In our formula (3.21) giving surface tension the corrective surface term can again be neglected. Introducing, then, the values (3.07) and (3.09) we obtain

$$\gamma = kTn_1 \int_0^\infty [1 - \exp(-(u-u_1)/kT)]dh, \quad (10.01)$$

[3] Brereton Baker, J. Chem. Soc. **101**, 2339 (1912); **121**, 568 (1922). For further references see A. Findlay, *The Phase Rule* (Longmans, Green and Company, London, New York, Toronto, 1931), seventh edition, p. 20.

[4] H. S. W. Massey and C. B. O. Mohr, Proc. Roy. Soc. **A141**, 434 (1933); **144**, 188 (1934).

[5] Mg makes a strange exception with $Q = 2.31$. It seems that the experimental determination of L^* is at default in this case.

where u is given in general by (2.04), (2.07), and u_1 by (2.14). It should be mentioned that $(u-u_1)$ is always positive and γ, therefore, comes out positive. In the limit $(u-u_1)/kT \to 0$ the dynamic formula (10.01) reduces to a form which might be obtained by the usual static procedure.

In what follows we shall be satisfied to make use of the first approximation which assumes the molecular density n to be constant even in the surface layer. Then u takes the form given by (2.10), (2.11) and γ can finally be written in the form

$$\gamma = kTn_1\sigma^*, \tag{10.02}$$

where

$$\sigma^* = z\sigma_1. \tag{10.03}$$

Here z is a pure number given by

$$z = I_5 + I_6 \tag{10.04}$$

and I_5, I_6 represent the integrals

$$I_5 = \int_0^1 \{1-\exp[(\pi n_1/kT)(\psi(\sigma_1) - \xi\sigma_1\chi(\sigma_1))]\}d\xi, \tag{10.05}$$

and

$$I_6 = \int_1^\infty \{1-\exp[(\pi n_1/kT)(\psi(\sigma_1\xi) - \xi\sigma_1\chi(\sigma_1\xi))]\}d\xi. \tag{10.06}$$

It is easy to see that z will be of the order of 1, presumably somewhat larger than 1. For, I_5 is at the utmost equal to 1, and I_6 will depend on the distance up to which the molecular forces are noticeable and will tend towards zero as this distance becomes shorter. Altogether σ^* measures what might be called the "average thickness of the surface layer."

This statement suggests a different form for (10.02). The product $n_1\sigma^*$ defines the number of particles per cm² in the surface layer and we may look upon this surface layer as a separate phase with a surface density

$$\nu_1 = n_1\sigma^*. \tag{10.07}$$

The "equation of state" for this phase[6] will then be given by

$$\gamma = \nu_1 kT. \tag{10.08}$$

[6] M. Born and R. Courant, Physik. Zeits. **14**, 731 (1913) have stressed, long ago, the point that the Eötvös formula should be considered as an equation of state.

If, furthermore, we call a surface which contains one mole of liquid a molar surface S^*, we can write

$$\nu_1 = N_0/S^*, \tag{10.09}$$

and the equation of state assumes the form

$$\gamma S^* = RT. \tag{10.10}$$

It is known that Eötvös, in establishing his law, was led by the law of corresponding states. He, therefore, introduced a molar surface tension $\Gamma = \gamma(Mv_1)^{\frac{2}{3}}$, referring it to a spherical volume of liquid which would contain one mole. Our derivation shows that the true analogy with the gaseous phase is brought out, not if a volume containing a mole is considered, but if the surface phase itself contains one mole.

The equations (10.08) and (10.10), suggestive as they are, cannot be compared in significance with the corresponding laws for gases or solutions. This is due to the fact that ν_1 is not independently variable (as density in gases or concentration in solutions) but is an implicit function of the temperature. Therefore, neither ν_1 nor S^* are known *a priori*. They obtain a definite meaning only if defined by the integrals involved in the expression (10.04) for z. On the other hand, the argument may be reversed and the thickness of the surface layer determined from the experimental knowledge of the surface tension.

TABLE IV. Comparison of theoretical and empirical data[*] (γ = surface tension, k_E = Eötvös' constant.)

1	2	3	4	5	6	7	8
Liquid	σ_1 $\times 10^8$	σ^* $\times 10^8$ 20°C	γexp at b.p.	γtheor at b.p.	$4\sigma\Gamma/3$	k_E exp	k_E theor
Mercury	5.0	28.5	394	394	0.60	0.9–1.3	1.09
Bromine	6.7	8.8	34.7	34.6	0.80	2.00	1.95
Carbon disulfide	6.9	8.1	28.5	29.3	0.78	2.1	1.86
Acetone	7.5	7.2	19.1	26.4	0.71	1.90	2.13
Carbon tetrachloride	8.1	10.8	20.0	22.7	0.84	2.21	2.16
Chloroform	7.7	9.0	21.6	25.2	0.76	2.1	2.03
Ethyl ether	8.1	7.3	15.3	19.5	0.79	2.25	2.04
Benzene	7.9	10.7	20.0	24.0	0.86	2.22	2.27
Ethyl alcohol	7.3	5.13	17.5	34.5	0.50	1.15	2.55
Water	4.8	5.43	58.9	79.1	0.42	1.20	2.48

This procedure affords a first test for the correctness of our formula since reasonable values for the thickness of the surface layer should be obtained. Again it should be pointed out that this test is entirely independent of the special law of molecular interaction.

We have calculated σ^* for our ten liquids starting from the experimental values of the surface tension at 20°C. The values thus obtained are to be found in column 3 of Table IV. They are, without exception, of the order of magnitude which might have been anticipated.

Furthermore, if the values of σ^* are compared with the values of σ_1 as determined in Part I (Table IV, column 2) it will be seen that there is a remarkable agreement between the two series (except in the case of mercury where σ^* is five to six times as large as σ_1). This agreement suggests the interpretation that the surface phase, anyway in many cases, consists just of one molecular layer. However, we have pointed out previously (p. 475, Part I) that the values of σ_1 determined in Part I may be somewhat too large. If that is true the surface phase would consist of somewhat more than one layer. This is, of course, equally acceptable.

The situation becomes less satisfactory if an attempt is made to calculate the surface tension in a quantitative way from the potentials determined in Part I. This proves feasible, without serious modification of the potential, only in the case of mercury. In the case of the other nine liquids the potentials of the form (7.01) with the constants as given in Table II (Part I) do not fall off sufficiently quickly with larger distances. This calls for a general remark.

In order that the integral (10.06) may become convergent the potential $\varphi(r)$ (p. 464, Part I) must fall off at least as $1/r^4$. For the calculations carried through in Part I it was only required that $\varphi(r)$ fall off at least as $1/r^3$. No attention was given to the more stringent requirement involved in the calculation of the surface tension, and most of the potentials tabulated in Table II are not in agreement with it.

However, this is no serious difficulty. It was stated (p. 474, Part I) that the theoretical values given in Table I (Part I) depend astonishingly little on the individual choice of the exponents λ or μ. The calculation of the surface tension, however, is strongly dependent on the individual value of μ (this μ determining the depth to which the molecular forces are sensible). It is, therefore, possible to introduce values of μ which make (10.06) convergent without sensibly affecting the agreement obtained for the other physical constants.

The theoretical value of γ can be increased indefinitely by letting the exponent μ approach its lower limit $\mu=4$. On the other hand, γ can be decreased only to a limiting value which is reached as λ and μ tend towards equality. The limiting value of the exponent is given with sufficient accuracy by $\lambda_0=\mu_0=(\beta/\gamma)^{\frac{1}{3}}+(\alpha/\gamma)$, in the notation of Section VIII. If, then, $\lambda=\lambda_0+\epsilon$ and $\mu=\lambda_0-\epsilon$ (with ϵ a small number) it is easy to develop formulae for all physical quantities including γ. They become independent of ϵ in the limit $\epsilon\to 0$ and agree closely with those tabulated in Table II, Part I. The values of λ_0 lie between 5.62 for Br_2 and 4.26 for H_2O.

However, the values of γ thus obtained are still too large by a factor which increases (in the order of our tables) from about 2 for Br_2 to at least 10 for H_2O. This discrepancy may be due to two reasons: the values of σ_1 as determined in Part I may be too large, and the potentials may fall off too slowly (even in the limiting case sketched above).

It was pointed out in Section VIII that the knowledge of σ_1 is not required for the determination of a, b, L, and c_v. Thus the agreement obtained for these constants would not be affected by a change of the values of σ_1. Only the relation (7.05) which has an approximate character would have to be modified. The knowledge of σ_1, on the other hand, is decisive for the calculation of γ and it would seem reasonable to determine σ_1 in such a way as to make γ fit the empirical data. However, such a procedure would necessitate changing σ_1 by more than seems reasonable from the uncertainty in σ_1.

Therefore, we prefer to make the potential itself responsible for the greater part in the observed discrepancy. A value of μ between 5 and 4.26 makes the surface layer extend over 3 to 10 molecular layers which is in contradiction to the direct evidence mentioned above. Thus, there can hardly be a doubt that μ should be at least 5 to make the surface tension fit empirical data. Consequently a potential of the form (7.01) does not seem adequate to describe the properties of liquids in a complete quantitative way: If the constants are determined by the elastic and thermal behavior of the liquid the potential will

fall off too slowly to give a quantitative agreement with observed surface tensions.

This situation is, after all, not astonishing. The elastic and thermal behavior of a liquid is determined by the form of the potential in the immediate neighborhood of a molecule, i.e., up to the distance σ_1. The surface tension, on the other hand, depends in a decisive way upon the decrease of the potential beyond that distance and a potential of the form (7.01) may not have sufficient flexibility to meet both exigencies.

A potential with an exponential decrease beyond σ_1 would, no doubt, be better fitted to give a quantitative description of most liquids. In order to avoid lengthy numerical calculations we have adopted, as a first very rough approximation, the procedure to "cut off," at the distance σ_1, the potentials as determined in Part I. Accordingly we assume that our potential $\varphi(r)$ is zero for $r>\sigma_1$. The same will hold, then, for $\psi(r)$ and $\chi(r)$ and the integral I_6 of (10.06) becomes zero. The numerical calculations show that the exponential in I_5 is sufficiently small for all liquids (except Hg) to make it negligible. The integral I_5 then has the value 1 and γ assumes the simple form

$$\gamma = kTn_1\sigma_1. \tag{10.11}$$

We have computed γ from this formula for our liquids (with the exception of Hg) for the chosen standard temperatures, i.e., the respective boiling points. The calculated values are compared with the empirical values in Table IV (columns 4 and 5). The empirical values had to be interpolated, and for Br_2 extrapolated, from the observed values. The agreement is about as good as might be expected from the rough approximation involved, except for the "associating" liquids alcohol and water.

It will be noticed that the theoretical values are, as a rule, too large. This would indicate that our values of σ_1 are, on the average, 30 percent too large. This is, of course, a lower limit for the deviation involved since a greater part of the error would fall on σ_1 if the potential were not to be cut off so abruptly.

We have not discussed the case of mercury yet. This liquid presents special conditions in two regards. The theoretical value $\mu=6$ could be assigned (owing to the high bulk coefficient) and the thickness of the surface layer is much larger than in all other cases (Table IV, column 3). These circumstances render it possible to fit γ to the empirical value without cutting off the potential (7.01). We have evaluated for Hg the integral (10.06) by graphical methods (the evaluation of (10.05) is immediate). If the constants as given in Table II are used a value of $\gamma=306$ is obtained as compared with the measured value $\gamma=394$. Thus, in this case the theoretical value is even too small and μ must be lowered. With the assumption $\mu=5.32$ (which leads to $\lambda=12.86$) the agreement is complete and the constants of Table I are hardly affected.

Eötvös' Law

The temperature dependence of γ is rather involved according to our formula (10.08). At first sight it would seem that γ should increase with the temperature in contradiction to empirical facts. However, n_1 and σ^* decrease with rising temperature and a general decrease may result. We shall limit ourselves to showing that Eötvös' law follows from our formula as a limiting law for $\lim (u-u_1)/kT\to 0$.

Under this assumption the quantity Γ considered by Eötvös:

$$\Gamma=\gamma(Mv_1)^{\frac{1}{3}}=\gamma(N_0/n_1)^{\frac{1}{3}}, \tag{10.12}$$

can be written in the form

$$\Gamma=\pi N_0^{2/3}n_1^{4/3}\left\{\int_0^{\sigma_1}(h\chi(\sigma_1)-\psi(\sigma_1))dh + \int_{\sigma_1}^{\infty}(h\chi(h)-\psi(h))dh.\right. \tag{10.13}$$

Therefore we obtain

$$\frac{d\Gamma}{dT}=\frac{4}{3n_1}\frac{dn_1}{dT}+\frac{\pi}{2}n_1^{4/3}N_0^{2/3}\sigma_1^3\varphi(\sigma_1)\frac{\partial\sigma_1}{\partial T}. \tag{10.14}$$

This expression is always negative since $(1/n_1)(dn_1/dT)=-a$, and since $\varphi(\sigma_1)$ is positive and $\partial\sigma_1/\partial T$ is negative for the equilibrium distance.

If we now introduce the special potential (7.01) and make use of the approximate formulae

(7.04) and (7.12) we find

$$\frac{d\Gamma}{dT}=-\frac{4}{3}a\Gamma+\frac{R}{4N_0^{\frac{1}{3}}}\left(\frac{\delta}{2\pi}\right)^{\frac{1}{3}}\frac{\delta\varphi(\sigma_1)}{kT}\frac{\varphi(\sigma_1)}{\sigma_1\varphi'(\sigma_1)}. \quad (10.15)$$

Thus, in the limit $\varphi/kT\to 0$ the Eötvös constant, $k_E=-d\Gamma/dT$, should approach the value $4a\Gamma/3$. In this form the relation can be tested, without reference to the form of the molecular interaction, by the insertion of the experimental values for a and Γ. It will be seen from Table IV (columns 6 and 7) that $4a\Gamma/3$ has the correct order of magnitude but gives less than half of the experimental values.

Under actual conditions the second term in (10.15) is of the same order of magnitude as the first. We have calculated it making use of the values determined in Section VIII. This is a legitimate approximation since the second term in (10.15) has its origin in the first integral of (10.13). Hence the value of this term is not affected by the fact that the potential has to be modified *beyond* σ_1 in order to give correct values for γ itself.

Column 8 of Table IV contains the values which we have calculated from the complete expression (10.15), for the standard temperatures, using the empirical data for a and Γ. The agreement between observed (column 7) and calculated values is almost better than might have been anticipated since the assumption $(u-u_1)/kT\ll 1$ is not fulfilled for the standard temperatures. Under these circumstances it should be stressed only that $d\Gamma/dT$ comes out negative and of the proper order of magnitude. The main contribution in making $d\Gamma/dT$ negative comes from $\partial\sigma_1/\partial T$ as in the case of thermal expansion (see p. 474, Part I). It need hardly be mentioned that k_E is not a true constant but itself depends on temperature as is also shown by experimental evidence.

XI. NEIGHBORHOOD OF THE CRITICAL POINT

In deriving the potential for the surface layer we have assumed that the contribution on the vapor side can be neglected. As pointed out previously (p. 465, Part I) this assumption restricts our treatment, as far as surface terms have been considered, to the case where the molecular density in the vapor is small compared to that in the liquid. In order to obtain formulae which hold up to the critical point we must first generalize the expressions for the potential in the transition layer.

In doing so we shall not write down the formulae which correspond to (2.04) and (2.07) and which hold if the density is treated as variable within the surface layer. We shall be satisfied to establish the first approximation which assumes the densities in the two adjacent phases to be constant up to the geometrical boundary. Consequently there will be a discontinuity of the density in this boundary. Furthermore, we shall disregard the dependence of σ, the average distance of nearest neighbors, upon the change of potential within the layer (see p. 470, Part I). Then σ_1 and σ_2 become parameters independent of space within the respective phases and only dependent on the temperature and the average molecular density in the way established in Section V.

If we now call h_1 the normal distance from the boundary in the liquid the potential of a point at the depth h_1 becomes, by straight forward integrations,

$$u=\pi n_1[\psi(\sigma_1)+h_1\chi(h_1)]+\pi n_2[\psi(\sigma_2)+(h_1/\sigma_1)(\psi(\sigma_1)-\psi(\sigma_2))-h_1\chi(h_1)],\quad 0\le h_1\le\sigma_1, \quad (11.01)$$

and

$$u=\pi n_1[2\psi(\sigma_1)-\psi(h_1)+h_1\chi(h_1)]+\pi n_2[\psi(h_1)-h_1\chi(h_1)],\quad \sigma_1\le h_1<\infty. \quad (11.02)$$

These formulae reduce, of course, to (2.10) and (2.11) if n_2 is negligibly small compared with n_1.

Counting h_2 in the analogous way from the boundary into the vapor phase we obtain

$$u=\pi n_1[\psi(\sigma_1)-h_2\chi(\sigma_1)]+\pi n_2[\psi(\sigma_2)+h_2\chi(\sigma_2)],\quad 0\le h_2\le\sigma_1, \quad (11.03)$$

$$u=\pi n_1[\psi(h_2)-h_2\chi(h_2)]+\pi n_2[\psi(\sigma_2)+h_2\chi(\sigma_2)],\quad \sigma_1\le h_2\le\sigma_2, \quad (11.04)$$

and

$$u=\pi n_1[\psi(h_2)-h_2\chi(h_2)]+\pi n_2[2\psi(\sigma_2)-\psi(h_2)+h_2\chi(h_2)],\quad \sigma_2\le h_2<\infty. \quad (11.05)$$

These expressions make the potential a continuous function across the boundary, varying from the negative value (2.14) in the interior of the liquid to the negative value of smaller amount (2.15) in the interior of the vapor (see reference 7, Part I). In the geometrical boundary we have

$$u_0=\pi[n_1\psi(\sigma_1)+n_2\psi(\sigma_2)]. \qquad (11.06)$$

It should be noticed that, on the vapor side u is different from u_2 even if the contributions of n_2 are neglected. For $n_1=n_2$ the potential (11.01) to (11.05) becomes constant throughout as it should.

With the potential thus generalized the partition function leads to an expression for the "work function" identical with (3.10) if only (3.06) is replaced by

$$q_\tau=\Pi=\Pi_1V_1+\omega_1S+\Pi_2V_2+\omega_2S. \qquad (11.07)$$

Here, Π_1 and Π_2 are defined by (3.07) and (3.08) and the two surface terms are given by

$$\omega_i=\int_0^\infty[\exp(-u/kT) - \exp(-\mu_i/kT)]dh_i, \quad i=1,2. \qquad (11.08)$$

It should be mentioned that ω_1 is negative whereas ω_2 is positive.

S, of course, refers to the common surface of the two phases. This will be spherical under our assumptions, as previously proved (p. 467, Part I). The vapor phase will necessarily have an exterior surface S_2 and this should give a contribution to q_τ depending on the interaction between the vapor and the walls of the containing vessel. We are not interested here in this surface effect and have disregarded it.

With the new form of Π, (11.07), most of the formulae of Section III take slightly modified forms which are easy to establish. The changes regard the corrective surface terms which are of negligible influence anyway. The only significant change concerns the surface tension. Instead of (3.21) we obtain

$$\gamma=-kTn_1\frac{\omega_1}{\Pi_1}\Big/\left(1+\frac{\omega_1S}{\Pi_1V_1}\right) - kTn_2\frac{\omega_2}{\Pi_2}\Big/\left(1+\frac{\omega_2S}{\Pi_2V_2}\right). \qquad (11.09)$$

If this expression is evaluated as in the preceding section our final formula (10.02) is augmented by additional terms which do not vanish even if all terms involving n_2 are neglected. However, it can be shown that the additional terms are numerically irrelevant as long as the density of the vapor is small compared to that of the liquid. Thus the procedure adopted in Part I and in Section X is legitimized. The corrected form of γ, (11.09), vanishes, as do ω_1 and ω_2, if n_1 and n_2 become equal.

We are now prepared to study the equilibrium of the two phases in the neighborhood of the critical point. Proceeding in exactly the same way as in Section IV we obtain, instead of (4.06) and (4.05) the following two conditional equations:

$$\Omega_1=\Omega_2=\Omega \qquad (11.10)$$

and

$$\Pi_1-n_1\Omega+2\omega S/3V_1=\Pi_2-n_2\Omega. \qquad (11.11)$$

Here we have introduced the notations

$$\omega=\omega_1+\omega_2 \qquad (11.12)$$

and

$$\Omega_i=\frac{\partial\Pi_i}{\partial n_i}+\frac{S}{V_i}\frac{\partial\omega}{\partial n_i}, \quad i=1,2. \qquad (11.13)$$

The conditional equations (11.10) and (11.11) now hold for all values of n_1 and n_2, including the critical region. It can be proved that, with the assumptions regarding $\varphi(r)$ which we made in the beginning (p. 464, Part I), a critical point will exist.[7] The critical data will be given, in the usual way, by the equation of state[8] together with the two conditions

$$\frac{\partial p_1}{\partial V_1}=0, \quad \frac{\partial^2 p_1}{\partial V_1^2}=0. \qquad (11.14)$$

It will be seen presently that the relative size of the two phases in the immediate neighborhood of the critical point is fixed by the conditions of equilibrium. However the solution for the critical data will still involve corrective surface terms. In a strict sense, therefore, one should speak of a "critical region." However, the critical data can

[7] See Appendix I, this paper.

[8] The exact expression for the pressure in the liquid phase is now given by the left-hand side of (4.05) with ω substituted from (11.12). The pressure in the vapor phase is given by a similar expression with the last term missing.

be obtained with sufficient accuracy by the use of the abbreviated equation of state (6.04). If required, the exact data could, then, be calculated by a procedure of successive approximations.

For what follows we assume the critical data n_c, p_c, and T_c to be determined. For the neighborhood of the critical point we set

$$n_1=n_c+\nu_1, \quad n_2=n_c+\nu_2, \quad T=T_c+\tau, \quad (11.15)$$

and develop the conditional equations (11.10) and (11.11) with regard to the small quantities ν_1, ν_2, and τ. The zero-order terms yield

$$\frac{S}{V_1}\left(\frac{\partial\omega}{\partial n_1}\right)_c=\frac{S}{V_2}\left(\frac{\partial\omega}{\partial n_2}\right)_c, \quad (11.16)$$

where the subscript c refers to the critical point. This equation determines the relative size of the two phases. The first-order terms yield

$$\nu_1\left[\left(\frac{\partial^2\Pi_1}{\partial n_1^2}\right)_c+\frac{S}{V_1}\left(\frac{\partial^2\omega}{\partial n_1^2}\right)_c-\frac{S}{V_2}\left(\frac{\partial^2\omega}{\partial n_2\partial n_1}\right)_c\right]-\nu_2\left[\left(\frac{\partial^2\Pi_2}{\partial n_2^2}\right)_c+\frac{S}{V_2}\left(\frac{\partial^2\omega}{\partial n_2^2}\right)_c-\frac{S}{V_1}\left(\frac{\partial^2\omega}{\partial n_1\partial n_2}\right)_c\right]$$
$$=-\left[\frac{S}{V_1}\left(\frac{\partial^2\omega}{\partial n_1\partial T}\right)_c-\frac{S}{V_2}\left(\frac{\partial^2\omega}{\partial n_2\partial T}\right)_c\right]\tau \quad (11.17)$$

and

$$\nu_1\left[\frac{1}{3}\left(\frac{\partial\omega}{\partial n_1}\right)_c\right]-\nu_2\left[\left(\frac{2}{3}+\frac{V_1}{V_2}\right)\left(\frac{\partial\omega}{\partial n_2}\right)_c\right]=\frac{2}{3}\left(\frac{\partial\omega}{\partial T}\right)_c\tau. \quad (11.18)$$

From these equations ν_1 and ν_2 can be determined as functions of τ.

We shall not attempt to investigate the solution of (11.17) and (11.18). However, one point is of interest. From the form of the equations it is evident that ν_1 and ν_2 will be proportional to τ, and the same result, therefore, will hold for $\nu_1+\nu_2$. This expresses the rule of the "rectilinear diameter" established by Cailletet and Mathias. Our deduction, of course, holds only for the neighborhood of the critical point and there is no indication, without the study of higher terms, why the rule holds over a comparatively wide domain of temperatures. This fact, however, appears connected with the corresponding fact that the surface tension is practically a linear function of the temperature.

Finally we shall derive the value of the Kamerlingh Onnes constant K under the assumption of the special potential (7.01). The complete knowledge of the critical point requires, besides the determination of n_c, p_c, and T_c, that of the equilibrium distance σ_c at the critical point. The necessary four equations are given by the equation of state, the two conditions (11.14) and the equation (5.05) which is characteristic of our theory and which connects σ, T, and n.

Neglecting surface terms we start from the equation of state in the form (6.04), with U_1 given by (6.03) and (7.03). The combination of the two equations (11.14) yields σ_c:

$$\sigma_c^{\lambda-\mu}=f\lambda^2(\lambda+3)(\mu-3)/(g\mu^2(\mu+3)(\lambda-3)). \quad (11.19)$$

Substitution of this value into either of Eqs. (11.04) gives a relation between the critical temperature and critical density

$$kT_c=(2\pi/9)n_c f\sigma_c^{-\lambda+3}\lambda(\lambda+3)\times(\lambda-\mu)/(\mu(\lambda-3)), \quad (11.20)$$

and if this is substituted into the equation of state, an expression for K is obtained:

$$K=RT_c/p_cV_c=(\lambda+3)(\mu+3)/\lambda\mu. \quad (11.21)$$

Here V_c stands for the molar volume at the critical point. Lennard-Jones and Devonshire[9] have derived, by the "cell method," a formula for K which is equivalent to (11.21). The exponents introduced by these authors refer, however, not to the intermolecular potential but to a function defining, in an arbitrary way, the average volume occupied by each atom.

We have compared the expression (11.21) with the experimental critical data as far as they are

[9] J. E. Lennard-Jones and A. F. Devonshire, Proc. Roy. Soc. **A163**, 53 (1937).

available for our ten liquids. The calculated and the observed values of K are given in columns 6 and 7 of Table III. The calculated values are consistently too small by 25 to 33 percent (if H_2O is excluded). This suggests a systematic error as in the case of the heat of vaporization. However, the discrepancy is hardly larger than one would expect with the special form of potential adopted if it is taken into account that the coefficients involved (Table II, Part I) have been determined from measurements at the ordinary boiling point.

If we want to summarize the results we should distinguish between the general theory and the deductions based on the special form of potential (7.01). The general theory seems satisfactory in the following regards: It reestablishes a random distribution of the molecules and gives the liquid a shape determined by surface tension. Furthermore, it proves the possibility of coexistence of vapor and liquid within certain limits of temperature and it leads automatically to kinetic expressions for the vapor pressure and for the surface tension.

As to the special form of the potential (7.01) it has been shown that it represents the behavior of liquids of widely variable character in a general way. In the one case of mercury the representation covers the thermal and elastic behavior as well as the surface tension. In all other cases the potential has to be modified for larger molecular distances if it is to include surface tension quantitatively. Furthermore, there remain discrepancies of a systematic nature in the determination of the heat of vaporization and in the critical data. It has not been investigated how far association in one or both phases may be responsible for these deviations. However, even with these deficiencies, it seems satisfactory that the simplified assumption of extensionless mass points, with the very special form of potential (7.01), gives our model practically all properties of real liquids with an almost quantitative agreement.

APPENDIX I

It has to be shown that, for sufficiently high values of the temperature, the equations of state for the two phases admit of only one solution for the molecular density n. The proof proceeds in two steps. First surface terms are neglected. In the limiting case $\varphi/kt \to 0$ the parameter σ becomes independent of T and assumes the geometrical value $\sigma=(1/2\pi n)^{\frac{1}{3}}$ of Hertz (p. 470, Part I). From this fact, and from the assumed form of $\varphi(r)$ (p. 464, Part I), it follows that p, as determined from (6.04), increases monotonically with decreasing V. This proves the point in the absence of surface terms. To complete the proof we call the unique solution which exists for sufficiently high values of T, in the absence of surface terms n_0 and investigate whether two solutions of the form $n_1=n_0+\nu_1 S/V_1$ and $n_2=n_0+\nu_2 S/V_2$ can be obtained. If these expressions are introduced into the formulae for the pressure[8] it follows that $n_1=n_2$ *to all orders of approximation*. Hence there is only one solution and no surface of separation can exist. As it has been proved previously (Appendix I, Part I) that there are at least two solutions for sufficiently low temperatures there must be an upper limit of temperature (eventually depending on surface terms) for which more than one solution can be obtained.

In Appendix I, Part I we have given two forms for the conditional equations, either Eqs. (a) and (c) or Eqs. (d) and (e). As surface terms were not considered in Appendix I, Part I, it should be mentioned that both sets yield only a zero approximation for a procedure of successive approximations. Furthermore, it should be pointed out that the two sets are *not* equivalent. Eqs. (d) and (e) are a necessary consequence of Eqs. (a) and (c) but not vice versa. The reason for this situation is that the transition from (a) and (c) to (d) and (e) involves a differentiation. For the calculation of the exact critical data the set (d) and (e) represents a much more adequate zero solution than (a) and (c) since (a) makes the pressure zero.

Letters to the Editor

Nuclear Energy Levels in Fe^{56} from the Decay of Mn^{56} and Co^{56}

L. G. Elliott and M. Deutsch
Massachusetts Institute of Technology, Cambridge, Massachusetts
March 25, 1943

THE radiations accompanying the radioactive decay of Mn^{56} have been studied by a number of authors.[1] However, no consistent energy level scheme could be con-

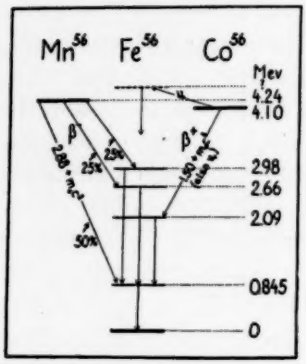

FIG. 1. Nuclear energy levels of Fe^{56} from radioactive disintegrations.

structed to agree with the beta-ray, gamma-ray, and coincidence measurements. We have therefore studied the *photoelectrons* produced in lead by these gamma-rays using our magnetic lens spectrometer, with considerably improved resolution. This study has revealed, in addition to two gamma-rays of 0.845 ± 0.015 and 2.13 ± 0.05-Mev energy,[1] the emission of a 1.81 ± 0.04-Mev gamma-ray, about as abundant as the 2.13-Mev radiation. It had escaped detection in previous experiments because of the inadequate resolution of the Compton recoil method. All of the experiments may now be represented consistently by the disintegration scheme shown in the left half of Fig. 1.

The gamma-ray energies from a mixture of Co^{56}, Co^{57}, and Co^{58} have been previously reported by us.[2] A study of the decay of these gamma-rays, and a separate investigation of Co^{58},[3] allows us to assign to Co^{56} gamma-rays of energies 0.845 ± 0.015, 1.24 ± 0.04, 3.4 ± 0.2 Mev, and others of as yet undetermined energy between 1.5 and 3 Mev and of lower abundance. The energy of the 0.845-Mev gamma-ray is identical with that from Mn^{56} to within 5 kev. The 15-kev probable error given above refers to the absolute energy values; the relative energies are known much more accurately. The maximum energy of the positrons was found in the beta-ray spectrometer to be 1.50 ± 0.05 Mev. Abundant K x-rays and the relatively low intensity of the annihilation radiation indicate the occurrence of orbital electron capture.

The number of positron-gamma-ray coincidences per positron counted in the spectrometer was found to be independent of positron energy (above 0.2 Mev), in agreement with the results of Cook and McDaniel.[4] The efficiency of the gamma-ray counter for gamma-rays of 0.8- and 1.3-Mev energy was determined by coincidence measurements on Mn^{54}, Mn^{56}, Fe^{59}, Co^{58}, Co^{60}. The latter three disintegration schemes have been previously reported by us. With the aid of this calibration it was deduced from the observed coincidence rate in Co^{56} that each positron is accompanied by a 1.24-Mev and a 0.845-Mev gamma-ray in cascade as shown in the right half of Fig. 1. The dependence of the coincidence rate on the amount of lead absorber between source and gamma-ray counter was found to be consistent with this scheme. Further studies of the gamma-rays accompanying orbital electron capture in Co^{56} are in progress and a complete report on these experiments will be published soon.

Taking the mass of the neutral Fe^{56} atom to be 55.9572, we deduce 55.9612 for that of Mn^{56} and 55.9621 for Co^{56}. The threshold for a (p,n) reaction on Fe^{56} should be 5.5 Mev.

[1] E.g.: Townsend, Proc. Roy. Soc. **177**, 357 (1941); Langer, Mitchell, and McDaniel, Phys. Rev. **56**, 427 (1939); Deutsch and Roberts, Phys. Rev. **60**, 362 (1941); and others.
[2] M. Deutsch, A. Roberts, and L. G. Elliott, Phys. Rev. **61**, 389A (1942).
[3] Am. Phys. Soc. Bull. **18**, 1 (1943).
[4] C. S. Cook and P. W. McDaniel, Phys. Rev. **62**, 412 (1942).

The Carbon Arc in Oxygen for the Spectrochemical Determination of Potassium

L. T. STEADMAN
Department of Radiology, The University of Rochester, School of Medicine and Dentistry, Rochester, New York
March 29, 1943

IT is well known that the analytical measurement of very small amounts of potassium by the intensity of its spectrum line 4044.14A in the carbon arc is limited by the high background and the lines of the cyanogen bands. The N_2 of the air responsible for this effect may be replaced to a certain extent by O_2 without impairing the strength of the potassium line, as is the case when CO_2 is used. Johnson and Norman[1] recently have used a CO_2 atmosphere for removing the CN bands in their successful measurement of Cl and Br by means of the high voltage spark method of excitation.

The following technique for measuring potassium has proved very useful when employed with the rotating sector method of measuring line intensities. The lower cathode spectrographic carbon is arranged coaxially in a brass tube 3 cm in diameter which is open at the top and closed at the bottom except for a gas inlet. The top is about 5 mm above the crater tip and has a small rectangular notch on the side facing the spectrograph. The gas supplied to the arc from a commercial oxygen tank is controlled by a pressure reducing valve and the pressure in the line is measured by means of a water manometer. Best results are obtained with an arc current of 8 amp., a gas pressure of 2 cm H_2O, a slit width of about 10 microns, and a high contrast emulsion (35-mm high contrast positive film). Purified National 0.25-inch diameter regular graphite electrodes are used. The cathode is focused on the collimator lens of a Bausch and Lomb medium quartz spectrograph. No other gases have been tried.

With this improvement for determining potassium, the spectrochemical method described by the author[2] for sodium in biological materials has been extended to include other elements so that blood serum is now routinely analyzed for Na, K, Ca, Mg, and P all at once. The use of O_2 does not materially influence the measurement of the elements other than K. To the cathode is added 0.01 ml of serum, which amount in the human normally contains 33.0 percent Na, 2.0 percent K, 1.0 percent Ca, 0.27 percent Mg, and 1.3 percent P. Also, 2.5 percent Rb is added as the internal standard for K and 100 percent Cd as the internal standard for all the other elements. The spectrum lines measured are Na 2680.3A, K 4044.1A, Ca 3006.9A, Mg 2783.0A, P 2535.6A, Rb 4201.8A, and Cd 2677.6A.

[1] W. W. A. Johnson and Daniel P. Norman, Ind. and Eng. Chem., Anal. Ed. **15**, 119 (1943).
[2] L. T. Steadman, J. Biol. Chem. **138**, 603 (1941).